University Of Cyprus
Faculty of Pure and Applied Sciences Department Of Biological Sciences

Laboratory of Developmental Biology and BioImaging Technology
(Assistant Professor Paris A. Skourides)

ADDRESSING THE MOLECULAR BASIS OF MORPHOGENETIC MOVEMENTS DURING *XENOPUS* GASTRULATION WITH THE USE OF QUANTUM DOT NANOCRYSTALS

THE ROLE OF FOCAL ADHESION KINASE (FAK) DURING *XENOPUS* DEVELOPMENT

Ph.D. THESIS

PANAYIOTA STYLIANOU

NICOSIA, JUNE 2011

Πανεπιστήμιο Κύπρου
Σχολή Εφαρμοσμένων και Θετικών Επιστημών
Τμήμα Βιολογικών Επιστημών

Εργαστήριο Αναπτυξιακής Βιολογίας
και Βιοαπεικόνισης
(Επίκουρος Καθηγητής Πάρης Α. Σκουρίδης)

ΔΙΕΡΕΥΝΗΣΗ ΤΗΣ ΜΟΡΙΑΚΗΣ ΒΑΣΗΣ ΤΩΝ ΜΟΡΦΟΓΕΝΕΤΙΚΩΝ ΚΙΝΗΣΕΩΝ ΚΑΤΑ ΤΗΝ ΔΙΑΡΚΕΙΑ ΤΗΣ ΓΑΣΤΡΙΔΙΩΣΗΣ ΣΤΟ *XENOPUS* ΜΕ ΤΗ ΧΡΗΣΗ ΝΑΝΟΚΡΥΣΤΑΛΛΩΝ

Ο ΡΟΛΟΣ ΤΗΣ ΚΙΝΑΣΗΣ ΤΩΝ ΕΣΤΙΑΚΩΝ ΠΡΟΣΚΟΛΛΗΣΕΩΝ (FAK) ΚΑΤΑ ΤΗΝ ΑΝΑΠΤΥΞΗ ΤΟΥ ΒΑΤΡΑΧΟΥ *XENOPUS*

ΔΙΔΑΚΤΟΡΙΚΗ ΔΙΑΤΡΙΒΗ

ΠΑΝΑΓΙΩΤΑ ΣΤΥΛΙΑΝΟΥ

ΛΕΥΚΩΣΙΑ, ΙΟΥΝΙΟΣ 2011

ABSTRACT

Focal Adhesion Kinase (FAK) is a non-receptor tyrosine kinase originally identified as substrate of the oncogenic tyrosine kinase pp60 v-src. FAK as its name suggests localizes prominently at the integrin rich focal adhesions, which suggested a role in controlling cell behaviour resulting from interactions with the extracellular matrix. Later studies established a number of roles for FAK including those of a positive regulator of cell motility, cell survival, cell adhesion, migration and growth regulation. The importance of FAK during embryonic development was demonstrated by the embryonic lethal phenotype of FAK null mice. In *Xenopus*, *Drosophila* and the chick its expression suggests a role in gastrulation movements but there is no evidence to further support this.

We now show that integrin based FAK activity is necessary for mesoderm migration but not convergent extension. Inhibition of FAK by overexpression of the bona fide dominant negative FRNK (Focal adhesion Related Non-Kinase), blocks mesoderm spreading and migration both *in vitro* without affecting convergent extension highlighting the molecular differences between the two movements. In order to address the effects of blocking FAK *in vivo* we developed NIR QD based methodology which for the first time allowed *in vivo* visualization of deep movements in *Xenopus laevis* with single cell resolution. Using this approach we show that FAK is necessary for mesoderm migration *in vivo* and we provide quantitative *in vivo* data regarding migration rates and directionality of the mesoderm. These results implicate FAK as an important regulator of morphogenesis in *Xenopus* and demonstrate the power of the NIR QD methodology.

The essential role of FAK in mesoderm migration provided us with a tool with which to address the role of this movement during the process of gastrulation as a whole and to conclude that mesoderm migration is necessary for successful closure of the blastopore in *Xenopus*. Our results add to a growing body of evidence implicating FAK as a positive regulator of cell spreading and migration.

We go on to show that active tyrosine phoshorylated FAK is primarily found on the plasma membrane of blastomeres in both blastula and gastrula embryos suggesting that FAK becomes activated on the plasma membrane and that FAK may be activated via integrin-independent mechanisms at least prior to gastrulation. In an effort to identify the region of FAK responsible for membrane localization *in vivo* several mutants were generated and examined for their localization. These experiments revealed that the N-terminal FERM domain is both necessary and sufficient for plasma membrane localization of FAK in

integrin-free regions of the plasma membrane. Interestingly, expression of the FERM domain in *Xenopus laevis* embryos leads to elevated tyrosine phosphorylation of endogenous FAK and of downstream targets in a cell autonomous and Src-dependent manner. These data reveal a new role for the FERM domain as an activator of FAK. In addition, our findings confirm an essential role of the FAK autophosphorylation site Tyr397 on cell spreading and migration and also suggest a possible role for FAK in mesodermal patterning and polarity.

Finally, we show that both the N- and C- termini of FAK are required for FAK targeting to the plasma membrane in the highly morphogenetic dorsal mesoderm and generated a new promising dominant negative construct designed upon these findings. Using this putative dominat negative construct in several *in vivo* and *in vitro* assays with we reveal that FAK is necessary for morphogenesis, affecting both cell-extracellular matrix and cell-cell based movements of the mesoderm, in addition to an essential role in mitosis.

Table of Contents

I. LIST OF TABLES AND FIGURES 5
A. TABLES 5
B. FIGURES 5
II. LIST OF MOVIES (CD) 9
1. INTRODUCTION 10
1.1 XENOPUS LAEVIS AS AN EXPERIMENTAL MODEL 10
1.2 GASTRULATION IN XENOPUS LAEVIS 13
1.2.1 Morphogenetic movements 13
1.2.2 Mesoderm migration 15
1.3 QUANTUM DOTS (QD'S) 17
1.3.1 Synthesis and optical properties of QD's 17
1.3.2 Characteristics of Quantum Dots 18
1.3.3 Biological applications 19
1.4 CELL ADHESION-FOCAL ADHESIONS 23
1.5 FOCAL ADHESION KINASE (FAK) 26
1.5.1 Introduction 26
1.5.2 Molecular structure and function of Focal Adhesion Kinase 28
- FERM (band 4.1 and ezrin, radaxin, moesin proteins) 28
- Proline Rich Domain 1 and Linker Domain 31
- Kinase – Catalytic Domain 32
- Proline Rich Domain 2, Linker, Proline Rich Domain 3 32
- Focal Adhesion Targeting (FAT) 33
- FRNK 33

1.5.3 The role of Focal Adhesion Kinase in cell adhesion and migration 35
1.5.4 The Focal Adhesion Kinase in early development 36
2. ANALYSIS AND DESCRIPTION OF METHODOLOGY 42
2.1 INTRODUCTION 42
2.1.1 Obtaining, housing & feeding Xenopus laevis 43
2.2 GENERAL METHODS 45
2.2.1 Inducing ovulation 45

2.2.2 Isolating the testes 45
2.2.3 Manual egg collection 46
2.2.4 In vitro fertilization 47
2.2.5 Preparing embryos for manipulation 48
- Dejellying embryos 48
- Removing the Vitelline Membrane 48
2.2.6 Microinjections 49
2.2.7 Animal Cap Isolation 51
2.2.8 Dissociation and Reaggregation of Animal Caps 52
2.2.9 Isolation of Posterior Dorsal Mesoderm from mid-gastrula stage embryo 52
2.3 SPECIFIC METHODS 54
2.3.1 Embryos, explants and Microinjections 54
2.3.2 Antibodies and surface labelling 55
2.3.3 Whole-mount In Situ Hybridization (WISH) 58
2.3.4 Plasmids and Cloning strategy 59
2.3.5 Cell Migration assays, FN spreading, adhesion assays and convergent extension assays 61
2.3.6 Immunoblotting (Western Blot Analysis) and Immunoprecipitation 61
2.3.7 Calculation of in vivo migration rates 62
2.3.8 Quantum Dot labelling and NLS conjugations 64
2.3.9 In vivo Imaging and Notes on QD toxicity 64
3. RESULTS 66
3.1 DEVELOPING NEAR INFRA RED (NIR) QUANTUM DOT (QD'S) BASED IMAGING TOOLS FOR IMAGING OF DEEP TISSUE MORPHOGENETIC MOVEMENTS IN XENOPUS IN VIVO 66
3.1.1 Fluorophore evaluation 66
3.1.2 Imaging the migrating anterior mesoderm using NIR QD's 66
3.1.3 Functionalized Quantum Dot probes 70
3.2 FOCAL ADHESION KINASE IS PRESENT AT FOCAL ADHESION COMPLEXES AND IS NECESSARY FOR ACTIVE MESODERM MIGRATION IN XENOPUS EMBRYOS IN VITRO AND IN VIVO 73
3.2.1 Visualization focal adhesion on migrating mesodermal cells 73
3.2.2 Focal Adhesion Kinase is necessary for mesoderm migration 76
3.2.3 Imaging FRNK expressing mesoderm in vivo 79

3.3 THE ROLE OF THE AUTOPHOSPHORYLATION SITE TYROSINE 397 OF FOCAL ADHESION KINASE DURING XENOPUS DEVELOPMENT 84
3.3.1 Y397FFAK overexpression leads to the failure of blastopore closure (Activation of FAK is important during gastrulation (phenotype in vivo)) 84
3.3.2 Phosphorylation of the Y397 autophosphorylation site of FAK is important for the spreading of mesodermal cells in vitro 91
3.4 EXPLORING THE EXPRESSION AND PHOSPHORYLATION OF FOCAL ADHESION KINASE AND ITS DOWNSTREAM TARGETS 99
3.4.1 Expression and phosphorylation of Focal Adhesion Kinase during Xenopus development 99
3.4.2 Down-stream targets of Focal Adhesion Kinase show similar patterns of phosphorylation during early Xenopus embryogenesis 108
3.5 INITIAL INDICATIONS THAT FAK IS REGULATED BY INTEGRIN-INDEPENDENT MECHANISMS IN XENOPUS EMBRYOS 113
3.5.1 FAK morpholino fails to downregulate FAK and inhibit the phosphorylation of FAK during early development of Xenopus laevis 113
3.5.2 FRNK overexpression does not act as a dominant negative in Xenopus laevis embryos 116
3.5.3 FAK becomes activated in Xenopus laevis embryos not exclusively by integrin-depended mechanisms. 119
3.6 INVESTIGATION OF THE FUNCTION OF VARIOUS FOCAL ADHESION KINASE DOMAINS IN XENOPUS EMBRYO 122
3.6.1 Generation and initial characterization of different constructs of Focal Adhesion Kinase 122
3.7 THE FERM DOMAIN IS RESPONSIBLE FOR THE PLASMA MEMBRANE LOCALIZATION OF FAK IN INTEGRIN-FREE AREAS AND IT ACTIVATES FAK IN A SRC- DEPENDANT MANNER 133
3.7.1 The FERM domain of the Focal Adhesion Kinase can autonomously localize at the plasma membrane in Xenopus embryos. 133
3.7.2 The FERM domain is necessary for the localization of FAK on the membrane 138
3.7.3 FERM overexpression leads to activation of endogenous FAK. 140
3.7.4 FERM expression results in endogenous FAK activation in a Src dependent manner. 143

3.8 THE FERM/FRNK CONSTUCT IS CAPABLE OF TARGETING FAK TO THE PLASMA MEMBRANE AND MAY BE A PROMISSING DOMINANT NEGATIVE 147
3.8.1 The FERM and FAT domains cooperate to target FAK on the plasma membrane 147
3.8.2 FERM/FRNK expression blocks convergent extension by regulating the levels of c-Cadherin 155
4. DISCUSSION 158
4.1 DEVELOPING NEAR INFRA RED (NIR) QUANTUM DOTS (QD'S) BASED IMAGING TOOLS FOR IMAGING OF DEEP TISSUE MORPHOGENETIC MOVEMENTS IN XENOPUS IN VIVO 159
4.2 FOCAL ADHESION KINASE IS PRESENT AT FOCAL ADHESION COMPLEXES AND IS NECESSARY FOR ACTIVE MESODERM MIGRATION IN XENOPUS EMBRYOS IN VITRO AND IN VIVO 162
4.3 THE ROLE OF TYROSINE 397 AUTO-PHOSPHORYLATION SITE OF FOCAL ADHESION KINASE DURING XENOPUS DEVELOPMENT 165
4.4 FOCAL ADHESION KINASE IS ACTIVATED BY INTEGRIN-INDEPENDENT MECHANISMS IN THE CONTEXT OF THE EMBRYO 167
4.5 THE FERM DOMAIN IS RESPONSIBLE FOR THE PLASMA MEMBRANE LOCALIZATION OF FAK IN INTEGRIN-FREE AREAS AND IT ACTIVATES FAK IN A SRC- DEPENDENT MANNER 170
4.6 FERM/FRNK IS A PROMISSING DOMINANT NEGATIVE OF FAK 174
5. CONCLUSIONS AND FUTURE PLANS 176
REFERENCES 178
ANNEXES 192
I. ABBREVIATIONS 192
II. PUPLICATIONS* 194
III. CONFERENCE ANNOUNCEMENTS 194

I. LIST OF TABLES AND FIGURES

A. Tables

Table 1: Concentrations of mRNA microinjections…….53
Table 2: Concentrations of the used Antibodies for Imunofluorescence……..……..55
Table 3: Concentrations of the used Antibodies for Whole mount IF…….....56
Table 4: Cloning strategy for FAK constructs…….59
Table 5: FAK (100pg) can partially rescue the FRNK (1ng) induced blastopore closure failure.....79

B. Figures

Figure 1: *Xenopus laevis*……..10
Figure 2: Clevage of a frog egg……....11
Figure 3: *Xenopus laevis* life cycle……...12
Figure 4: Cell movements during *Xenopus* gastrulation……..16
Figure 5A: Emission and sizes of quantum dots of different composition.....18
Figure 5B: Absorption (upper curves) and emission (lower curves) spectra of four CdSe/ZnS qdot samples.....18
Figure 6: QD labeling of *Xenopus* embryos at different stages and specific QD intracellular localizations.....20
Figure 7: Comparison of QD's and RG-D (Rhodamine Green Dextran) for resistance to photobleaching.....21
Figure 8: NIR QD sentinel lymph node mapping in the mouse……...22
Figure 9: Temporal and spatial expression patterns of E-, C- and N-cadherins.....24
Figure 10: FAK structural features…….,,,,,,,,...26
Figure 11: FERM "clover leaf" Structure……29
Figure 12: Autoinhibited FAK and Sequential Model of Activation……...30
Figure 13: Comparison of *Xenopus* (XL_U11078) and chicken (NM_205435) FAK in amino acid level (ClustalW2)……...39
Figure 14: Natural mating……42
Figure 15: *Xenopus laevis* Facility…….……..44
Figure 16: Priming a female *Xenopus laevis*.....45
Figure 17: Squeezing of female frogs and manual collection of eggs.....46
Figure 18: *In vitro fertilization*.....47

Figure 19: Fate map for the 32-cell stage of *Xenopus laevis*.....50
Figure 20: Microinjector and micromanipulator.....50
Figure 21: Microinjection system consiting of micromanipulator, injector and stereoscope.....50
Figure 22: Microscope Zeiss Axio Imager Z1.....56
Figure 23: Stereoscope (Discovery V12).....57
Figure 24: Correction of the migration speed for *in vivo* measurements.....62
Figure 25: NIR QD´s can be used to label and image mesodermal cells during gastrulation.....68
Figure 26: Injection of non targeted NIR QD´s at the 32 cell stage enables visualization of the mesodermal mantle with single cell resolution.....69
Figure 27: NLS peptide conjugated QD´s display size based exclusion from the nucleus.....71
Figure 28: Migrating mesodermal cells form focal adhesion complexes and FRNK displaces FAK from its signaling complexes.....74
Figure 29: FRNK can inhibit mesodermal cell spreading and migration but has no effect on convergent extension movements.....77
Figure 30: FRNK injection inhibits mesoderm migration and results in failure of blastopore closure which often prevents neural tube closure.....80
Figure 31: Injection of Qtracker QD´s at mid gastrula enables visualization of the mesodermal mantle with single cell resolution. FRNK expressing cells fail to migrate directionally.....81
Figure 32: Different variants of FAK injected to embryos and these gastrulated normally but blastopore closure was delayed……..…...85
Figure 33: Dose response of Y397FFAK injected embryos……86
Figure 34: Y397FFAK phenotype can be rescued with wild type FAK……..87
Figure 35: Phosphorylation status of the embryos after the overexpression of the mutants…….88
Figure 36: Y397FFAK can inhibit mesodermal cell spreading……...93
Figure 37: Rescue of spreading using 100pg HA FAK……...94
Figure 38: *Whole mount in situ hybridization* in controls and Y397FFAK injected embryos……95
Figure 39: Xbra expression indicates that mesoderm specification in not affected in Y397FFAK injected embryos……..96
Figure 40: Expression and phosphorylation of FAK on tyrosine residues.....101

Figure 41: Phosphorylation status of the autophosphorylation site Tyrosine 397 of FAK……102
Figure 42: Phosphorylation status of the residure Tyrosine 576 in the activation loop of the kinase domain of FAK.....103
Figure 43: Phosphorylation status of the residue Tyrosine 861 of FAK……....104
Figure 44: Phosphorylation status of the residue Tyrosine 925 of FAK……....105
Figure 45: Phosphorylation of Paxillin on residue Tyrosine 31……109
Figure 46: Phosphorylation of Akt at the residue Ser473……..110
Figure 47: FAK expression in morphant embryos. Slight delay of the blastopore closure during gastrulation……..112
Figure 48: FAK morphant embryos does not effectively block FAK function *in vivo* during early development.....113
Figure 49: Exogenous FRNK localization and activated FAK. FRNK is not a dominant negative in *Xenopus laevis* embryos……..116
Figure 50: FAK becomes activated in *Xenopus laevis* independently of integrin-based complexes……...119
Figure 51: Constructs that generated……..121
Figure 52: Initial characterization of the constructs.....122
Figure 53: Localization of the mutants at AP of the embryo……124
Figure 54: Localization of the mutants at the DMZ of the embryo…….....125
Figure 55: Localization of the mutants in the apical surface of the cells of the animal cap cells in the embryo and localization of non-activated and activated endogenous FAK……126
Figure 56: Mutants of FAK and GFPFAK localization at Animal pole cells……....127
Figure 57: The FAT domain is partially responsible for the plasma membrane localization of FAK……130
Figure 58: The FERM can autonomously localize on the plasma membrane……134
Figure 59: The FERM domain of FAK is localized on the plasma membrane through a membrane-based mechanism……135
Figure 60: The FERM domain is necessary for localization of FAK to the membrane…….....137
Figure 61: FERM overexpression leads to activation of endogenous FAK……...140
Figure 62: FERM overexpression activated endogenous FAK in a Src-dependent manner……143

Figure 63: The FERMY397F construct fails to activate endogenous FAK and downstream signaling molecule paxillin……144
Figure 64: The FERM/FRNK construct competes with FAK for the membrane localization…….149
Figure 65: FERM/FRNK phenotype can be rescued when injected with wild type FAK……150
Figure 66: FERM/FRNK and FERMY397F/FRNK phenotypes during *Xenopus* development.....151
Figure 67: Overexpression of the HA FERM/FRNK construct leads to the formation of anaphase bridges in dividing cells *in vivo* and *in vitro* and to the mislocalization of P-Ser732…….152
Figure 68: HA FERM/FRNK blocks convergent extension by regulating the levels of C-cadherin……..155
Figure 69: Model for integrin-independent activation of FAK caused by the FERM domain……171

II. LIST OF MOVIES (CD)

1. Time-lapse movie of an embryo injected with NIR QD's at the DMZ at the 32 cell stage. Frames are 2D maximum intensity projections of deconlvolved z-stacks. Individual cells are clearly visible as they migrate towards the top of the BCR.

2. Close up of movie 1

3. Time-lapse movie of an embryo injected into one out of two dorsal blastomeres at the marginal zone at the four-cell stage with GFP-FRNK followed by QD injections of two blastomeres (one on the left and one at the right hemisphere) with NIR QD's at the 32 cell stage. Cells from the GFP negative side of the embryo are seen migrating directionally on the BCR while the majority of the cells from the GFP positive site fail to do so and move randomly.

1. INTRODUCTION

1.1 *Xenopus laevis* as an experimental model

Amphibians are a convenient system for studying vertebrate development for several reasons: Not only are they vertebrates, but amphibians are tetropods, so they have all of the fundamental features of land-dwelling vertebrates. They undergo external development, so they can be observed and relatively easily manipulated. In the present thesis *Xenopus laevis*, the African clawed frog has been used as an experimental model for studying early development (Figure 1). *Xenopus laevis* can easily lay eggs repeatedly with a simple hormone injection (details in section: materials and methods) (Sive, H. L., Grainger, R. M. et al. 2000). The eggs can be fertilized *in vitro* in a dish by adding sperm in a simple media. The embryos are large, they are approximately 1 to 1.4 mm in diameter, which is an order of magnitude larger than a mouse oocyte (10 folds larger). The large size allows the developmental biologist for micromanipulation, microinjections and microdissections.

The mature *Xenopus* egg has a dark, pigmented animal region and a pale, yolky, and heavier vegetal region. Before fertilization the egg is enclosed in a protective vitelline membrane and a gelatinous coat. Also the vegetal pole of the eggs contains a high percentage of yolk which enables the embryo to survive and develop in very simple buffer in the lab environment. Egg activation begins with a cortical reaction and a transient calcium wave that passed across the egg. Their development is relatively rapid; they go from fertilization through neurulation in approximately 18 hours at 22^{o}C (Gilbert, S. 2006).

Figure 1. ***Xenopus laevis***

The development of the embryos begins with the first cleavage that occurs along animal-vegetal axis within 90 minutes of fertilization, and this divides the embryo into equal halves. Further cleavages follow rapidly at intervals of about 20 minutes. The cells derived from cleavage divisions are called blastomeres (Figure 2). Cells at the vegetal pole are larger than those at the animal pole. A fluid–filled cavity, the blastocoel, develops in the animal region of the embryo, and when this occurs the embryos is then referred to as a blastula. At mid-blastula stage, there is the mid-blastula transition (MBT), which is the beginning of the zygotic genome transcription (Gilbert, S. 2006; Winklbauer, R. 2009).

At the blastula stage, the mesodermal and endodermal germ layers are located in the equatorial and vegetal regions, while the ectoderm is still confined to the animal region. The belt of tissue that plays a critical role in future development is known as the marginal zone. The blastula is in the form of a hollow sphere with radial symmetry. The cell movements of gastrulation convert this into a three layered structure with clearly recognizable anterior-posterior and dorsal/ventral axes and bilateral symmetry. Gastrulation involves extensive cell movements and rearrangement of the tissues of the blastula so that cells become localized to their proper positions in relation to the overall body plan of the animal.

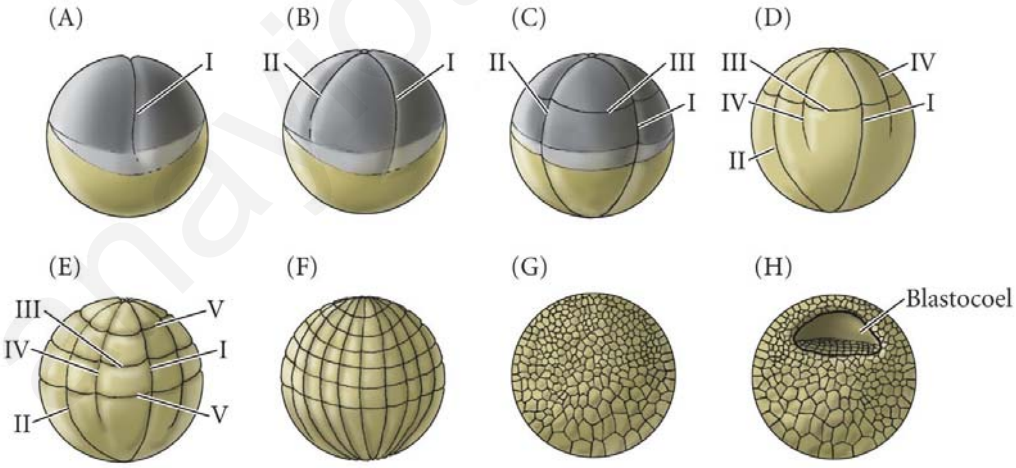

Figure 2. Cleavage of a frog egg. (A, B) Because the vegetal pole has yolk, the second division begins in the animal region of the egg before the first division has divided the vegetal cytoplasm. (C) The third division is displaced toward the animal pole. (D-H) the vegetal hemisphere contains larger and fewer blastomeres than the animal half. (H) Represents a cross section though a mid-gastrula stage embryo. Adopted from (Gilbert, S. 2006).

Gastrulation is completed by neurulation. Neurulation creates neural tube, neural crest and the bona fide epidermis, which covers the neural tube when it is created. While the notochord and somites are developing, the neural plate ectoderm above begins to develop into neural tube and the embryo is then called a neurula. Neurulation is completed by organogenesis. The embryo begins to look like a tadpole and we can recognize the main vertebrate features. At the anterior end the brain is already divided up into a number of regions and the eye and ear have begun to develop and posterior tail is formed last. After organogenesis is completed, the mature tadpole hatches out of its jelly covering and begins to swim and feed (Figure 3). Later, the tadpole larva will undergo metamorphosis to give rise to the adult frog (Gilbert, S. 2006).

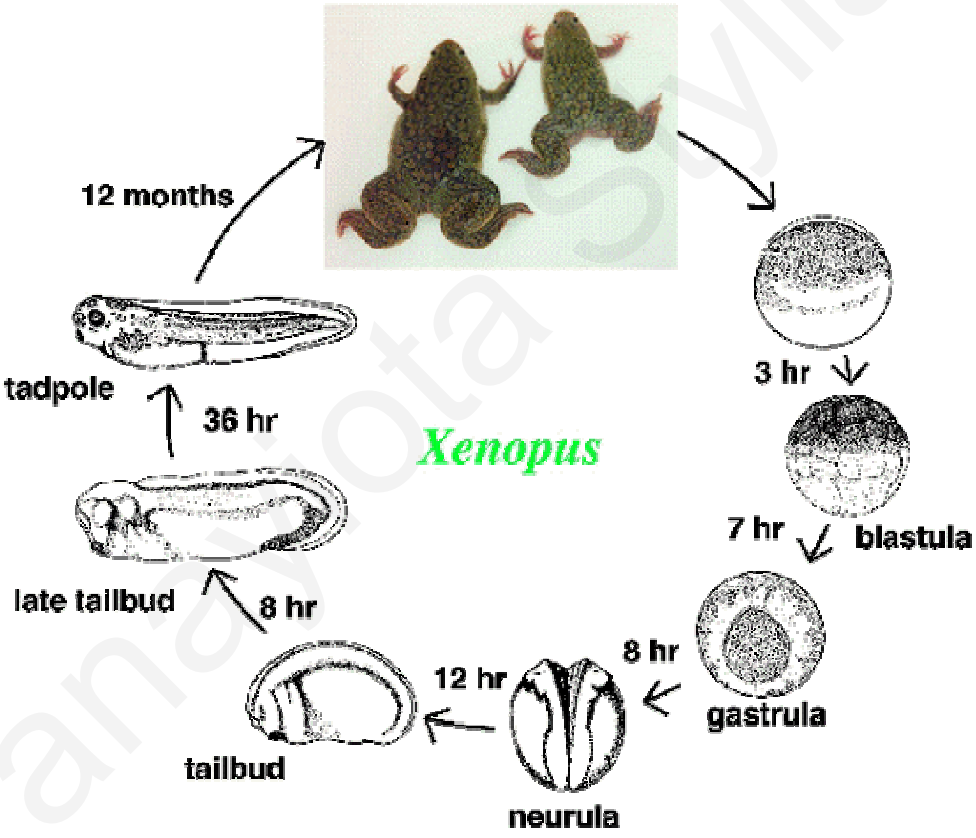

Figure 3. ***Xenopus laevis*** **life cycle**. Adopted from Xenbase: *Xenopus* web source.

1.2 Gastrulation in *Xenopus laevis*

The process of gastrulation involves highly integrated and regulated cell movements which result in the correct placement of tissues and the formation of the basic body plan of the embryo, including the physical construction of the rudimentary primary body axes. *Lewis Wolpert* (1986): *"It is not birth, marriage, or death, but gastrulation, which is truly the most important time in your life."* In vertebrates the first movements of embryogenesis (morphogenetic movements) occur at the onset of gastrulation. As a result of the movements of gastrulation, cells are brought into new positions, allowing them to interact with cells that are initially not near them. This paves the way for inductive interactions, which are the hallmark of neurulation and organogenesis. During gastrulation the three primary germ layers are established. The primary germ layers (endoderm, mesoderm, and ectoderm) are formed and organized in their proper locations. Endoderm, the most internal germ layer, forms the lining of the gut and other internal organs. Ectoderm, the most exterior germ layer, forms skin, brain, the nervous system, and other external tissues. Mesoderm, the middle germ layer, forms muscle, the skeletal system, and the circulatory system (Gilbert, S. 2006).

1.2.1 Morphogenetic movements

Morphogenetic movements in *Xenopus laevis* have been studied extensively at the cellular level but more recently a lot of molecular information has begun to be uncovered (Figure 4). The first morphogenetic movement, is a process called epiboly in which the cells of the prospective ectoderm located on top of the spherical embryo move downward toward the equator (Keller, R. E. 1980). Epiboly is mediated at the cellular level by radial intercalation of the deep layers of the animal cap cells. The animal cap which is made of three cell layer during gastrulation becomes a two layered structure as the cells of the lower layer intercalate radially. This creates a larger surface area which pushes the cells to move down toward the equatorial region. While fibronectin has been suggested to be required for this process nothing is known about the molecular mechanism underlying this active intercalation behaviour (Marsden, M. and DeSimone, D. W. 2001; Longo, D., Peirce, S. M. et al. 2004).

The second movement, convergent extension, is a movement whereby the cells located in the dorsal region of the equatorial region converge and extend toward the dorsal midline (Keller, R. E., Danilchik, M. et al. 1985). Convergent extension is mediated at the cellular

level by active movement of dorsal equatorial cells providing convergence and also mediolateral intercalation which ultimately gives rise to the extension of the anterior-posterior axis (Keller, R. E., Danilchik, M. et al. 1985). The cells adapt a clear polarity in their morphology during these movements. At the molecular level experiments performed in *Xenopus* and *Zebrafish* have demonstrated that the Wnt pathway, mediated by Disheveled plays a crucial role in the establishment of cell polarity (Smith, J. C., Conlon, F. L. et al. 2000; Tada, M. and Smith, J. C. 2000; Wallingford, J. B., Rowning, B. A. et al. 2000).

The third movement is involution, a process during which cells become internalized by invaginating and rolling over the blastopore lip. The first site of involution is right below the dorsal marginal zone (DMZ) and an epithelial sheet rolls inward to form an underlying layer. The first pioneering cells which become internalized will form the prechordal plate (head mesoderm) and they are immediately followed by the cells of the axial mesoderm, contributing to the notochord. Involution then expands mediolaterally and finally ventrally until the invaginating cells form a full circle called the blastopore. Involution is preceded by the formation of bottle cells, which demarcate the site of invagination initially in the dorsal side (Keller, R. E. 1981). The activin/nodal pathway as well as the activation of the Wnt pathway have been shown to induce the formation of ectopic bottle cells, but no additional molecular information is available about involution (Hardin, J. and Keller, R. 1988; Kurth, T. and Hausen, P. 2000).

In the fourth morphogenetic movement, vegetal rotation, the cells of the endoderm located at the lower part of the embryo (vegetal pole), undergo upwelling movements. These endodermal cell movements are assumed to occur in order to push and maintain the mesodermal precursors juxtaposed to the ectoderm. Nothing is known about the molecular aspect of endodermal movements (Winklbauer, R. and Schürfeld, M. 1999).

1.2.2 Mesoderm migration

Mesodem migration is a well studied morphogenetic movement that takes place during the *Xenopus* gastrulation and we deal with it in the present thesis. Once invaginated inside the embryo they become apposed to the animal cap, the cells of the prechordal plate and notochord adhere to the extracellular matrix (ECM) and start moving toward the top of the BCR by crawling on the blastocoel roof (Figure 4) (Nakatsuji, N. and Johnson, K. E. 1983b; Nakatsuji, N. 1986; Winklbauer, R. 1990). Once involuted, mesodermal cells adhere to the fibronectin of the ECM of the blastocoel roof, they become flat and create a shingled arrangement and extend numerous filopodia and lamellipodia. Integrins mediate cell-ECM interactions and are essential for morphogenesis. Integrin dependent adhesive activity is regulated both in space and time during gastrulation and cell adhesion to the Arg-Gly-Asp (RGD, a sequence present in fibronectin's type III repeats and is responsible for cell adhesion onto FN) containing central cell-binding domain of fibronectin has been shown to be necessary for gastrulation in *Xenopus* (Alfandari, D., Ramos, J. et al. 1996). The assays used to address the role of mesoderm migration, relied on blocking adhesion of mesodermal cells extracellularly using antibodies against fibronectin or peptides containing the RGD sequence, which were injected in the blastocoel cavity (Ramos, J. W. and DeSimone, D. W. 1996; Winklbauer, R. and Keller, R. 1996). The aim of these experiments was to block the FN-Integrin interactions, and, as a result, block mesoderm migration. A comparison of the phenotypes resulting from experiments where researchers are interfering with the FN-Integrin interactions leads to the conclusion that morphogenesis is disrupted in many ways (Ramos, J. W. and DeSimone, D. W. 1996; Winklbauer, R. and Keller, R. 1996; Marsden, M. and DeSimone, D. W. 2001).

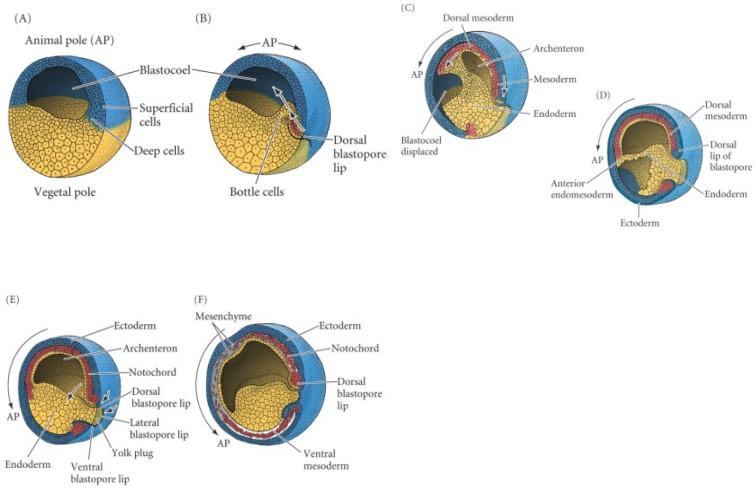

Figure 4. Cell movements during *Xenopus* gastrulation. (A, B) Early gastrulation. The bottle cells of the margin move inward to form the dorsal lip of the blastopore, and the mesodermal precursors involutes under the roof of the blastocoels. AP marks the position of the animal pole, which will change as gastrulation continues. (C, D) Mid-gastulation. The archenteron forms and displaces the blastocoel and the cells migrate down toward the vegetal region. (E, F) Toward the end of gastrulation, the embryo becomes surrounded by ectoderm, the endoderm has been internalized and the mesodermal cells have been positioned between the ectoderm and the endoderm. Adopted from (Gilbert, S. 2006).

The complexity of these movements together with our inability to image them *in vivo* forced researchers to study each movement isolated from the others. The movements themselves are studied by breaking them down into their component events, which is a useful first step. Yet if we are to truly comprehend the way morphogenetic movements give rise to form, we need to begin integrating what we know back to the embryo and view gastrulation as a unified process rather than individual components. In order to achieve this we need to have the ability to image movements *in vivo* with high resolution so that questions regarding involvement of specific proteins and pathways can be addressed in the embryo. Although imaging technologies like Optical Coherence Microscopy, MRI, Ultrasound Biomicroscopy and Optical Coherence Tomography are capable of deep tissue imaging they do so at low resolution creating the need for better methodology (Boppart, S. A., Tearney, G. J. et al. 1997; Needles, A., Yang, V. X. D. et al. 2003; Haskell, R. C., Williams, M. E. et al. 2004; Papan, C., Boulat, B. et al. 2007).

1.3 Quantum Dots (QD's)

1.3.1 Synthesis and optical properties of QD's

The optical properties of Quantum Dots are a result from their chemical synthesis and their physical characteristics. Quantum Dots are nanometer-scale semiconductor crystallites (known as nanocrystals or quantum dots) which have the potential to revolutionize biological imaging. They have dimensions in the range of 2-10nm and they constituted from 200-1000 atoms. The nanocrystals are often composed of atoms from groups II-VI (eg. CdSe, CdTe, CdS and ZnSe) or III-V (e.g InP and InAs) elements in the periodic table and are defined as particles with physical dimensions smaller than the exciton Bohr radius (Chan, W. C., Maxwell, D. J. et al. 2002; Michalet, X., Pinaud, F. F. et al. 2005).

All semiconductors and the Quantum Dots have three basic energy bands: the conduction band, the valence band and in between them the band gap (energy gap) (Chan, W. C., Maxwell, D. J. et al. 2002) that depending on from each other distances determines the properties and characteristics of semiconductors. The electrons that occupy levels of energy under the band gap are found in the valence band while electron that occupies levels above the energy gap are found in the conduction band.

As mentioned before, QD's are single crystals of few nanometers size and shape and this feature can be controlled by the duration and temperature used during synthesis and by the ligand molecules which are used for their synthesis. This leads QD's to have composition and size dependent absorption and emission (Figure 5A). The range of emission wavelength is 400 to 1350 nm and it depends on the size which varies from 2 to 9.5 nm (Michalet, X., Pinaud, F. F. et al. 2005). QD's absorb photons when the excitation energy exceeds the band gap resulting in the creation of an electron hole pair (exciton). During this process, electrons are promoted from the valence band to the conduction band. Measurements of UV to visible spectra reveal a large number of energy states in QD's. This leads to a broadband absorption spectrum in marked contrast to standard fluorophores. The lowest excited energy state is shown by the first observable peak, known as the confinement peak. Excitation at shorter wavelengths is possible because multiple electronic states are present at higher energy levels. In Quantum Dots this energy (from the energy gap) is expressed as fluorescence. The molar extinction coefficient gradually increases towards shorter wavelengths. This is an important feature for biological applications because it allows simultaneous excitation of multicolor QD's with a single light source. Also if the energy is smaller than Bohr exciton radius, the energy level is

quantized and the value is directly related with the quantum dot size (Smith, A. M., Duan, H. et al. 2008).

In summary, the smaller the size of the Quantum Dot, the larger the energy gap (band gap) between the two energy bands (conduction and valence) will be, therefore the energy that it emits increases and thus leads to a smaller wavelength of fluorescence (Figure 5B).

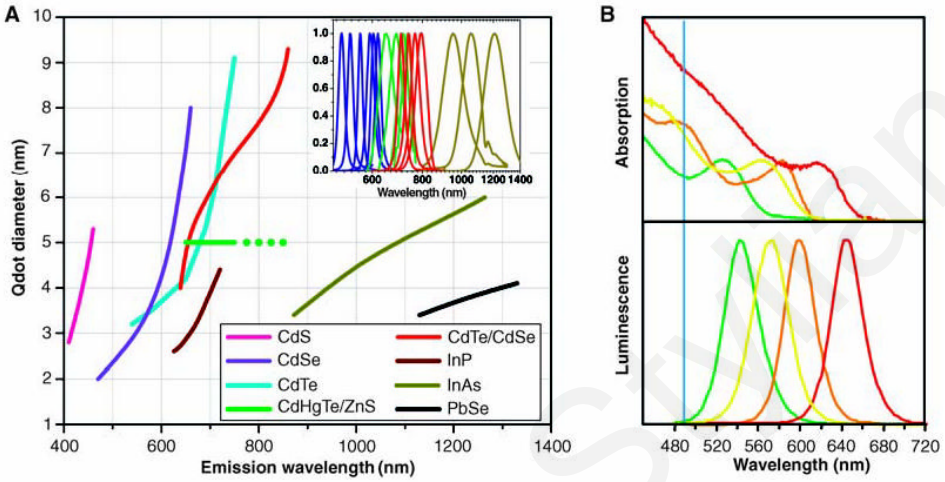

Figure 5. A. Emission and sizes of quantum dots of different composition. Quantum dots can be synthesized from various types of semiconductor materials (II-VI: CdS, CdSe, CdTe. III-V: InP, InAs and IV-VI: PbSe) characterized by different bulk band gap energies. The curves represent experimental data from the literature on the dependence of peak emission wavelength on qdot diameter. The range of emission wavelength is 400 to 1350 nm, with size from 2 to 9.5 nm. Inset: Representative emission spectra for some materials. **B. Absorption (upper curves) and emission (lower curves) spectra of four CdSe/ZnS qdot samples.** Adopted from (Michalet, X., Pinaud, F. F. et al. 2005).

1.3.2 Characteristics of Quantum Dots

Quantum Dots provide distinct advantages over traditional fluorescent markers and they are 10 to 100 times brighter (Kawasaki, E. S. and Player, A. 2005; Smith, A. M., Duan, H. et al. 2008). These colloidal particles act as robust, broadly tunable nanoemitters that can be excited by a single light source and provide distinct advantages over current *in vitro* and *in vivo* markers (e.g., organic dyes and fluorescent proteins). In addition to extremely high fluorescence intensity QD's offer a wide excitation spectrum, which makes the use of a single excitation filter possible. They have narrow and tunable emission spectra, which

reduce spectral overlap making the simultaneous use of more colors possible. Therefore it is possible to use all the excitation wavelengths without having problems of bleed-through between each other (Arya, H., Kaul, Z. et al. 2005; Michalet, X., Pinaud, F. F. et al. 2005). Also the large stokes shift increases the detection sensitivity, which provides large separation between the excitation and the emission is an important advantage. Sensitivity of QD's is higher than the conventional fluorescence dyes. The separation of the absorption and emission peaks increases the sensitivity by reducing the autofluorescene of the sample being examined.

One of the most important advantage of the QD's is the resistance to photobleaching (Medintz, I. L., Uyeda, H. T. et al. 2005; Michalet, X., Pinaud, F. F. et al. 2005). Phobleaching is a process in which the molecular structure of a dye is destroyed as a result of the excitation light and then it is non fluorescent anymore. In simple words this leads to photodegratation of the dye (Arya, H., Kaul, Z. et al. 2005). QD's are remarkably photostable, 100 to 1000 folds from the commercial fluorophores. This attribute is due to their transparent ZnS shells which enables their fluorescence to extinguish at a slow rate. The long fluorescence lifetime of QD's enables the use of time-gated detection and to separate their signal from that of shorter lived species (such as background autofluorescence which exists in the cells).

Summarizing, the characteristics of the Quantum Dots, mentioned above makes them good imaging-tool candidates in the world of bio-imaging and biological applications in basic and applied biology.

1.3.3 Biological applications

QD's have properties that provide advantages beneficial for a number of different science applications as compared to the standard fluorophores. The improved brightness and photostability exhibited by QD's are justification for their increased use in imaging and labeling experiments. The robustness of their signal strength also affords utility in targeting and detection applications. Over the years QD's have been tested in lots of applications including immunofluorescence assays, DNA and RNA targeting (fluorescence in situ hybridization in chromosomes) and *in vivo* targeting of cancer cells or bacteria. The most successful use of QD's have been the immunofluorescene assay labeling proteins, microtubules, actin, nuclear proteins of fixed cells and tissues (Michalet, X., Pinaud, F. F. et al. 2005; Xing, Y. and Rao, J. 2008; Walling, M. A., Novak, J. A. et al. 2009).

Successful experiments *in vitro* prompted investigators to use QD's for *in vivo* applications. Experiments showed that visible spectrum emitting QD´s can be used successfully to obtain single cell resolution (superficial tissues) of the events of early *Xenopus* development including gastrulation (Dubertret, B., Skourides, P. et al. 2002). They performed *in vivo* imaging by microinjecting QD's in early stage *Xenopus* embryo in a single blastomere. The fluorescence of the nanocrystals could be followed from the time of the injection to the tadpole stage thus showing that the QD's were stable *in vivo* (Figure 6).

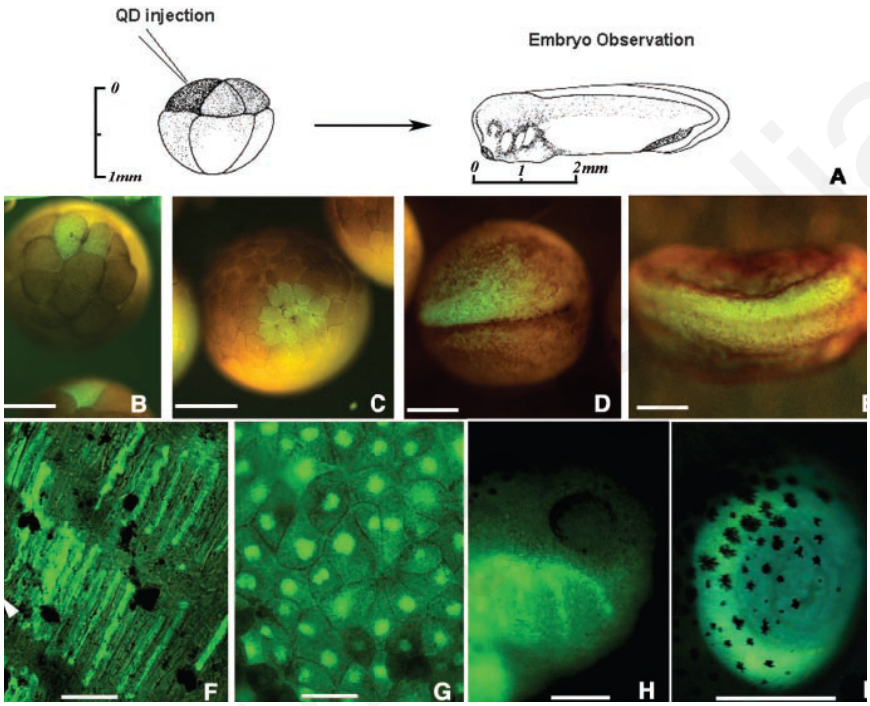

Figure 6. QD labeling of *Xenopus* embryos at different stages and specific QD intracellular localizations. (A) Schematic showing the experimental strategy. QD-micelles, were injected into an individual blastomere between 1.5 and 3 nl of QD's. (B) to (E), transmission and fluorescence images have been superposed. Injection of one cell out of an eight-cell-stage embryo resulted in labeling of individual blastomeres. (F) Intracellular labeling of an axon (arrow) and somites at tadpole stage 40. (G) QD's localized in the nucleus during mid-blastula stages. (H) Labeled neural crest cells migrating into the branchial arches. (I) QD's fluorescence observed in the gut of an injected embryo. Adopted from (Dubertret, B., Skourides, P. et al. 2002).

QD's, as mentioned, are much more resistance to photobleaching than other fluorophores as proven by *in vitro* experiments (Bruchez, M., Jr., Moronne, M. et al. 1998). This resistance also remains as shown by *in vivo* experiments. After 80 minutes of constant UV excitation (at 450nm) under the microscope the intensity of the Quantum Dot remained the same but the membrane GFP (injected to the embryos as QD's) had photobleached (Figure 7). This shows the great photostability of QDs during time in biological systems (Dubertret, B., Skourides, P. et al. 2002).

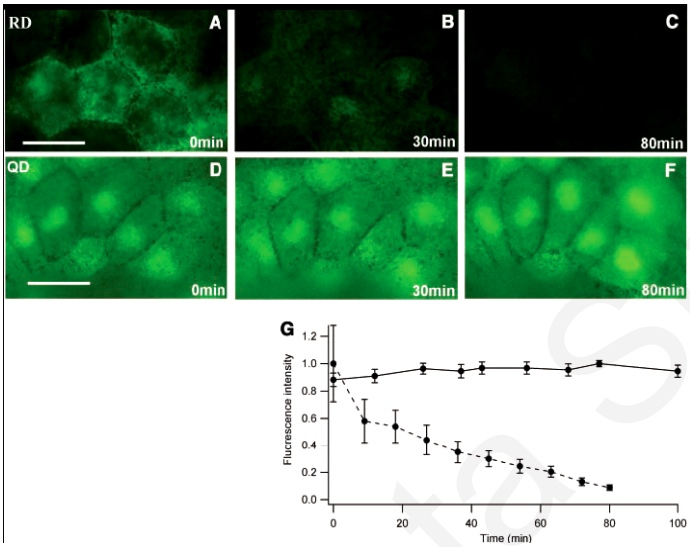

Figure 7. Comparison of QD's and RG-D (Rhodamine Green Dextran) for resistance to photobleaching. (A to C) Consecutive images of RG-D injected *Xenopus* animal pole blastomeres. (D to F) Consecutive images of QD's injected *Xenopus* animal pole blastomeres. During each experiment, the injected embryos were excited continuously at 450 nm. (G) Graph presenting the variation of fluorescence intensity of one cell of the RG-D–injected embryo (dotted line) and of one cell of the QD-injected embryo (solid line). Adopted from (Dubertret, B., Skourides, P. et al. 2002).

In addition, the Near Infra Red (NIR) region of the spectrum (700–950 nm) is ideal for imaging through tissues because light scattering diminishes with increasing wavelength, and hemoglobin electronic and water vibrational overtone absorptions approach their minimum over this spectral domain (Hawrysz, D. J. and Sevick-Muraca, E. M. 2000; Intes, X., Ripoll, J. et al. 2003; Kalchenko, V., Shivtiel, S. et al. 2006 ; Rao, J., Dragulescu-Andrasi, A. et al. 2007). NIR QD´s have been used for imaging of tumors and sentinel lymphnodes in mice and pigs respectively (Figure 8) (Kim, S., Lim, Y. T. et al. 2003; Stroh, M., Zimmer, J. P. et al. 2005).

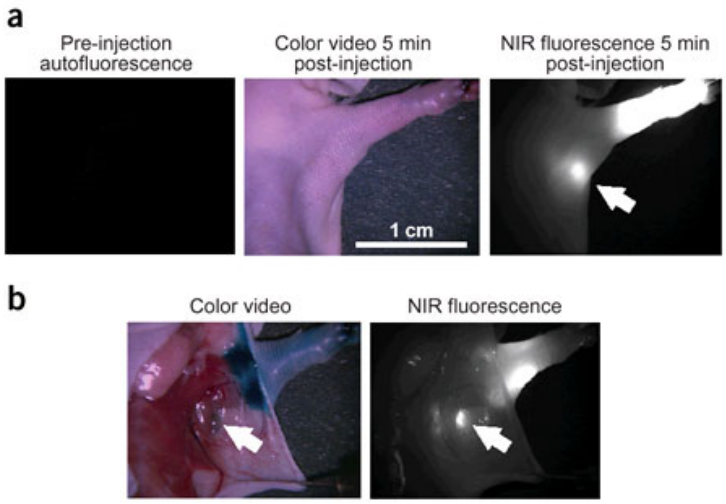

Figure 8. NIR QD sentinel lymph node mapping in the mouse. (a) Images of mouse injected intradermally with 10 pmol of NIR QD's in the left paw. Left, pre-injection NIR autofluorescence image; middle, 5 min post-injection white light color video image; right, 5 min post-injection NIR fluorescence image. Arrow indicates the putative axillary sentinel lymph node. (b) Images of the mouse shown in a 5 min after reinjection with 1% isosulfan blue and exposure of the actual sentinel lymph node. Isosulfan blue and NIR QD's were localized in the same lymph node (arrows). Adopted from (Kim, S., Lim, Y. T. et al. 2003).

Furthermore, living tissue auto fluorescence also reaches a minimum at this range and the fluorescent signal can, even in the case of organic fluorophores, be detected *in vivo* at subnanomolar quantities and at depths sufficient for experimental or clinical imaging (Weissleder, R., Tung, C. H. et al. 1999; Tung, C. H., Mahmood, U. et al. 2000).

This raised the possibility of using QD´s emitting in the NIR region for *in vivo* imaging of morphogenesis in *Xenopus laevis*. Specifically we aimed to visualize a process called mesoderm migration using NIR QD's nanocrystals.

1.4 Cell adhesion-Focal Adhesions

During embryonic development in which a multicellular organism forms proper regulation of cell adhesion takes place. Cell adhesion is very important because they take part to compose of a variety of differentiated cell types. Cells are stuck together by adhesion molecules, which are proteins carried on the cell surface that can bind to other molecules on cell surface or in the extracellular matrix. There are two different types of adhesion, the cadherin-based cell-cell adhesion (intercellular adhesion) the integrin-mediated cell substratum adhesion (ECM: extracellular matrix) (Yano, H., Mazaki, Y. et al. 2004).

The first type of adhesion, cell-cell adhesion, is necessary for many developmental processes like cell fate specification, gastrulation, moprhogenesis and organogenesis. Adherens junctions (AJs) consist of cadherin-catenin complexes which play an important role during the above processes. AJs are not only present in contacts at the cell-cell junctions but they involved in epithelial - mesenchymal and mesenchymal - epithelian transitions (Stepniak, E., Radice, G. L. et al. 2009) Cadherins are a large family of calcium dependent cell-cell adhesion proteins. During vertebrate morphogenesis different cadherins are expressed to different extents in different tissues. In *Xenopus laevis* cadherins (E, C and N, Type I cadherins) have a temporal and spatial expression pattern during development. C-cadherin is expressed throughout early development (major cadherin) and is required for cell adhesion in the blastula. E-cadherin expression begins at the onset of gastrulation from the animal cells of the blastula that gives rise to the ectoderm. N-cadherin expression starts at the end of gastrulation when the ectoderm becomes segregated into dorsal neural ectoderm. E-cadherin continues to be expressed as the ectoderm becomes the epidermis (Choi, Y. S., Sehgal, R. et al. 1990; Ginsberg, D., DeSimone, D. et al. 1991). It is very interesting that the expression of one type of cadherin is replaced by another cadherin (Figure 9). This leads to the conclusion that all of the cadherins are required for normal development during morphogenesis and they regulate different aspects of gastrulation and an important mechanism that leads to different types of tissues in the embryo (Nandadasa, S., Tao, Q. et al. 2009).

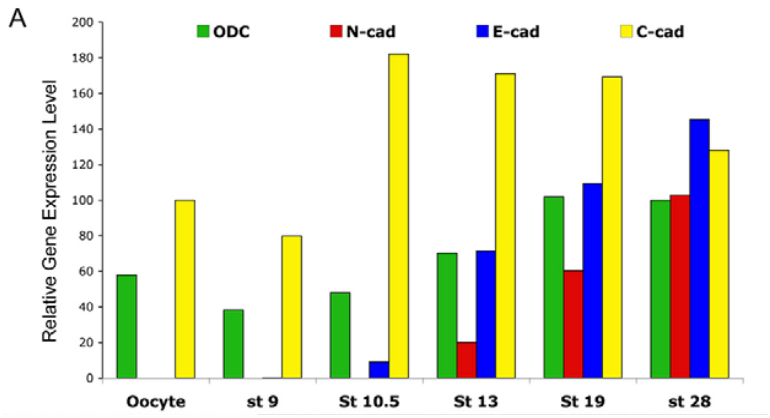

Figure 9. Temporal and spatial expression patterns of classical E-, C- and N-cadherins. (A) Real-time RT-PCR analysis of cDNA isolated from *Xenopus* embryos at different stages showing the temporal expression pattern of N- (red), E- (blue) and C- (yellow) cadherin. Green bars show levels of the loading control, ODC. Adopted from (Nandadasa, S., Tao, Q. et al. 2009).

The second type of adhesion, adhesion between cell and extracellular matrix is required for normal development. Attachment of cells to the extracellular matrix (ECM) is primarily mediated by the integrin family receptors. The extracellular domain of integrins interacts with the actin cytoskeleton. The intracellular domain of integrin mediated adhesions contains a large number of proteins, some of which directly mediate the mechanical linkage between ECM and the cytoskeleton, while others participate in adhesion mediated signaling (Hynes, R. O. 1992; Hynes, R. O., George, E. L. et al. 1992). Cell adhesion leads to the clustering of integrins and recruitment of numerous proteins to form multi-protein complexes on the cytoplasmic face of the plasma membrane termed focal adhesions (Burridge, K., Fath, K. et al. 1988). Focal adhesions serve to anchor the actin cytoskeleton to the plasma membrane and to provide linkage between the extracellular environment and the cytoplasm (Burridge, K. and Chrzanowska-Wodnicka, M. 1996). Focal adhesions are found both at the cell periphery and more centrally, associated with the ends of stress fibers in cells cultured on two dimensional rigid surfaces. Adherent mammalian cells have been known to attach to the extracellular matrix through these complexes and a large number of proteins like the Focal Adhesion Kinase (FAK) have been identified which are consistently localized at focal adhesions (vinculin, talin, tensin and paxillin). The cell is capable of continuously remodeling focal complexes to focal adhesions and vice versa, in order to migrate. Src and FAK are two of the major kinases found in focal adhesions and bind to different partners to regulate focal adhesion dynamics and cell behavior. Both proteins are important regulators of the focal adhesion turnover (Parsons, J. T. and Parsons, S. J. 1997).

FAK-/- fibroblasts have larger and more stable focal adhesions but they lose random migration, suggesting that FAK has a significant role in focal adhesion turnover (Ilic, D., Furuta, Y. et al. 1995).

Such complexes (focal adhesion complexes) have been recently visualized in dorsal mesodermal explants plated onto FN coated surfaces by immunofluorecence and by overexpression of a paxillin-GFP fusion protein (Iioka, H., Iemura, S. et al. 2007). In addition, disruption of focal adhesion complexes has been reported to inhibit convergent extension another well studied morphogenetic movement (Iioka, H., Iemura, S. et al. 2007). Finally, there are no known proteins that are selectively involved in this type of mesodermal cell behaviour and as a result there has been no way to specifically inhibit mesoderm migration without affecting other morphogenetic movements or cell fate to test its relevance. Xbra however has been suggested to function as a switch between convergent extension and mesoderm migration (Kwan, K. M. and Kirschner, M. W. 2003).

Both types of adhesion are essential during embryonic development. For example during gastrulation in *Xenopus* mesodermal migration is a collective migration so both cell adhesion interactions are needed (Winklbauer, 2009). Cell migration is a process that is based on cell and ECM interactions and has a fundamental role in early embryogenesis. During cell migration, the cells form cytoplasmic protrusions at their leading edges which extend and attach to the substratum and the cell body of the cells detaches and contracts at the trailing edge (Winklbauer, 2009). There are indications that integrin mediated cellular events can intercommunicate with cadherin based interactions. FAK and paxillin which are integrin based signaling molecules were proposed to participate in processes regulating N-cadherin on cell-cell adhesion (Yano, H., Mazaki, Y. et al. 2004).

1.5 Focal Adhesion Kinase (FAK)

1.5.1 Introduction

A specific cytoplasmic non-receptor tyrosine kinase: Focal Adhesion Kinase (FAK) is one of the proteins we propose to examine in regards to its involvement in *Xenopus* gastrulation in this proposal. FAK expressed in a variety of species including human, mice, chicken (Schaller, M. D., Borgman, C. A. et al. 1992) and *Xenopus* (Hens, M. D. and DeSimone, D. W. 1995; Zhang, X., Wright, C. V. et al. 1995). It is a highly conserved 125kDa protein that is recruited to focal adhesions following ECM interactions, leading to the activation of its kinase activity and in turn the continuous tyrosine phosphorylation of multiple signaling molecules and pathways (Schaller, M. D., Borgman, C. A. et al. 1993; Zachary, I. 1997). FAK is constituted from a central tyrosine kinase domain flanked by a large N- and C- terminal noncatalytic domains surrounding phosphorylation sites and Proline rich regions (Pro-1 to Pro-3) (Figure 10) which are binding sites for Src homology (SH3) domain containing proteins such as the adaptor protein p130Cas (Hayashi, I., Vuori, K. et al. 2002). FAK contains six major sites of tyrosine phosphorylation (Y397, Y407, Y576, Y577, Y861 and Y925) (Grigera, P. R., Jeffery, E. D. et al. 2005). A proline-rich region at amino acids 711-718 serves as the primary binding site of the SH3 domain of p130Cas and a second proline-rich region at amino acids 878-881 contributes to this interaction.

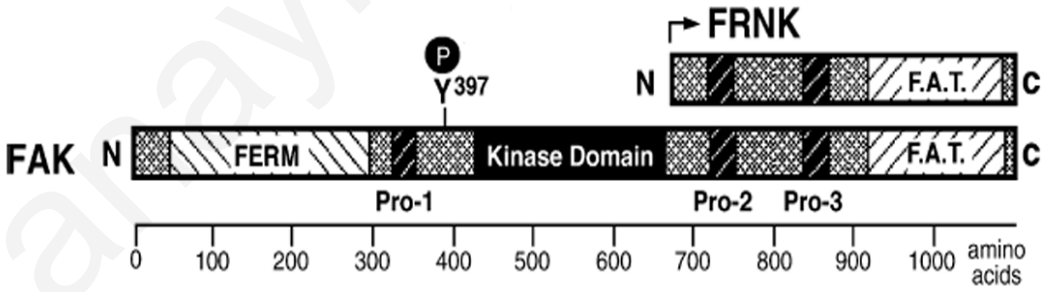

Figure 10. FAK structural features. FAK is composed of an N-terminal FERM homology domain, a central kinase domain, and a 150 amino acid FAT region within the C-terminal domain. FAK also contains three proline-rich (Pro-1 to Pro-3) regions that serve as Src-homology 3 (SH3) domain docking sites. The major FAK phosphorylation site is at Tyr-397. The FAK C-terminal domain termed FRNK is also expressed as a separate mRNA transcript and is identical to residues 668– 1052 of FAK. FRNK functions as a competitive inhibitor of FAK signaling. Adopted from (Schlaepfer, D. D., Mitra, S. K. et al. 2004).

FAK was first identified as a protein phosphorylated in response to Src transformation and shown to localize to focal contacts and adhesions as its names implies (Schaller, M. D., Borgman, C. A. et al. 1992). It is localizes to focal adhesions through its C-terminal domain (FAT domain, details below) which is crucial for its signaling function (Hildebrand, J. D., Schaller, M. D. et al. 1993). At focal adhesions it forms focal contacts with substances of the extracellular matrix, like fibronectin *in vitro*, through connection of integrins at the end of actin filaments and *in vivo* (Hanks, S. K., Calalb, M. B. et al. 1992; Furuta, Y., Ilic, D. et al. 1995). At these contacts FAK becomes activated via phosphorylation on tyrosine residues and acts like scaffold for the recruitment of other signaling proteins (Zachary, I. 1997). It has been shown that FAK localizes predominantly at the integrin rich focal adhesions, which suggested a role in controlling cell behavior resulting from interactions with the extracellular matrix (Hanks, S. K., Ryzhova, L. et al. 2003; Schlaepfer, D. D. and Mitra, S. K. 2004). FAK can phosphorylate other proteins involved in cell migration and spreading, like paxillin and tensin (Otey, C. A. 1996). Mutants of FAK that failed to localize to focal adhesions, exhibit impaired autophosphorylation and are unable to phosphorylate FAK substrates in response to focal adhesion (Shen, Y. and Schaller, M. D. 1999).

FAK is activated via autophosphorylation at tyrosine Tyr 397 which is initiated by integrin engagement with its ligand (Schaller, M. D., Hildebrand, J. D. et al. 1994; Eide, B. L., Turck, C. W. et al. 1995). Clustering of FAK into focal adhesions enhances this phosphorylation and this cluster becomes a binding site for tyrosine kinase Src (Src homology 2, SH2), which phosphorylates FAK at Tyr576 and Tyr577 to further activate FAK. Tyr 397 can also be phosphorylated by Src; hence it is not strictly an autophopshorylation site. Other adhesion regulated sites of FAK phosphorylation are 407, 861 and 925 (Calalb, M. B., Polte, T. R. et al. 1995). Src phosphorylates Tyr861 and Tyr925 creating docking sites for other SH2 domain bearing molecules such as Src kinase, PI3-kinase (PI3K), Grb2 adaptor protein and SOS complex (Lim, S. T., Mikolon, D. et al. 2008). Finally, data indicates that phosphorylation of Tyr861 might enhance the phosphorylation of Tyr397 (Leu, T. H. and Maa, M. C. 2002).

Autophopshorylation site (Tyr397) and activation loop phosphorylation sites (Tyr576/577) are required for maximal FAK catalytic activation. Mutants of both show a great reduction in the phosphotyrosine levels of the expressing FAK in $FAK^{-/-}$ cells (Owen, J. D., Ruest, P. J. et al. 1999). Constitutively activate FAK variants have been described. Super FAK (glutamine substitutions of two lysine residues 578 and 581 in the activation loop of FAK)

and FAK6.7 (two brain exons were engineered into avian FAK) when they expressed in chicken embryo cells exhibited increased catalytic activity *in vitro* compared with the wild type FAK. These mutants were regulated by adhesion complexes because both of them reduced catalytic activity from cells in suspension (Gabarra-Niecko, V., Keely, P. J. et al. 2002). Also exogenous expression of FRNK acts as a dominant negative mutant to inhibit FAK signaling (details in the section below). FRNK expression localizes to focal contacts and promotes FAK tyrosine dephosphorylation at the Tyr397/SH2 binding site. The expression of a leucine to serine mutation within FRNK (FRNK S1034) did not act as an inhibitor of FAK because it does not localized to focal contacts as strong as FRNK does. Therefore, its expression does not promote FAK dephopshorylation compared to FRNK expression in $FAK^{-/-}$ cells (Sieg, D. J., Hauck, C. R. et al. 1999). Deletions of the FAK N-terminal domain result in constructs possessing higher levels of FAK activity *in vivo* and *in vitro* (Cooper, L. A., Shen, T. L. et al. 2003).

1.5.2 Molecular structure and function of Focal Adhesion Kinase

- **FERM (band 4.1 and ezrin, radaxin, moesin proteins)**

FERM is the amino terminal domain of FAK which contains amino acids 36 to 362. It is involved in protein – protein interactions which link FAK to growth factor receptors at the plasma membrane, such as EGF, PDGF and HGFR and also interacts with the cytoplasmic tails of integrin β1 *in vitro* (Schaller, M. D., Otey, C. A. et al. 1995; Chen, T. H., Chan, P. C. et al. 2011). The FERM domain consists of a three lobed structure, F1 to F3 and it is arranged in a "clover leaf" shaped structure (Lim, S. T., Mikolon, D. et al. 2008). The F1 lobe has a ubiquitin-like fold, F2 lobe has a acyl-CoA binding protein (BP)-like subdomain and F3 lobe has a PH/PTB/EVH-like subdomain (exhibits plecktrin homology phosphotyrosine binding domain) (Figure 11) (Dunty, J. M., Gabarra-Niecko, V. et al. 2004). In addition, the F2 lobe contains the NLS signal (Nuclear localization signal) of FAK, whereas the F1 lobe has the first NES signal (Nuclear export signal) of FAK. The second NES is in the kinase-catalytic domain (Ossovskaya, V., Lim, S. T. et al. 2008).

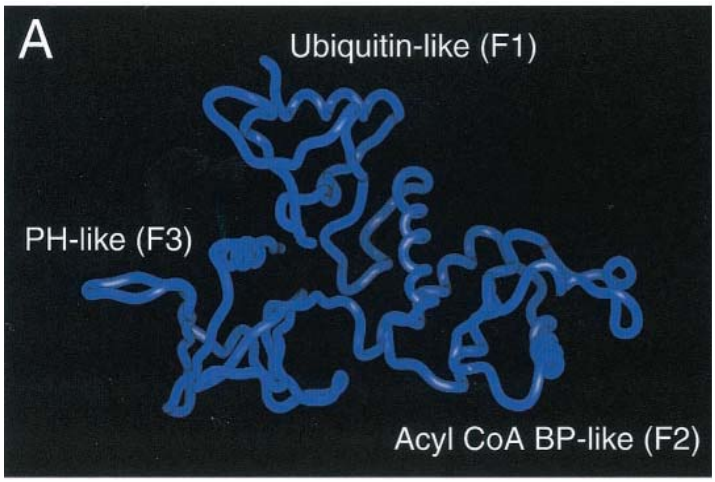

Figure 11. FERM "clover leaf" Structure. The backbone of the model of the FERM domain of FAK is shown. This model contains FAK residues 60 to 349. The ubiquitin-like subdomain (F1), acyl-CoA binding protein (BP)-like subdomain (F2) and PH/PTB/EVH-like subdomain (F3) are indicated. Adopted from (Dunty, J. M., Gabarra-Niecko, V. et al. 2004).

FERM can regulate the activation and the inhibition of FAK. The clover leaf structure binds directly to the kinase C-loop when FAK is autoinhibited impeding access to the active site and protecting the FAK activation A-loop from phosphorylation by Src. There are three major points of regulatory contact: binding of the F1 FERM lobe to a linker segment containing Y397, a hydrophobic pocket within the F2 FERM lobe binding to F596 residue within the kinase domain and the PxxP motif (residues Arg368 to Pro374) in the linker docking to the F3 lobe of FERM (Lim, S. T., Mikolon, D. et al. 2008). FERM interacts with FAK through F1 and FAK can be activated when it is released from the closed state by binding of a protein or lipid partner to its FERM domain. These partners bind FERM to F1 or F2 subdomains and open the protein permitting autophosphorylation of FAK on Tyr397 and Src binding through SH2 domain and through SH3 domain to PxxP. This leads to the phosphorylation of Tyr576 and Tyr577 residues in the activation A-loop by Src which fully activates FAK (Figure 12) (Lietha, D., Cai, X. et al. 2007).

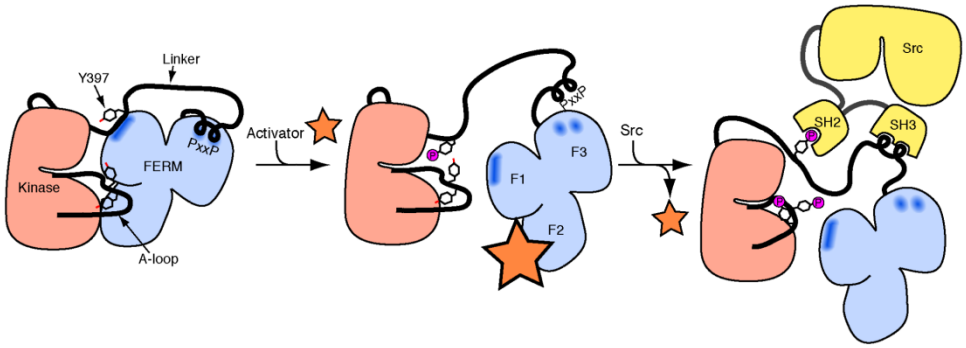

Figure 12. Autoinhibited FAK and Sequential Model of Activation. In the inactive state (left), the FERM domain blocks the kinase active site and sequesters the Tyr 397 and activation loop phosphorylation sites. FAK activation will be initiated by displacement of the FERM domain by competitive binding of an activating protein (orange star) to the FERM F2 surface. Disassembly of the autoinhibited conformation allows rapid autophosphorylation of the linker residue Tyr397 and exposes the Src docking sites in the linker (center panel). In a subsequent step, Src is recruited and activated via SH2 binding to pTyr397 and SH3 binding to the PxxP sequence in the linker region. Localized Src then phosphorylates the activation loop residues Tyr576 and Tyr577 of FAK (right panel). Phosphorylation of the activation loop yields full catalytic activity and, even in the event of activator dissociation, will not allow kinase inhibition by the FERM domain. Adopted from (Lietha, D., Cai, X. et al. 2007).

These findings where supported from *in vitro* assays. *In vitro* binding assays have shown that FERM domain binds directly with the catalytic-kinase domain of FAK *in trans* (intermolecular interactions) and inhibits the activation of the protein (Cooper, L. A., Shen, T. L. et al. 2003). Also substitution of the residue Lys 38 with Alanine (K38) has shown an up-regulation of FAK activity but a reduction of the interaction between FERM and the kinase domain. This residue is near the linker, suggesting the possibility to destabilize the linker-FERM interaction (Cohen, L. A. and Guan, J. L. 2005). A possible way which the FERM domain can stop its interaction with the kinase domain is through FERM and phosphatidylinositol-4,5-bisphosphate (PtdIns(4,5)P_2) interaction. *In vitro* studies with PtdIns(4,5)P_2 vesicles showed that these lipids are cabable of changing FAK structure. Modified levels of PtdIns(4,5)P_2 caused by the use of inositol polyphosphate 4-phosphatase, change FAK structure *in vivo* (Cai, X., Lietha, D. et al. 2008). Another possible way, is the interaction of FERM with other proteins and the recruitment of FAK at other protein complexes.

FERM can also activate FAK by an indirect way. This is through an intermolecular interaction between FERM and FAK *in vitro*. It is believed to take place through some basic amino acids on the surface of the F2 lobe, called "basic patch" (216-KAKTLR-221). This interaction is necessary for FAK activation and the recruitment of Src in order to cause the phosphorylation of tyrosine residues on FAK (Tyr576/577) and stimulate cell migration (Dunty, J. M., Gabarra-Niecko, V. et al. 2004). Additionally, as a result of the activation of FAK, another interaction of FAK through FERM is demonstrated which directly interacts with the HGF receptor (HGFR: hepatocyte growth factor receptor). The "Basic patch" (216-KAKTLR-221) in the FERM domain interacts with HGFR, phosphorylates the residue Y194 and this interacts with the basic residues. The intramolecular FERM-kinase interaction may be relieved and this allows the kinase to interact *in trans* with another FERM domain. Therefore, FAK autophosphorylates on Tyrosine397 recruits the binding of Src and finally full activation of FAK by phosphotylaton Tyr576/577 in the activation A-loop (Chen, T. H., Chan, P. C. et al. 2011).

- **Proline Rich Domain 1 and Linker Domain**

Proline Rich Domain 1 and Linker Domain contains the region from amino acids 362 to 428. Within the linker domain the major autophosphorylation site of FAK, residue Tyr397which is essential for the majority of FAK functions is found (Schaller, M. D., Hildebrand, J. D. et al. 1994; Eide, B. L., Turck, C. W. et al. 1995). Tyr397 autophopshorylation site and flanking in the linker from an antiparallel β strand interaction with the FERM F1 lobe. When residue Tyr397 becomes phosphorylated the activation loop is exposed for Src phosphorylation and disassembly the interactions among FERM, linker and kinase regions (Lietha, D., Cai, X. et al. 2007). The phosphorylated Tyr397 is the binding site for proteins with SH-2 domain (Src homology) such as: PI3 kinase, Phospholipase C-γ, Grb7 and Src family kinase (Michael D. Schaller, 1994). The binding of Src in this site is enhanced by the interaction of the SH-3 domain of Src with the first proline rich domain of FAK upstream the Tyr397 site (371-374 amino acids) (Thomas, J. W., Ellis, B. et al. 1998). Binding of Src causes more phosphorylation of FAK at other sites like Tyr575 and Tyr577 within the activation A loop in the catalytic domain. The phosphotylation of the above three residues increases FAK activity. Although the autophosphorylation of FAK can theoriticaly happen intermolecularly, it happens with an intramolecular reaction and is less sensitive to inhibition by N terminal domain. Moreover, *in vitro* dimerzation of FAK is cabable of causing phosphorylation on Tyr397 (Toutant, M., Costa, A. et al. 2002).

- **Kinase – Catalytic Domain**

The catalytic domain is between amino acids 428 to 697. The kinase domain contains a kinase C-loop and an activation A-loop (A loop: 576-600 animo acids). The F2 loop of FERM binds a site on the C loop of the kinase centered on Phe596 and causes the inhibition of FAK. The Kinase domain also contains two of the six major phosphorylation sites of FAK, the Tyr576 and Tyr577. These two are highly conserved residues and located at the activation loop of kinase domain (Calalb, M. B., Polte, T. R. et al. 1995). Phosphorylation of these residues is achieved by binding of Src to the phosphorylated Tyr397 and this leads to the maximal activation of FAK and downstream signaling pathways (Calalb, M. B., Polte, T. R. et al. 1995; Lietha, D., Cai, X. et al. 2007). Also phosphorylation of FAK on Tyr576 and Tyr577 by Src likewise acts to stabilize the catalytic loop in an active conformation which permits stable interaction with protein substrates. Mutation of these residues reduces the catalytic activity of FAK (Calalb, M. B., Polte, T. R. et al. 1995).

- **Proline Rich Domain 2, Linker, Proline Rich Domain 3**

This region is between amino acids 668 to 920 and contains two proline regions (Pro2 and Pro3), which have many proline residues throughout the sequence region and a linker domain between them (Schlaepfer, D. D., Hauck, C. R. et al. 1999).

Proline rich domain 2 (residues 711-718 amino acids, PxxP718: site I motif) is one of the two binding sites of p130Cas to FAK through an SH3 domain (Harte, M. T., Hildebrand, J. D. et al. 1996).

Proline rich-3 domain (residues 878-881 amino acids, PxxP881: site II motif) is the second binding site of p130Cas to FAK through an SH3 domain (Harte, M. T., Hildebrand, J. D. et al. 1996).

The Linker domain contains four sites of serine phosphorylation which were newly identified : Ser722, Ser843, Ser846 and Ser910 (Grigera, P. R., Jeffery, E. D. et al. 2005). Also phosphorylation of Ser732 is involved in the regulation of centrosomal functions in endothelial cells during mitosis (Park, A. Y., Shen, T. L. et al. 2009). Thr700 and Ser708 surround a potential site of caspase cleavage and they are just downstream of the acidic amino acid linker region that separates the kinase domain from the C-terminal domain. These sites are conserved in human, mouse and frog (Gervais, F. G., Thornberry, N. A. et al. 1998). In addition, Tyr861 which is a phosphorylation site of the linker domain (one of the six major sites of FAK phosphorylation), is phosphorylated by Src and enhances FAK

autophosphorylation at Tyr397 (Calalb, M. B., Zhang, X. et al. 1996; Leu, T. H. and Maa, M. C. 2002).

- **Focal Adhesion Targeting (FAT)**

The C-terminal region of FAK is called focal adhesion targeting (FAT) region and it is necessary and sufficient for the localization of FAK to newly formed and existing focal adhesions (Hildebrand, J. D., Schaller, M. D. et al. 1993). FAT domain appears to be conserved thought the species. The residues that constitute FAT are 921 to 1046. The crystal structure of FAT indicates that it forms four helix bundle which are straight, closely antiparallel and give rise to an symmetrical bundle (Hayashi, I., Vuori, K. et al. 2002).

FAT binds paxillin through two hydrophobic regions at the surface of FAT by two Luecine- rich ("LD") motifs within the N-terminal half of paxillin. Point mutations confirm the importance of the helical bundle for paxillin binding, because mutations in the hydrophobic core lead to the loss of the interaction (Hayashi, I., Vuori, K. et al. 2002). Paxillin binds to the cytoplasmic domains of integrin receptors and the focal adhesion protein vinculin, and it may act as a docking partner for FAK (Hildebrand, J. D., Schaller, M. D. et al. 1995). The FAT domain contains one of the major phosphorylation sites of FAK, the Tyr 925 which is phosphorylated by Src after its binding to FAK at Tyr397. Tyr 925 lies on the first turn following helix α1 so it is accessible for phopshorylation. The phosphorylation creates binding site for the SH2 domain of Grb2 (adaptor protein) and leads the formation of signaling complex that includes Ras (small GTP binding protein) and SOS (nucleotide exchange factor) (Schlaepfer, D. D. and Hunter, T. 1996). Phosphorylation of other residues of FAK increases the binding via integrins but phosphorylation of FAK at Tyr925 has been found to cause FAK loss from the focal adhesions. The tyrosine phosphorylation of the Tyr925 may be important for the regulation of FAK loacalization to focal adhesions (Katz, B. Z., Romer, L. et al. 2003; Deramaudt, T. B., Dujardin, D. et al. 2011).

- **FRNK**

FRNK (a splice variant form of FAK, called FRNK: Focal adhesion Related Non-Kinase) contains the C-terminus portion of FAK (668-1052 amino acids, 40kDa protein product, residues Met 668 to His 1052) but lacks the kinase domain while at the same time maintains the focal adhesion localization sequence (Schaller, M. D., Borgman, C. A. et al. 1993; Taylor, J. M., Mack, C. P. et al. 2001). It is expressed through an alternative intronic promoter between 3 'most exon of the catalytic domain (kinase domain) and the 5' most

exon of the C-terminal domain of FAK (Nolan, K., Lacoste, J. et al. 1999). FRNK mRNA is encoded by a novel exon that resides within an intron of the full length gene FAK. FRNK is expressed in variety embryonic tissues like the 18 day old chick embryo lung, intestine and muscle but low levels in other organs, including spleen, heart and brain. Data strongly shows the expression of FRNK is not limited to avian species but it presents in other species like rodents (highly expression in lungs, aorta but not on skeletal muscle) and cell lines like vascular smooth muscle cells (Nolan, K., Lacoste, J. et al. 1999; Taylor, J. M., Mack, C. P. et al. 2001).

The C-terminal region of FAK is rich in protein-protein interaction sites and contains a 100 residue sequence for focal adhesion targeting (FAT) which directs FRNK to adhesion complexes (Taylor, J. M., Mack, C. P. et al. 2001). The FAT domain is present in other adhesion proteins, including vinculin and it is the binding site for the focal adhesion protein paxilin (Parsons, 2003). By competing with FAK at the focal adhesions, it acts as a strong negative regulator of focal adhesion formation (Schaller, M. D., Borgman, C. A. et al. 1993; Gilmore, A. P. and Romer, L. H. 1996; Heidkamp, M. C., Bayer, A. L. et al. 2002). Overexpression of GFP-FRNK has displaced FAK from focal adhesions by competitive binding to paxillin via its identical FAT sequence. In the cells overexpressing GFP-FRNK, endogenous FAK appeared mainly perinuclear and paxillin distributed diffusely throughout the cell (Heidkamp, M. C., Bayer, A. L. et al. 2002). Because of the identical 360 amino acids of C-terminal of FAK (involved in binding p130Cas, Grb2, GRAF and paxillin) FRNK may also act as an alternative substrate of Src family proteins which bind and activate FAK, thus competing with FAK for specific binding partners in downstream signaling pathways (Heidkamp, M. C., Bayer, A. L. et al. 2002).

In most cells, FRNK overexpression inhibits cell spreading, cell migration and growth factor mediated signals to MAP kinase (Schaller, M. D., Borgman, C. A. et al. 1992; Taylor, J. M., Mack, C. P. et al. 2001). FRNK acts as a dominant negative form of FAK by blocking the formation of focal adhesions on fibronectin substrates and causing reduction of tyrosine phosphorylation of FAK. Localization of FRNK to focal adhesions caused by reduction autophopshorylation or transphopshorylation of FAK at tyrosine 397. The reduction of cell spreading correlates to some degree with the reduction of tyrosine phosphorylation of FAK and can be overcome by coexpression of wild type FAK (Richardson, A. and Parsons, T. 1996; Taylor, J. M., Mack, C. P. et al. 2001). Overexpression of FRNK can inhibit endothelial cell migration in cultured cell wound healing assays (Gilmore, A. P. and Romer, L. H. 1996). From the results it is believed that

FRNK acts as a competitive inhibitor of FAK and acts as an endogenous regulator of FAK activity.

1.5.3 The role of Focal Adhesion Kinase in cell adhesion and migration

Considering the knowledge about FAK and focal adhesions a great deal of evidence has implicated FAK in the regulation of cell migration. Numerous studies have shown that the promotion of cell migration is from integrin signaling through FAK and pointed to FAK as a positive regulator of cell spreading and migration.

FAK knockout studies showed an early embryonic lethal phenotype with extensive mesodermal deficiency while deficient FAK ($FAK^{-/-}$) embryonic fibroblast from these mice have defects in migration as a reduction of the rate of cell spreading providing more direct evidence for the role of FAK as a positive regulator of migration. In these fibroblasts there is an increase in the number and size of the peripherally localized adhesions. Cells cultured from these embryos display decreased motility *in vitro* (Ilic, D., Furuta, Y. et al. 1995; Corsi, J. M., Houbron, C. et al. 2009). Overexpression of FAK in various cells including $FAK^{-/-}$ mouse embryonic fibroblasts (MEFs) promotes migration of fibronectin substrate (Owen, J. D., Ruest, P. J. et al. 1999; Sieg, D. J., Hauck, C. R. et al. 1999). Also stable overexpression of FAK in CHO (Chinese hamster ovary) cells results in increased cell motility in fibronectin and it depends on both Y397 and the p130Cas proline rich binding sites. It is believed that FAK regulated CHO cells migration through two different pathways, one involving FAK/Src with p130Cas which binds FAK at Y397 and the other pathway initiated by PI 3-kinase binding to FAK Y397 (Reiske, H. R., Kao, S. C. et al. 1999).

FAK deficient cells ($FAK^{-/-}$) (FAK null mouse embryo cells) spread more slowly on extracellular matrix proteins (fibronectin substrate), exhibit an increased number of prominent focal adhesions and migrate poorly in response to chemotactic and haptotactic signals (Ilic, D., Furuta, Y. et al. 1995; Sieg, D. J., Hauck, C. R. et al. 1999). Overexpression of FAK deficient cells with wild type FAK restores cell migration and spreading when plated on fibronectin but expression of FAK mutants lacking kinase activity (K545RFAK mutant), or the ability to bind Scr family kinases (Y397FFAK mutant) fails to restore cell migration (Sieg, D. J., Hauck, C. R. et al. 1999). FAK autophosphorylation site (Y397) and activation loop phosphorylation sites (Y576/577) are critical for induced FAK activation and for enhanced cell spreading and migration

responses, while Y397FFAK (autophosphorylation defective variant) has a negative effect on cell migration of $FAK^{-/-}$ cells (Owen, J. D., Ruest, P. J. et al. 1999). These studies support the conclusion, made by using different experimental systems, of a positive role for FAK in cell spreading and migration.

FAK is the first example of a tyrosine kinase regulated by a domain under the control of an alternative intronic promoter and the first example of a focal adhesion protein regulated in this manner (Nolan, K., Lacoste, J. et al. 1999). This domain is an isoform of FAK that has been identified in a number of cell types and is well characterized. It is a non-catalytic isoform, called FAK related non-kinase (FRNK) (Richardson, A. and Parsons, T. 1996). FRNK is identical in sequence to the C-terminal domain of FAK at the nucleotide and amino acid level and a splice variant of FAK which inhibits cell spreading, cell migration and growth factor mediated signals to MAP kinase in most cells when overexpressed *in vitro* (Schaller, M. D., Borgman, C. A. et al. 1993; Sieg, D. J., Hauck, C. R. et al. 1999; Taylor, J. M., Mack, C. P. et al. 2001).

Overexpression of FRNK in cells can rescue the inhibition of cell spreading using full length FAK and FAK mutants. Specific K454RFAK (Kinase-dead, the catalytic residue is mutated) mutant could efficiently restore cell migration but Y397FFAK (autophosphorylation defective variant) was unable to restore the normal kinetics of cell spreading as in FAK deficient cells (Richardson, A. and Parsons, T. 1996; Sieg, D. J., Hauck, C. R. et al. 1999). From these results it is believed that FRNK acts as a competitive inhibitor of FAK. In addition, cell spreading in this system has been shown to correlate with paxillin and not tensin phopshorylation. This suggested that phosphorylation of paxillin by the FAK/Src complex regulates cell spreading (Richardson, A., Malik, R. K. et al. 1997).

1.5.4 The Focal Adhesion Kinase in early development

The signaling pathways that FAK is involved in are thought to be activated by cell-extracellular matrix interactions, because of the co-localization of FAK with integrins (Zachary, I. 1997). However, *in vivo,* it is possible that FAK is involved also in cell-cell interactions at the apicolateral membrane because of its expression on the apical surface of epithelial cells. This suggests that FAK may not only interact with integrins *in vivo* and it is possible that there are also other proteins and other kinds of interactions (Ridyard, M. S. and Sanders, E. J. 1999).

Numerous studies have established a number of roles for FAK including those of a positive regulator of cell motility, cell survival and growth regulation. FAK gene knockout in mouse causes early lethality with extensive cardiovascular defects. It has been reported that FAK-null ($FAK^{-/-}$) mice cannot survive beyond the embryonic day 8.5 (E8.5) (Ilic, D., Furuta, Y. et al. 1995). These mice can initiate gastrulation normally but in the late phase of gastrulation, there is mesodermal defect similar to that caused by fibronectin deficiency. This indicates that at least for these stages FAK is mediated only by fibronectin and integrin interactions (Furuta, Y., Ilic, D. et al. 1995). Endothelial cells from FAK null embryos cannot organize themselves into vascular networks and that is the reason why there are defects in the blood vessel morphogenesis during the embryonic development of $FAK^{-/-}$ mice (Ilic, D., Kovacic, B. et al. 2003). FAK mutant knockin mouse models were also generated by researchers to explore the role of FAK signaling pathways in development and function *in vivo*. Mutant FAK^{Δ} (deleted exon 15 which contains major phosphorylation site Y397) is expressed at normal levels and as an active kinase but embryos $FAK^{\Delta/\Delta}$ display various defects (hemmorahages, edema, multiple organ abnormalities) and overall developmental retardation at E13.5-14.5 and then died (Corsi, J. M., Houbron, C. et al. 2009). Mutant embryos $FAK^{K454R/K454R}$ (K454 mutated to R in the catalytic domain) also exhibited embryonic lethality (lethal at E9.5) and extensive defects in blood vessel formation and disorganized EC (endothelial cells) pattering in embryos (Lim, S. T., Chen, X. L. et al. 2010). These results suggested that FAK kinase activity (autophosphorylation at Y397) is necessary for normal development.

In *Xenopus*, *Drosophila* and the chick its expression suggests a role in gastrulation but there are no data to further support this (Hens, M. D. and DeSimone, D. W. 1995; Zhang, X., Wright, C. V. et al. 1995; Fox, G. L., Rebay, I. et al. 1999; Fujimoto, J., Sawamoto, K. et al. 1999).

Sequence of *Xenopus* FAK has 89-91% similarity to chicken, mouse and human FAK homologs (Figure 13). In the catalytic domain the amino-acids are identical up to 97%. With Northern blot analysis the mRNA level of FAK is present in eggs (maternal mRNA), decreases slightly from cleavage stages and blastula stages. At the onset of gastrulation the levels of mRNA slightly increase and then decrease by the late gastrula. At neurula stage the levels continue to drop and thena steady increase begins until tailbud and tadpole stages (Hens, M. D. and DeSimone, D. W. 1995; Zhang, X., Wright, C. V. et al. 1995). Certain residues that are important in FAK activation and function are conserved and they including Y403 (equivalent with Y397 in chicken) and K647 (equivalent with K454 in

chicken). Some regions of amino-acids are present in *Xenopus* only and not found in other species. Despite the fact that M705 (begging of the alternative gene product, FAK related nonkinase, FRNK) is present in *Xenopus* amino acids FRNK expression at the mRNA or protein level has not been detected in *Xenopus* embryos (Hens, M. D. and DeSimone, D. W. 1995). Also the three major domains are present in *Xenopus* FAK the FERM, catalytic - kinase and FAT domain.

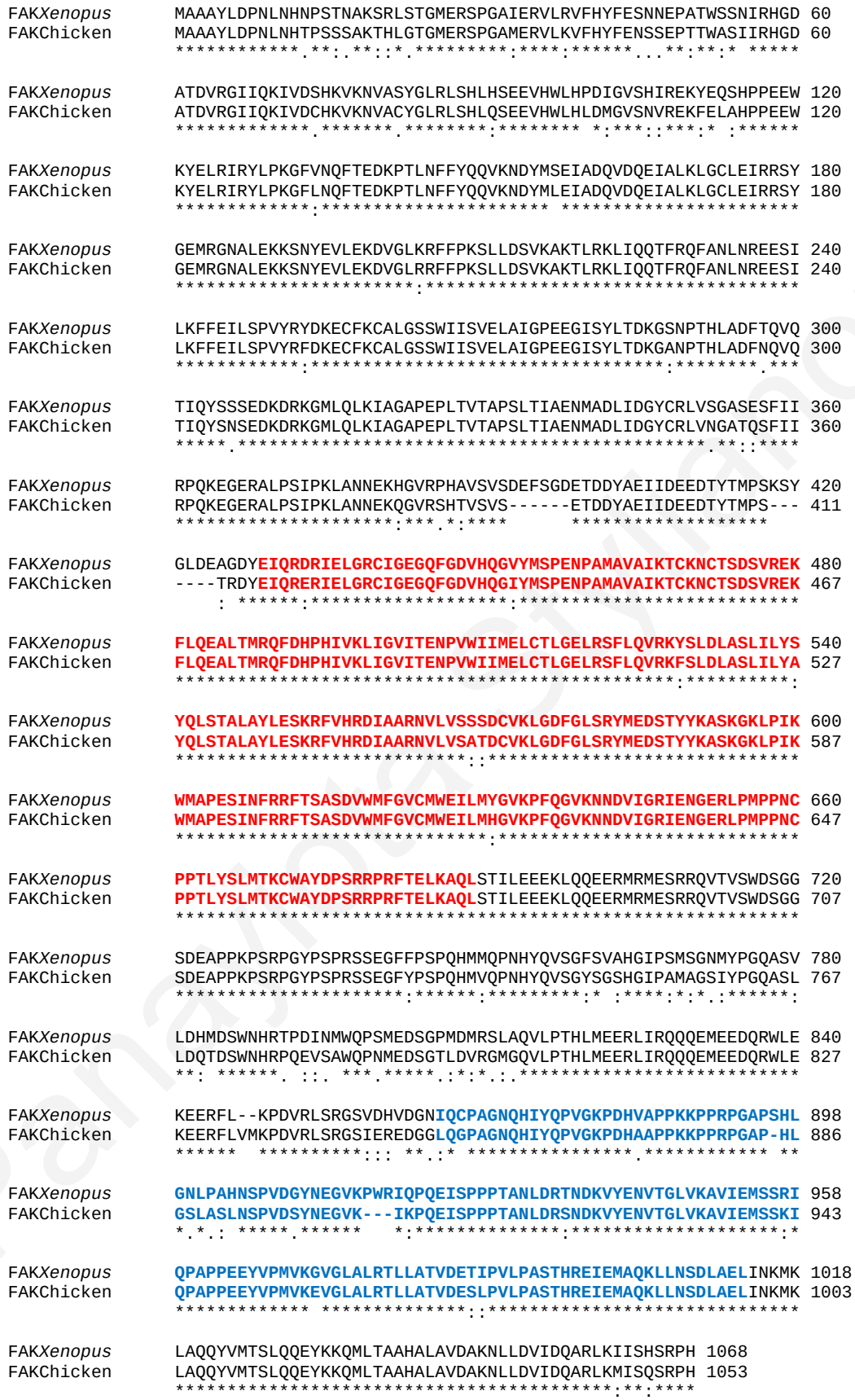

Figure 13. Comparison of *Xenopus* (XL_U11078) and chicken (NM_205435) FAK in amino acid level (ClustalW2) Kinase Donain in Red and FAT domain in blue.

In *Xenopus* FAK is required and a key component of the molecular machinery that drives somite formation. Injections of FRNK mRNA at four-cell stage into regions fated to be somites leads to defects in somite rotation, misoriented cells and disruption of intersomitic boundaries (Kragtorp, K. A. and Miller, J. R. 2006). Also it was shown that FRNK overexpression resulted in a significant decrease in autophosphorylation of FAK, indicating that FRNK is an effective inhibitor of FAK activity *in vivo*. Low levels of tyrosine-phosphorylated FAK first appear during gastrulation but levels increase through stage 17 and beyond (Hens, M. D. and DeSimone, D. W. 1995).

During gastrulation FAK expression increases significantly and is detected in mesoderm, marginal zone ectoderm and cells of the blastopore roof and during stages 21-22, it is at somites and remains there until stage 35. The highest levels of FAK expression were between somites. With the help of *whole mount in situ hybridization*, FAK expressed (embryo stage 35) in structures of the central nervous system and in the head and truck. Specifically FAK was expressed in the retina, lens, rhombomeres, forebrain, midbrain and hindbrain. The above expression patterns indicate that FAK functions through integrin-depended adhesion interactions (Hens, M. D. and DeSimone, D. W. 1995).

In summary, FAK is expressed from fertilization to tadpole stage and phosphorylation (phosphorylated on tyrosine residues) is temporally regulated (Hens, M. D. and DeSimone, D. W. 1995).

In *zebrafish* the expression and phosphorylation FAK changes dramatically after gastrulation. FAK is concentrated at the sides of cell-cell adhesion in the epithelial enveloping layer and may associate with actin cytoskeleton at epithelial junctions containing cadherins. FAK is phosporylated at these epithelial junctions on pY576, pY861, pY925 but not on pY397 during epiboly and gastrulation (Crawford, B. D., Henry, C. A. et al. 2003). Phosphorylation on pY397 is detectable by the begging of somitogenesis. All the residues of tyrosines are increased at that stage. No evidence has been reported about the differential phosphorylation of tyrosine residues in FAK in the context of possible interactions with focal adhesion proteins in *Xenopus*. Activation of FAK is present at the notochord periphery and is expected to have a potential role in the promotion of directional intercalation of notochord cells during notogenesis and maybe involved in somitogenesis. This is based on the fact that FAK and phosphorylated FAK become concentrated to the recently formed somite boundaries during somitogenesis and myotome develpoment (Henry, C. A., Crawford, B. D. et al. 2001).

In summary, activated FAK (Phosphorylated on Tyr397) in *zebrafish* is first seen at the end of gastrulation (Crawford, B. D., Henry, C. A. et al. 2003), whereas in *Xenopus* it is detectable from the onset of gastrulation (Hens, M. D. and DeSimone, D. W. 1995) and in mice, after the late mid-gestation stage (Jean-Marc Corsi, 2009).

2. ANALYSIS AND DESCRIPTION OF METHODOLOGY

2.1 Introduction

The large size (1mm) and the rapid developmental rate (within 2 days tadpoles are observed) of *Xenopus laevis* embryos make them ideal for the developmental biologist. The large size of *Xenopus laevis* embryos allows micromanipulation and microinjections and makes them a good animal model for examination of early vertebrate development. *Xenopus laevis* embryos can be obtained by inducing ovulation and fertilizing the eggs *in vitro* or by natural mating (Figure 14). A good female frog can lay hundreds of eggs in a single day. The actual number of eggs laid and the efficiency of fertilization are unpredictable so ovulation should be induced in more than one female every day of the experiments (3 or 4 females every time). Females can be induced to lay repeatedly for some years, but rest periods of four months are required between ovulations. The testes from one male contains sufficient sperm to fertilize several thousand eggs (can kept in 4^{o}C for few days in a certain media) (Sive, H. L., Grainger, R. M. et al. 2000).

Figure 14. *Xenopus laevis* natural mating

2.1.1 Obtaining, housing & feeding *Xenopus laevis*

We obtained our adult frogs from several international suppliers such as NASCO (United States) and *Xenopus* express (France/UK). Frogs were shipped in peat moss during the spring and autumn. Shipping during summer months was avoided due to the extreme heat, respectively female and male frogs were kept in separate tanks of the aquarium. New frogs were kept separately from the older ones and a resting period of two weeks was allowed after receiving each new shipment of frogs. This resting period was crucial and helped to increase the quality of oocytes.

Housing and feeding frogs was important and always a priority in our lab during the day. The frogs should be comfortable in the tanks. Four females or six males (males are much smaller than females) are comfortable in approximately 16 litres of fresh water (Sive, H. L., Grainger, R. M. et al. 2000). The animals were kept in the aquarium tanks of the system (12 tanks of 90L each, Figure 15). This particular setup was very effective due to the large number of frogs we were housing in our lab. The system has a holding capacity of approximately 300 frogs and contains about 1700 litres of water. The system drips fresh water in and out continuously and prevents accumulation of wastes. The toxic waste is kept low and solid waste is drained continuously.

The quality of the ingoing water was monitored to ensure it was optimal for the frogs. Several parameters were measured once a week such as: pH (6.5 to 7 is optimal for *Xenopus*), conductivity (hardness of the water), gH, kH, NO_3, NH_4, NO_2 and we monitored the system with the help of Aquacontroller (system observation online). In order to keep the conductivity stable at 1200μS a salt solution (NaCL and Ocean salt) was gradually dispensed (in a drip wise fashion) into the incoming water of our aquarium system (Godfrey, E. W. and Sanders, G. E. 2004). High concentration of calcium and high gH value results in higher survival rates and normal development of *Xenopus* embryos. The hardness of the water improves the firmness of the oocytes, early development of the embryos and their survival and normal development (Godfrey, E. W. and Sanders, G. E. 2004). Also the water was pumped through biological filter to remove ammonia, nitrites and finer particles and across four high capacity UV lights to kill bacteria and other pathogens, before being pumped back to the tanks. With this environment we were able to keep the frogs in excellent health. The frogs were kept on a regular light-dark cycle of 12 hours light and 12 hours dark (controlled system of light cycle in the animal lab) (Figure 15). Some investigators believe that egg quality improves when frogs are exposed to sunlight equivalent light levels (Hilken, G., Dimigen, J. et al. 1995). *Xenopus* enjoy light

but it is important to have dark areas, like opaque plastic pipes, so they can hide from the light if they want to. The temperature of the room and the water in the aquarium was kept at 18^{o}C which is optimal for the frogs and for all the stages of embryonic development (Sive, H. L., Grainger, R. M. et al. 2000).

The frogs were fed three times a week in the morning (Monday, Wednesday, Friday) with floating food and pellets (Hilken, G., Dimigen, J. et al. 1995).

Figure 15. *Xenopus laevis* Facility

2.2 General methods

2.2.1 Inducing ovulation

Ovulation was induced by administering an injection of human Chorionic Gonadotropin (hCG, Chorulon 1500 IU) into the dorsal lymph sac of the female frog. For the induction of full ovulation, 600-750 units of hCG (Intervet International B.V., Medivet Suppliers LTD, Chorulon 1500 IU), depending on frog size, was injected into the dorsal lymph sac. The injection was performed with a fine needle (26-30 gauge) attached to a 1ml syringe laterally toward the dorsal midline, across the lateral line "stitch" marks to the dorsal lymph sac (Figure 16). When the needle penetrated the sac we injected the liquid (approximately 600-750 units hCG in 1ml liquid). After the injection we waited few seconds and then slowly pulled out the needle. The frogs were kept at 16 °C and started laying eggs approximately 14 hours after injection (the hours for laying eggs depends from the temperature, (Sive, H. L., Grainger, R. M. et al. 2000).

Figure 16. Priming a female *Xenopus laevis*

2.2.2 Isolating the testes

One male frog was sacrificed every week. The male was euthanized by submersion into a 0.05% benzocaine solution for 30 minutes to 1 hour at room temperature. Using scissors and forceps the testes were removed from the body. The testes lie at the base of the fat bodies and were easily recognized. They are about 1cm long. The isolated testes were placed in a solution that contained 10% serum (newborn calf serum), 90% Leibovitz (L-15 Medium Leibovitz without L-glutamine from Sigma cat#L5520) with antibiotic (0.05

mg/ml gentamycin) and stored at 4ºC. Under these conditions, testes can be stored for at least 5 to 7 days, after which sperm viability drops.

2.2.3 Manual egg collection

After induction of ovulation, the cloaca becomes red and sensitive, so we avoid touching it when picking up the female frog. The eggs are collected in a sac near to cloaca and simultaneous lateral and vertical pressure is needed to expel them. In order to do so the frog is held with two hands and the belly is gently massaged with one thumb over a clean glass petri dish (90cm) containing 0.33X MMR (Marc's Modified Ringers solution) (Ubbels, G. A., Hara, K. et al. 1983). The frog should begin to lay eggs within less than a minute (Figure 17). Egg collection did not continue for more than 2-3 minutes total. Egg collection was carried out every hour for the first 2-3 hours of laying and then more often as the day progresses. Females usually laid eggs for about 8 hours. A maximum of 6-8 collections are expected from a frog in 1 day. Each batch of oocytes obtained from the female frog were kept in a separate glass petri dish. Fertilization was performed as soon as possible after laying. Primed females were kept separately from the aquarium so each one could be observed independently.

A frog can be induced to lay eggs repeatedly, but it must rest between ovulations as mentioned previously. Rest periods of four months appear to be optimal. So it was useful to keep accurate records and dates of ovulations (Sive, H. L., Grainger, R. M. et al. 2000).

Figure 17. Squeezing of female frogs and manual collection of eggs

2.2.4 *In vitro fertilization*

Before *in vitro fertilization* most of the 0.3xMMR buffer must be removed from the eggs in the petri dish using a plastic pipette. Forceps and scissors (cleaned with 70% ethanol before use) were used to macerate a piece of testis and mix to distribute the tissue over the eggs (Figure 18A). The eggs are tough at this point and will not break easily. The first sign of fertilization (within few minutes, approximately 20min) is a concentration of the pigmented animal hemisphere to less than one half of the egg. The eggs rotate within the vitelline membrane so that the animal hemisphere faces upward (Ubbels, G. A., Hara, K. et al. 1983) (Figure 18B). A fertilized egg is more elastic and resistant to deformation than an unfertilized egg. This is due to the thickening of the vitelline membrane after fertilization. To assess egg quality, test fertilization is performed every day on a few eggs of the first batch. If the fertilization efficiency was poor, we tested the eggs from a second batch because the egg quality can vary from one laying to the next. Also to verify that the testes were viable we crushed a little on a microscope slide, rinsed it with 0.3XMMR (MMR activates the sperm to begin swimming), covered with coveslip and viewed under the microscope. The sperm were easy to identify by their fine helical shape and the characteristic movement. Good quality eggs and sperm produced fertilization efficiencies of 80-100% (Sive, H. L., Grainger, R. M. et al. 2000). These batches of embryos were used in all the experimental procedures.

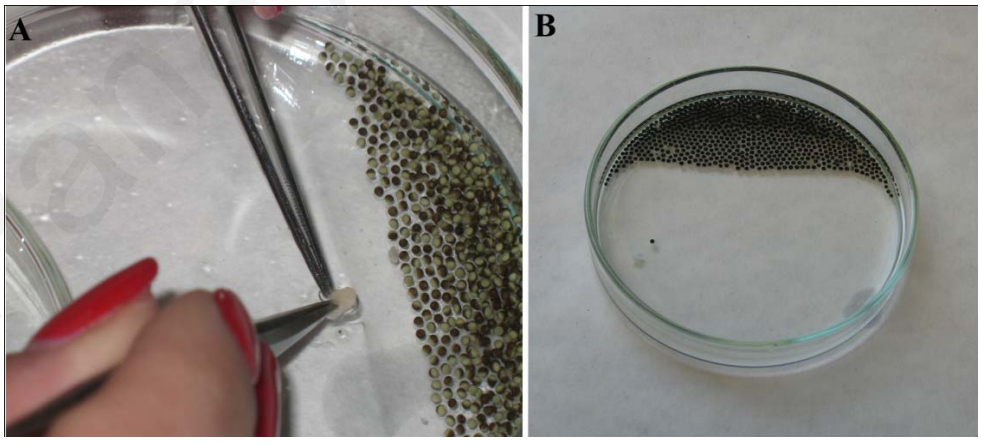

Figure 18. A. *In vitro fertilization* and B. 20 minitues after fertilization: 100% fertilization

2.2.5 Preparing embryos for manipulation

Embryos are surrounded by a series of thick, protective gelatinous membranes. Removal of these membranes is the first step in most micromanipulation procedures, which is achieved by hatching the embryos in 1.8% cysteine (L-cyteine 97%, cat#W32,630-5) pH 7.8 as describes below. The membranes must be completely removed for embryo dissection. For microinjection, membranes can be completely or partial removed. The second important technique in embryo preparation is the removal of the vitelline membrane.

- **Dejellying embryos**

The embryos were dejellied by removing buffer 0.33X MMR and swirling in 0.33X MMR with 1.8% (w/v) cysteine at pH 7.8. The eggs were gently swirled for 2-4 minutes until the jelly coats were visible in the solution and the eggs started to come together. Dejellying was completed in about 4 minutes, but depends on the frog and must be titrated for each animal. It was safest to monitor each dish of embryos during the dejellying process and not to depend on timing alone. When the embryos began packing together closely and fragments of jelly could be seen floating in the buffer, the cysteine was promptly decanted and the fertilized eggs were rinsed at least 10 times in an excess of 0.33X MMR (Sive, H. L., Grainger, R. M. et al. 2000).

It was important to rinse embryos thoroughly in a clean petri to remove all traces of the cysteine. The vitelline membrane thickens during the first 30 minutes post fertilization so it was best not to dejelly until after this stage. Dejellying of the embryos is best performed after the first division because the thickened membrane offers some protection to the fragile embryo. After dejelling, the embryos were placed in a clean dish keeping them at low density in 0.1X MMR or 4% Ficoll in 0.33X MMR (if the embryos were going to used for microinjection procedures) and the dead embryos removed promptly (Ubbels, G. A., Hara, K. et al. 1983).

- **Removing the Vitelline Membrane**

Vitelline membrane was loosened by digestion with proteinase K (10μg/ml) for a few minutes or manually with the help of forceps and tweezers. The procedure using proteinase K was carried out in glass vials (5ml glass vials) containing 0.1X MMR. Longer exposure to proteinase K results in the destruction of the vitelline membrane and damages the embryo. For this reason, mainly manual removal of the vitelline membrane was performed

for micromanipulation procedures. The procedure was facilitated by coating the bottom of the dish with 1% agarose (electrophoresis grade) in 0.1X MMR. With two forceps, one to hold the embryo steady and the other (sharper pair), to make tear in the vitelline membrane. If the tear was large enough, the embryo could pop out. In both ways; with proteinase K or manual removal, the naked embryos were stored in 0.1X MMR or fixed and used for the future experiments.

2.2.6 Microinjections

Most of the experiments of the thesis included microinjection technique performed on embryos. Embryos were microinjected with mRNA and DNA constructs. RNA injection has the advantage of allowing uniform expression over a large region of the embryo. Embryos are very sensitive to the volume of nucleic acid injected. Therefore, volumes for one cell to four cells were kept below 10nl and less for injection of later stage embryos (Smith, W. C. and Harland, R. M. 1991). After fertilization, the dorsal side of the embryo can be distinguished accurately by the lighter pigmentation characteristic of the animal hemisphere (Ubbels, G. A., Hara, K. et al. 1983). This allowed specific targeting of the injections. A complete fate map of 32 cell stage (Figure 19) embryos has been drawn (Dale, L. and Slack, J. M. 1987) and so at that stage it was quite possible to inject specific blastomeres; however the volume was kept below 3nl. The embryos at 32 cell stage were injected with Quantum dots (NIR QD's) and used for *in vivo* migration assays (Figure 19). Embryos are sensitive to perturbation were therefore treated gently during the injection process. Completely dejellied embryos were transferred to dishes containing a solution Ficoll 4% in 0.33X MMR. Ficoll collapses the vitelline space, reduces the pressure on the embryo and therefore prevents leakage due to the microinjection procedure.

The reagents and the equipment for the microinjection and manipulation were prepared before the beginning of any microinjection procedure. For the microinjections we needed microinjectors, micromanipulators, needles, injection slides, forceps, tweezers and Ficoll 4% (Figure 20, 21). The injection slides were made from sylgard (Sylgard 184 elastomer, Dow Corning Corp.). The volume of the elastomer can be adjusted to produce slides of different thickness (1mm: for early stages of the embryos). The injection volume was very important. Injections of embryos with more than 5ng of mRNA and 100pg of DNA most of the times leads to abnormal development and death during gastrulation. Therefore, the volume was calibrated very carefully. The needle was backfilled with a long narrow tip and with certain amount of RNAse free water (usually 2μl). The injection volume was

calculated by the number or injections made with 2μl of RNAse free water (ex. 200 pulse for 2μl so every pulse corresponds to 10nl).

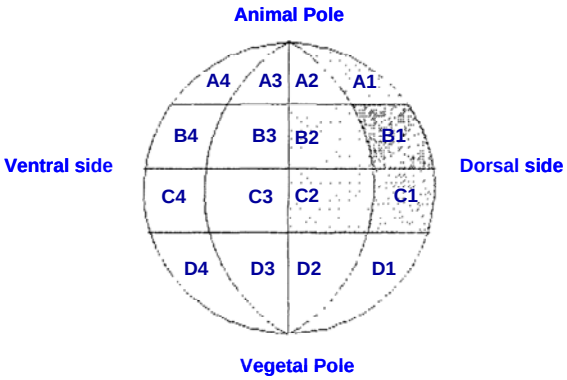

Figure 19. Fate map for the 32-cell stage of *Xenopus laevis* adopted from (Dale, L. and Slack, J. M. 1987).

Figure 20. Microinjector and micromanipulator

Figure 21. Microinjection system consiting of micromanipulator, injector and stereoscope.

2.2.7 Animal Cap Isolation

The first step in every microdissection procedure is dejellying removing the vitelline membrane from the embryos as described in above sections. The animal cap refers to the tissue around the animal pole of a blastula stage embryo. The fate of this tissue is to become cement gland-neuroectoderm on the dorsal side and epidermis on the ventral side. Animal caps are very useful because they are composed of pluripotent cells that can be induced to from endodermal, mesododermal, or ectodermal cell types (Ariizumi, T., Sawamura, K. et al. 1991; Takashi Ariizumi, Naomi Moriya et al. 1991). With quite a bit of practice the removal of the animal cap is a relatively easy dissection process. The animal cap was removed with care in order to obtain only pure ectodermal cell populations, without contaminating with mesodermal cells. For every experiment caps from embryos of the same stage and batch were used (most of the times from the same frog) so to be sure that the tissue was as homogeneous as possible.

During the next step of the procedure, the embryos were placed in glass petri dishes coated with agarose 1% in 0.5X MMR. With the help of a sharp pair of forceps and eyebrow hair knife we cut the cap. Then, the animal cap is removed, cleaned from mesodermal cells or any adherent vegetal yolk cells and the explants cultured in different solutions depending on the experiments they will be used (cultured in 0.5X MMR or CMFM for dissociation). Animal caps were used for migration assays, convergent extension assays and immunofluorescence assays.

2.2.8 Dissociation and Reaggregation of Animal Caps

Single cells derived from animal caps were used in all the experiments for migration assays, immunofluorescence assays and localization assays. Animal caps can be dissociated by exposure to a medium lacking Ca^{++} and Mg^{++} ions (CMFM, Calcium Magnesium Free Medium). Animal caps transferred to 1% agarose (agarose in CMFM) coated dishes containing Ca^{++} /Mg^{++} ion free buffer (CMFM) and activin 10μg/ml (Asashima, M., Nakano, H. et al. 1990). Approximately ten animal caps were placed into a single well of a 12 well non-treated dish. The caps were incubated and swirled at room temperature for approximately 45-60 minutes. During this time the inner cap cells separate from the outer layer. The outer epithelial layer was discarded at this point and the cells were dissociated. For immunofluorescence and migration assays the cells were transferred to fibronectin (50μg/ml) coated coveslips (charged before with HCl and cleaned with distilled water, 5 minutes each) or slides (mentioned below) (Ramos, J. W. and DeSimone, D. W. 1996).

If the dissociated cells were used for reaggregation; the cells were removed from the Ca^{++} /Mg^{++} ion free buffer and placed in a 1% agarose (agarose was prepared in 0.1X MMR solution) coated glass petri dish with 0.5X MMR. The cells were incubated swirled at room temperature for 4-5 hours. We later noticed that it was easier to put the dissociated cells in an eppendorf tube (reaggregation in this way is completed in less than 2 hours). The reaggregated caps were fixed in fixation buffer (1X MEMFA) and used for the subsequent experiments (immunofluorescence).

2.2.9 Isolation of Posterior Dorsal Mesoderm from mid-gastrula stage embryo

Mid-gastrula dejellied embryos (stage 9) were selected and the vitelline membrane removed. Two superficial slits were made, one on each side of the dorsal blastopore in order to mark the dorsal region. By extending the slits anteriorly to the blastocoel a third slit was made in the blastocoel. The dorsal ectoderm was peeled as far as the blastopore so as to expose the mesoderm. The ectoderm was then cut off. Starting from the blastopore, two additional cuts were made into the mesoderm; one on each side of the dorsal midline. The dorsal mesendoderm was peeled as far back as the anterior extent of the archenteron (Sive, H. L., Grainger, R. M. et al. 2000). The piece of the explants were cultured in 0.5X MMR and used in migration or immunofluorescence assays.

2.3 Specific methods

2.3.1 Embryos, explants and Microinjections

Xenopus laevis embryos from induced spawning (Winklbauer, R. 1990) were staged according to Nieuwkoop and Faber (1967). *Xenopus* embryos were fertilized *in vitro* and dejellied using 0.33X MMR with 2% (w/v) cysteine at pH 8 and then maintained in 0.1X MMR. Microinjections were performed in 4% Ficoll in 0.33X MMR. The embryos were injected with RNA at the 2 and 4-cell stage according to established protocols (Smith, W. C. and Harland, R. M. 1991). For example, FRNK was injected at 500 pg per blastomere (up to 1ng total), memGFP at 100 pg per blastomere and FAK at 50 pg per blastomere (Table 1). Also we used FAK-specific antisense morpholino to target sequences upstream of the start codon of *Xenopus* FAK (within the 5'UTR). The sequence of the morpholino that was used was the following: 5'- TCCAGGTAAGCCGCAGCCATAGCCT - 3' (referred as: FAK MO). After injections the embryos were cultured in 4% Ficoll in 0.33X MMR until stage 8 and then cultured in 0.1XMMR at room temperature for phenotype experiments. For elongation assays, animal cap explants were prepared from stage 8 (stages according to Nieuwkoop) embryos and treated with activin A protein (10 ng/ml).

Table 1. Concentrations of mRNA microinjections

mRNA *	Concentration** (total pg per embryo)
FAK	100-200
FRNK	500-1000
Y397FFAK	250-500
K454RFAK	250-500
D395AFAK	250-500
FAKΔFAT	250-500
Y397FFAKΔFAT	250-500
FERM/FRNK	250-500
FERMY397F/FRNK	250-500
FERM	250-500
FERMY397F	250-500
Δ375FAK	250-500
FAT	250-500

* Sometimes mRNA coinjected with histoneGFP, membraneGFP or membraneCherry (total 100pg for each one).

** Site of injection depended on the experiment. Most of the mRNA's injected in Animal pole (AP, dorsally) and in Dorsal Marginal Zone (DMZ).

2.3.2 Antibodies and surface labelling

Indirect immunofluorescence assays were performed as described (Skourides, P. A., Perera, S. A. et al. 1999; Demetriou, M. C., Stylianou, P. et al. 2008) with some modifications. Animal caps were dissociated in CMFM (Sato, S. M. and Sargent, T. D. 1989) and induced in activin 10ng/ml until the sibling embryos reached stage 9 (Asashima, M., Nakano, H. et al. 1990). Ectoderm was removed and the remaining cells seeded on glass coverslips. The coverslips used were first coated with 50μg/ml fibronectin incubated for 1 h at 37^{o}C in humidified chamber and washed three times with ice cold phosphate buffered saline (PBS) containing 0.5 mM MgCl2 and 0.5 mM $CaCl_2$ (PBS++). The seeded cells were then fixed for 10 min in 4% paraformaldehyde solution in PBS++. Fixation was followed by the addition of 50 mM glycine solution in PBS++ and then the cells were permeabilized using 0.2% Triton-X solution in PBS2++ for 10 min. Permeabilized cells were blocked using 10% normal donkey serum (Jackson Immunoresearch) for 30 min at room temperature (RT) in humidified chamber. Primary antibodies were added to the 5% normal donkey serum solution in PBS++ and cells were incubated in the antibody solution for 45 min RT. Primary antibodies used included the following: a-FAK polyclonal (2A7, Upstate Biotechnology) (Kragtorp, K. A. and Miller, J. R. 2006), Vinculin (VN 3-24, Hybridoma bank) (Kragtorp, K. A. and Miller, J. R. 2006), Phospho-FAK antibodies (PY397 monoclonal from Chemicon and polyclonals PY576, PY861 from Biosource Invitrogen), Paxilin (MAB3060, Chemicon Millipore). Secondary antibodies that used were alexa 633, alexa 488 and phalloidin 555 from Molecular Probes (Table 2). Coverslips were mounted on microscope slides using prolong antifade mounting media. Cells were then imaged on a Zeiss Axio Imager Z1 using a Zeiss Axiocam MR3 and the Axiovision software 4.6 (Figure 22). Aquired multichanell images were spectrally unmixed using Axiovision software 4.6.

Table 2. Concentrations of used Antibodies for Immunofluorescence assays

Antibodies	Dilutions in block solution
a-FAK (2A7, Upstate Biotechnology)	1/250
Vinculin (VN 3-24, Hybridoma bank)	1/50
PY397FAK (MAB1144, Chemicon Millipore)	1/250
PY576 FAK (44652G, eBiosource Invitrogen)	1/250
PY861 FAK (44-626G, eBiosource Invitrogen)	1/250
Paxillin (MAB3060, Chemicon Millipore)	1/500
Alexa 488 (Molecular probes, Invitrogen)	1/500
Alexa 633 (Molecular probes, Inivtrogen)	1/250
Phalloidin 555 (Molecular probes, Invitrogen)	1/500

For **whole mount immunostaining** embryos were fixed in 3.7% formaldehyde in MEMFA (2 hours at room temperature) and the vitelline envelope was removed manually. Following vitelline envelope removal embryos were sectioned saggitally or animal caps sections (depends of the experiment). The embryos were permeabilized for at least 5 hours in 0.5% Triton, 5% BSA, 1% DMSO (PBDT) and blocked for 2 hours in 0.5% Triton, 5% BSA, 1% DMSO and 1% Normal Goat or Normal Donkey serum. Primary antibody staining followed using a-FAK polyclonal (Kragtorp, K. A. and Miller, J. R. 2006), Phospho-FAK antibodies, Paxillin, c-Src, pPaxillin, pAkt, GFP and HA one at a time or in combination. Embryos were incubated with primary antibodies diluted at 1:500 (depending on the primary antibody the dilutions ranged from 1:50 to 1:1000, table) overnight at 4^{o}C (Table 3). Embryos were then washed three times in PBDT for 10min, incubated for 2hours RT with secondary antibodies (Alexa 633, Alexa 488 goat anti mouse and anti rabbit from Molecular Probes and Cy3 donkey anti mouse and rabbit from Jackson Immunoresearch) at 1:500 dilution RT and then washed three times in PBDT again (Table 3). For negative control experiments the embryos incubated after block solution only with secondary antibodies and no specific staining was expected. The sections were kept flat with the help of a coverslip and silicone grease. The embryos were imaged on a Zeiss Axio Imager Z1 same way as the cells mentioned above (Figure 22). Cleared whole embryos were imaged and mounted in a similar fashion as described above. Clearing of embryos was performed by immersion the embryos in two parts benzyl benzoate and one part benzyl alcohol after dehydration (Murray's Clearing Medium). The refractive index of BB:BA closes matches the refractive index of yolk thereby rendering *Xenopus* embryos

nearly transparent. Optical sectioning was achieved using a Zeiss Apotome structure illumination system (Figure 22).

Table 3. Concentrations of used Antibodies for Whole Mount IF

Antibodies	Dilution in Block solutions (PBDT)
a-FAK (2A7, Upstate Biotechnology)	1/100
PY397FAK (ab4803, Abcam)	1/1500
PY397FAK (MAB1144, Chemicon Millipore)	1/100
PY576 FAK (44652G, eBiosource Invitrogen)	1/500
PY861 FAK (44-626G, eBiosource Invitrogen)	1/500
Paxillin (MAB3060, Chemicon Millipore)	1/250
pPaxillon Tyr31 (sc-14035, Santa Cruz)	1/50
pAkt (Ser 473) (sc-7985, Santa Cruz)	1/50
c-Src (sc-18 Santa Cruz)	1/50
HA mouse (sc-7392 Santa Cruz)	1/100
HA rabbit (NB600-363, Novus)	1/500
Alexa 488 anti mouse (Molecular probes, Invitrogen)	1/500
Alexa 488 anti rabbit (Molecular probes, Invitrogen)	1/500
Alexa 633 anti mouse (Molecular probes, Inivtrogen)	1/500
Alexa 633 anti rabbit (Molecular probes, Inivtrogen)	1/500
Cy3 anti mouse (Jackson Immunoresearch)	1/500
Cy3 anti rabbit (Jackson Immunoresearch)	1/500

Figure 22. Microscope Zeiss Axio Imager Z1

2.3.3 Whole-mount In Situ Hybridization (WISH)

Whole mount in situ hybridization was performed on *xenopus* embryos stage 10, 12 and 13 using digoxygenin-rUTP labelled RNA probes as described by Harland (1991) (Hens, M. D. and DeSimone, D. W. 1995). Antisense Digoxigenin-labeled Xbra probe (mesoderm marker, MBT to stage 10), Chordin (mesoderm marker, neural tube), Sox2 (neural plate marker) and Sox3 (neural plate marker) were synthesized by *in vitro* transcription of linearized plasmid CS2++ with restriction enzyme NotI using RNA polymerase SP6 and ribonucleotide mixture in which UTPS were labeled with Digoxigenin (DIG-UTP cat#11277073910, Roche). After proteinase K treatment (remove vitelline membrane), as mentioned before in the text, the embryos were fixed, dehydrated, rehydrated, permeabilized, hybridized in a solution containing the probe and washed with Maleic Acid Buffer (MAB, pH 7.5 solution that contains levamisole-inhibits endogenous phosphatases) (protocol detailed in protocols appendix). Bound probe was detected by alkaline phosphatase-conjugated anti-digoxigenin (Anti-Dogoxigenin-AP fragments, Roche cat#11093274910) using BM Purple substrate (BMP from Roche cat#11442074001). It's a four day protocol and the whole embryos were imaged using bright-field optics on a stereoscope (Discovery V12) using software AxioVision 4.7 (Figure 23).

Figure 23. Stereoscope (Discovery V12)

2.3.4 Plasmids and Cloning strategy

GFP FAK and GFP FRNK (kindly provided by Kevin Pumiglia**)** constructs in the adenoviral shuttle vector, pShuttle were cloned into the CS2++ vector by restriction enzyme digest with BglII –XbaI, BglII-NotI respectively, and transcribed into capped mRNA using mMessage mMachine Sp6 kit (Ambion) and the mRNAs were purified using the Mega Clear kit (Ambion). EGFP fused to a Ras farrnesylation sequence (memGFP), EGFP fused to histone sequence (hGFP) and membrane Cherry (memCherry) in the CS2++ vector (kindly provided by Chembei Chan) transcribed into capped mRNA using mMessage mMachine Sp6 kit (Ambion).

Microinjections were performed as above. RNAs that were not fused with GFP co-injected with memGFP or hGFP or memCherry mRNA (total 100pg) per embryo.

Four mutant constructs which were expected to perturb focal adhesion kinase function were used. One was Y397F FAK (mutant in the major autophosphorylation/activation site on FAK) (Eide, B. L., Turck, C. W. et al. 1995), the other was K454R FAK (Kinase-dead, the catalytic residue is mutated (Hildebrand, J. D., Schaller, M. D. et al. 1993) and the D395 FAK (allows Src binding to pY397, but not PI3K) (Reiske, H. R., Kao, S. C. et al. 1999) all in pKH3 vector (kindly provided from Guan lab). They were HA tagged (contains triple influenza virus HA tag) so primers were designed to PCR out the mutants from pKH3 vector. CS2++HAY397FFAK, CS2++ HAK454RFAK, CS2++ HAD395AFAK plasmids were constructed using PCR and sequencing to verify the correct sequence. The F397, R454 and D395 point mutants had the expected nucleotide substitution after sequencing reactions (Magrogene).

Also Δ375 mutant (N-term 375 residues are truncated, making FAK hyperactive) (Cooper, L. A., Shen, T. L. et al. 2003) in pKH3 vector (kindly provided from Guan lab). From FAK (full length) in plasmid pKH3 (kindly provided from Guan lab) FRNK and FAT removed by PCR using following primers (Table 4) and the product was inserted into the pCS108 vector with NotI/XhoI restriction enzymes. With the help of these plasmids new constructs were designed and most of these were sequenced (Magrogene). Primers that have been used to PCR out the constructs, the enzymes and the vectors that were inserted are analyzed in the following table. All plasmids were transcribed into capped mRNA using mMessage mMachine Sp6 kit (Ambion).

Antisense RNA of Xbra (mesoderm marker, MBT to stage 10), Chordin (mesoderm marker, neural tube), Sox2 and Sox3 (neural plate marker) were transcribed from CS2++ vector (kindly provide by Ali Brivanlou) and used for whole mount in situ hybridization.

Table 4. Cloning strategy for FAK constructs

Template plasmid (pKH3)	Primers (Forward and Reverse)	New Vector* NotI/XhoI sites
FAK	5'-ATGCGGCCGCATG*TACCCATACGATGTTCCAGATTACGCT*-3' TTTCTCGAGTTAGTGGGGCCTGGACTGGCTGATCATTTT	CS2++ FAK
GFPFAK (plasmid: CS2++)	5'-AAGCGGCCGCATG*TACCCATACGATGTTCCAGATTACGCT*ATGGA ATCCAGGCGA-3' 5'-TTTCTCGAGTTAGTGGGGCCTGGACTGGCTGATCATTTT-3'	pCS108 FRNK
Y397FFAK	5'-ATGCGGCCGCATG*TACCCATACGATGTTCCAGATTACGCT*-3' 5'-TTTCTCGAGTTAGTGGGGCCTGGACTGGCTGATCATTTT-3'	CS2++ Y397FFAK
K454RFAK	5'-ATGCGGCCGCATG*TACCCATACGATGTTCCAGATTACGCT*-3' 5'-TTTCTCGAGTTAGTGGGGCCTGGACTGGCTGATCATTTT-3'	CS2++ K454RFAK
D395AFAK	5'-ATGCGGCCGCATG*TACCCATACGATGTTCCAGATTACGCT*-3' 5'-TTTCTCGAGTTAGTGGGGCCTGGACTGGCTGATCATTTT-3'	CS2++D395AFAK
FAK	5'-ATGCGGCCGCATG*TACCCATACGATGTTCCAGATTACGCT*-3' AACTCGAGTCTTCACGCCTTCGTTGTAGCTGTCCACGGGG	pCS108 FAKΔFAT**
Y397FFAK	5'-ATGCGGCCGCATG*TACCCATACGATGTTCCAGATTACGCT*-3' 5'-AACTCGAGTCTTCACGCCTTCGTTGTAGCTGTCCACGGGG-3'	pCS108 Y397FFAKΔFAT**
FAK	FERM: 5'-ATGCGGCCGCATG*TACCCATACGATGTTCCAGATTACGCT*-3' 5'-TTT**TCTAGA**ATCTATTATCTCTGCATAGTCATCTGT-3' FRNK: 5'AAA**TCTAGAGGTAGCGGCAGCGGTAGC**AGGTTTACTGAACTTAA AGCAC **(Linker)** -3' 5'-TTTCTCGAGTTAGTGGGGCCTGGACTGGCTGATCATTTT-3'	pCS108 FERM/FRNK***
Y397FFAK	FERM: 5'-ATGCGGCCGCATG*TACCCATACGATGTTCCAGATTACGCT* TTT**TCTAGA**ATCTATTATCTCTGCAAAGTCATCTGT-3' FRNK: 5'AAA**TCTAGAGGTAGCGGCAGCGGTAGC**AGGTTTACTGAACTTAA AGCAC **(Linker)**-3' TTTCTCGAGTTAGTGGGGCCTGGACTGGCTGATCATTTT	pCS108 FERMY397F/FRNK***
FAK	5'-ATGCGGCCGCATG*TACCCATACGATGTTCCAGATTACGCT*-3' 5'-TTTCTCGAGTTAATCTATTATCTCTGCATAGTCATCTGT-3'	pCS108 FERM
Y397FFAK	5'-ATGCGGCCGCATG*TACCCATACGATGTTCCAGATTACGCT*-3' 5'-TTTCTCGAGTTAATCTATTATCTCTGCAAAGTCATCTGT-3'	pCS108 FERMY397F
Δ375FAK	5'-ATGCGGCCGCATG*TACCCATACGATGTTCCAGATTACGCT*-3' 5'-TTTCTCGAGTTAGTGGGGCCTGGACTGGCTGATCATTTT-3'	CS2++ Δ375FAK
GFPFAK (plasmid: CS2++)	5'-AAGCGGCCGCATG*TACCCATACGATGTTCCAGATTACGCT*AT CAAGCCACAGGA-3' 5'-TTTCTCGAGTTAGTGGGGCCTGGACTGGCTGATCATTTT-3'	pCS108 FAT

* All of the plasmids contain HA tag (influenza virus HA tag) HA sequence: *TACCCATACGATGTTCCAGATTACGCT*

** Constructs missing FAT domain (responsible for localization for FAK to focal adhesions)

*** Constructs missing kinase domain (responsible for the fully activation of FAK). Two PCR reactions, 1st FERM and 2nd **linker** + FRNK. Common internal restriction site is **XbaI**.

2.3.5 Cell Migration assays, FN spreading, adhesion assays and convergent extension assays

Dorsal Marginal Zone (DMZ) explants (from stage 11 embryos) and animal caps (from stage 8) were dissociated in CMFM (Sato, S. M. and Sargent, T. D. 1989) with the addition of 1mM EDTA for 10 minutes. Dissociated cells from animal caps were induced in activin 10ng/ml for 1 hour RT (Asashima, M., Nakano, H. et al. 1990). Cells were then placed in four well plates from which the plastic bottom had been removed and a glass cover slip was attached using Silicone Grease. The glass had been previously coated with fibronectin (FN 50μg/ml). If more than one cell population was going to be filmed at the same time small Petri dishes were coated with a thin film of agarose and small wells were created by punching through the agarose with a cut pipette tip. The individual wells were then coated with FN and cells were placed in them after being dissociated. Cells were then observed under a Zeiss Axio Imager Z1 microscope and time lapse movies were made using a Zeiss Axiocam MR3, the Axiovision software 4.6 and the average speed of migration was calculated using ImageJ software. Cells were tracked for 60 min for each experiment. For convergent extension assay animal caps explants from stage 8 embryos, were treated with 0.5X MMR and induced in activin 10ng/ml to form mesoderm and elongate.

2.3.6 Immunoblotting (Western Blot Analysis) and Immunoprecipitation

Protein lysates were prepared by homogenizing explants or embryos (embryos in different stages) in ice cold RIPA lysis buffer (50mM TrisHCl pH7.4, 150mM NaCl, 2mM EDTA, 1% NP-40, 0.1% SDS, 1% deoxycholate 24mM) supplemented with phosphatase inhibitors (5mM Na_3VO_4) and protease inhibitors (1mM PMSF from Sigma cat#, Protease cocktail from Sigma, P8340). Homogenates were cleared by centrifugation at 15000g for 30min at 4^{o}C (Kragtorp, K. A. and Miller, J. R. 2006). The embryo samples were separated on SDS-polyacrylamide gels and proteins were blotted on PVDF (Figure 13). Membrane and blots were then blocked in 5% milk in TBSTw (TBS buffer + 0.1%Tween). Blots were incubated with anti-FAK (1:500, monoclonal from Millipore, 05-537) or phospho-FAK antibodies (1:2000 FAKpY397 polyclonal from Abcam ab4803 and polyclonals 1:500 FAKpY576, FAKpY861 from Biosource Invitrogen) in 5%milk in TBSTw overnight at 4^{o}C. Visualization was performed using HRP-conjugated antibodies (Santa Cruz Biotechnology anti-Rabbit and mouse) and detected using the Amersham kit (GE

Healthcare kit). For loading control actin (1:1000 actin polyclonal from Santa cruz cat#sc-1616) was used in every blot.

For immunoprecipitation, protein lysates were prepared by homogenizing embryos (embryos at different stages) in ice cold MK's modified lysis buffer (50 mM Tris HCl pH8, 150 mM NaCl, 1 mM EGTA, 0.5% NP-40, 0.5% Triton-X100, 5mM NaF) supplemented with phosphatase inhibitors (5mM Na_3VO_4) and protease inhibitors (1mM PMSF from Sigma cat#P7626, Protease cocktail from Sigma, P8340). Homogenates were cleared by centrifugation at 15000g for 30min at 4^{o}C (Kragtorp, K. A. and Miller, J. R. 2006). The lysates were incubate with 0.5-1 µL (HA monoclonal from Santa Cruz ca# sc-7392) of antibody and rotated for 1-4 hours at 4°C. 40µL protein-A-agarose (Santa Cruz cat# sc-2002) was added to the lysates and incubated for 1-2 hours at 4°C. The beads were recovered by centrifugation at 4°C for 2 minutes at 2000 rpm. The samples were washed three times using MK's buffer, high salt wash buffer (50mM Tris-HCl pH 7.5, 500mM NaCl, 0.1% Nonidet 40, 0.05% sodium deoxycholate) and low salt wash buffer (50mM Tris-HCl pH 7.5, 0.1% Nonidet 40, 0.05% sodium deoxycholate). After the last centrifugation, loading dye (Laemmli + ßME) was added to the beads (heat at 80°C for 5 minutes) and beads were spun to the bottom of the tube. The samples were separate on SDS-polyacrylamide gels and the rest of the procedure was the same as above (immunoblotting procedure).

2.3.7 Calculation of *in vivo* migration rates

The migration rates for *in vivo* experiments were calculated using the following formula $\gamma=2\pi r\mu/360$ (**γ**: arc, **µ**: 2θ angle) considering that the embryo is a sphere with r: 0.5mm (see Figure). The tracked distance in the 2D projection combined with the starting point and end point z-positions were used to calculate the chord between the two points for each cell (start-point and end-point). Then, since migration inside the embryo is very directional, we assumed a straight line path for each cell and calculated the arc for each given chord using the circle defined by the start and end points plus the center of the sphere. This gives a circle of approximately 1mm in diameter (the diameter of the embryo) and the central angle **θ** can be calculated for each cell using the chord length and the radius $\mathbf{\sin(\theta/2) = C/2r}$ (where **C** is the chord length and **r** the radius). We then went onto calculate the arc length for each cell using the central angle and the radius, using the following formula $\mathbf{\gamma=2\pi r\mu/360}$ assuming that the embryo is a sphere with **r**: 0.5mm. A right angle triangle

may then be formed, in which the radius from the center of the sphere to the end-point of migration corresponds to one side, a perpendicular line from the start point of migration to the radius corresponds to the other side, and the cord **C** corresponds to the hypotenuse. The pythagora's theorem was applied to this right angled triangle to find the hypotenuse and the formula **sin(θ/2) = C/2 r** was used to find the angle θ. So, using the formula **γ=2πRμ/360 (μ=2θ)** we calculated the arc length, corresponding to the migration from the start to the end point (Figure 24). Given that migration is timed we observed an average increase of 0.3μm/ min of the migration rates. For these assays, embryos were injected with QTracker 800 Cell Labeling Kit (Invitrogen Q25071MP) in the blastocoel cavity or non targeted QDot800 nanocrystals (Invitrogen Q21071MP) at the 32 cell stage. The embryos were injected at 32 cell stage, in one out of 32 cells, at the dorsal marginal zone (DMZ) (blastomeres B1 or C1, Figure). The embryos were transferred into siliconized glass slides with 0.95mm deep wells so that once a coverslip was placed on top of the embryo it would slightly depress the vitelline membrane and thus immobilize the embryo. Regarding the reference point the time lapse movies were two channels including a reference reflected light frame with each fluorescence frame. The reference point was a selected superficial cell at the top of the BCR and only embryos in which the reference cell had not changed position (XYZ) in all the relevant frames were used for tracking and measurements.

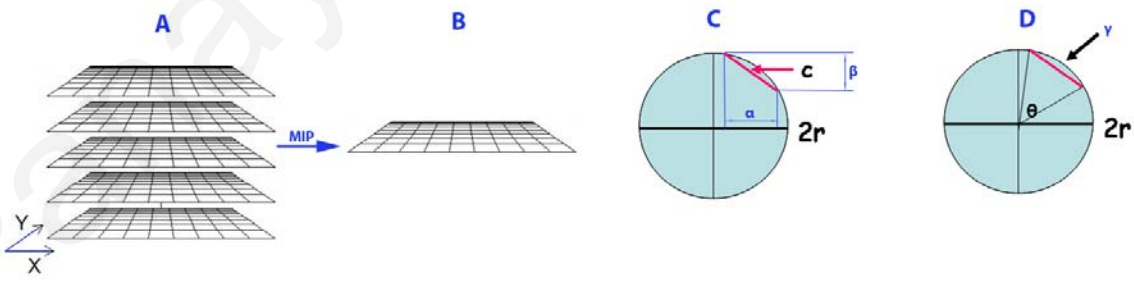

Figure 24. Correction of the migration speed for *in vivo* mesurements. (A) z-stacks. (B) Maximum intensity projection (MIP) after deconvolution. (C) Calculation of the cord (**C**: cord, **α** and **β** form a right angle triangle in which the cord (**C**) is the hypotenuse, **r**: 0.5mm). (D) Calculation of the arc (**γ**: arc, γ=2πrμ/360).

2.3.8 Quantum Dot labelling and NLS conjugations

For *in vivo* assays, embryos were injected with QTracker 800 Cell Labeling Kit (Invitrogen Q25071MP) in the blastocoel cavity or non targeted QDot's 800nm nanocrystals (Invitrogen Q21071MP) at the 32 cell stage. The embryos were injected at 32 cell stage, one out of 32 cells, at the dorsal marginal zone (blastomeres B1, C1) (Figure 19). In order to ensure that the embryos did not move during filming they were transferred into siliconized glass slides with ~0.95mm deep wells so that once a coverslip was placed on top of the embryo it would slightly depress the vitelline membrane thus immobilize the embryo. For each time lapse movie the reference point was a selected superficial cell at the top of the BCR and only embryos in which the reference cell had not changed position (XYZ) in all the relevant frames were used for tracking and measurements. Individual cell migration rates were calculated from 10 embryos (minimum of 10 individual cells measured from each embryo).

Coupling of biotinylated peptides (NLS, Biotin-Lys-Gly-Gly-Gly-Pro-Lys-Lys-Lys-Arg-Lys-Val-COOH, CASLO Laboratory ApS) to streptavidin conjugated QD´s were performed according to the manufacturer's protocol (Invitrogen Corporation). For the direct Conjugation of Qdot® ITK™ Carboxyl Quantum Dots to the purified NLS peptide 2 nmol Qdot® ITK™ Carboxyl Quantum Dots (in 50 mM sodium borate, pH8.3) were diluted to 1 μM using 10 mM borate buffer, followed by the addition of the NLS peptide solution. This was followed by the addition of 57 μL of 10 mg/ml N-ethyl-N'-dimethylaminopropyl-carbodiimide (EDC). The solution was stirred for 2 hours and then filtered through a 0.2 um PES membrane unit and transferred to a clean centrifugal ultrafiltration unit and spun in a centrifuge for 5 buffer exchanges with 50 mM borate buffer to remove unconjugated peptides. Finally the conjugate was filtered through a 0.2 μm syringe filter. Conjugates were then be electrophoresed to ensure that the conjugation was successful. The successful conjugates were injected to the embryos and used for the *in vivo* assays.

2.3.9 In vivo Imaging and Notes on QD toxicity

Embryos were imaged on a Zeiss AxioImager, with a Zeiss Apochromat 5X/0.25 lens. A Zeiss Axiocam MR3 and the Axiovision software 4.6 were used to aquire the images. Acquired z-stacks were deconvoluted (Inverse Filter) using a theoretical PSF using 800-nm and maximum intensity projections were created using the Zeiss Axiovision software. For

the visualization of QD nanocrystals we used customized filter sets with excitation between 530 and 585 nm and emission between 775 and 825 nm. Although optimal excitation of the QD's requires wavelengths around 400 nm and use of suboptimal longer wavelength excitation resulted in lower signal to noise ratio images and required longer exposure times under the same conditions observation using this filter resulted in much lower photodamage to the embryo. All organic fluorophores were detected using narrow band filter sets recommended by the manufacturers to achieve the maximum background rejection possible.

Different batches of nanocrystals from Invitrogen showed differences regarding the overall toxicity observed in the absence of excitation. Some batches displayed such high toxicity that divisions of injected blastomeres would halt immediately after injection. In addition non-targeted 700 nm QD's from evident technologies (eFluorTM 700NC) consistently showed high toxicity making them unsuitable for *in vivo* experiments in *Xenopus*. In an effort to determine whether the observed toxicity was due to the QD's themselves or due to chemical contaminants in the buffer, QD batches that displayed toxicity were diluted in PBS (100 μl of QD solution to 2500 μl of PBS) and re-concentrated using an Amicon Ultra-4 Centrifugal Filter (Ultracel _100k) back to their initial volume. This process did not appreciably affect the overall toxicity of the QD solutions suggesting that the source of toxicity are the QD's. This leads to the conclusion that variations in the coating of different batches of QD's and differences in stability of the different coating systems, employed by invitrogen and Evident technologies, result in differences in toxicity. Evidently, there is a need for improved methodology leading to the creation of water soluble, biocompatible QD's, as well as a need for better quality control of the (currently available) final product.

3. RESULTS

3.1 Developing Near Infra Red (NIR) Quantum Dot (QD's) based imaging tools for imaging of deep tissue morphogenetic movements in *Xenopus in vivo*

3.1.1 Fluorophore evaluation

We began our study by evaluating a number of fluorophores emitting both in the visible and the NIR region (organic and inorganic) in an effort to identify the region of the spectrum as well as the type of fluorophore best suited for this study. This was achieved by injecting each fluorophore into the animal pole of early embryos and assessing the signal to noise ratio and the toxicity in the presence and absence of excitation (data not shown). The advantages of using the NIR region of the spectrum for lineage tracing became apparent in our initial experiments comparing NIR QD´s to visible range QD´s. *Xenopus* embryos are highly auto-fluorescent due to the large amount of yolk present, especially at early stages. As seen in Figure 25A, B the *in vivo* detection of QD labeled superficial animal pole cells is vastly improved when all visible wavelengths are filtered out, a clear demonstration of the advantages of using the NIR region for this type of experiment. In addition our comparison of different fluorophores indicated that NIR QD´s from Invitrogen (Qtracker 800 non-targeted quantum dots) were the most suitable for our study, having higher signal to noise ratio and significantly better photostability than any of the NIR or far red organic fluorophores (IrDye800, Alexa680, Cy3, Cy5, Alexa750) that were tested (data not shown). However despite the clear advantages of QD´s it should be noted that there was significant variation in the quality of QD´s from Invitrogen from different batches. More details can be found in the materials section of the thesis proposal.

3.1.2 Imaging the migrating anterior mesoderm using NIR QD's

In order to test if NIR QD labelled mesodermal cells could be visualized *in vivo* through the cells of the animal cap non targeted NIR QD´s were microinjected in the dorsal marginal zone of 8 cell embryos. The embryos were then allowed to develop to stage 10.5 and imaged on an epifluorescence equipped microscope. This type of experiment allowed the visualization of the leading edge of the anterior mesoderm through the animal cap of wild type embryos during gastrulation (Figure 25E- H) while injection of both dorsal and ventral marginal zone blastomeres enabled visualization of the mesodermal mantle closure (Figure 25M - P). This type of injection however failed to provide clear delineation of

individual cells due to the uniform nature of the labelling (Figure 25E - H). Non targeted NIR QD´s label cells uniformly and are evenly inherited by the progeny of the injected cells making cell boundaries hard to distinguish especially when the tissue being imaged is deep within the embryo, leading to diffuse signal. Despite this we were able to obtain time lapse movies showing the progress of the leading edge (Figure 25E- H) and calculate the average displacement rate of the front *in vivo* which was 1,9 ± 0.28μm/min (average from 20 embryos at 20-22 **°C**). These measurements refer to the speed with which the anterior mesoderm front is approaching the top of the BCR assuming that the mesoderm is migrating on the surface of a 1mm sphere (details regarding the calculations can be found in the materials and methods section). These rates did not vary as much as previously recorded *in vitro* rates (1-3μm/min) (Winklbauer, R. 1990; Winklbauer, R. and Nagel, M. 1991; Winklbauer, R. and Keller, R. 1996) is slower than previously published *in vivo* rates (~4μm/min) (Davidson, L. A., Hoffstrom, B. G. et al. 2002) but is faster than the rate calculated from the analysis of *in vivo* MRI based time lapse movies (~1,3μm/min) (Papan, C., Boulat, B. et al. 2007; Papan, C., Boulat , B. et al. 2007). The differences between the rates measured by us and others are most likely due to differences in the temperature at which the embryos or explants were filmed. It should be noted that an embryo develops 25% slower at 20 **°C** versus 22 °C (Sive, H. L., Grainger, R. M. et al. 2000).

In an effort to track single cells embryos were injected at the 16 cell stage. Injection of one blastomere at this stage restricted labeling to a sufficiently small number of cells and enabled visualization of individual migrating cells (Figure 26C and D). Improved visualization of single cells was achieved by the injection of 32 cell embryos at blastomeres C1 or B1 (Figure 26A - E, movie 1 and 2). Using this approach individual cells can be tracked and migration rates can be easily determined. In addition the resolution is sufficient to monitor cell shape changes and protrusions of individual cells (Figure 26A-E magnified insets and movie2). Tracking of anterior mesodermal cells reveals an overall highly directional and highly persistent movement of these cells towards the top of the BCR (tracks on Figure 26E). Individual cell migration rates were calculated from 10 embryos (minimum of 10 individual cells measured from each embryo) and they ranged between 1.9μm/min and 2.9μm/min (Figure 2F). The lowest rate is in agreement with the average rate of the front as measured before (1,9 ± 0,28μm/min, Figure 1E- H). One would expect that if the front is moving at a certain rate that rate would be the minimum observed for individual cells. However these measurements show that individual cells can attain sustained migration rates, which are significantly higher than the migration rate of the

mesoderm front. In *Xenopus*, prechordal mesoderm moves as a multilayered coherent cell mass held together by cadherin based cell-cell adhesion (Winklbauer R., Nagel M. et al. 1996). However it is clear from the QD based visualization of the anterior mesoderm that there is free movement of individual cells within the cell mass and that a surprising amount of mixing takes place during this movement (movie 1). Individual cells break free from their neighbours and become interspersed within non labelled regions (Figure 25D). In addition cells can be seen undergoing division and the daughter cells follow different paths (Figure 26B-E small icons lowest green track and movie 2). These data are in agreement with previously published work suggesting that contacts between individual dorsal marginal zone cells are significantly less stable than those between ventral marginal zone cells (Reintsch, W. E. and Hausen, P. 2001).

Another approach that resulted in single cell visualization was the use of Qtracker® 800 Cell Labeling QDs (Invitrogen Qtracker 800 Cell Labeling Kit). These were injected in the blastocoel (BC) of late blastula to early gastrula embryos and were taken up by cells facing the inside of the blastocoel cavity. The viscosity of the Qtracker® 800 solution causes it to remain at the lower region of the BC labeling vegetal and mesodermal cells without labeling animal pole cells. Late blastula and early gastrula injections resulted in relatively homogeneous staining enabling the visualization of the entire mesodermal mantle but making single cells hard to track (Figure 25I - L). However mid gastrula injections enabled single cell visualization and tracking albeit with lower resolution than single blastomere injections (Figure 31F-G). Labeling of individual cells using this approach is not homogeneous with some cells taking up higher amounts of nanocrystals than others. In addition the Qtracker® 800 Cell Labeling QD´s tend to aggregate inside the cells and the signal from labeled cells does not persist as long as that of non targeted QD´s.

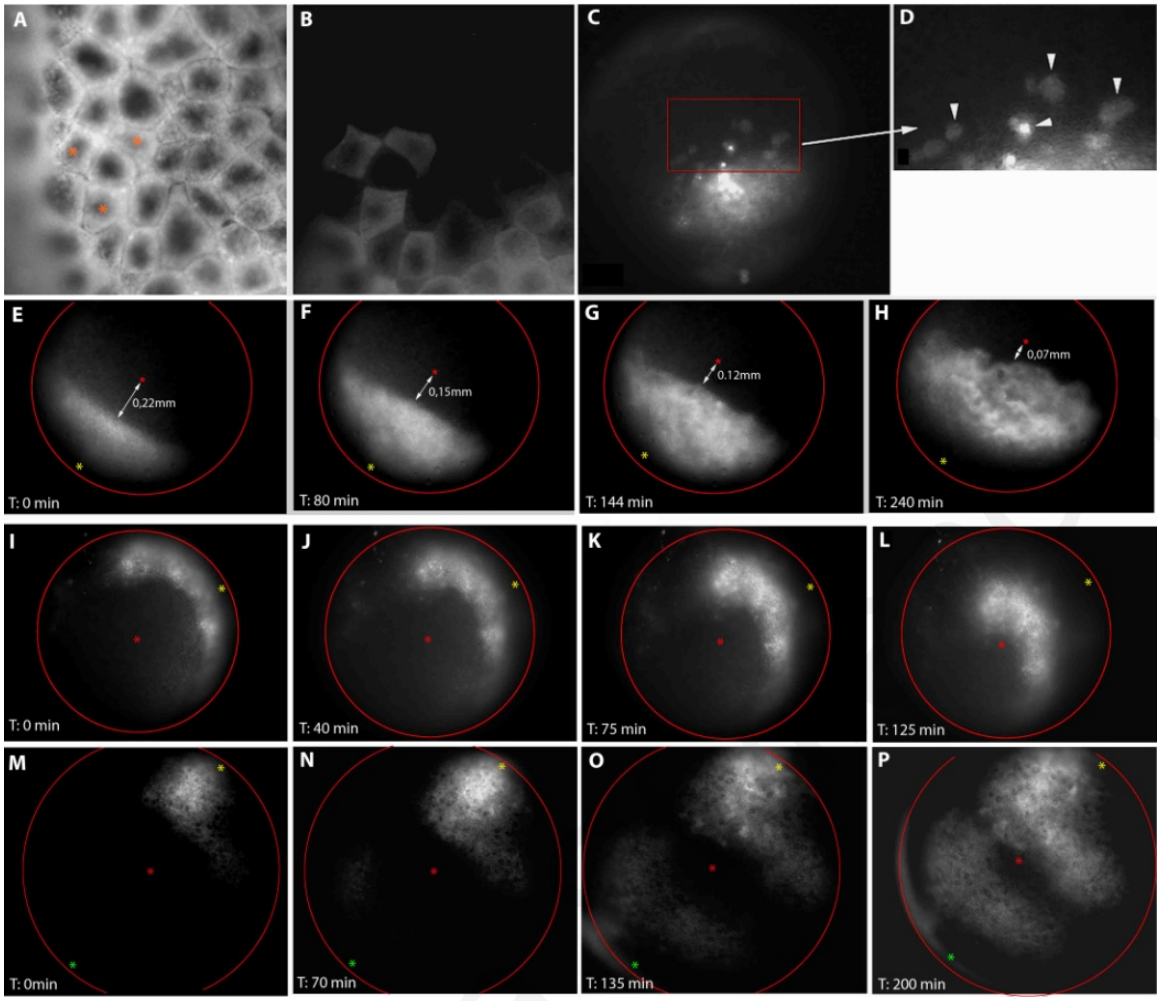

Figure 25. NIR QD´s can be used to label and image mesodermal cells during gastrulation. (A, B) NIR QD (800nm peak emission) labelled animal pole cells in a living embryo viewed with two filter sets. (A) The embryo was imaged with 600nm long pass emission filter allowing all wavelengths above 600nm to reach the camera and in B the same area of the same embryo was imaged with an 800nm long pass filter set allowing all wavelengths above 800nm to reach the camera. Autofluorescence in the 600nm to 750nm range is so intense that the labelled cells (three indicated with red stars in A) cannot be differentiated from unlabeled neighbouring cells. (C, D) NIR QD's labelled cells break free from their neighbours and become interspersed within non labelled regions and can be visualized through the pigmented animal cap. (E-H) Four frames from a time lapse movie of an embryo injected at the DMZ (yellow star) at the four cell stage with NIR QD´s. The mesodermal front becomes clearly visible as it moves towards the top of the blastocoel (red star). (I-L) Four frames from a time lapse movie of an embryo injected with cell tracker QD´s at early gastrula. The Qtracker QD´s were injected into the blastocoel cavity. Using this approach QD´s labelled vegetal pole cells (not visible) and the mesodermal belt (DMZ yellow star, top of the BCR red star, VMZ green star). (M-P) Injection of NIR QD´s at both the DMZ (yellow star) and VMZ (green star) enables visualization of the mesodermal mantle closure (DMZ yellow star, top of the BCR red star, VMZ green star) (Stylianou, P. and Skourides, P. A. 2009).

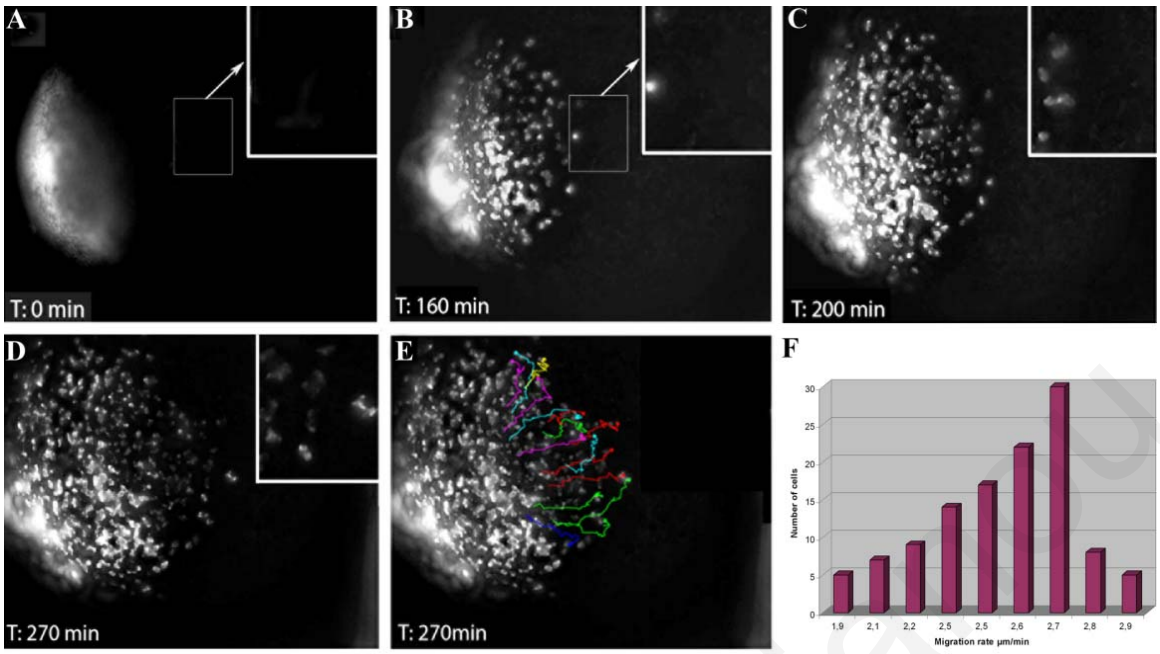

Figure 26. Injection of non targeted NIR QD´s at the 32 cell stage enables visualization of the mesodermal mantle with single cell resolution. (A-E) Five frames from a 4D time lapse movie of an embryo injected at the DMZ at the 32 cell stage. Frames are 2D maximum intensity projections of deconvolved z-stacks. Individual cells are clearly visible as they migrate towards the top of the BCR. Cells appear to have freedom of movement and display varying migration rates however they all display a high degree of directionality as indicated by their tracks (E). (F) Distribution of individual cell migration rates from *in vivo* tracking of NIR QD injected embryos as in A-E (10 embryos were used and a minimum of 10 cells were tracked from each embryo) (Stylianou, P. and Skourides, P. A. 2009).

3.1.3 Functionalized Quantum Dot probes

Despite the fact that injections of *Xenopus* embryos at the 32-cell stage can provide single cell resolution imaging of migrating mesoderm, injections at this stage are relatively difficult especially when the targeting of a specific blastomere is required. However injections of earlier stage embryos result in homogeneous staining of the progeny making it impossible to identify individual cells (Figure 25E-H). An improved NIR QD probe would be one that concentrates in the nucleus. Individual nuclei are well spaced within the embryo in all dimensions creating better contrast. In addition the concentration of a fluorophore in the nucleus would further enhance the signal to noise ratio due to higher localized signal intensity. We tested four different streptavidin conjugated QD´s (Qdot 565, Qdot 605, Qdot 705, Qdot 800) which we pre incubated with a synthetic biotinylated SV40 nuclear localization signal (NLS) peptide. Using this approach only the NLS

Qdot565 QD´s became localized to the nucleus whereas all longer wavelength QD´s were either completely excluded from the nucleus or only showed partial concentration in the nucleus (Figure 27 and data not shown). It appears that size limitations preclude NIR QD´s from accumulating in the nucleus. In an effort to minimize the diameter of the NIR QD´s we used reactive carboxyl QD's and created covalent NLS-QD conjugates (Qdot 800). However the Qdot800 CdSe/ZnS core shell QD-NLS conjugates also failed to accumulate in the nucleus (data not shown). We went on to test InAr/ZnS core shell QDs synthesized by the Bawendi group (Zimmer, J. P., Kim, S. W. et al. 2006). These QD´s have similar emission spectra with the QDot 800 from invitrogen but significantly smaller hydrodynamic radii (Zimmer, J. P., Kim, S. W. et al. 2006) and readily accumulate in the nucleus (Figure 27). Such localization allows tracking of individual cells even in homogeneously labelled regions of the embryo. However the quantum yield of these lab synthesized particles is relatively low (6-9%), compared to the commercially available CdSe/ZnS core shell QD´s making them unsuitable for deep tissue imaging at this time (Zimmer, J. P., Kim, S. W. et al. 2006). Their relatively low quantum yield requires the use of higher amounts before the signal intensity reaches sufficient levels for *in vivo* detection in deep tissues and such amounts are toxic to the embryo. These results point to the need for smaller biocompatible NIR QD´s with higher quantum yields. Such material would further improve both the depth penetration and the resolution of QD based *in vivo* imaging.

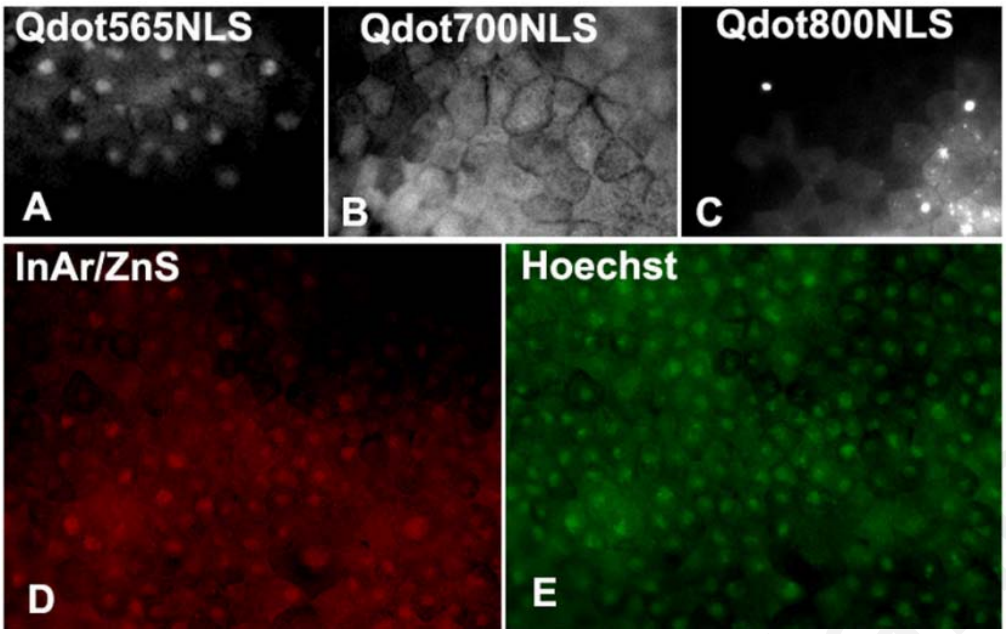

Figure 27. NLS peptide conjugated QD´s display size based exclusion from the nucleus. Visible spectrum CdSe/ZnS streptavidin NLS-QD´s accumulate in the nucleus (A) while NIR NLS-QD´s either do not concentrate sufficiently (B) or are completely excluded (C). InAr/ZnS core shell QD´s are efficiently transported into the nucleus (Red InAr/ZnS core shell QD´s, green labelled with *Hoechst)*. (F) QD injected cells spread and display the same morphology as controls (Stylianou, P. and Skourides, P. A. 2009).

3.2 Focal Adhesion Kinase is present at focal adhesion complexes and is necessary for active mesoderm migration in *Xenopus* embryos *in vitro* and *in vivo*

3.2.1 Visualization focal adhesion on migrating mesodermal cells

It became clear from our above experiments that quantum dots can be used to track migrating mesodermal cells during gastrulation *in vivo* and thus enable us to analyze intrinsic and extrinsic signals that control gastrulation movements in live embryos. We decided to analyze the role of focal adhesions and specifically the Focal Adhesion Kinase (FAK) in mesodermal cell migration using QD´s. As prechordal mesoderm migrates along the fibronectin matrix of the BCR during *Xenopus* gastrulation, focal adhesions and molecules involved in formation of focal adhesion complexes would be expected to play an important role in this process. To test this possibility, we first examined the distribution of known focal adhesion proteins in migratory *Xenopus* mesodermal cells. To confirm the presence of focal adhesions in migrating mesodermal cells we used antibodies directed against a number of well characterized focal adhesion proteins. We detected characteristic linear focal adhesions (FAC´s) in adherent mesodermal cells that were plated on FN coated coverslips (Figure 28). Optical sectioning of these cells revealed that the linear structures observed are only present in the coverlip/cell interface further confirming that the complexes imaged are focal adhesions (data not shown). FAK colocalizes with both Vinculin and Paxillin on these complexes (Figure 28A-F). FAK localized at the FAC´s is phosphorylated on all three sites examined (PY397, PY576, PY861) as evidenced by staining with phospho specific FAK antibodies (Figure 28 and data not shown). FAC´s were mainly concentrated at the cell periphery especially in cells with a motile phenotype and were weaker and smaller than the ones seen on mammalian cells grown on FN. Double labeling of vinculin and actin revealed that the focal adhesion complexes formed at the ends of actin filaments (Figure 28G, H) in a similar fashion as described in mammalian adherent cells (Maher, P. A., Pasquale, E. B. et al. 1985; Yap, A. S., Stevenson, B. R. et al. 1995).

Efforts to visualize focal contacts *in vivo* were not successful, even though all focal adhesion proteins we examined (FAK, Vinculin, Paxillin) were enriched in the interface between the BCR and the adherent mesodermal cells including phosphorylated FAK (Figure 28I and data not shown). Work by other groups using substrates of varying flexibility has shown that cells plated in relatively flexible substrates display a less organized cytoskeleton and absence of linear focal adhesions. Instead they form focal

adhesion like structures that appear punctuate and are much smaller (Robert, J. P. and and Wang, Y.-L. 1997). Since the BCR is less rigid than glass it is likely that focal contacts in the embryo are very small compared to the ones formed *in vitro* making them hard to image however the concentration of focal adhesion proteins in the interface between mesendoderm and the BCR suggests that such complexes do indeed form in the embryo.

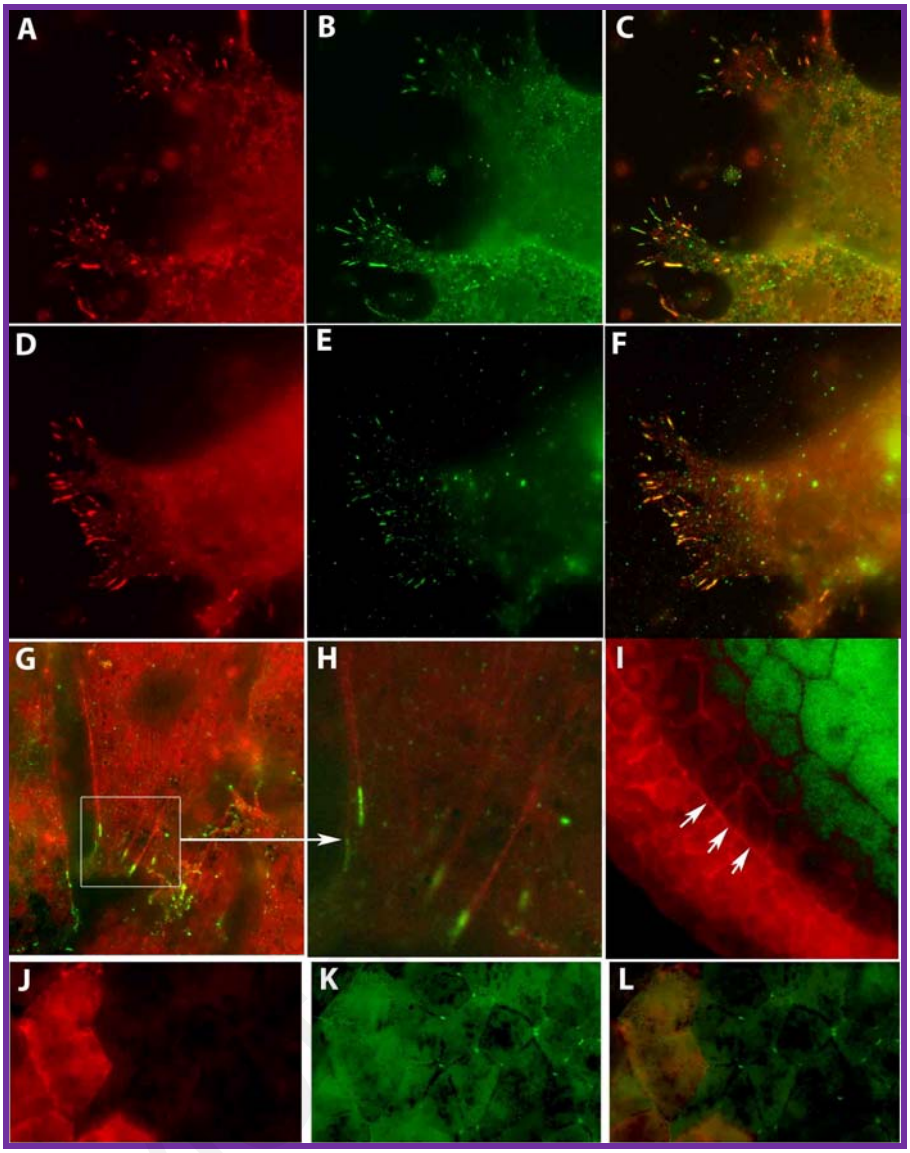

Figure 28. Migrating mesodermal cells form focal adhesion complexes and FRNK displaces FAK from its signaling complexes. (A-C) Colocalization of FAK PY861 (red) with Vinculin (green) at the focal adhesions formed by mesodermal cells plated on fibronectin. (D-F) Colocalization of Paxillin (red) with FAK PY576 (green) (G) Staining with phalloidin (red) and Vinculin (green) reveals that focal adhesions are formed at the end of actin filaments. (H) Higher magnification (of the boxed region of G). (I) Sagittal section of 10 ½ stage embryo staining with anti-FAK PY576 (secondary antibody alexa633) reveals a concentration of phosphorylated FAK at the interface between mesoderm and deep ectoderm. (J-L) FRNK-HA (red) can compete FAK (green) from its signaling complexes. FRNK-HA (500pg) was injected in one out of two blastomeres of two cell stage embryos at the animal pole and then the embryos were allowed to develop to stage 11 fixed and processed for whole mount immunostaining. FRNK-HA was stained with an HA specific antibody while endogenous FAK (green) was visualized using a FAK polyclonal antibody raised against the N-terminus of FAK that does not recognize FRNK. Note the

diffuse signal of endogenous FAK (green) in the FRNK expressing cells (red) compared to the neighbouring control cells (Stylianou, P. and Skourides, P. A. 2009).

3.2.2 Focal Adhesion Kinase is necessary for mesoderm migration

FAK is a positive regulator of cell migration, integrating integrin and growth-factor signals (Sieg, D. J., Hauck, C. R. et al. 1999; Sieg, D. J., Hauck, C. R. et al. 2000; van Seventer, G. A., Salmen, H. J. et al. 2001; Hanks, S. K., Ryzhova, L. et al. 2003; Schlaepfer, D. D. and Mitra, S. K. 2004; Schlaepfer, D. D., Mitra, S. K. et al. 2004). It is expressed in *Xenopus* migrating mesodermal cells and we have shown that it is localized at the focal adhesions formed by these cells (Hens, M. D. and DeSimone, D. W. 1995; Zhang, X., Wright, C. V. et al. 1995). In addition it has been shown that FAK has a role in somitogenesis (Kragtorp, K. A. and Miller, J. R. 2006). Its expression and localization at the tissues undergoing mesoderm migration suggest a potential role in this movement. In order to examine the possibility that FAK is important for mesoderm migration we used influenza hemagglutinin (HA) tagged versions of both FAK and FRNK, a dominant negative splice variant as well as GFP tagged versions of both proteins (Schaller, M. D., Borgman, C. A. et al. 1993; Richardson, A. and Parsons, T. 1996; Richardson, A., Malik, R. K. et al. 1997). We first addressed the possible effects of FRNK over-expression on the localization and tyrosine phosphorylation of endogenous FAK in *Xenopus* cells. Tyrosine phosphorylation of FAK is a good indicator of its activity, and cycles of phosphorylation and dephosphorylation are believed to be essential for cell migration (Du, Q. S., Ren, X. R. et al. 2001; Leu, T. H. and Maa, M. C. 2002). In agreement with previously published data (Kragtorp, K. A. and Miller, J. R. 2006) over-expression of FRNK leads to a significant reduction in the levels of tyrosine phosphorylated FAK on residue 397 (data no shown). Furthermore FRNK over-expression leads to the redistribution of endogenous FAK from its complexes to the cytoplasm (Figure 28J-L). This is in agreement with findings that FRNK expression leads to the redistribution of FAK from the focal adhesions to the cytoplasm in rat myocytes (Heidkamp, M. C., Bayer, A. L. et al. 2002), and also supports the hypothesis that FRNK functions by competing FAK off its signaling complexes (Richardson, A. and Parsons, T. 1996; Crawford, B. D., Henry, C. A. et al. 2003). The fact that FRNK, competes FAK from its complexes and reduces its phosphorylation level suggests that it is, as reported previously, functioning as a bona fide dominant negative in the context of the developing *Xenopus* embryo (Richardson, A. and Parsons, T. 1996; Leu, T. H. and Maa, M. C. 2002).

To examine the role of FAK in the process of mesoderm migration, FRNK was co-injected with mem-GFP in the DMZ of four cell stage embryos. Following injection embryos were allowed to develop to late blastula stages and then the DMZ was dissected and dissociated. A mixture of injected and uninjected DMZ cells were then plated on FN coated wells and imaged. Dissociated FRNK over-expressing cells adhere but fail to spread (Figure 29N) and their migration rate is comparable to that of ectodermal controls (Figure 29M compare bar 2 and 5). The same is true for small anterior mesodermal explants, which remain rounded and do not spread on FN (Figure 29A-C). Furthermore, co-injection of FAK together with FRNK rescues spreading, and most of the FAK + FRNK co-expressing cells exhibit a migratory morphology, however their average migration rate is lower than that of uninjected controls (Figure 29D-F and M bar 3). In addition overexpression of FAK in ectodermal cells does not induce a migratory phenotype, nor does it increase the rate of migration of mesodermal cells (data not shown). These results suggest that FRNK can specifically and cell autonomously inhibit mesoderm migration on FN *in vitro* and suggest that FAK is necessary but not sufficient for this morphogenetic movement.

Recent data from Iioka et al have implicated paxillin, vinculin and tallin in convergent extension movements (Iioka, H., Iemura, S. et al. 2007). In order to address a potential role of FAK and focal adhesions in convergent extension two cell stage embryos were injected with FRNK (1ng) and memGFP (200pg, as a lineage tracer) at the animal pole, and animal caps were cut at late blastula. After activin induction the explants were either placed on BSA coated wells or on FN treated wells and were then allowed to develop until sibling controls reached late neurula. The explants that were placed in FN coated wells spread into a monolayer except in the regions expressing FRNK, which blocked spreading as well as intercalative behaviour towards the substratum (Figure 29D-F). Uninjected induced explants completely spread into a monolayer (data not shown). On the other hand, explants in BSA coated wells healed and underwent convergent extension movements leading to their elongation, which was identical in extent to that of uninjected control explants suggesting that FRNK expression does not affect convergent extension (Figure 29J-L).

FRNK has been shown to disrupt focal adhesion complexes (Heidkamp, M. C., Bayer, A. L. et al. 2002) and its expression in these explants although clearly disruptive with respect to spreading and adhesion on FN has no effect on the intercalative behavior of explants undergoing convergent extension. Despite this radial intercalation of adherent explants is blocked possibly due to the fact that underlying cells are unable to move and allow the overlying cells to intercalate towards the substratum. These results suggest that FAK is not

important for convergent extension but is required for mesoderm migration. The differences are most likely due to the cell-cell vs. cell-ECM interactions required by convergent extension and mesoderm migration respectively.

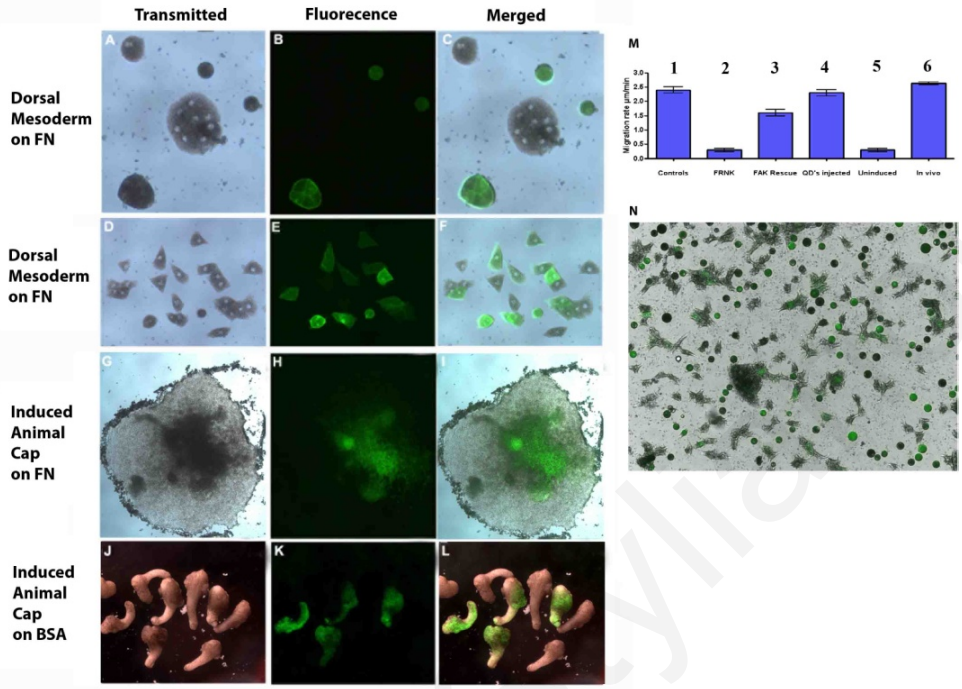

Figure 29. FRNK can inhibit mesodermal cell spreading and migration but has no effect on convergent extension movements. (A-C) Small dorsal marginal zone explants and individual cells are inhibited from spreading by FRNK overexpression (note the visibility of the nuclei in the GFP negative cells indicating that these cells are spread). MemGFP (100pg) coinjected with FRNK (500pg DMZ injection one out of two blastomeres) serves as linage tracer of FRNK expressing cells. (D-F) Co-injection of FAK (50pg) can rescue the FRNK phenotype. The majority of cells expressing both FAK and FRNK together with memGFP as a marker spread and display a migratory morphology. (G-I) FRNK expressing regions of activin induced animal caps placed on fibronectin coated slides exhibit no intercalative behaviour towards the substratum and remain multilayered appearing dark *in trans*mitted light illumination (G). A total of 500pg of FRNK was injected in two out of four animal pole blastomeres of four cell stage embryos and the animal caps were dissected (stage 8) induced with activin and placed on FN coated wells. (J-L) Expression of FRNK (two blastomeres of two-cell stage embryos were injected at the animal pole with FRNK 500pg per blastomere) does not affect convergent extension. FRNK was co injected with memGFP and GFP positive explants elongate to the same extent as controls (20 injected embryos and 20 controls embryos were used). (M) Migration rates of FRNK expressing mesodermal cells (1) are similar to those of animal cap controls (5). FRNK was injected in both blastomeres (500pg per blastomere) of two cell stage embryos. Co injection of FAK (50pg per blastomere) with FRNK raises the migration rates of these cells significantly (3). QD labeling does not affect migration rates of induced mesodermal cells (4). *In vivo* migration rates (6) are slightly higher than the rates

of *in vitro* rates (1). (N) Merged still frame from a time lapse movie used to calculate migration rates of FRNK expressing (GFP positive) and control mesodermal cells. The majority of FRNK expressing cells remain rounded up. 500pg of FRNK was injected with 100pg of GFP in one out of two blastomeres of two cell stage embryos (Stylianou, P. and Skourides, P. A. 2009).

3.2.3 Imaging FRNK expressing mesoderm *in vivo*

Since FRNK can inhibit mesoderm migration *in vitro*, we wanted to determine the effects of FRNK expression *in vivo.* Dorsal mesoderm is the tissue most actively engaged in this type of morphogenetic movement (Wacker, S., Brodbeck, A. et al. 1998). We therefore injected FRNK at the dorsal marginal zone of four cell stage embryos in both dorsal blastomeres (the injections were made at the dorsal most region of the embryo as close to the cell-cell boundary as possible, 500pg per blastomere). Figure 30A shows the range of deformities observed. In most embryos the blastopore failed to close, which led to neural tube closure problems in the more severe cases. 83% (n=31) of FRNK injected embryos failed to reach blastopore closure compared to 0% (n=27) of mem-GFP injected embryos (Table 5). The FRNK injected embryos which gastrulated normally were morphologically normal but blastopore closure was delayed. These results are in agreement with previous data showing that use of adhesion blocking antibodies and peptides (Ab´s against fibronectin and RGD containing peptides) leads to a delay of or failure of blastopore closure (Ramos, J. W. and DeSimone, D. W. 1996; Winklbauer, R. and Keller, R. 1996). Evidence of the specificity of the FRNK phenotype was established by co-injection of FAK which can rescue the FRNK phenotype and significantly reduce (but not eliminate) the number of embryos failing to reach the tadpole stage. 43% (n=44) of FAK co injected embryos failed to reach blastopore closure compared to 83% (n=31) of FRNK alone. The partial rescue of the FRNK phenotype by co-expression of FAK is consistent with the partial rescue observed in dissociated cells (Figure 30D – F and M).

Since the dorsal most mesoderm is more migratory, we postulated that FRNK expression in less active tissues would be less detrimental to the gastrulation process. This prediction was tested by marginal zone injections of FRNK into four cell stage embryos that were progressively more lateral. As the injections become more lateral (away from the DMZ) the percentage of embryos failing to close their blastopore decreases dramatically further supporting the prediction that blocking mesoderm migration in less active tissues should result in milder phenotypes (Figure 30C). Whole mount in situ staining of stage12, 12 ½ embryos injected with FRNK (at the DMZ of four cell embryos) shows that FRNK expression does not affect mesoderm specification as evidenced by the undisturbed

expression of Xbra. However the positioning of chordamesoderm in FRNK injected embryos is mildly affected as shown in Figure 30D, E (compare FRNK injected to control).

We went on to image FRNK expressing mesoderm *in vivo* with the use of NIR QD´s. Four cell embryos were injected with FRNK-GFP mRNA (1ng) in both dorsal blastomeres at the marginal zone. Embryos were allowed to develop to the 32 cell stage and were then injected at the B1 or C1 blastomeres with QD´s. Unlike controls where individual cells are seen migrating towards the animal pole, in embryos injected with FRNK at both dorsal blastomeres no QD labeled cells were detected migrating on the BCR (data not shown). In an effort to visualize FRNK expressing cells we went on to inject four cell stage embryos with FRNK-GFP mRNA (500pg) in one out of two dorsal marginal zone blastomeres. At the 32 cell stage two blastomeres one on the uninjected and one on the FRNK-GFP injected side were injected with non targeted QD´s. The embryos were allowed to develop and imaged at gastrula stage. As shown in Figure 31 (A-E) very few cells can be seen migrating out of the GFP positive region (movie 3). Despite the fact that GFP negative cells can be seen reaching the top of the BCR the FRNK injected embryos failed to produce cells that were clearly separated as in the controls suggesting that FRNK expression in one hemisphere influences the migration of cells in the other (Figure 31 A-E). In addition the few cells coming out of the GFP positive region lack directionality and only a small number of these cells reach the top of the BCR. The experiment was repeated using stage 9.5 injections in the blastocoel with Qtracker® 800 Cell Labeling QD´s. As seen in Figure 31 (Figure 31F-G), FRNK positive cells that are in direct contact with GFP negative cells initially migrate directionally towards the top of the BCR possibly pulled by neighbouring FRNK negative cells but are soon left behind and move randomly. GFP positive cells that are not in close proximity to GFP negative mesodermal cells fail to migrate towards the top of the BCR. This is to our knowledge the first time that inhibition of this morphogenetic movement has been imaged *in vivo* and offers strong evidence regarding the *in vivo* inhibition of mesoderm migration by FRNK (Figure 31K-O). The behavior of the FRNK expressing cells correlates well with the *in vitro* data further strengthening our conclusion that FAK is necessary for this movement.

Table 5- FAK (100pg) can partially rescue the FRNK (1ng) induced blastopore closure failure.

	memGFP	FRNK+memGFP	FRNK+FAK+memGFP

Normal	27/100%	5/17%	25/67%
Gastrulation failure due to Blastopore closure failure	0/0%	26/83%	19/43%
Total number injected	27/N/A	31/N/A	44/N/A

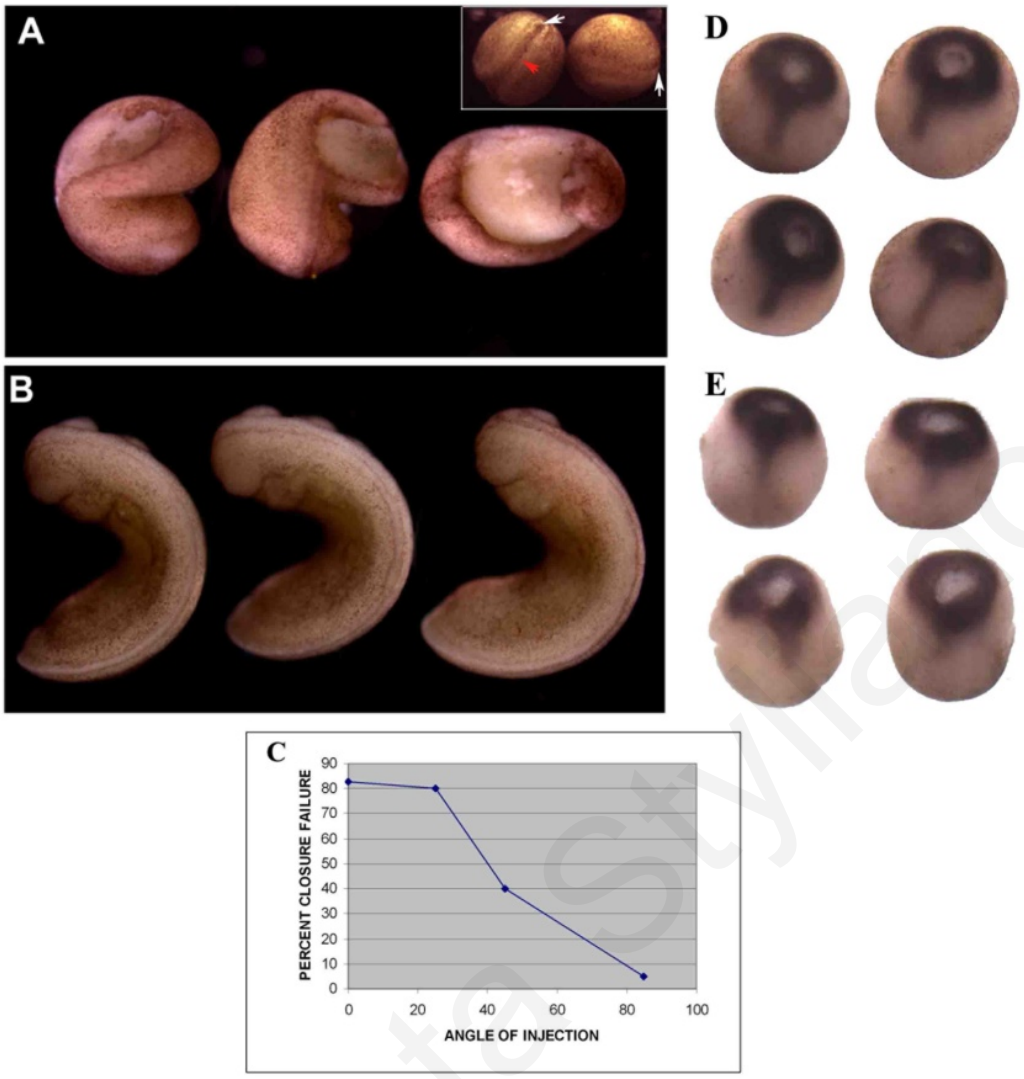

Figure 30. FRNK injection inhibits mesoderm migration and results in failure of blastopore closure which often prevents neural tube closure. FRNK injected embryos (two blastomeres of four-cell stage embryos were injected at the dorsal marginal region with FRNK 500pg per blastomere) fail to close their blastopore (A) compared to uninjected sibling embryos (B). This often leads to failure of closure of the posterior regions of the neural tube. Coinjection of FAK (50pg per blastomere) rescues the phenotype (inset of A) and the blastopore closes completely in the majority of embryos (white arrows). (C) As the injections become more lateral (away from the DMZ) the percentage of embryos failing to close their blastopore decreases dramatically. (D-E) *Whole mount in situ hybridization* for Xbra indicates that mesoderm specification is not affected in FRNK expressing embryos (two blastomeres of four-cell stage embryos were injected at the dorsal marginal region with FRNK 500pg per blastomere). Injected embryos (E) appear to have a slightly shortened trunk compared to controls (D) (Stylianou, P. and Skourides, P. A. 2009).

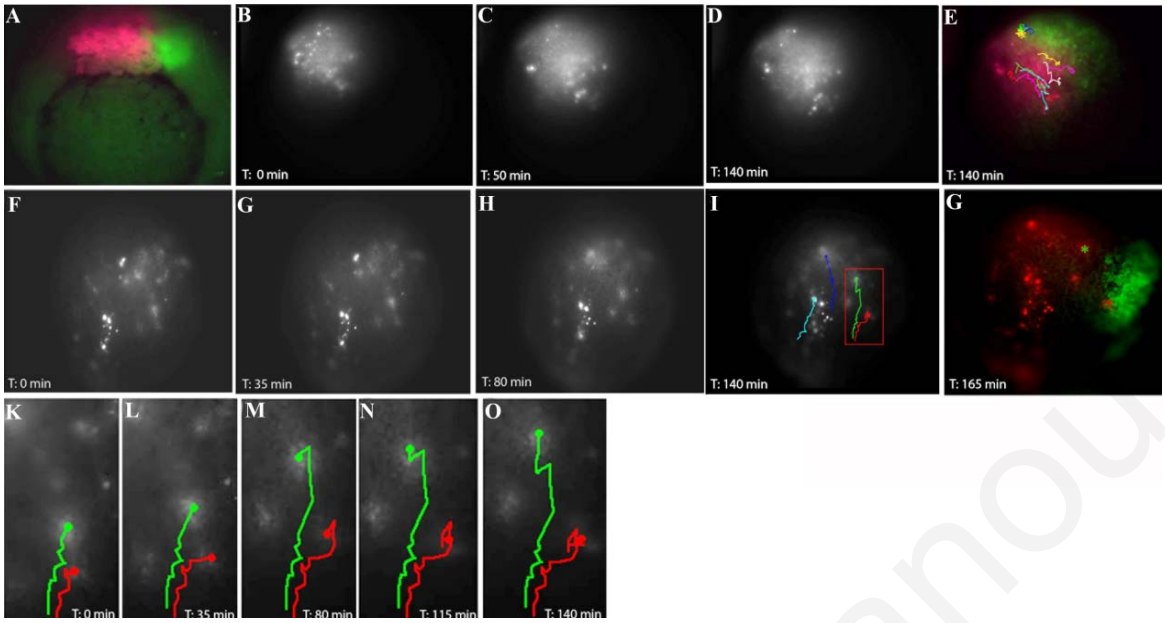

Figure 31. Injection of Qtracker QD´s at mid gastrula enables visualization of the mesodermal mantle with single cell resolution. FRNK expressing cells fail to migrate directionally. (A-E) Five frames from a 4D time lapse movie of an embryo injected with NIR QD's at the DMZ at the 32 cell stage. Frames are 2D maximum intensity projections of deconvolved z-stacks. Individual cells are clearly visible as they migrate towards the top of the BCR. One out of two blastomeres was injected with GFP-FRNK (500pg) at the four cell stage followed by QD injections of two blastomeres (one on the left and one on the right hemisphere) with NIR QD´s at the 32 cell stage. (F) Shows the GFP and QD labelled regions around the dorsal lip of the blastopore. Cells from the GFP negative side of the embryo are seen migrating directionally on the BCR (see tracks in I) while the majority of the cells from the GFP positive site fail to do so and move randomly. (F-G) Five frames from a time lapse movie of an embryo injected with Qtracker NIR QD´s inside the blastocoel. The embryo was injected with GFP-FRNK (500pg) at the four cell stage in one out of two dorsal blastomeres. FRNK expressing cells fail to migrate towards the BCR. (K-O) Same embryo as in (F) through (G) magnified and tracked (tracked region boxed in I). Tracking of cells at the border area between the FRNK expressing and non expressing regions of the embryo (FRNK expressing-red track, non expressing-green track). Initially the FRNK expressing (GFP positive) cells move towards the top of the BCR with the non expressing cells but then begin to slow down and move randomly. Final positions of tracked cells shown in (G) (green star GFP negative cell red star GFP positive cell)(Stylianou, P. and Skourides, P. A. 2009).

3.3 The role of the autophosphorylation site Tyrosine 397 of Focal Adhesion Kinase during *Xenopus* development

3.3.1 Y397FFAK overexpression leads to the failure of blastopore closure (Activation of FAK is important during gastrulation (phenotype *in vivo*))

Transgenic studies in the mouse have addressed the role of FAKs major site of autophosphorylation Tyr397 as well as the role of the kinase activity. Mutant FAK^{Δ} (deleted exon 15 which contains major phosphorylation site Y397) is expressed at normal levels and retains its kinase activity but $FAK^{\Delta/\Delta}$ mouse embryos display various defects (haemorrhages, edema, multiple organ abnormalities) and overall developmental retardation at E13.5-14.5 followed by death (Corsi, J. M., Houbron, C. et al. 2009). $FAK^{K454R/K454R}$ (K454 mutated to R in the catalytic domain) mutant embryos also exhibited embryonic lethality (lethal at E9.5) and extensive defects in blood vessel formation and disorganized EC (endothelial cells) pattering (Lim, S. T., Chen, X. L. et al. 2010). These results suggested that both FAK kinase activity and autophosphorylation on Tyr397 are necessary for normal development.

Since FAK is nessesary for mesoderm migration and in order to get a better understanding of the role of FAK in this type of cell movement we decided to examine the role of specific residues of FAK in *Xenopus*. We examined the Y397FFAK (mutant in the major autophosphorylation/activation site on FAK) (Eide, B. L., Turck, C. W. et al. 1995), K454RFAK (Kinase-dead, the catalytic residue is mutated) (Hildebrand, J. D., Schaller, M. D. et al. 1993) and D395AFAK (allows Src binding to pY397, but not PI3K) (Reiske, H. R., Kao, S. C. et al. 1999) point mutants.

The three point mutants were initially evaluated to determine their effect on the overall development by expressing them in the dorsal involuting mesoderm. We coinjected GFP (100pg) with either FRNK (as a positive control for the experiment), FAK, Y397FFAK, K454RFAK, Y397FΔFAK or D395AFAK at the dorsal marginal zone of four cell stage embryos in both dorsal blastomeres. The injections were made at the dorsal region of the embryo as close to the cell-cell boundary as possible (125pg total per blastomere). Figure 32 shows a slight delay in blastopore closure which was observed in all mutant-FAK injected embryos. FRNK injected embryos that were used as a positive control of the experiment showed a delay of the blastopore closure which was more pronounced than the other mutants that were used albeit at a higher dose (Figure 32E, 500pg per blastomere). Of the three point mutants used, surprisingly Y397FFAK gave the strongest phenotype

since injected embryos were delayed the most in terms of blastopore closure (Figure 32B). The reasons behind this difference we believe lie in the fact that in the trasgenics no requirement for dominant negative function is present since no endogenous WT FAK is present in these animals. However in the *Xenopus* context we would see an effect only if the injected construct acts as a dominant negative. Unlike Tyr397 in the K454RFAK mutant can be *in trans* phosphorylated by endogenous FAK enabling recruitment of Src and downstream signaling (Figure 35C). On the other hand Y397FFAK would presumambly be able to compete FAK off of its signaling complexes but would then be unable to recruit Src thus blocking downstream signaling. Expresison of K454RFAK led to a slight delay while the D395AFAK mutant did not have any discernible phenotype at this stage (Figure 32C, F). The experiment was repeated with 500pg total RNA coinjected with 100pg GFP using the Y397FFAK and K454RFAK mutants. The phenotypes using this amount of RNA were more prominent. In the case of Y397FFAK, most of the embryos failed to close the blastopore however the blastopore of K454RFAK injected embryos closed normally (Figure 32H, I).

Since the expression of Y397FFAK led to a strong phenotype with regards to gastrulation movements, we decided to examine this mutant more closely and determine what effects the expression of this point mutant has on cell movements. We begun by undertaking a more careful dose response experiment. Injections were made at the dorsal region of the embryo as close to the cell-cell boundary as possible, as described above (Figure 33, total amount for both DMZ blastomeres). Figure 33 shows the range of Y397FFAK that was injected into embryos and the phenotypes at stages 12-13 and 27. As the amount of the RNA, injected increased, the failure of bastopore closure was more intense. At the amount of 260pg, 90% of the embryos gastrulated normally and 10% of the embryos failed to close the blastopore (Figure 33A, B). However, when injecting embryos with 520pg to 1040pg, the blastopore failed to close which in turn led to neural tube closure defects and in the more severe cases were followed by death (Figure 33C-E).

In order to establish the specificity of the Y397FFAK phenotype, rescue experiments were carried out. Coinjection of FAK (50pg per blastomere) can partially rescue the Y397FFAK phenotype and significantly reduce the number of embryos failing to reach the tadpole stage (Figure 34H, st.40). Figure 34 shows embryos injected at different stages at the DMZ with either Y397FFAK (as above) or with FAK for rescue. During early stages (stage 12) most of the FAK injected embryos survived and a partial rescue the Y397FFAK phenotype was observed (Figure 34B, C). At later stages however, fewer embryos from both mutant

and rescue injected groups survived (Figure 34E-F, H-I). These results indicate that phosphorylation on Tyr397 may be critical during gastrulation in *Xenopus* embryos.

These results are in agreement with our previous published data showing that FRNK injected embryos failed to reach blastopore closure which led to neural tube closure problems compared to the non injected embryos (controls) (Stylianou, P. and Skourides, P. A. 2009). From our results it seemed as though autophosphorylation of FAK was required for blastopore closure during gastrulation of the embryo. Therefore, we wanted to test its importance in the process of mesoderm migration.

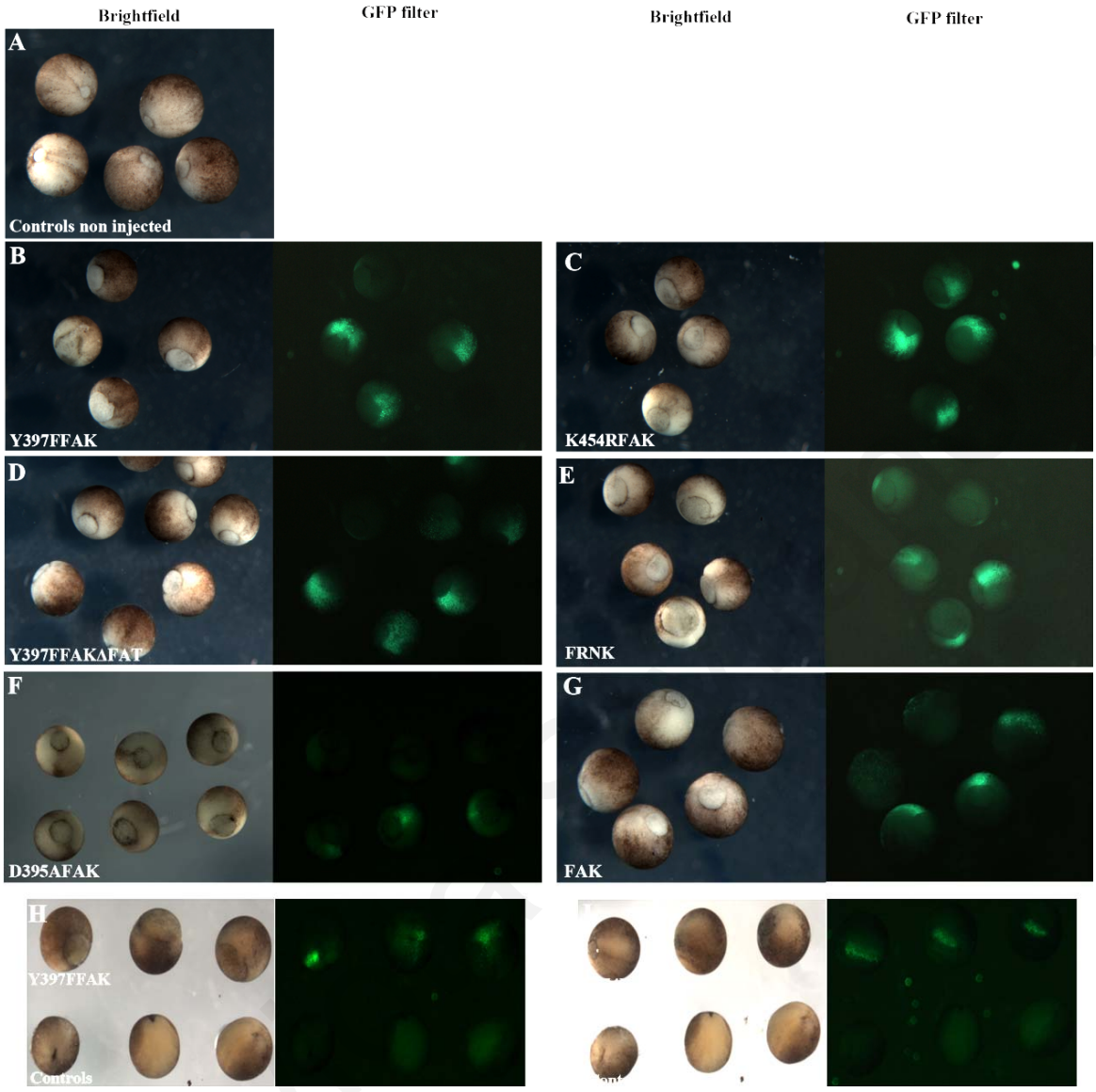

Figure 32. Different variants of FAK injected to embryos and these gastrulated normally but blastopore closure was delayed. (A) Controls non injected embryos at stage 12. (B-G) Co injected GFP 100pg with each mutant at the dorsal marginal zone of four cell stage embryos. The injections were made at the dorsal region of the embryo as close to the cell cell-cell boundary as possible. (H-I) Repeated the injections with Y397FFAK (H) and K454RFAK (I) with 500pg total RNA. Y397FFAK injected embryos (H) blastopore failed to close as the controls embryos gastrulated normally.

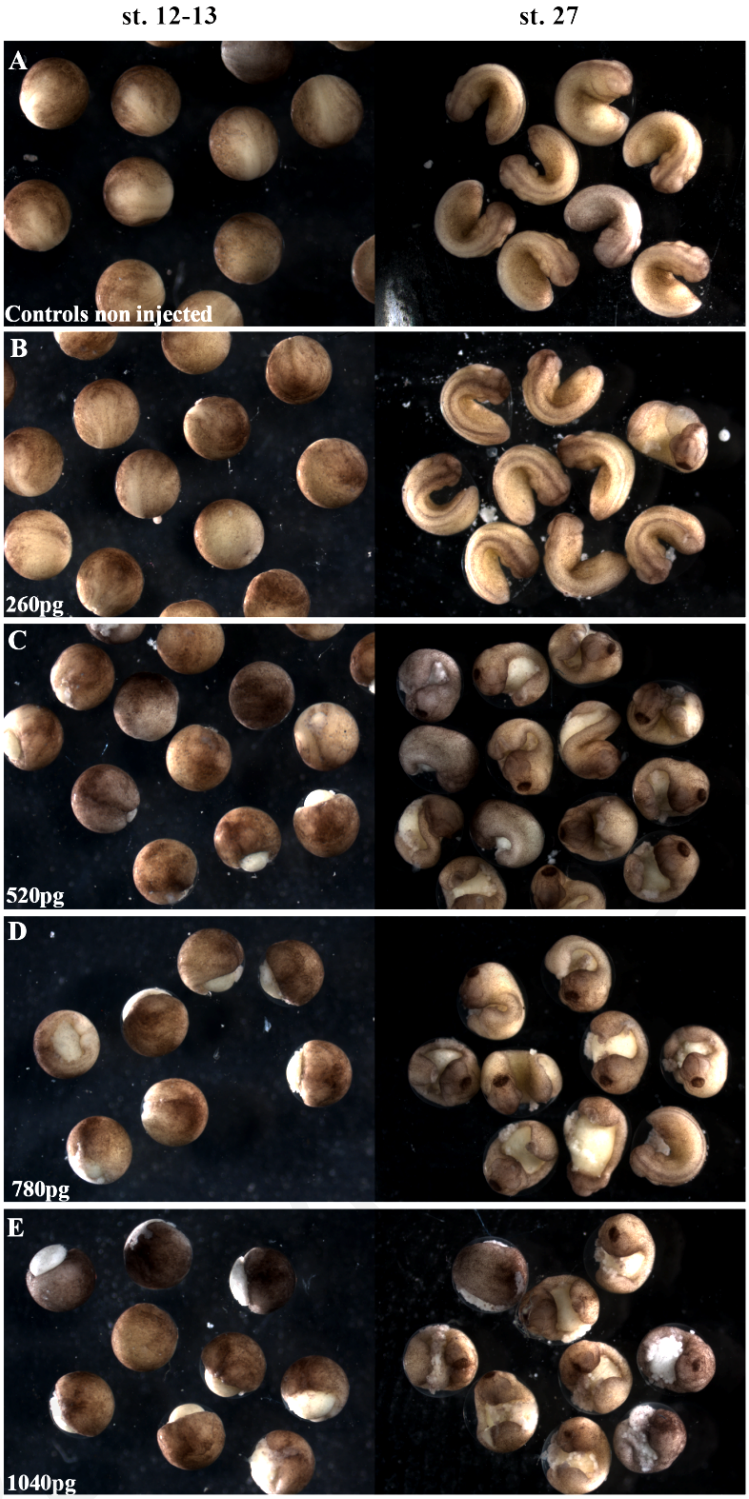

Figure 33. Dose response of Y397FFAK injected embryos. (A) Images of non-injected control embryos at the same stages as the injected embryos. (B -E) Embryos injected at the dorsal side into two blastomeres of the four cell stage embryo. The injections were made at the dorsal region of the embryo as close to the cell cell-cell boundary as possible. First column at stage 12-13 and second column at stage 27. Total RNA concentration injected was 260pg (B), 520pg (C), 780pg (D) and 1040pg (E). From the images it's obvious that more RNA causes more severe phenotype at the injected embryos. In most embryos the blastopore failed to close which led to neural tube closure problems (C-E).

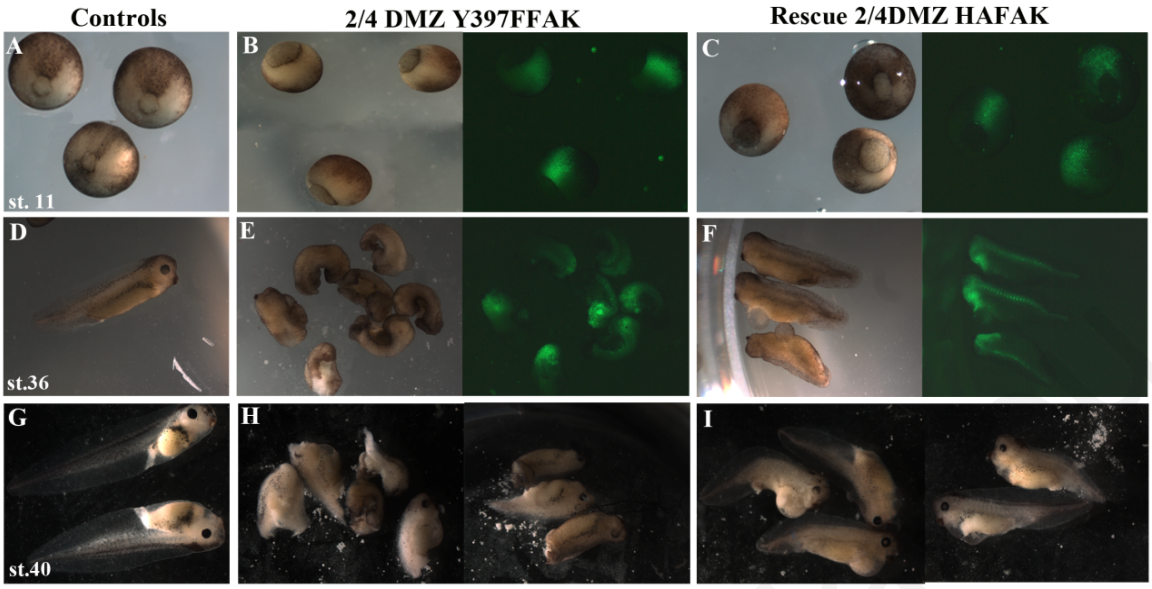

Figure 34. Y397FFAK phenotype can be rescued when injected with wild type FAK. (A-C) Embryos imaged at stage 12. Injected embryos show a delay in blastopore closure (B) compared with the controls (A) and it seems as though this phenotype can be partially rescued (C). Embryos were co-injected with GFP 100pg and either 500pg Y397FFAK or FAK (100pg total) into both dorsal blastomeres of the four cell stage embryo and left to develop. . (D-F) At stage 36 most of the embryos died, however, the ones which survived showed blastopore closure defects which led to neural tube closure problems (E). Partial rescue of Y397FFAK phenotype by expression of FAK led to the closure of the neural tube (F). (G-I) Same embryos left to develop to stage 40 (G) all live embryos were imaged. Most of the embryos injected with Y397FFAK either died or showed with posterior defects (H) (shorter trunks) and the embryos that expressed FAK were partially rescued (I).

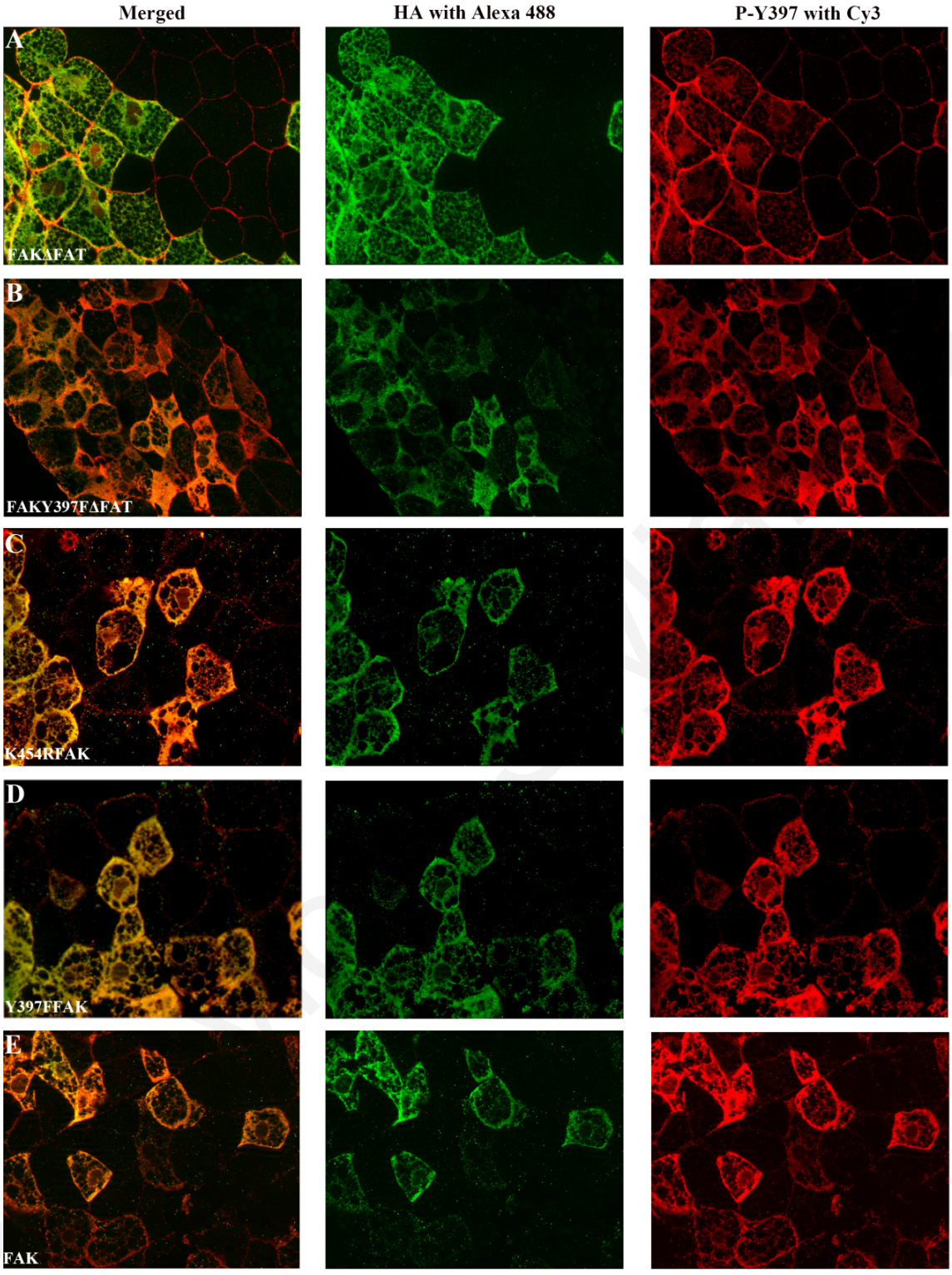

Figure 35. Phosphorylation status of the embryos after the overexpression of the mutants. (A-E: first column) Merged images of mid-sagittal optical section of stage 12 embryos with double staining. 500pg of each mutant were injected in the DMZ site of the embryo, fixed at stage 12, sagittaly sectioned, permeabilized and proceed to immunofluorescence assay. For HA mutants monoclonal HA antibody was used stained with Alexa 488 (second column: green) and for activated FAK polyclonal anti-FAKPY397 used stained with Cy3 (third column: red).

3.3.2 Phosphorylation of the Y397 autophosphorylation site of FAK is important for the spreading of mesodermal cells *in vitro*

It has been shown that the Tyr397 autophosphorylation site of FAK is crucial for the normal kinetics of cell spreading. In fact, expression of the dominant negative mutant Y397FFAK in FAK null cells has an inhibitory effect on cell spreading and cell migration (Cary, L. A., Chang, J. F. et al. 1996; Owen, J. D., Ruest, P. J. et al. 1999). A requirement for FAK Tyr397 in cell spreading response was also indicated by the fact that inhibition of spreading by FAK C-terminal domain (FRNK) cannot be rescued by co-expression of the Y397FFAK mutant. Moreover, the same FRNK expressing cells can be significantly rescued by co-expression of a kinase defective mutant (K454RFAK) (Richardson, A., Malik, R. K. et al. 1997). Also, overexpression of K454RFAK in CHO cells increases migration and total phopshorylation of the endogenous FAK (Cary, L. A., Chang, J. F. et al. 1996).

Since Y397FFAK expression can block blastopore closure *in vivo*, we wanted to determine the effects of Y397FFAK expression on mesoderm morphogenesis. Dorsal mesoderm is the most moprhogenetically active tissue during gastrulation; therefore, the failure of the balstopore closure may be due to a problem with mesoderm migration or convergent extension. For this reason we examined the effect of Y397FFAK expression on these two movements using well established *in vitro* assays.

Injections of histone GFP (100pg) with mutants of FAK (250pg) in one animal blastomere at the four cell stage were carried out. Following injections, embryos were allowed to develop to stage eight and then animal caps were dissected and dissociated in CMFM. Dissociated cells were induced with activin 10ng/ml and seeded on fibronectin (50μg/ml) coated coverslips. 95% of dissociated Y397FFAK overexpressing cells failed to spread and remained rounded (Figure 36A) compared to the control non injected cells (10% percentage).

It is known that FAT region is necessary and sufficient for the localization of FAK to focal adhesions (Hildebrand, J. D., Schaller, M. D. et al. 1993). In order to further examine the way that Y397FFAK mutant excerts its effect in this context we generated a Y397F mutant in which the FAT domain was deleted. If the mutant was acting via competition of FAK off of focal adhesions complexes in a similar fashion as FRNK has been shown to act we would expect this deletion to abolish the effect on cell spreading. Surprisingly however, overexpresson of the Y397FΔFAT showed a similar level of spreading inhibition as full length FAK (Figure 36B, D). To further examine these mutants and the specificity of the

phenotype, we continued with rescue experiments. Half of the embryos that were injected with mutants of FAK (250pg with memGFP 100pg) were rescued with 100pg of FAK (coinjected with memcherry 50pg, 2 out of 4 AP blastomeres) and the embryos were left to develop to stage 8. At late blastula animal caps were dissected and dissociated in CMFM. After activin induction cells were plated on fibronectin coated coverslips (50μg/ml) and imaged. Co-injection of FAK together with Y397FFAK rescued spreading and most of the FAK+Y397FFAK co-expressing cells (up to 91%) exhibited typical spreading morphology (Figure 37A). The same results were observed in FAK+K454RFAK coexpressing cells but at percentage lower than 78% (Figure 37B). Additionally, FAK+Y397FΔFAT coexpressing cells up to 72% of the cells spread (Figure 37C). Overall these results suggest that the Y397F mutant does not excert its effect at the FAs but rather acts on signaling complexes of FAK unrelated to FAs.

It is known that embryonic fibroblasts of $FAK^{-/-}$ mice have defects in migration and reduction in the rate of cell spreading. These fibroblasts show an increase in the number and size of the peripherally localized adhesions (Ilic, D., Furuta, Y. et al. 1995; Corsi, J. M., Houbron, C. et al. 2009). Similar types of adhesions appear in $FAK^{\Delta/\Delta}$ cells (deleted exon 15 which contains major phosphorylation site Y397) which exhibit multiple thinner membrane protrusions and show delayed spreading compared to $FAK^{+/+}$ mouse embryonic fibroblasts (MEFs) cultured *in vitro* (Corsi, J. M., Houbron, C. et al. 2009). These results are in agreement with our findings showing a spreading defect in adherent mesodermal cells expressing the Y397F mutant. Also MEFs from $FAK^{K454R/K454R}$ exhibit enhanced focal adhesion formation but decreased cell migration (Lim, S. T., Chen, X. L. et al. 2010). This is also in agreement with the limited effect that this mutant has on mesoderm migration.

As discussed above the failure of the blastopore to close in Y397FFAK injected embryos could be due to effects on either convergent extension or mesoderm migration. In order to address the potential role of the autophopshorylation site of FAK and focal adhesions in convergent extension, two cell stage embryos were injected with Y397FFAK (250pg per blastomere) and histoneGFP (50pg per blastomere, as a lineage tracer) at the animal pole. Animal caps were dissected at the late blastula stage and after activin induction (15ng/ml) the explants were placed in agarose coated wells. The embryos were allowed to develop until the sibling controls reached late neurula stage. The injected explants healed but they did not elongate. The uninjected control explants healed and underwent convergent extension movements leading to their elongation which suggests that Y397FFAK

expression does affect convergent extension (Figure 37D, white stars: control caps). The above phenotype could not be rescued using overexpression of full length FAK (data not shown). The above results suggest that expression of the Y397FFAK mutant somehow blocks convergent extension movements and mesoderm migration. However the inability of WT FAK to rescue the convergent extension movements suggests that expression of Y397FFAK leads to irreversible changes in the tissue. It is important to note that in the animal cap elongation assays correct tissue polarity needs to be preserved. Cells not only need to retain the ability to intercalate but they need to do so in precise orientation. So while the mesoderm migration assays only tests a cell autonomous effect the convergent extension assays tests tissue polarity as well which may be difficult to rescue. Another possibility is that expression of this mutant leads to changes in cell fate specification and specifically that it may affect mesoderm specification. If this is the case one would expect both these movements to be affected.

To address this possibility *Whole mount in situ hybridization* analysis was performed on stage 12 and stage 13 embryos which were injected with Y397FFAK in order to examine if this FAK mutant affects embryonic mesoderm specification. For these experiments either one of the two DMZ blastomeres at four cell stage or one of two AP blastomeres of two cell stage embryos were injected with Y397FFAK. Expression of Y397FFAK decreased the expression levels of the mesoderm marker Xbra (half of the Xbra is missing) (Figure 38B). However, Y397FFAK did not affect Chordin (mesoderm marker, neural tube), Sox2 (neural plate marker) or Sox3 (neural plate marker) expression (Figure 38D, F, H). These markers showed levels of expression comparable to uninjected controls embryos (Figure 38A, C, E, G). We then went on to detect the Y397FFAK positive cells in the embryo with the help of an immunofluorescence assay. After whole mount in situ hybridization, half of the embryos were saggitaly sectioned and an immunofluorescence assay was carried out (Figure 39A-D). We couldn't detect a correlation with loss of Xbra and injection sites; only a reduction in the belt of the Xbra expression in the whole embryo (Figure 39E). RT PCR analysis was performed in order to obtain more quantitative data and in this case Y397FFAK expression lead to a clear reduction of Xbra (Figure 39F). These results were quite diffucult to explain since Y397FFAK expression appears to reduce the expression levels of Xbra but this appears to be a non cell autonomous effect. However it is possible that expression of this construct alters mesodermal patterning without blocking mesoderm induction. This would explain the inability to rescue convergent extension since the amount of FAK used for the rescue would in theory affect the type of mesoderm being

induced. Failure to specifically induce chordal mesoderm would in effect abolish convergent extension movements even if prechordal or lateral mesoderm were in fact induced. More work is required in order to point the precise effects of Y397FFAK expression on mesoderm patterning and polarity in order to determine precisely why a) Y397FFAK expression blocks convergent extension movements b) why this block cannot be rescued by WT FAK expression c) how the expression of a cytosolic protein affects Xbra expression in a cell non autonomous manner.

In summary, our results add to a growing body of evidence implicating FAK as a positive regulator of cell spreading and migration. Our findings confirm the essential role of the FAK autophosphorylation site Tyr397 on cell spreading and migration and in addition suggests a possible role for FAK in mesodermal patterning and polarity.

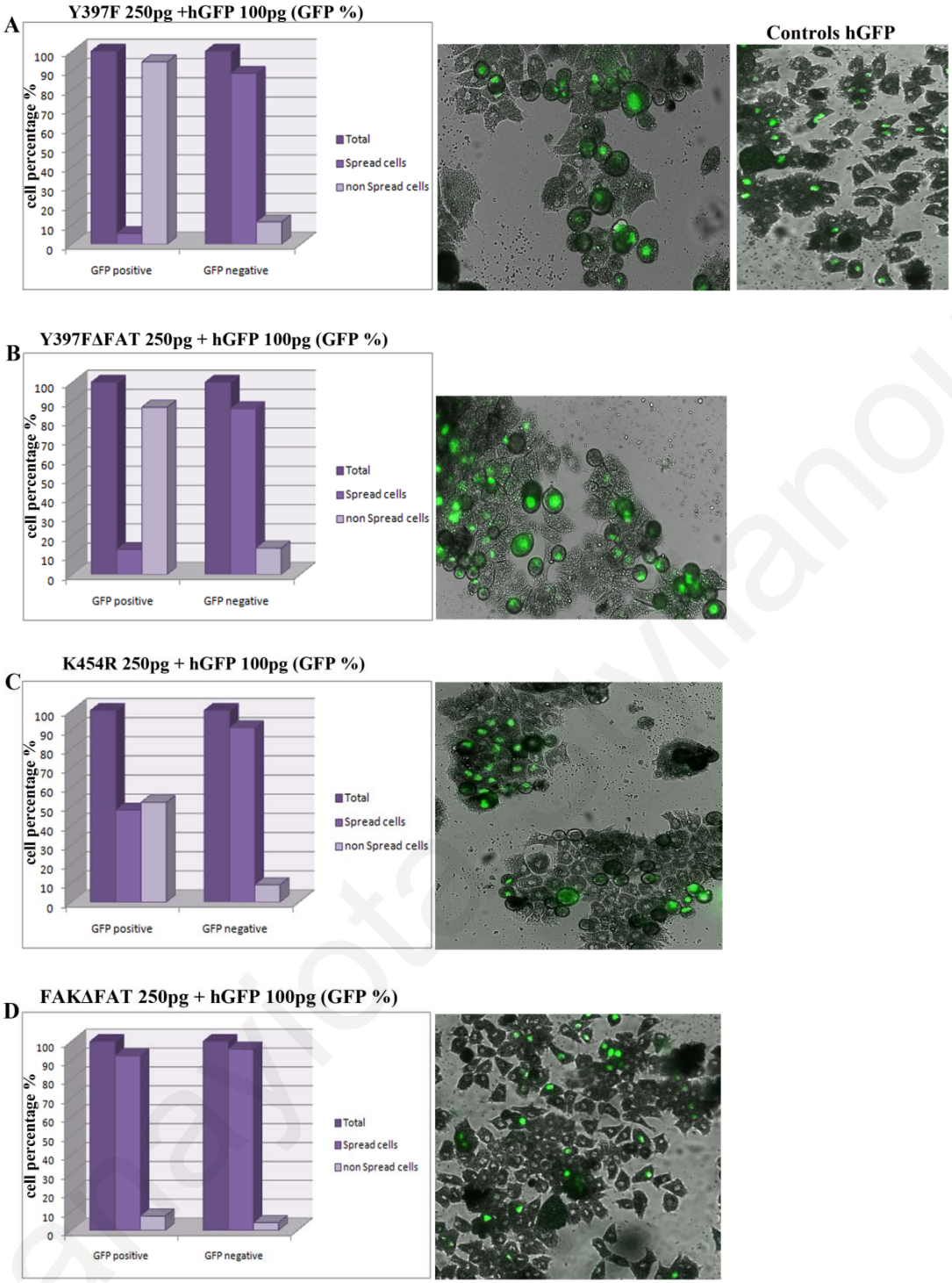

Figure 36. Y397FFAK can inhibit mesodermal cell spreading. (A-D, first column) Percentage of GFP positive (expressing mutants) and GFP negative cells (controls) in terms of spreading. Second column the images are an example of merged still frame used to calculate the percentage of spreading and non-spreading cells which expressed each of the mutants on fibronectin coated coverslips. HistoneGFP positive cells are the cells that expressed the mutants. 94.5% (A), 87% (B) 52% (C) and 7.6% (D) of mutants expressing cells are rounded up. Third column the image is an example of merged still frame of injected cells only with histoneGFP. All cells are spreading normally.

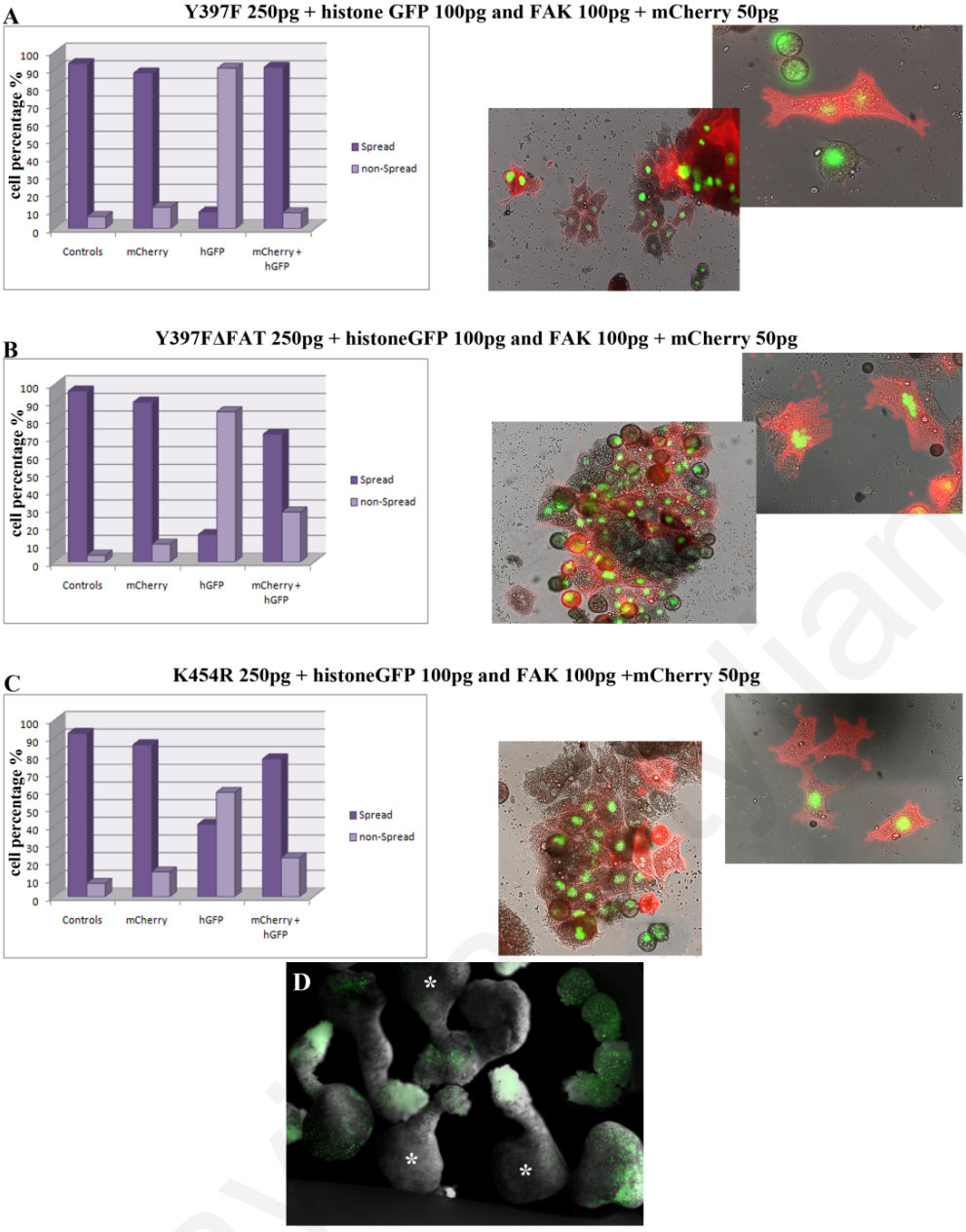

Figure 37. Rescue of spreading using 100pg HA FAK. (A-C, first column) Percentage of spreading and non spreading cells in four categories: control (non-injected) embryos, FAK 100pg (memcherry 100pg for lineage tracing), mutant 250pg (hisGFP 100pg for lineage tracing) and co-injected FAK with mutant. Second column: the images are an example of merged still frame used to calculate the percentage of spreading and non-spreading cells which expressed each of the mutants on fibronectin coated coverslips. HisGFP + memcherry positive cells are the cells that expressed the mutants rescue with full length FAK. Y397FFAK+FAK expressing cells are almost totally rescue (91.2%, A). The cells display a typical spreading morphology. (D) Expression of Y397FFAK (two blastomeres of two cell stage embryos were injected at the animal pole with Y397FFAK 250pg per blastomere) does affect convergent extension. Y397FFAK co-injected with histoneGFP explants do not elongate to the same extent as the non-injected controls embryos (white stars).

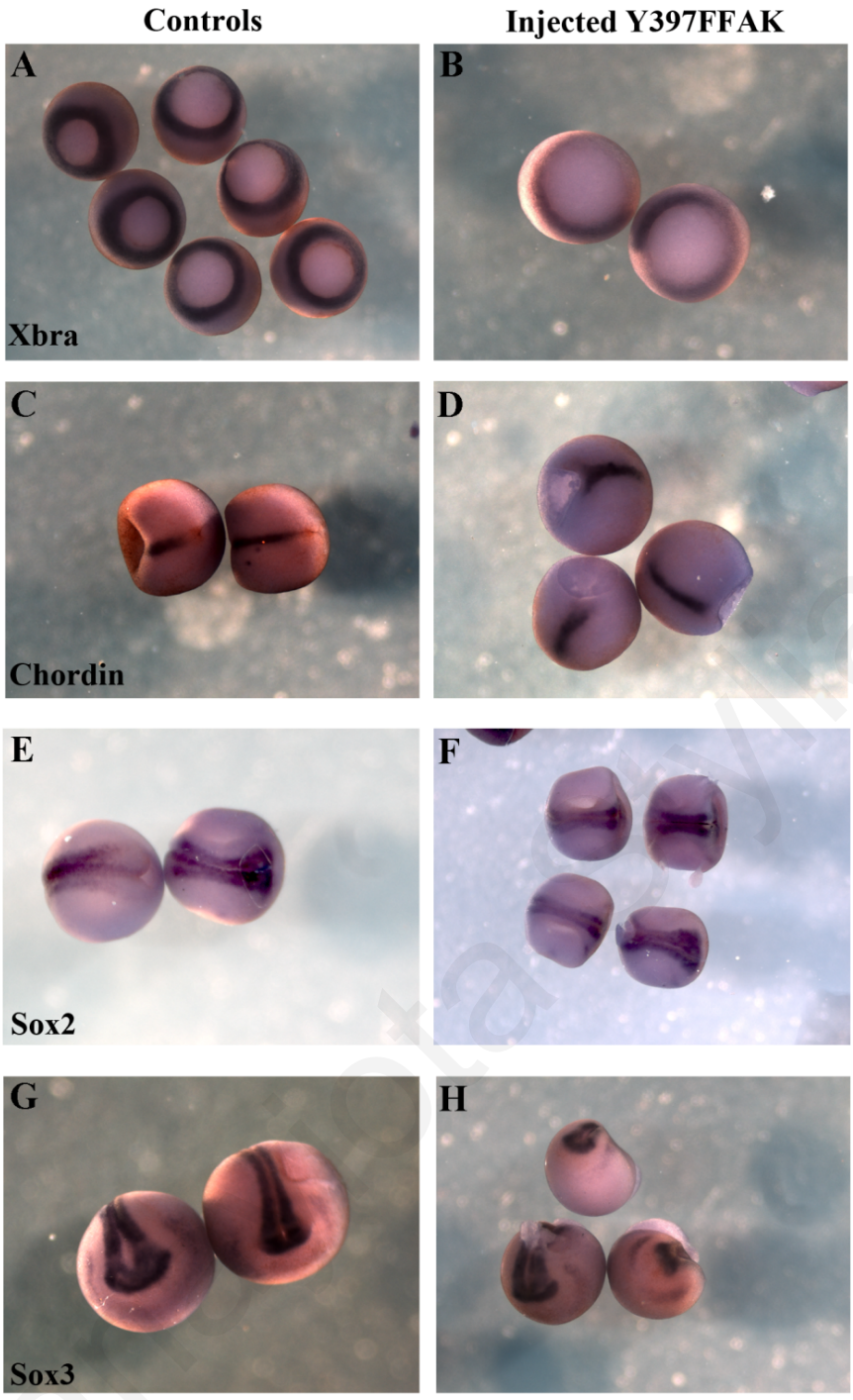

Figure 38. *Whole mount in situ hybridization* in controls and Y397FFAK injected embryos. (A, B) *Whole mount in situ hybridization* for Xbra indicates small reduction of the expression of the marker (half region of the belt missing) in the injected embryos with Y397FFAK (B) compared to the controls (A). (C, D) The expression of chordin is the same as the control embryos and the embryos injected with Y397FFAK. The injections of the embryos (B, D) were performed in one of the two dorsal blastomeres of four cell stage. The injections were made at the dorsal region of the embryo as close to the cell-cell boundary as possible. Similar expression patterns of Sox2 (E, F) and Sox3 (G, H) markers between controls (E, G) and injected embryos with Y397FFAK were observed (F, H). One dorsal blastomere of the animal pole of four cell stage embryo was injected.

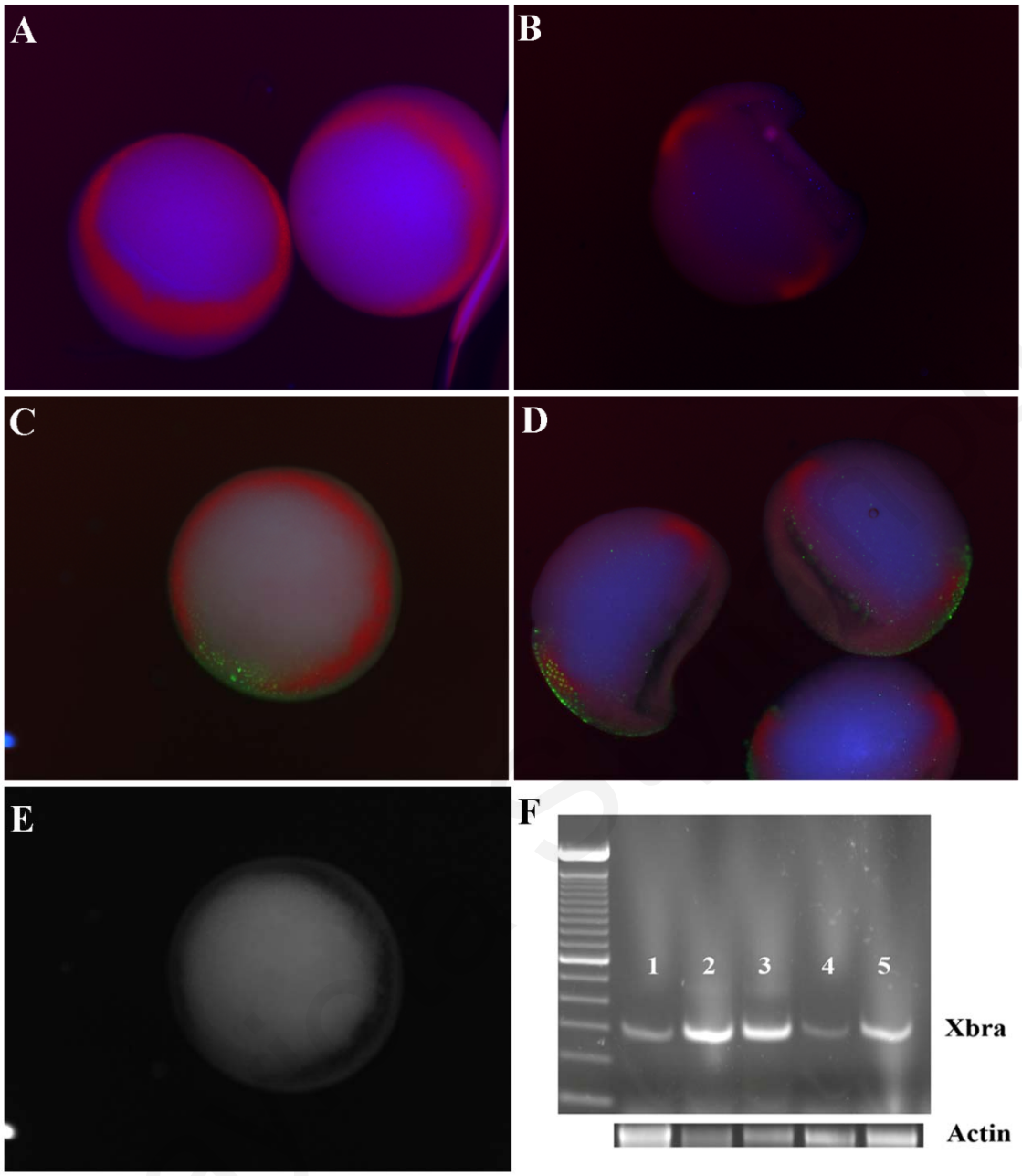

Figure 39. Xbra expression indicates that mesoderm specification in not affected in Y397FFAK injected embryos. (A, B) Control embryos, whole (A) and sagittal sectioned (B) expressing Xbra. (C, D) Injected embryos with Y397FFAK, whole (C) and saggital sectioned (D). In whole embryos a part of Xbra is missing (C) but in the sectioned (D) the pattern is the same as the control (B). (E) Injected embryo with Y397FFAK which shows absence of a portion of Xbra expression. (F) RT PCR from injected and control embryos. Lane 1-5: Y397FFAK animal caps, control non-injected animal caps, 2/2AP Y397FFAK injected whole embryo, 2/4DMZ Y397FFAK injected whole embryo, control non injected whole embryos. Reduction of the expression of Xbra in the injected animal caps and whole embryos compared to the controls.

3.4 Exploring the expression and phosphorylation of Focal Adhesion Kinase and its downstream targets

3.4.1 Expression and phosphorylation of Focal Adhesion Kinase during *Xenopus* development

In our effort to characterize the effects of the Y397FFAK mutant of FAK we examined the endogenous levels of phosphorylation of FAK. We noted that FAK was phosphorylated on Tyrosine 397 in all regions of the *Xenopus* embryo with elevation in the highly morphogenetic mesodermal tissues. FAK is phosphorylated on several residues either because of autophosphorylation in response to integrin signalling or because of the activity of other kinases such as Src. In addition, FAK phosphorylation on Tyrosine 397 is a response to growth factors or growth factor receptor clustering (Thomas, J. W., Ellis, B. et al. 1998; Lietha, D., Cai, X. et al. 2007; Chen, T. H., Chan, P. C. et al. 2011). The most important phosphorylation site of FAK is believed to be the Tyrosine 397 residue, which activates FAK (Schaller, M. D., Hildebrand, J. D. et al. 1994; Eide, B. L., Turck, C. W. et al. 1995).

Clustering of FAK at focal adhesions enhances this phosphorylation and this cluster becomes a binding site for the tyrosine kinase Src, which phosphorylates FAK on Tyrosine 576 and 577 to further activate FAK (Thomas, J. W., Ellis, B. et al. 1998). Another site of FAK phosphorylation is Tyr861 which is the major site of phosphorylation by Src (Calalb, M. B., Zhang, X. et al. 1996). Tyr861 phosphorylation enhances FAKs autophosphorylation at Tyr397 implying that integrin-mediated FAK Tyr397 phosphorylation is also regulated through cis-phosphorylation mechanisms (Leu, T. H. and Maa, M. C. 2002). In addition the FAT domain contains another major phosphorylation site of FAK, Tyr925, which is phosphorylated by Src after its binding to FAK (Schlaepfer, D. D. and Hunter, T. 1996). Phosphorylation of FAK on Tyr925 after fibronectin stimulation creates a binding site for the SH2 domain of Grb2. This leads to the formation of a signaling complex that includes Ras (small GTP-binding protein) and Sos (nucleotide exchange factor) (Schlaepfer, D. D., Hanks, S. K. et al. 1994).

We decided to examine the pattern of expression and phosphorylation of FAK in more detail in order to get additional insights regarding its role during early *Xenopus* development. We used several phospho specific antibodies against the most important tyrosines on the FAK molecule including Tyr397, 576, 861 and 925. This was done by Whole Mount Immunofluorescene and Western Blotting using whole embryo extracts. As

mentioned previously, the *Xenopus* sequence is 90% identical with the mammalian FAK homologs and specific residues are conserved including Tyrosine 397 (autophosphorylation site) (Hildebrand, J. D., Schaller, M. D. et al. 1993; Eide, B. L., Turck, C. W. et al. 1995; Hens, M. D. and DeSimone, D. W. 1995).

Lysates from representative developmental stages were used for western blot. Equal amounts of the lysate were loaded onto each gel and were probed using different antibodies. The membranes were stripped and re-probed for actin which was used as a loading control. Results from these experiments demonstrated that FAK protein is expressed at very low levels in blastula stage embryos. FAK protein levels increase during gastrulation and protein levels remain constant during neurulation and persist though tailbud (Figure 40E). This pattern is consistent with previous observations in *Xenopus* (Hens, M. D. and DeSimone, D. W. 1995; Kragtorp, K. A. and Miller, J. R. 2006). Also, in *zebrafish* FAK protein is expressed throughout early development and expression increases slightly during somitogenesis as in our model organism (Henry, C. A., Crawford, B. D. et al. 2001; Crawford, B. D., Henry, C. A. et al. 2003). Low levels of tyrosine-phosphorylated FAK first appear at blastula stage and we observed a dramatic increase of the phosphorylation of FAK, on all tyrosine residues during gastrulation (Figure 40E). By the beggining of neurulation phosphorylation of all these residues decreases but when somitogenesis began, mostly the Tyr397 residue of FAK was increasingly phosphorylated (Figure 39E). These results are in contrast with Hens and DeSimone findings that low levels of tyrosine-phosphorylated FAK first appear during gastrulation but levels increase through stage 17 and beyond (Hens, M. D. and DeSimone, D. W. 1995). In *zebrafish* embryos, phosphorylation of FAK is first detectable at the end of gastrulation and increases only during somitogenesis. This happens for all the residues but is more obvious for Tyrosine 397 (Crawford, B. D., Henry, C. A. et al. 2003).

In order to examine the temporal and spatial phosphorylation of FAK, embryos at stage 12 (late gastrula) were fixed, sagittally sectioned and used for immunofluorescence experiments. By the end of gastrulation FAK and phosphorylated FAK (on Tyrosine 397, 576 and 861) were concentrated at the interface between mesoderm and deep ectoderm (Figure 40B-D). Also in animal caps FAK concentrated at the cell-cell contact sites (Figure 40A). Further examination of the phosphorylation status of FAK was performed using embryos from pre-gastrula to late gastrula. Embryos were fixed, sagittally sectioned as before and used for IF assays using the following primary antibodies: anti-FAK PY397, PY576, PY861 and PY925 (Figures 41, 42, 43, 44). Phosphorylated FAK on Tyr397,

Tyr576 and Tyr861 was detected throughout the entire *Xenopus* embryo with a stronger signal on the plasma membrane and cell-cell boundaries. We observed that phosphorylation was elevated in cells of the mesodermal belt and along portions of the blastocoel roof at stage 10 (Figures 41, 42, 43, 44 A and B). At later stages, phosphorylation of these residues was detected throughout the embryo, but was more intense in the mesodermal region. An exception was tyrosine 925 which was phosphorylated in the cells of the mesodermal belt at stage 7, but when gastrulation begins it became concentrated to the dorsal and ventral lip and later only on the apical side of the epithelial lining of the archenteron (Figure 44C, D). It is known that FAK becomes activated via autophosphorylation at Tyr397 and that phosphorylation increases under conditions associated with enhanced focal adhesion formation (Hanks, S. K., Calalb, M. B. et al. 1992). As mentioned in Figure 28I, the concentration of focal adhesion proteins in the interface between mesendoderm and the BCR suggests that such complexes do indeed form in the embryo. Autophosphorylation at Tyr397 appears to be important for tyrosine phosphorylation of focal adhesion associated proteins and phosphorylation at Tyr576/577 and Tyr861 enhances the phosphorylation on Tyr397 (Calalb, M. B., Polte, T. R. et al. 1995; Leu, T. H. and Maa, M. C. 2002). In contrast, phosphorylation of FAK on the residue Tyrosine 925 causes FAK loss from focal adhesions (Katz, B. Z., Romer, L. et al. 2003; Deramaudt, T. B., Dujardin, D. et al. 2011). The phosphorylation of FAK on these residues in the interface between mesoderm and deep ectoderm suggests that they are critical during mesoderm migration but also in various tissues during *Xenopus* embryogenesis.

In *zebrafish,* the expression and phosphorylation FAK changes dramatically after gastrulation. FAK is concentrated at the sides of cell-cell adhesions in the epithelial enveloping layer and may associate with actin cytoskeleton at epithelial junctions containing cadherins. FAK is phosporylated at these epithelial junctions on pY576, pY861 but not on pY397 (Crawford, B. D., Henry, C. A. et al. 2003). However, no evidence has been reported about the differential phosphorylation of tyrosine residues of FAK in the context of possible interactions with focal adhesion proteins in *Xenopus*.

Results from the time course analyses demonstrated that FAK protein is expressed from pre-gastrula (stage 8) to tailbud stage 33 (Figure 40E). FAK protein levels increase as gastrulation proceeds and remain constant during neurulation and oragnogenesis. Also low levels of phosphorylated FAK (all residues) appear from stage 8 but these levels increase during gastrulation. At the onset of neurulation, phosphorylation of all residues decreases

slightly until tailbud stage with an exception for the phosphorylation of residue Tyrosine 397 which is elevated at stage 33.

The fact that FAK is heavily phosphorylated on all major sites including the activation loop in pre gastrula stage embryos shows that the kinase has an early role independent of cell movements and integrin activation during *Xenopus* development. Despite the fact that FAK is found primarily in the cytoplasm of the cells in the embryo, the phosphorylated forms are only located at the plasma membrane including the apical membrane suggesting that FAK activation takes place on the membrane.

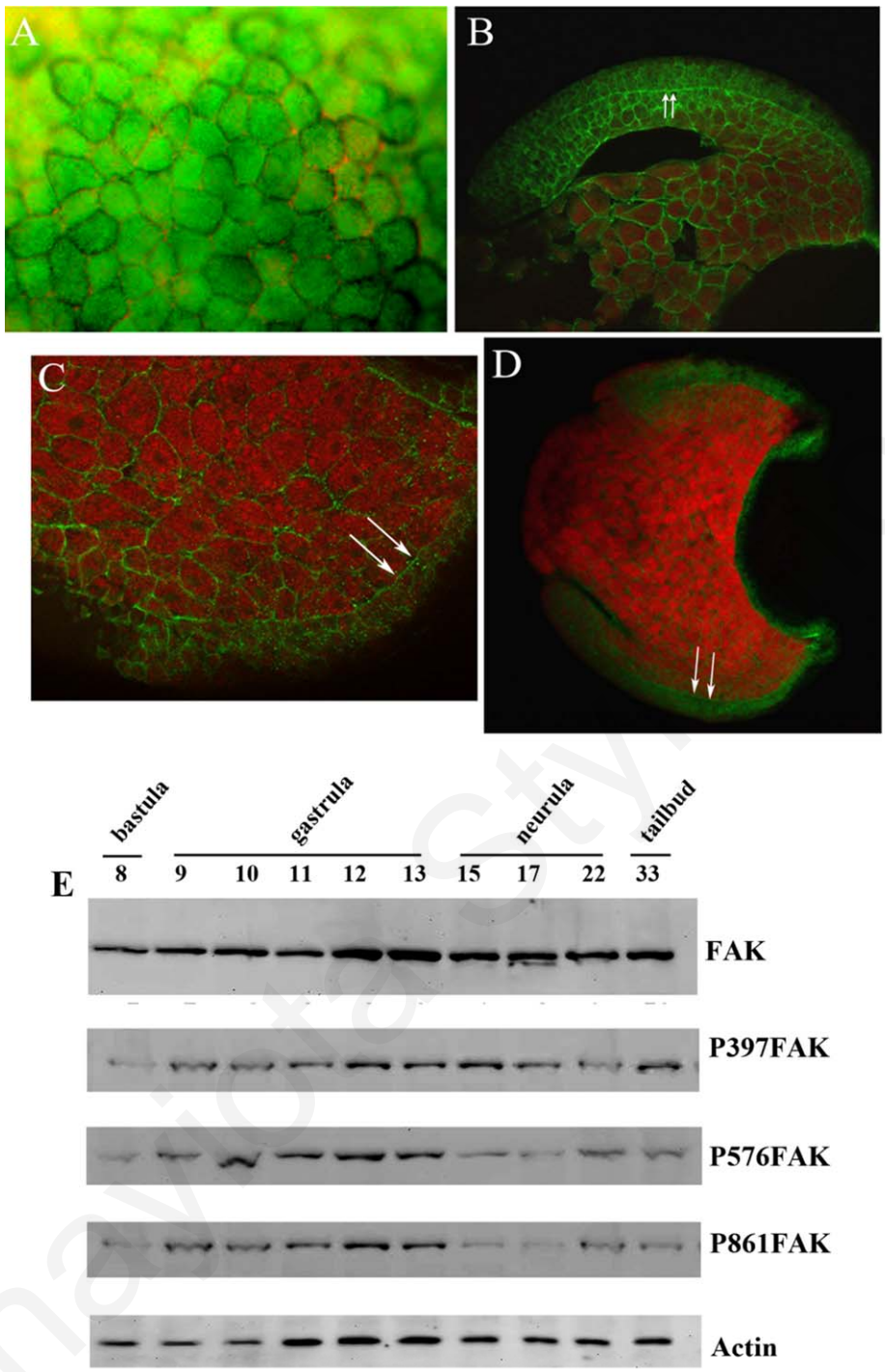

Figure 40. Expression and phosphorylation of FAK on tyrosine residues. (A) FAK is concentrated at sites of cell-cell adhesion in the animal cap. (B – D) Sagittal sections of stage 12 embryos stained with anti-FAK PY576 (B), anti-FAK PY397 (C) and anti-FAK PY861 (D) (secondary antibody cy3) reveals a concentration of phosphorylated FAK at the interface between mesoderm and deep ectoderm. (E) FAK and phosphorylated FAK are elevated during gastrulation. Each lane represents Western Blots from extracts of equal numbers of embryos probed with a monoclonal antibody against the C-terminus of FAK or polyclonal antibodies against the tyrosine residues (details in section: materials and methods). The last lane represents actin as a loading control.

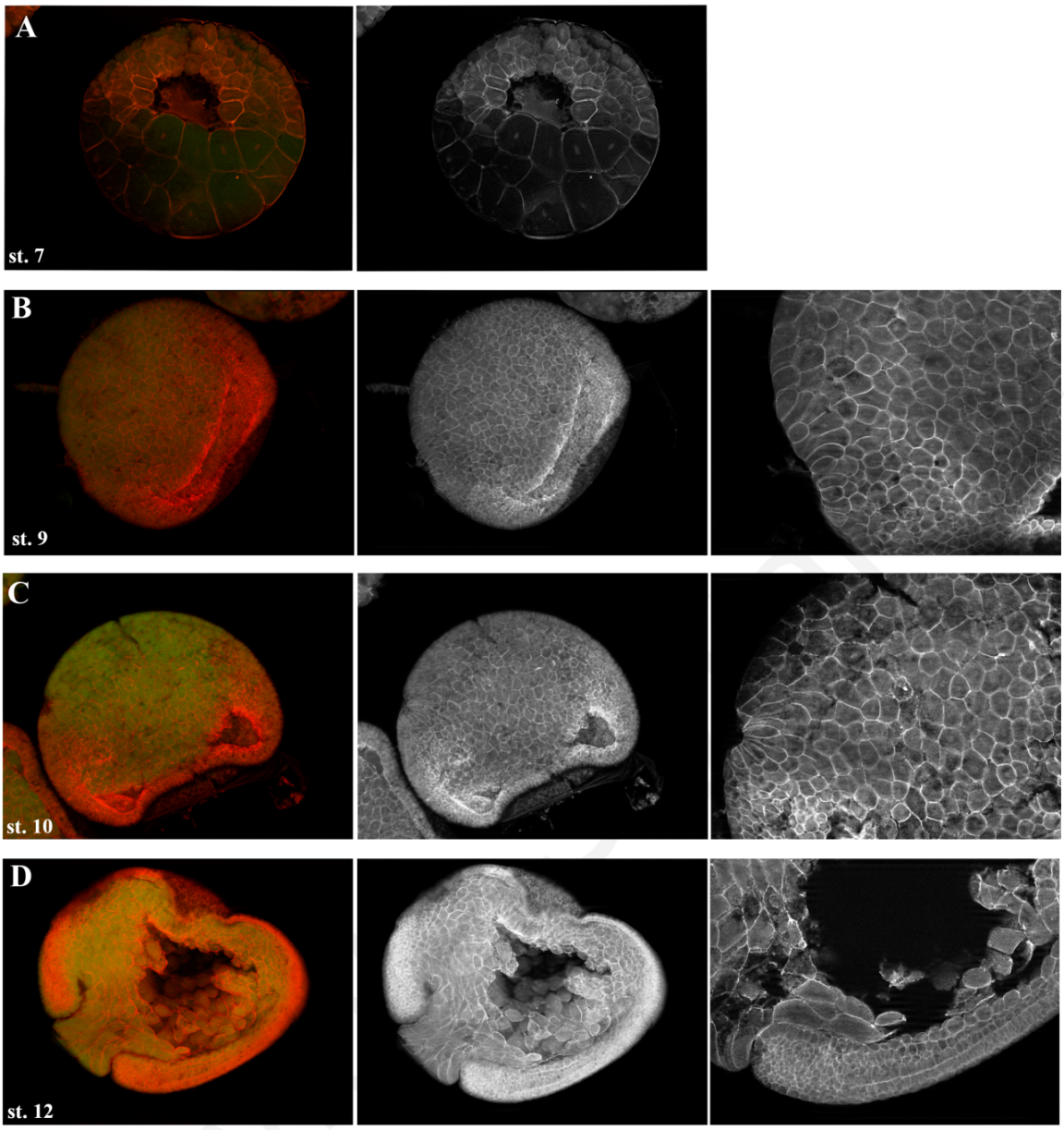

Figure 41. Phosphorylation status of the autophosphorylation site Tyrosine 397 of FAK. (A-D) Each row shows immunostaining with anti-FAK PY397 (secondary antibody Cy3) which is phosphorylated at cell-cell boundaries is observed throughout the embryo and is elevated at the involuting mesoderm; carried out on mid sagittal optical sections from blastula (A), early gastrula (B), mid gastrula (C) and late gastrula (D) stage embryos. The phosphorylation of PY397 is elevated at the involuting mesoderm during gastrula stages (B-D) and it's stronger at the interface between mesoderm and deep ectoderm. The right column shows higher magnification of the sagittal sections of B-D and is focused on the involuting marginal zone of the embryos.

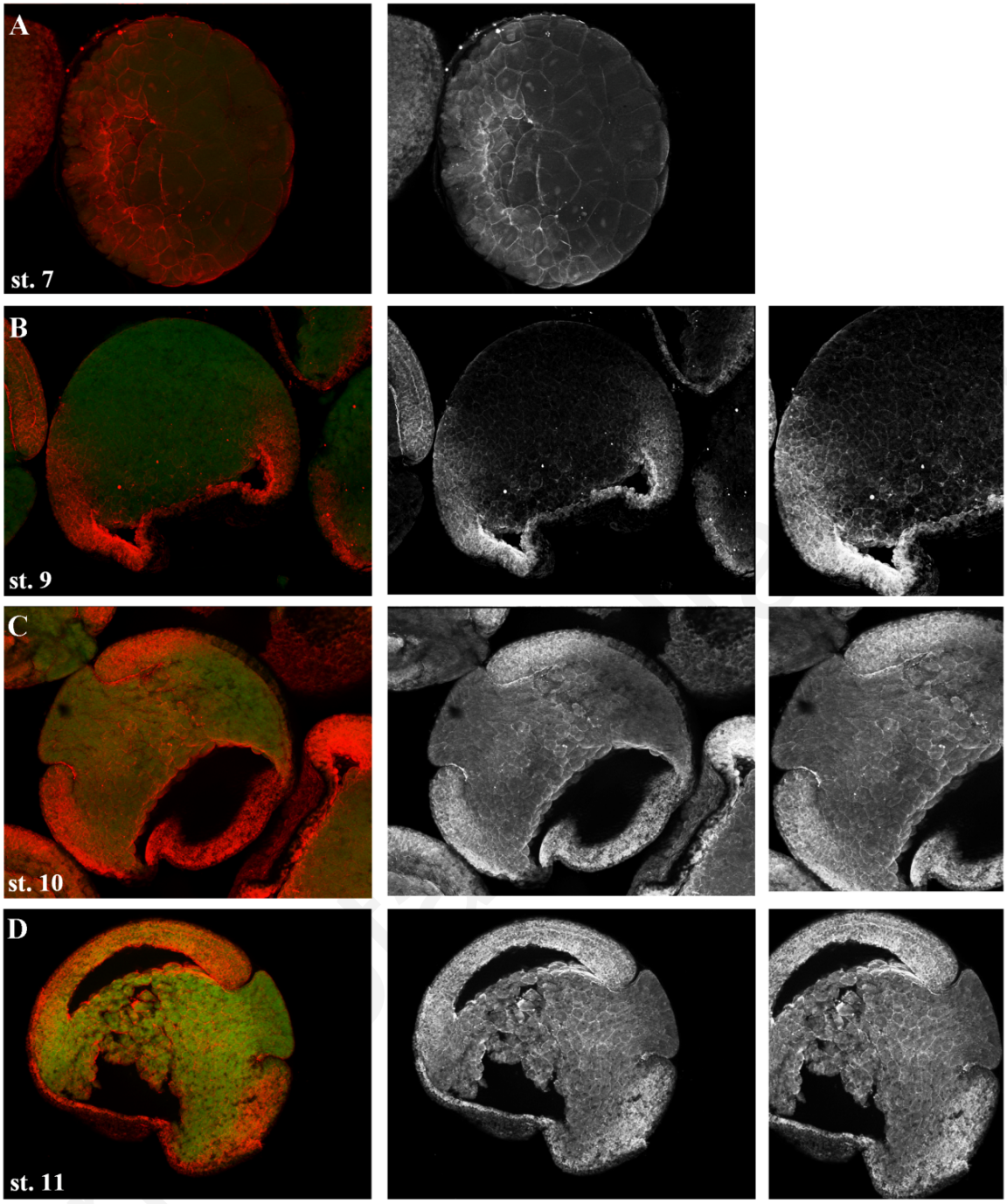

Figure 42. Phosphorylation status of the residure Tyrosine 576 in the activation loop of the kinase domain of FAK. (A-D) Each row shows immunostaining with anti-FAK PY576 (secondary antibody Cy3) which is phosphorylated at cell-cell boundaries all over the embryo and elevated at the involuting mesoderm, carried out on mid sagittal optical section from blastula (A), early gastrula (B), mid gastrula (C) and late gastrula (D) stage embryos. The elevation of the phosphorylation in more obvious at the involuting mesoderm during gastrula stages (B-D) and it's stronger at the interface between mesoderm and deep ectoderm. The right column shows higher magnification of the sagittal sections of B-D and is focused on the involuting marginal zone of the embryos.

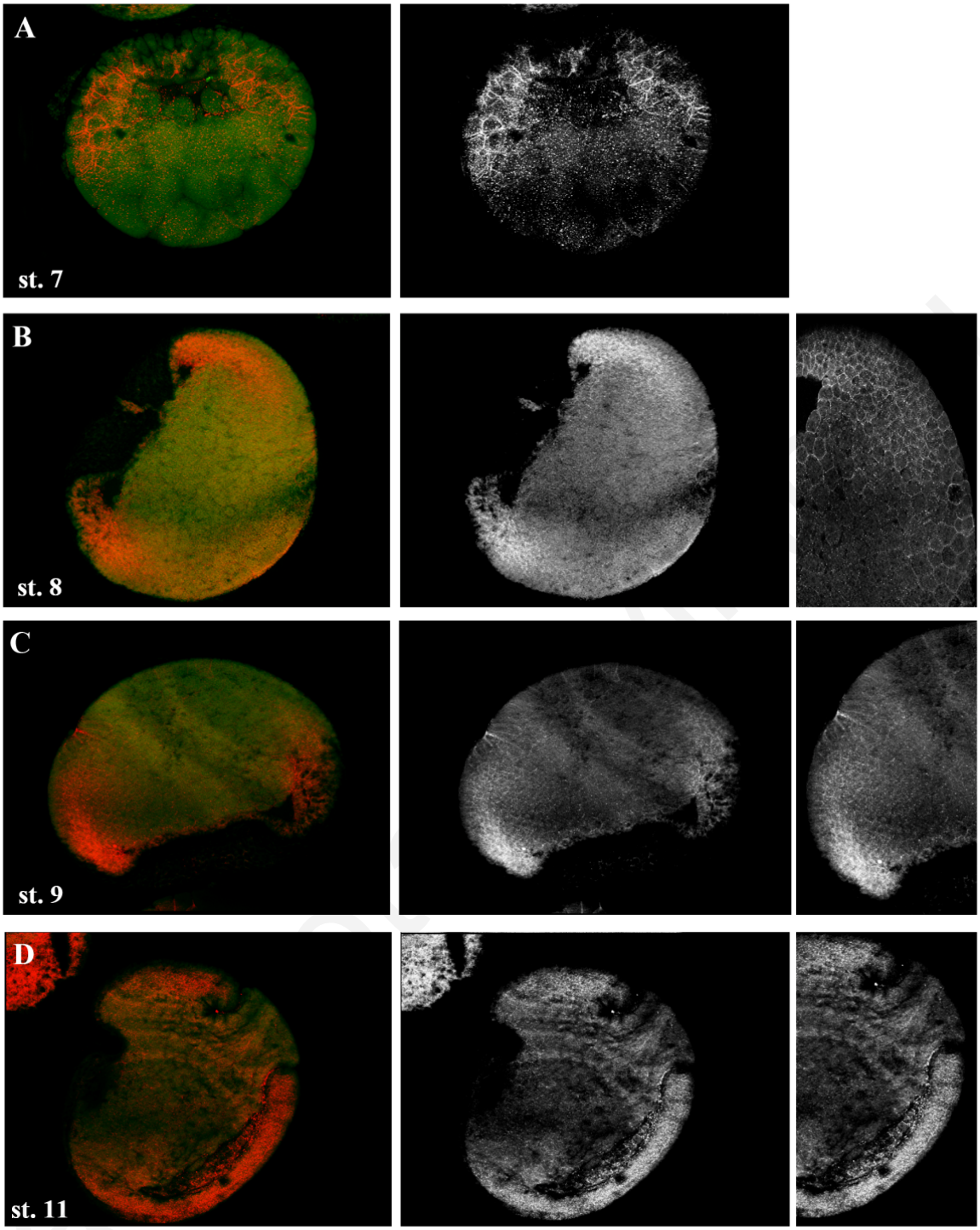

Figure 43. Phosphorylation status of the residue Tyrosine 861 of FAK. (A-D) Each row shows immunostaining with anti-FAK PY861 (secondary antibody Cy3) which phosphorylated at cell-cell boundaries (but not as strong as Tyrosine 576 and 397) all over the embryo and elevated at the involuting mesoderm; carried out on mid sagittal optical sections from blastula (A), early gastrula (B), mid gastrula (C) and late gastrula (D) stage embryos. The phosphorylation of PY861 is elevated at the involuting mesoderm during gastrula stages (B-D). The right column shows higher magnification of the sagittal sections of B-D and is focused on the involuting marginal zone of the embryos.

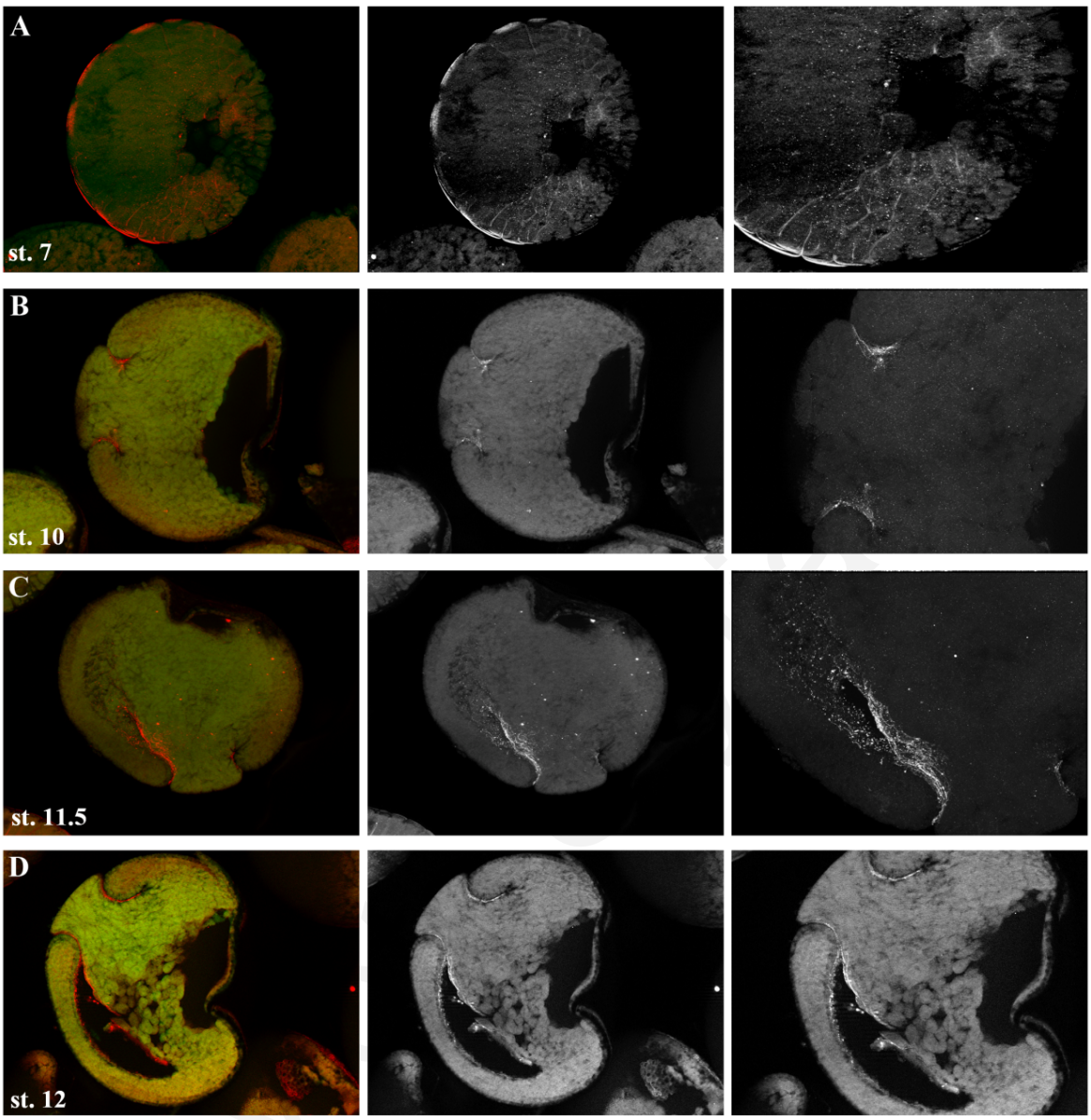

Figure 44. Phosphorylation status of the residue Tyrosine 925 of FAK. (A-D) Each row shows immunostaining with anti-FAK PY925 (secondary antibody Cy3) carried out on mid sagittal optical sections from blastula (A), mid gastrula (B) and late gastrula (C, D) embryos, (A) The phosphorylation appears to be only in the involuting mesoderm and as gastrulation begins (B) FAK is phosphorylated on Tyrosine 925 residue dorsal and ventral to the blastopore lip. At late gastrula stages (C, D) it is phosphorylated at the apical side of the archenteron and at the blastopore lip. The right column shows higher magnification of the sagittal sections of A-D and is focused on the phosphorylation of PY925.

3.4.2 Down-stream targets of Focal Adhesion Kinase show similar patterns of phosphorylation during early *Xenopus* embryogenesis

As previously mentioned, FAK becomes activated through phosphorylation of tyrosine residues and acts as a scaffold for the recruitment of other signaling proteins (Zachary, I. 1997). It can phosphorylate other proteins involved in cell migration and spreading like paxillin and tensin (Otey, C. A. 1996). Paxillin contains LD motifs (leucine-rich repeat motifs), LIM domains, SH3 and SH2 binding domains that serve as docking sites for cytoskeletal proteins, tyrosine kinases and others. Tyrosine 31, a Crk binding site of paxillin, is phosphorylated during integrin-mediated cell adhesion. The phopshorylation of paxillin is suggested to happen via a FAK/Src complex and is believed to regulate cell spreading (Richardson, A., Malik, R. K. et al. 1997). FAK binds paxillin through two hydrophobic regions at the surface of the FAT domain. These bind two leucine-rich repeat "LD" motifs (LDxLLxxL) within the N-terminal half of paxillin (Hayashi, I., Vuori, K. et al. 2002). This interaction results in phopshorylation of paxillin on Tyr31 and Tyr118 by the FAK/Src complex (Schaller, M. D., Otey, C. A. et al. 1995). The carboxyl terminus of paxillin consists of four tandemly repeated LIM domains essential for the localization to focal adhesions. Paxillin binds to the cytoplasmic domains of integrin receptors and the focal adhesion protein vinculin and may act as a docking partner for FAK (Hildebrand, J. D., Schaller, M. D. et al. 1995). Paxillin is only partially responsible for FAK promoted cell migration because analysis of the paxillin-FAK interaction after cell adhesion to fibronectin indicates that the interaction is constitutive and not significantly regulated by engagement of integrins with the ECM (Hildebrand, J. D., Schaller, M. D. et al. 1995).

We found that FAK is phosphorylated and thus in an active state from blastula to late gastrula and we wanted to compare the phosphorylation level of paxillin and FAK. Control embryos from stages 7 to 12 were fixed, sagittally sectioned and used for immunofluorescence with anti-pPax primary antibody and Cy3 secondary antibody. Important sites of phosphorylation of paxillin are Tyr31/118, Thr 403 and Ser481 which are conserved throughout most species (Crawford, B. D., Henry, C. A. et al. 2003). The phosphoshotylation pattern of paxillin Y31 is similar to the phosphorylation of the residues of FAK Tyr397, Tyr576 and Tyr861. The phosphorylated protein is abundant at all stages but is more pronounced in cells of involuting mesoderm and along portions of the blastocoel roof at stage 10 in a similar fashion to FAK (Figure 45A,B). In later stages, phosphorylated paxillin is abundant all over the embryo but is more concentrated in the mesodermal region (dorsally and ventraly) (Figure 45C, D). Thus the phosphorylation of

paxillin is similar to the phopshorylation of FAK especially during gastrulation at the involuting mesoderm. Both phosphorylated forms of the proteins are found at cell-cell boundaries. It is also known that paxillon Tyrosine phosphorylation caused by FAK overexpression in CHO cells is dependent on Tyr397 (Cary, L. A., Chang, J. F. et al. 1996). The similarity of the localization of both activated proteins and the above mentioned data suggest that as previously shown by a number of groups paxillin is a target of the FAK/Src complex and paxillin shows elevated phosphorylation in regions of the embryo where FAK is more active (Richardson, A., Malik, R. K. et al. 1997).

A second downstream target of FAK which was examined was the serine-threonine kinase Akt. Specifically, we examined the phosphorylation of Akt on residue 473. Serine 473 is the major phosphorylation site of Akt and is required for its activation (Franke, T. F., Kaplan, D. R. et al. 1997). The main autophosphorylation and activation site of FAK, residue Tyr397, (Eide, B. L., Turck, C. W. et al. 1995) is the binding site several SH2 containing proteins including: PI3 kinase, Phospholipase C-γ, Grb7 and Src family kinases (Schlaepfer, D. D., Hanks, S. K. et al. 1994). PI3K binds through its p85 subdomain and this binding results in the activation of the PI3K/Akt pathway which has a role in preventing cell apoptosis (Chen, H. C., Appeddu, P. A. et al. 1996; Cary, L. A. and Guan, J. L. 1999). It is known that blocking FAK function by a dominat negative or by pharmacologic inhibition impedes phopshorylation of the p85 subunit of PI3K and serine 473 of Akt. Also, constituively active FAK elevates p85 phosphorylation and Akt activity and regulates survival signals and cell viability (Xia, H., Nho, R. S. et al. 2004).

With the use of immunofluorescence the phosphorylation of Akt on Serine 473 was examined and again shown to be very similar to the phosphorylation of FAK. Phospho Akt was detected in all cells of the embryo at all stages but was elevated in the involuting mesoderm in a similar fashion to FAK and paxillin (Figures 46A -C). At early gastrula stages, the levels of the phosphorylation of Akt is more pronounced at the dorsal marginal zone (Figure 46B, C) but by the end of gastrulation Akt phsophorylation is elevated in both, the dorsal (more intense) and the ventral marginal zone (Figure 46D, E). At later stages (stage 12), phosphorylation is abundant all over the embryo at the cell-cell boundaries and in the nucleus but again is more elevated in mesodermal tissues (Figure 46D, E).

Results from this analyses demonstrate that phosphorylation of paxillin and Akt two well characterized downstream effectors of FAK begins prior to gastrulation (stage 8) and is maintained to late gastrula (stage12). At late gastrula the expression is elevated in the

mesodermal region of the embryos in a similar fashion to FAK. Overall, these results show that both FAK and its downstream targets are phosphorylated throughout development and that phosphorylation is elevated in the highly morphogenetically active mesodermal tissues during gastrulation. Interestingly this elevation is not restricted to the cell - ECM contact areas (for example: the region of mesendoderm in contact with the blastocoel roof) and suggests an involvement of FAK in mesoderm morphogenesis and not only mesoderm migration. The closely macthed pattern between the three proteins in terms of their phorphorylation status suggests that they are participating in similar developmental processes and are in agreement with *in vitro* work demonstarting that both Paxillin and Akt are downstream effectors of FAK (Hildebrand, J. D., Schaller, M. D. et al. 1995; Richardson, A., Malik, R. K. et al. 1997; Xia, H., Nho, R. S. et al. 2004).

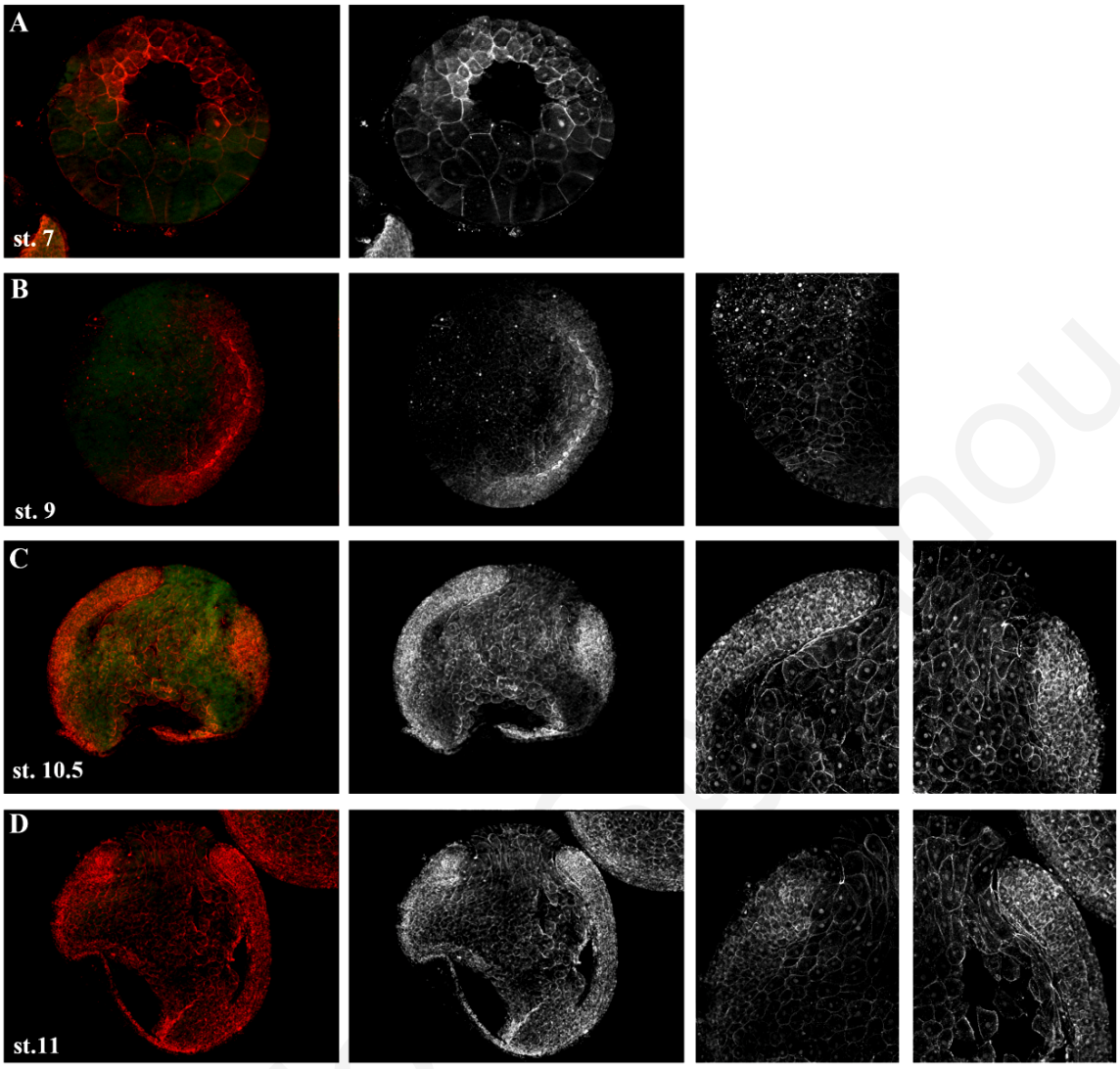

Figure 45. Phosphorylation of Paxillin on residue Tyrosine 31. (A-D) Each row shows mid-sagital optical sections from blastula (A), early gastrula (B) and late gastrula (C, D) stage embryos, immunostained with anti-paxillin PY31 (secondary antibody Cy3) which is concentrated at cell-cell boundaries, and in the nucleus throughout the embryo with an increase at the involuting mesoderm. The concentration of PY31 Paxillin increases at the involuting mesoderm during gastrula stages (B-D). The right two columns show higher magnification of the the involuting marginal zone from B-D.

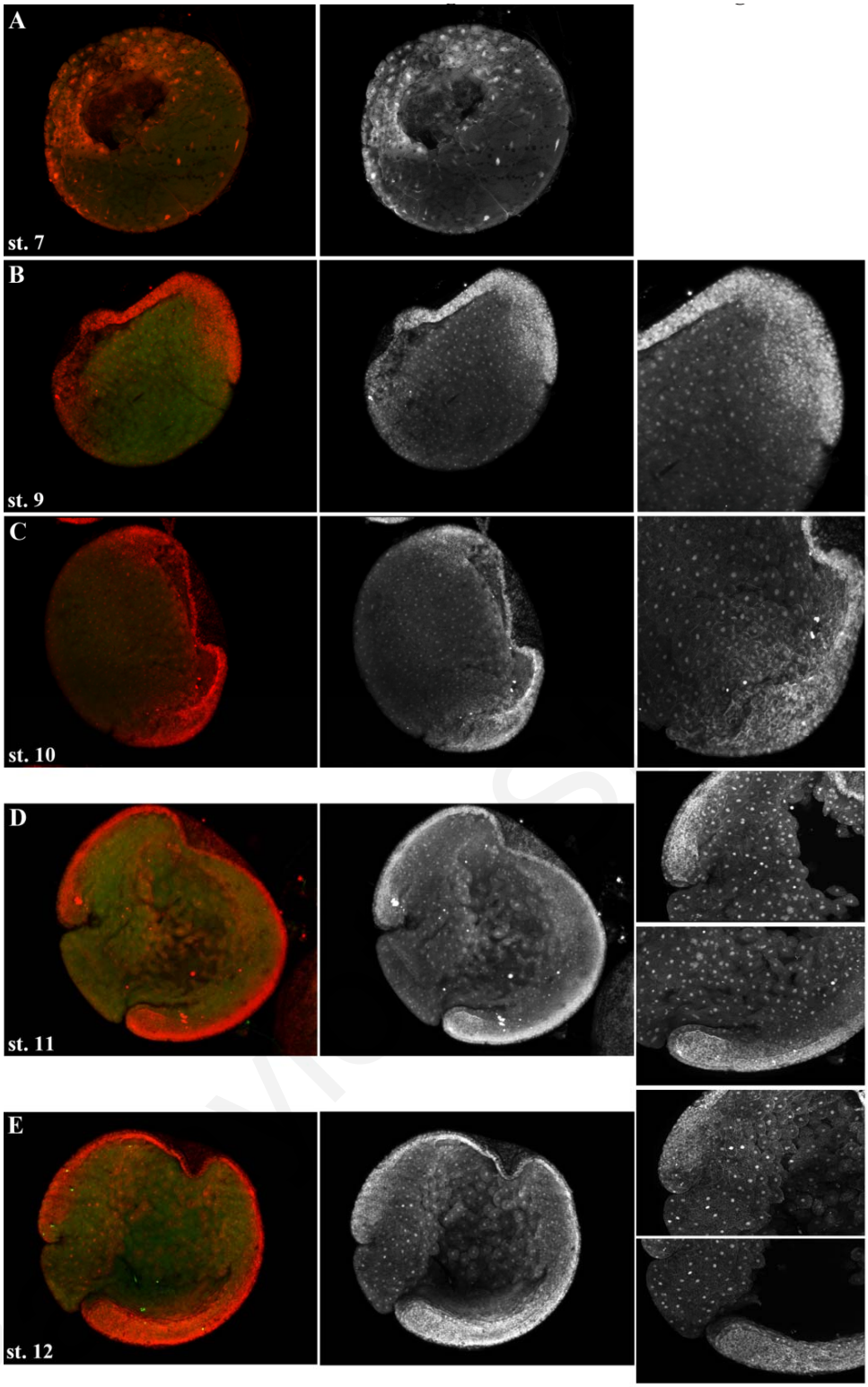

Figure 46. Phosphorylation of Akt at the residue Ser473. (A-D) Each row shows mid-sagital optical sections from blastula (A), early gastrula (B) and late gastrula (C, D) embryos, immunostained with anti-Akt Ser473 (secondary antibody Cy3) which concentrates at cell-cell boundaries, and in the nucleus throughout the embryo with an increase at the involuting mesoderm. The concentration of PYSer473 Akt increases at the involuting mesoderm during gastrula stages first dorsally and then ventrally (B-D). The right two columns show higher magnification of the the involuting marginal zone from B-E.

3.5 Initial indications that FAK is regulated by integrin-independent mechanisms in *Xenopus* embryos

3.5.1 FAK morpholino fails to downregulate FAK and inhibit the phosphorylation of FAK during early development of *Xenopus laevis*

To further address the role of FAK during early *Xenopus* development we generated an anti-sense morpholino to effectively block FAK *translation in vivo* in *Xenopus laevis* embryos. Studies that used anti-sense morpholino to minimize FAK function indicated that FAK is necessary for viability and cardiogenesis in *Xenopus*, however, no studies to date have addressed the use of FAK morpholino in earlier stages (Doherty, J. T., Conlon, F. L. et al. 2010).

We designed a FAK-specific antisense morpholino to target sequences upstream of the start codon of *Xenopus* FAK (within the 5'UTR). The sequence of the morpholino that was used was the following: 5'- TCCAGGTAAGCCGCAGCCATAGCCT - 3' (referred as: FAK MO). In order to establish that FAK MO effectively blocks FAK function *in vivo*, we injected 10 to 60ng of FAK MO with hGFP or mGFP (both 100pg total per embryo) into two blastomeres of four-cell stage embryos at the dorsal marginal zone.

Lysates from stage 12 were used for Western blot analysis and results showed that FAK protein expression in FAK morphant embryos was reduced (as the amount of FAK MO increases) compared to the control embryos (Figure 47A). Some of FAK morphant embryos were left to developed and then fixed at different stages during gastrulation (stage 9 to 12). The embryos which were allowed to develop past stage 12 had a slight delay with regards to blastopore closure compared to controls (Figure 47B, C). The embryos continued to develop normally until stage 40 (data not shown). The lack of effect on these early developmental stages is not very surprising because of the fact that heterozygous FAK null mice are viable and that FAK protein levels in our experiments were only reduced (Ilic, D., Furuta, Y. et al. 1995).

We continued with immunofluorescence experiments to examine the reduction of activated FAK at the site of the injected FAK MO. Primary antibodies used included the anti-FAK PY397 (secondary Cy3) to detect activated FAK and anti-GFP (secondary Alexa 488) to identify FAK MO injected cells. During gastrulation it appears that FAK MO was not able to reduce activated FAK (Figure 48A-C) but could do so in later stages (Figure 48D, E). At later stages FAK morphant embryos that were analyzed and sagitally sectioned in morpholino positive areas (GFP expression) exhibited abnormalities at the somites (Figure

48D, E arrows). This is in agreement with previously published data showing that FAK MO is only effective at later developmental stages (Doherty, J. T., Conlon, F. L. et al. 2010).

Morpholino (MO) based inhibition of translational initiation represents an attractive way to eliminate gene function during *Xenopus* development (Heasman, J., Kofron, M. et al. 2000). However, the degree to which a given target protein, like FAK, can be eliminated and the longevity of this effect during embryogenesis has not been documented. Also in our case it is not effective because the *Xenopus laevis* genome is tetraploid it may be necessary to design two MOs to achieve the desired loss of function phenotype (Nutt, S. L., Bronchain, O. J. et al. 2001). As previously reported, low levels of maternal FAK is present in fertilized eggs which persists throughout the onset of gastrulation (stage 10) at which time embryonic FAK protein becomes markedly induced (Hens, M. D. and DeSimone, D. W. 1995). Thus, maternal FAK is not depleted by FAK MO, which is designed to block translation of nascent transcripts.

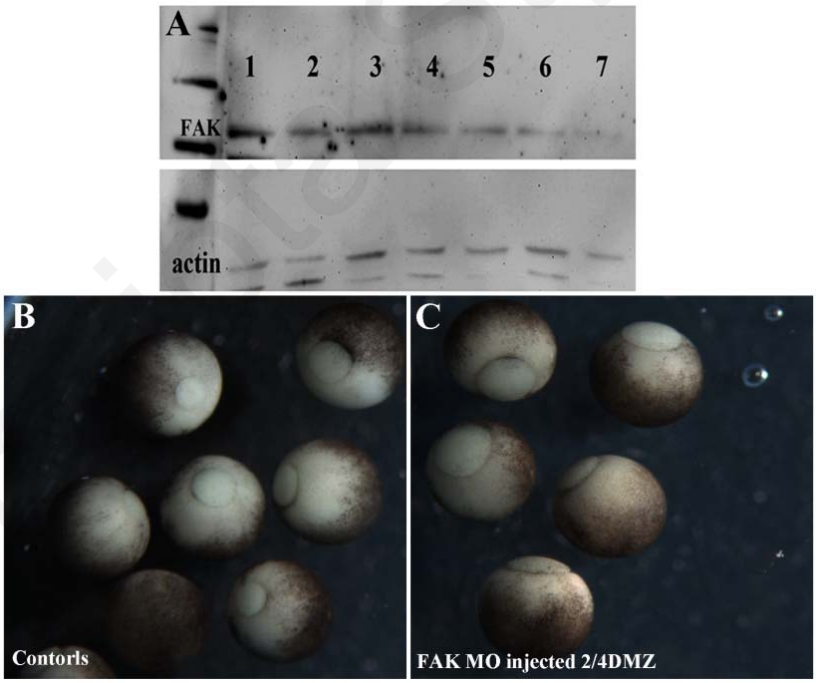

Figure 47. FAK expression in morphant embryos. Slight delay of the blastopore closure during gastrulation. (A) FAK MO (lane 2: 10ng, lane 3: 30ng, lane 4: 40ng, lane 5: 50ng and lane 6: 60ng) was injected into two blastomers of the four cell stage embryo at the DMZ and embryonic FAK protein levels were assessed at stage 12 by Western blotting. Levels of actin are shown as a loading control. (B) Control embryos and (C) injected embryos with FAK MO at stage 11. A slight delay of the bastopore closure can be seen in the injected embryos (C).

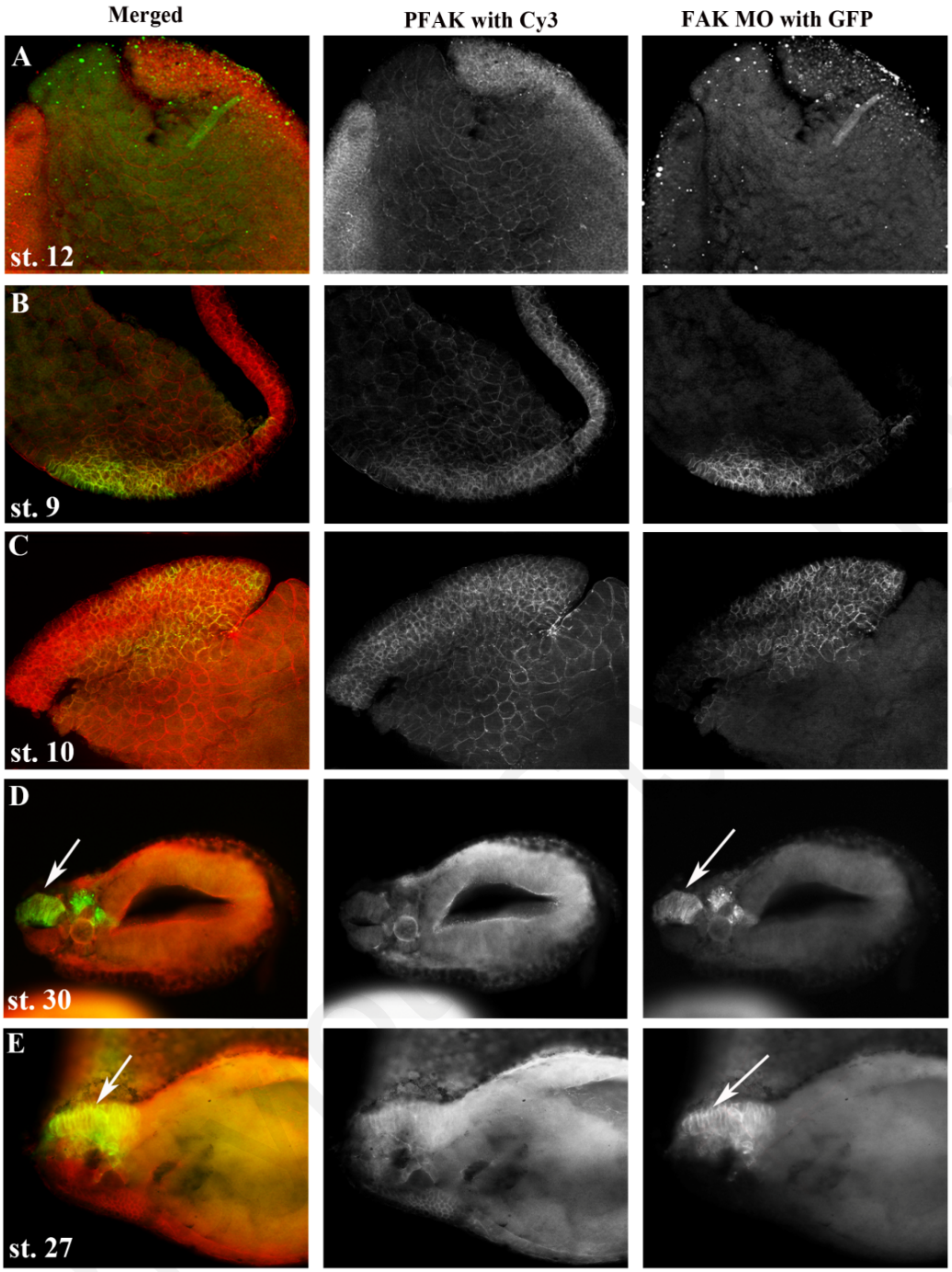

Figure 48. FAK morphant embryos does not effectively block FAK function *in vivo* during early development. FAK MO injected embryos (two blastomeres of four-cell stage embryos were injected at the dorsal marginal region with FAK MO) 10 ng (A, D), 20ng (B, E) and 40ng (C) co-injected with hGFP (100pg total) or memGFP (100pg total). During early development (A, B, C) activated FAK (second column, used anti-FAK PY397) seems to be no reduces in the site of the expressed morpholino (right column: FAK MO with GFP) but in later stages (D, E) a slightly reduction of activated FAK appears to the injected site. Also we can see a failure to the formation of the somites (arrows indicates injected sit: leads to expanded somite area) compared to the non injected site of the embryo. This may indicates the importance of activated FAK during somitogenesis in *Xenopus* embryos.

3.5.2 FRNK overexpression does not act as a dominant negative in *Xenopus laevis* embryos

Phosphorylated FAK is found in every single tissue in *Xenopus laevis* embryos, and its phosphorylation is elevated at the involuting marginal zone (IMZ) as shown in previous section 2.4.1. The presence of active FAK in all tissues suggests that plays an important role during early development especially in the highly morphogenetically active mesodermal tissues comprising of the involuting and non-involuting marginal zone.

Since the use of FAK MO couldn't provide downregulation of FAK during gastrulation we returned to the autonomously expressed C-terminal domain FRNK. FRNK as mentioned is the C-terminal region of FAK containing the FAT domain which is both necessary and sufficient for focal adhesion localization of FAK (Hildebrand, J. D., Schaller, M. D. et al. 1993). FRNK has been shown to act as a dominat negative by competing endogenous FAK from focal adhesions in several systems resulting in lower FAK phosphorylation as well as lower levels of phosphorylation of FAK´s downstream targets (Richardson, A., Malik, R. K. et al. 1997; Heidkamp, M. C., Bayer, A. L. et al. 2002; Kragtorp, K. A. and Miller, J. R. 2006; Stylianou, P. and Skourides, P. A. 2009). In order to tissue the specifically block FAK activation and address its role in different tissues FRNK was expressed via mRNA microinjection.

A total of 500pg of HA FRNK capped RNA was injected at the DMZ of four cell stage embryos (2/4 DMZ) and the AP of two cell stage embryos (1/2 AP) followed by IF. The effectiveness of FRNK in downregulating FAK was initially examined by monitoring the phosphorylation status at Tyr397 the major autophosphorylation site of FAK, which is considered a good indicator of the activation state of FAK (Eide, B. L., Turck, C. W. et al. 1995). Surprisingly despite the fact that FRNK could reduce the levels of phosphorylated FAK in FN plated mesodermal cells it failed to dowregulated the levels of phosphorylated FAK on Tyr397 in the embryo (Figure 49J-L). Examination of the localization of FRNK revealed that it partially localizes on the cell-cell boundaries (Figure 49D, E), in a diffuse manner but fails to localize at the apical region of the blastomeres suggesting that the C-ternimus is not sufficient for membrane localization (Figure 49G-I). Overall FRNK has a pattern of localization that is very similar to that of inactive FAK which is mostly cytoplasmic (Figure 49A-C) while active FAK (phosphorylated) is found exclusively at the sites of cell cell contact and the apical surface of superficial blastomeres (Figure 49F). Co-expression of HA FRNK with GFPFAK confirmed a close match between the localization patterns of the two constructs (Figure 49A-C). To confirm that FRNK is unable to act as a

dominant negative in the context of the *Xenopus* embryo, FRNK was overexpressed as described above and embryos were processed for whole mount immunofluorescence using a phospho specific antibody against tyrosine 576. This tyrosine is in the activation loop of the kinase domain and its phosphorylation confers full enzymatic activity to FAK. As described in a previous section this tyrosine is also heavily phosphorylated both pre and during gastrulation in normal embryos. As shown in Figure 49 (M-O) FRNK overexpression fails to reduce the levels of Tyr576 confirming that the FAK C-terminus is not sufficient for the competition of endogenous FAK from its complexes in the embryo. In agreement with this assertion FRNK expression in the *Xenopus* embryo does not lead to major phenotypic abnormalities. Other than inhibition of mesoderm migration FRNK expressing tissue appear normal and embryos that manage to close their blastopore are normal. This is contrast with results in the mouse where FAK knockout is lethal again suggesting that FRNK expression does not block FAK function in *Xenopus* (Ilic, D., Furuta, Y. et al. 1995). The relatively high levels of FAK phosphorylation prior to gastrulation and prior to the secretion of the major ECM components fibronectin and laminin suggest that FAK is largely activated in an integrin independent fashion in the embryo as opposed to the primarily integrin based activation observed in cells in culture as well as that seen in dissociated mesodermal cells plated on FN. The localization of FRNK suggests that active endogenous FAK may be targeted to the membrane through another domain and not FAT especially since FRNK cannot localize at the apical surface of superficial blastomeres and its localization to the cell - cell boundaries is weak compared to that of endogenous phospho-FAK.

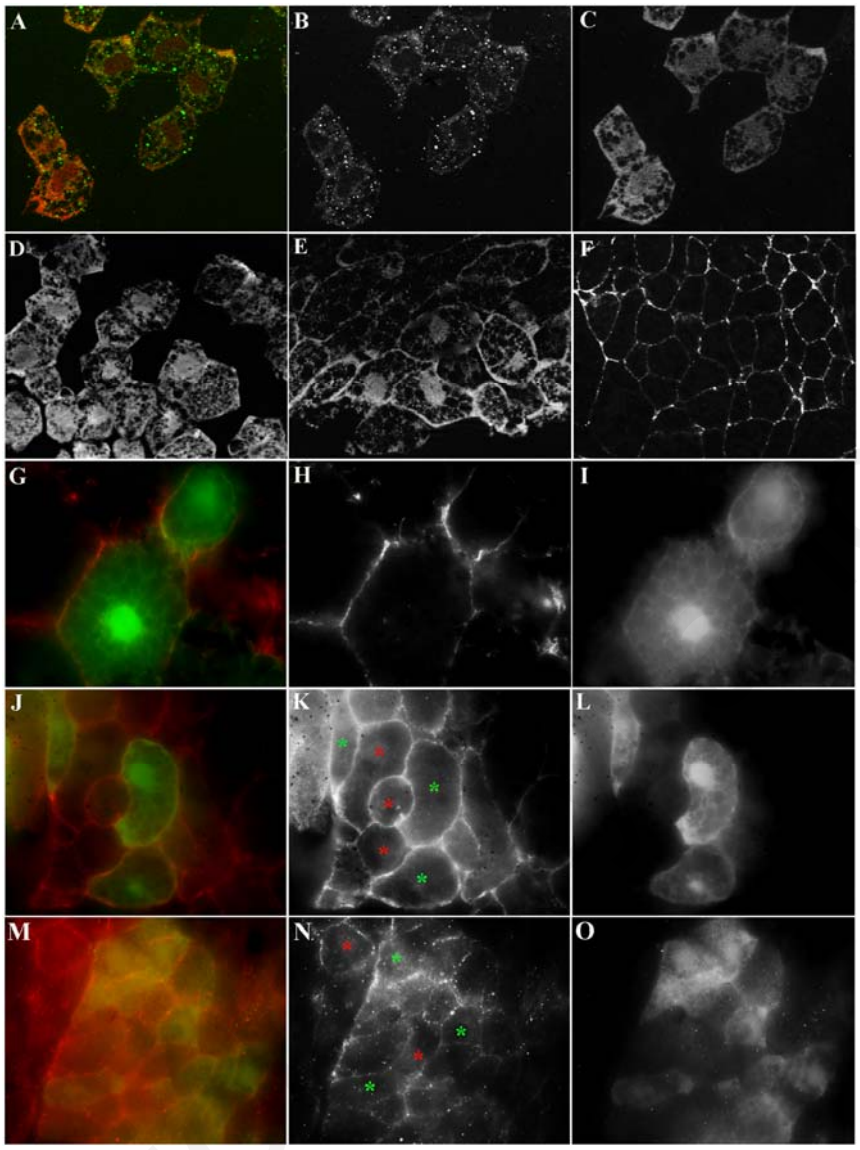

Figure 49. Exogenous FRNK localization and activated FAK. FRNK is not a dominant negative in *Xenopus laevis* embryos. (A) Colocalization of GFPFAK (B) (green) with FRNK (C) (red) at the animal pole of the overexpressed cells. (D) HAFRNK localization at the animal pole of the embryo when the embryo injected with 500pg of FRNK mRNA at two cell stage AP. (E) HAFRNK localization at the dorsal marginal zone when the embryo injected with 500pg at four cell stage embryo DMZ. (E) Activated FAK localizes tightly to the membrane. (G-I) DMZ cells which expressed FRNK (green, I) are not colocalize with activated FAK (red, H). (J-L) Localization of FRNK (green, L) and activated FAK at Tyr397 (red, K). HA FRNK (1ng) was injected in one out of two DMZ blastomeres of four cell stage embryos and did not cause any downregulation of the levels of phosphorylated FAK on Tyr397 site in whole embryos. Note the signal in the membrane of endogenous activated FAK in the FRNK expressing cells (K, green stars) compared to the neighbouring control cells which are the same level (K, red stars). (M-O) Localization of FRNK (green, N) and activated FAK at Tyr576 (red, O). The injections experiments performed as above. The expressions level of the injected cells (N, green stars) to their non injected neighbours is the same (N, red stars).

3.5.3 FAK becomes activated in *Xenopus laevis* embryos not exclusively by integrin-depended mechanisms.

The above data suggest that the activation of FAK in not exclusively through integrins in *Xenopus laevis* embryos because FRNK was found to act as a strong dominant negative of integrin based activation of FAK. This is supported by the fact that in early embryos (stage 8-blastula) fibronectin, the primary ECM component which is both necessary and sufficient for mesoderm migration in *Xenopus*, is still in the cytoplasm, and thus cannot engage integrin receptors (Danker, K., Hacke, H. et al. 1993). Yet FAK is already phosphorylated on residues Tyrosine 397, 576, 861 and 925 at this stage (Figures 41, 42, 43, 44 A). This strongly suggests that FAK phosphorylation prior to gastrulation is integrin independent. Laminin, the other major ECM phosphorylation component that integrins engage in the embryo is not expressed until stage 11 (Fey, J. and Hausen, P. 1990). Finally despite the fact that in gastrula stage embryos fibronectin is concentrated on the BCR both cells in contact with FN as well as cells that are not show high levels of phosphorylation once again suggesting that the bulk of FAK activation occurs in an integrin independent manner.

To further test this hypothesis, control embryos were stained with the FAK PY397 and/or integrin-β1 antibody. A5β1 is ubiquitously expressed and is the primary integrin heterodimer responsible for both mesoderm migration on FN as well as control of FN deposition by animal caps (AC) cells on the blastocoel roof (BCR) (Joos, T. O., Whittaker, C. A. et al. 1995). Activated FAK is localized tighly on the membrane (Figure 50A) in a similar fashion to integrin β1 at the sites of cell-cell contact (Figure 50C). However, no integrin-β1 staining can be seen on the apical surface of the outermost cell layer on the AC cells in control embryos in contrast to PY397FAK (Figure 50D, arrows and arrowhead). On the other hand in AC cells facing the blastocoels where fibronectin fibrils are assembled both integrins and activated FAK are found on the apical site of the membrane (Figure 50E, F, arrows). This suggests that FAK activation and localization on the plasma membrane can be independent of integrin clustering.

It is possible that FAK may be localized and activated on the cell membrane through cadherins. It has been shown that FAK can regulate cadherins and c-cadherin has been shown to localize on the apical side of the plasma membrane in certain cell types in *Xenopus* (Yano, H., Mazaki, Y. et al. 2004; Nandadasa, S., Tao, Q. et al. 2009). To examine this possibility we repeated the above experiment using an antibody against c-cadherin which is the only cadherin expressed in the embryo prior to gastrulation

(Heasman, J., Ginsberg, D. et al. 1994; Nandadasa, S., Tao, Q. et al. 2009). Control embryos were stained with c-cadherin antibody, alone (Figure 50B) or together with FAK PY397 antibody (Figure 50G, H, I) revealing that there is no colocalization between c-cadherin and activated FAK on the apical site of the plasma membrane of superficial cells (Figure 50G, arrow). This shows that endogenous FAK can become phosphorylated and thus activated in the absence of both integrins and cadherins.

This taken together with the activation of FAK prior to gastrulation and secretion of ECM components and the inability of FRNK overexpression to reduce endogenous FAK phosphorylation suggest that the bulk of FAK activation in the embryo occurs in an integrin-independent manner and probably through growth factor receptors on the plasma membrane.

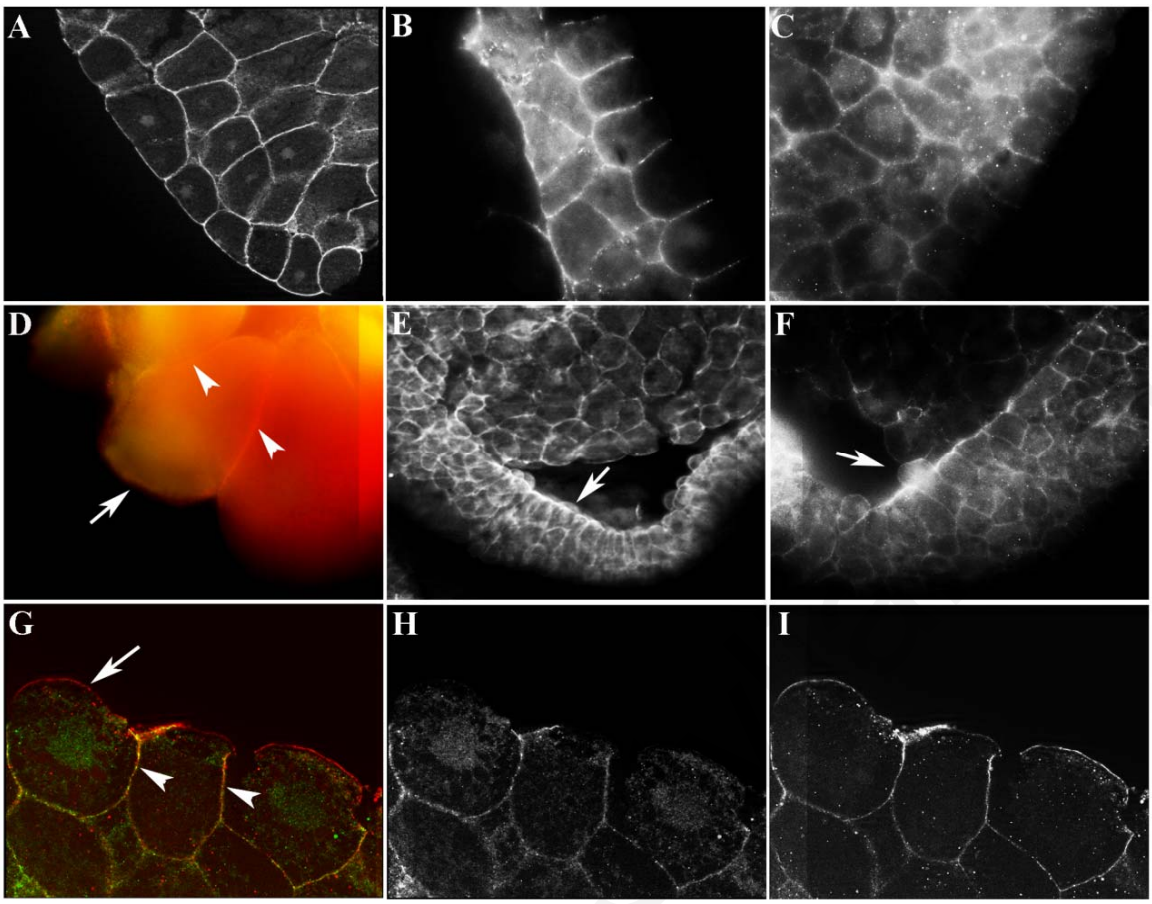

Figure 50. FAK becomes activated in *Xenopus laevis* embryos independently of integrins complexes. (A) Endogenous expression of Tyr397 FAK (B) cadherin and (C) integrin-β1 in control embryos fixed at stage 12 and sagittal sectioned. (D) Double staining in control embryos with anti-FAK PY397 (red) and integrin-β1 (green, arrowheads) which is obvious that in the apical surface of the embryo only activated FAK is detectable (red, arrow). (E-F) AC cells facing the blastocoels where fibronectin fibrils are assembled both integrins (F) and activated FAK (E) is found on the apical site of the membrane. (G) Double staining in control embryos with anti-FAK PY397 (red, arrow) and cadherin (green, arrowheads). Same as integrin only activated FAK is detectable in the apical surface of the whole embryo (I) and cadherin only in cell-cell boundaries (H).

3.6 Investigation of the function of various Focal Adhesion Kinase domains in *Xenopus* embryo

3.6.1 Generation and initial characterization of different constructs of Focal Adhesion Kinase

Experiments in the previous section suggested that the C-terminal domain of FAK which is both necessary and sufficient for focal adhesion targeting of FAK is not sufficient to target FAK on the plasma membrane or cell-cell contact areas in the *Xenopus* embryo. In an effort to identify the region of FAK responsible for membrane localization as well as the importance of residues known to facilitate some of FAKs interactions we generated and tested several constructs including: GFPFAK, HA FAK, HA Y397FFAK, HA K454RFAK, HA D395AFAK, HA FAKΔFAT, HA Y397FΔFAK, HA Δ395FAK, HA FERM/FRNK, HA FERMY397F/FRNK, HA FERM, HA Y397FFERM, GFPFRNK, HA FRNK and HA FAT (Figure 51, details materials and methods section). All constructs were *in vitro transcribed* to mRNA using mMessage mMachine Sp6 kit (Ambion) and run to 1% agarose (Figure 52A). mRNA's were quantified and used for microinjections after cleaning with lithium chloride and ethanol precipitation. Verification of the expression of these constructs at the protein level was made by Western Blot Analysis (Figure 52B).

To examine the localization most of the constructs that we generated, a total of 500pg of each mRNA was injected. The injections were performed on four cell stage embryos AP (2/4 AP) and DMZ (2/4DMZ) of four cell embryo. Following injection embryos were allowed to develop to mid gastrula (st.10), fixed, permeabilized, bleached and proceed for immunofluorescence using an HA antibody (HA monoclonal, Santa Cruz) and secondary alexa633. The embryos that were injected in the DMZ were sagittally sectioned and then treated as above. Most of the constructs had the same expression pattern as inactive FAK (Figure 53, 54). The localization of the generated mutants in several regions of the embryo DMZ, AP and Apical surface is shown in the following Figures: 53, 54 and 55.

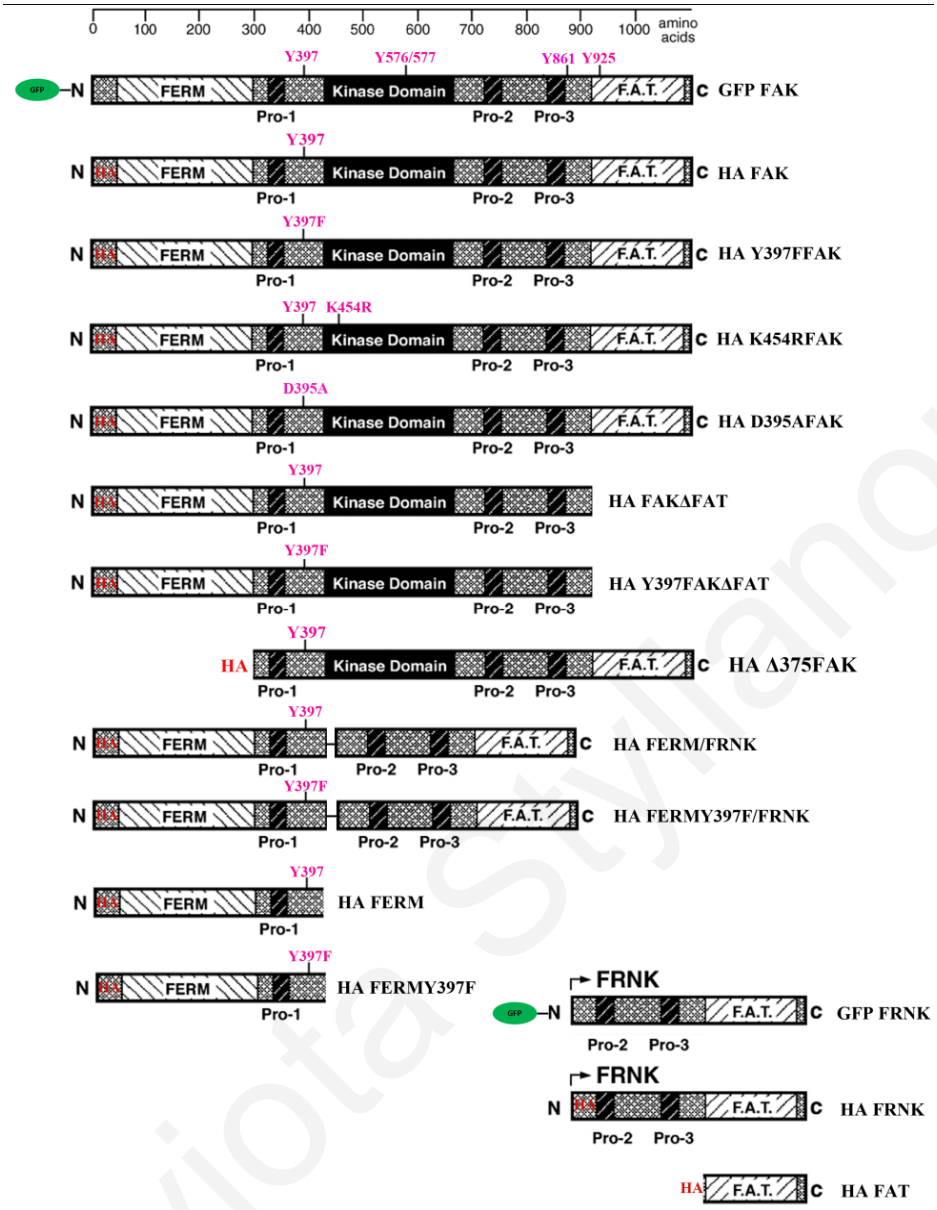

Figure 51. Constructs that generated. FAK proteins were HA-tagged on their NH_2-terminal, except GFP FAK and GFP FRNK, which are fused with GFP in their N-terminal. In all the HA-tagged constructs except HA Δ375FAK, HA FRNK and HA FAT, the HA epitope is replacing the first 30 amino acids (aa) of the N-terminal. In the Y397F containing constructs, the tyrosine 397 is substituted to phenylalanine and in the K454R construct, the lysine 454 is substituted to arginine. The ΔFAT constructs, do not contain the FAT domain (904-1068aa). The HA Δ375FAK construct, does not have the first 375 aa, which is the FERM domain, but it contains all the major phosphorylation sites. The HA FERM and HA FERMY397F mutants, contain the FERM domain, the first proline-rich region and the site 397. The HA FERM/FRNK and HA FERMY397F/FRNK constructs contain the FERM domain with the site 397, which is ligated with FRNK through a linker of six aa. They include the sites Tyr861 and Tyr925, but they do not have the major catalytic site Tyr576/577. The GFP FRNK and HA FRNK constructs contain the 2nd and 3rd proline-rich regions with the sites Tyr861 and Tyr925. The HA FAT construct, contains the 904-1068aa that are not included in the ΔFAT constructs with the Tyr925.

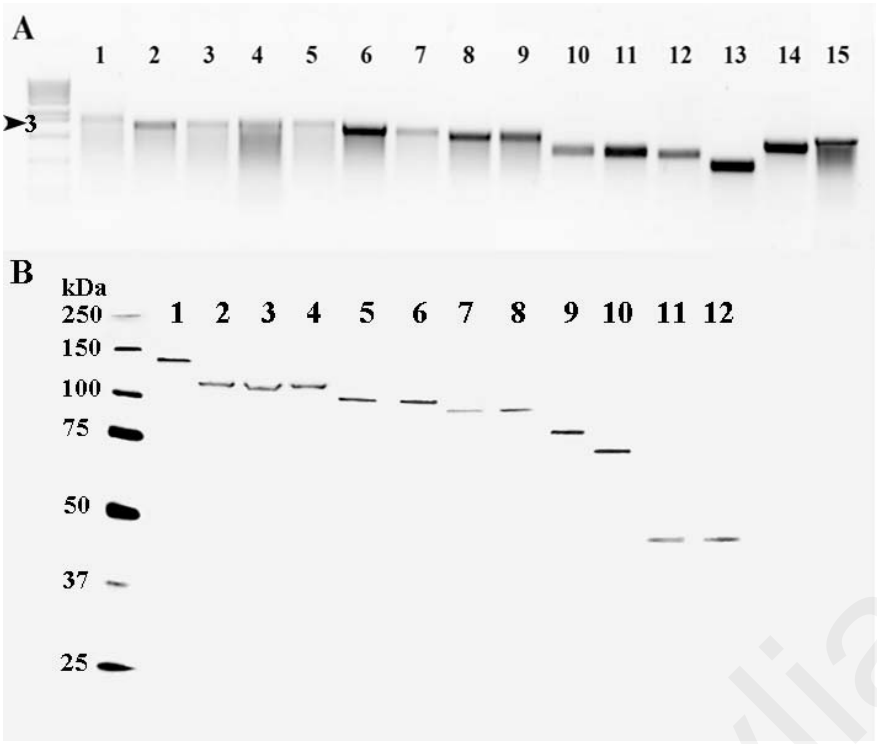

Figure 52. Initial characterization of the constructs. (A) Capped RNA generated through *in vitro transcription* of constructs. 1 to 15: GFP FAK, HA FAK, HA Y397FFAK, HA K454RFAK, HA D395AFAK, HA FAKΔFAT, HA Y397FFAKΔFAT, HA FERM/FRNK, HA FERMY397/FRNK, HA FERM, HA FERM397, HA FRNK, HA FAT, GFP FRNK and Δ375 FAK. (B) Expression of the constructs at protein level. Lane 1: GFPFAK, 2: HA FAK, 3: HA K454RFAK, 4: HA Y397FFAK, 5: HA FAKΔFAT, 6: HA FAKY397FΔFAT, 7: HA FERM/FRNK, 8: HA FERMY397F/FRNK, 9: HA Δ375FAK, 10: GFPFRNK, 11: HA FERM, 12: HA FERMY397F.

In AP cells all the constructs showed weak localization on the cell-cell boundaries and most of the signal was in the cytoplasm. The only two constructs showing a different pattern were the FERM (wild type and Y397F mutant) and FERM/FRNK constructs (wild type and Y397F mutant) which displayed strong cell-cell boundary localization similar to that of endogenous phosphorylated FAK (Figure 53 G-H, K-L). In addition both FERM and FERM/FRNK were localized on plasma membrane associated vesicles. The FERM domain was also found in the nucleus as expected since the FERM domain contains an NLS signal on the F2 loop (Ossovskaya, V., Lim, S. T. et al. 2008).

Interestingly when these constructs were expressed in the DMZ most of them had different localization from the one that they had at AP cells (Figure 53, 54). Wild type FAK and point mutants of FAK had the same localization but now FRNK and FAT showed relatively strong cell-cell boundary localization as well as nuclear staining (Figure 54). The localization of the FAT domain on cell-cell contact areas was even tighter than that of FRNK and surprisingly it was also strongly localized in the nucleus despite the fact that it does not contain any known NLS signals (Figure 54 G, H). Overall in these strongly morphogenetic cells the FAT domain showed a markedly better ability to target FAK at the cell-cell contact areas than it did in AP cells. In this context the FERM and FRNK domains show localizations that are quite similar but a striking change in localization occurs when the two domains are combined in the absence of the kinase domain. The combination leads to loss of the cytoplasmic pool seen in both FERM and FRNK and cell-cell contact localization becomes very strong (Figure 54I).

To confirm the above localizations another experiment was performed. Each domain was co-injected with 100ng GFPFAK at the AP of four cell stage embryos and the same procedure was used as above. An HA antibody was used for the different domains with secondary alexa 633 and for GFPFAK GFP antibody was used with secondary Cy3. Each embryo is different from the other, the pigmentation of the animal pole and the rate of the divisions, so we wanted to have an internal control for each construct. So with the co-injections of GFPFAK we had every time internal control of the expression and localization of full length FAK (Figure 56). As we saw before FERM and FERM/FRNK were the most tightly localized on the membrane in these cells with weak staining in the nucleus (Figure 56C, E). Also Δ375FAK when expressed at the AP of the embryos showed that the localization of this construct was similar to the endogenous FAK but with near complete loss of the plasma membrane component. More detailed analysis of the localization of these constructs will follow in later sections.

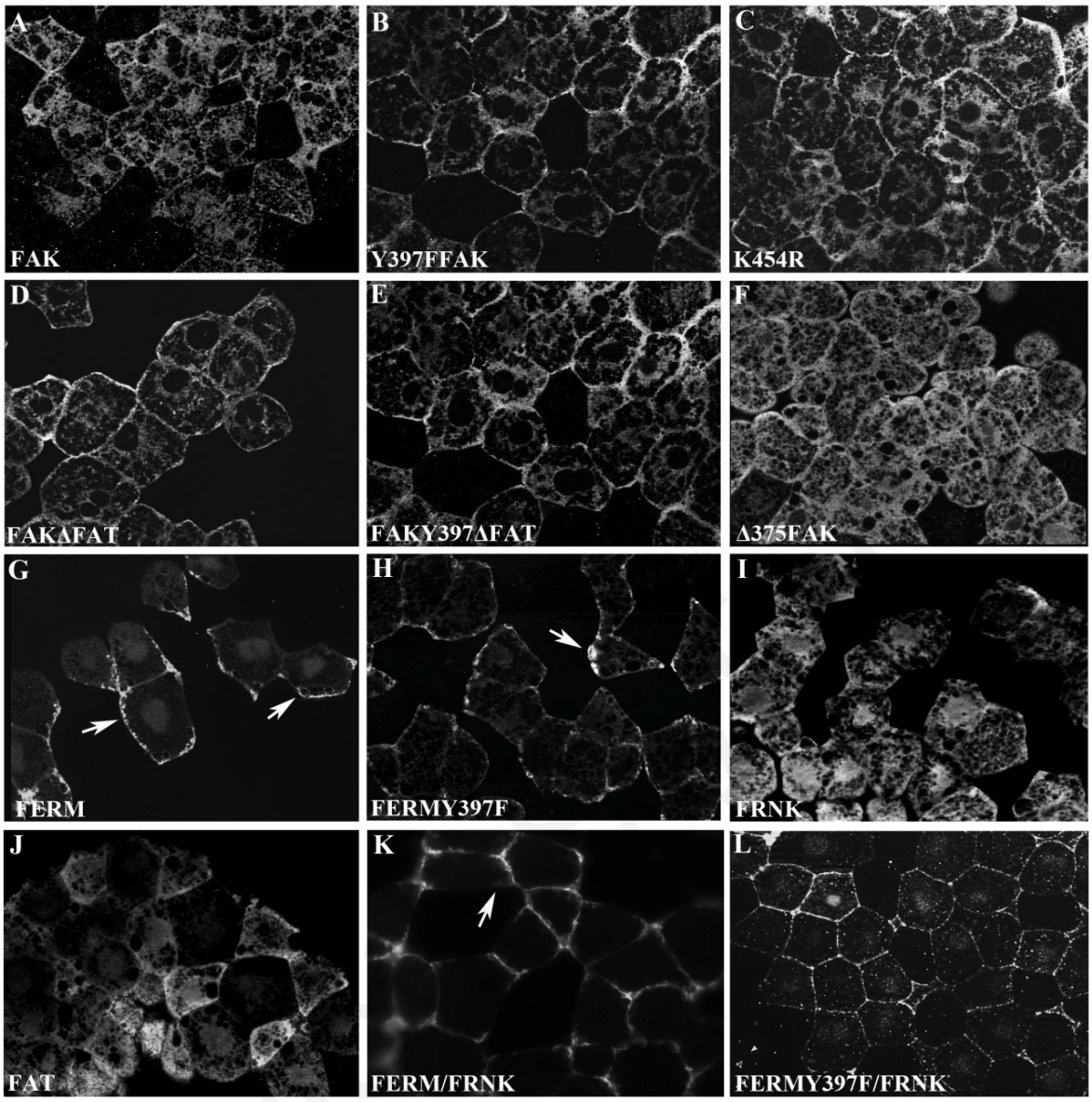

Figure 53. Localization of the mutants at AP of the embryo. (A-L) Optical section of animal views of stage 12 embryos after clearing with the use of BB/BA. 500pg of each domain was injected to one from two cell stage embryo at animal pole, fixed at stage 12, sectioned, permeabilized, bleached and proceed to immunofluorescence assay. HA monoclonal antibody was used and for secondary Cy3. (A-E) Mutants have similar localization to HA FAK (A). (F) Δ375FAK is diffused in the cytoplasm. (G-H) Mutants are tightly localized on the membrane and on the plasma membrane associated vesicles (arrow). (I-J) Mutants have similar localization to HA FAK (A). (K-L) Mutants are tightly localized on the membrane and on the plasma membrane associated vesicles (arrow).

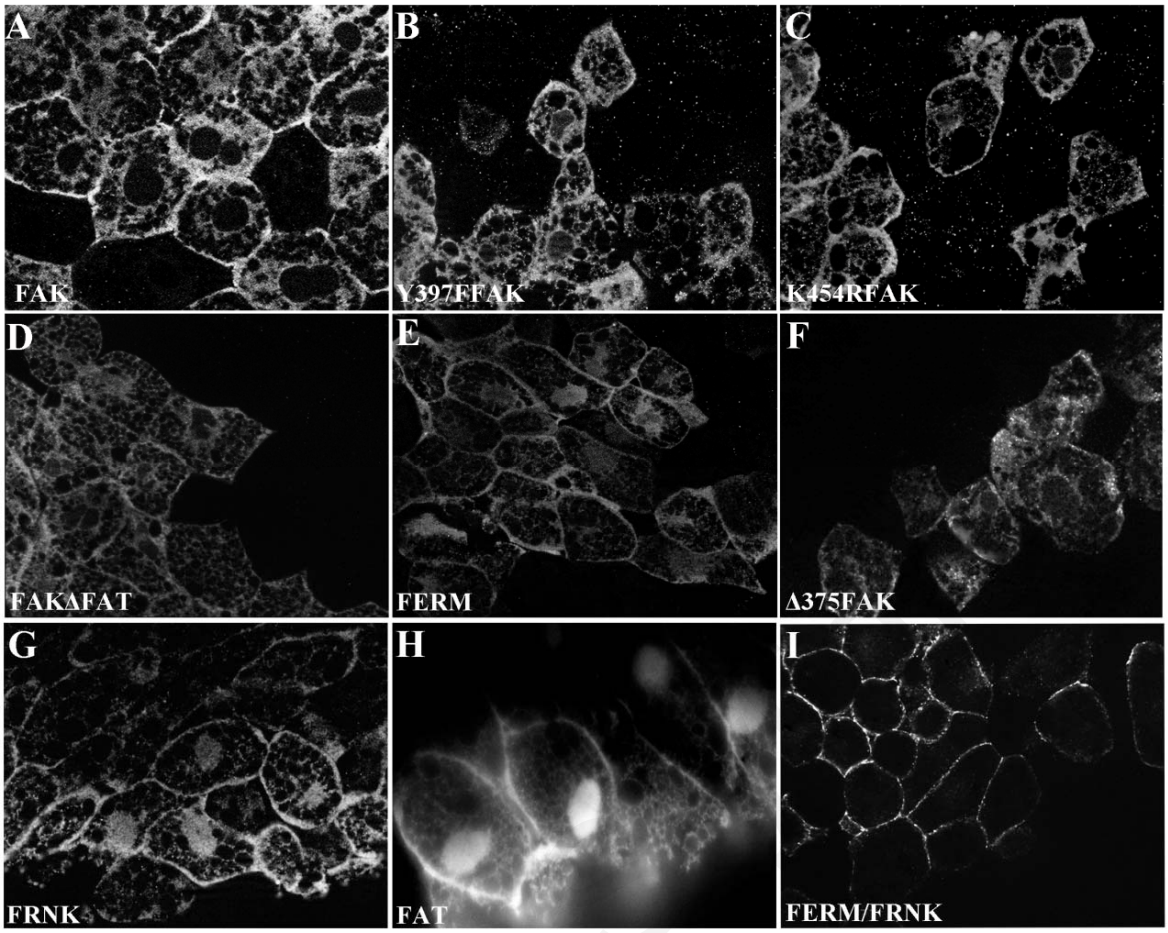

Figure 54. Localization of the mutants at the Dorsal Marginal Zone of the embryo. (A-I) Mid sagittal optical sections of dorsal views of stage 12 embryos after clearing with the use of BB/BA. 500pg of each domain was injected to one from four cell stage embryo at DMZ, fixed at stage 12, sagittal sectioned, permeabilized and proceed to immunofluorescence assay. HA monoclonal antibody was used and for secondary Cy3. (A) HA FAK is localized on the membrane, in the cytoplasm and in the nuclear. (B-C) Point mutants are on the plasma membrane and in the nuclear. (D) HA FAKΔFAT localized on the cortical cytoskeleton, partially on the plasma membrane. (E) HA FERM localized on the plasma membrane and in the nuclear. (F) Δ375FAK is diffused in the cytoplasm and on the plasma membrane. (G) HA FRNK is localized on the plasma membrane and in the nuclear. (H) HA FAT is localized on the plasma membrane and strongly in the nuclear. (I) HA FERM/FRNK is tightly localized on the plasma membrane.

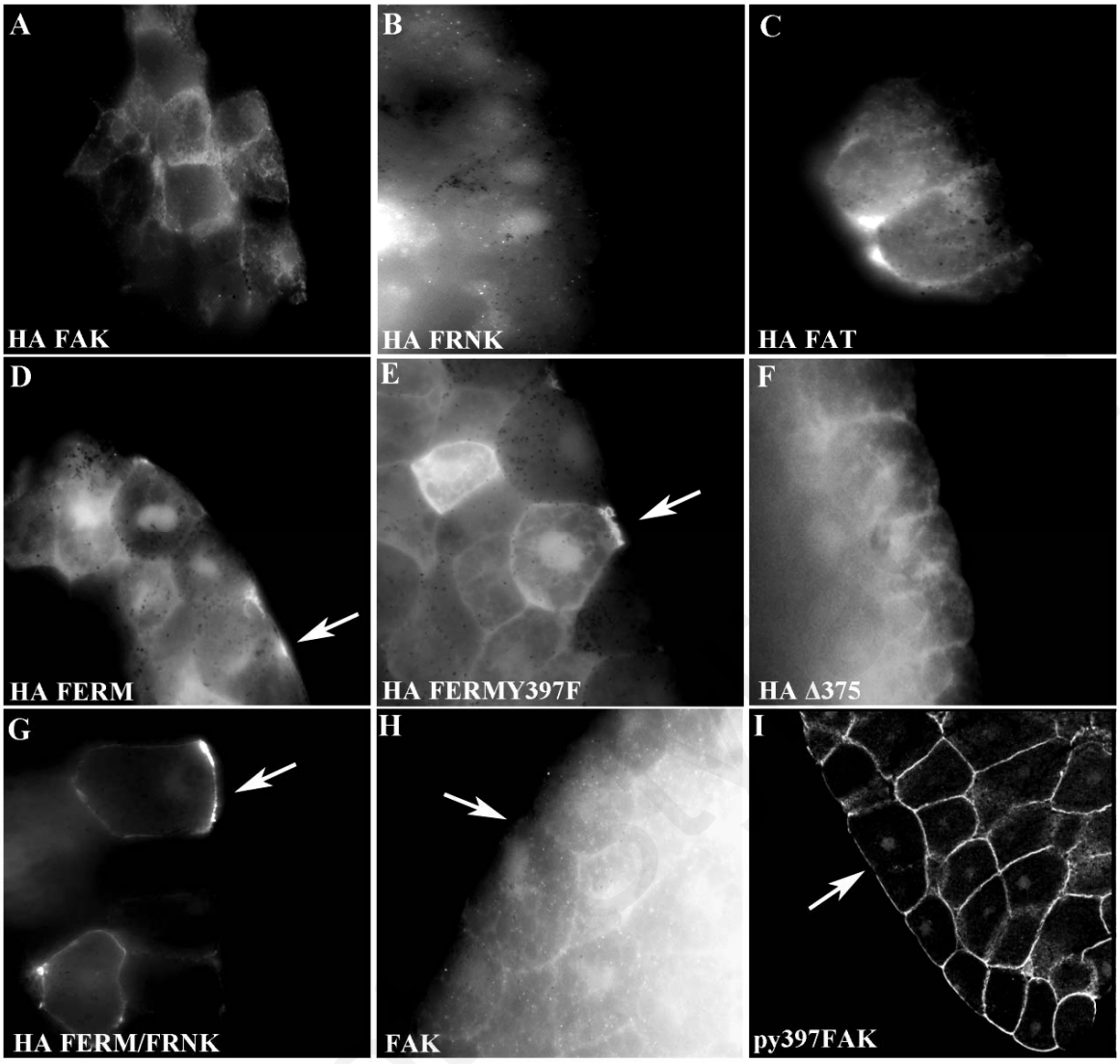

Figure 55. Localization of the mutants in the apical surface of the cells of the animal cap cells in the embryo and localization of non-activated and activated endogenous FAK. (A) HA FAK is localized on the apical surface. (B) HA FRNK, (C) HA FAT and (F) HA FAKΔ375 are not expressed on the apical surface. (D) HA FERM and (E) HA FERMY397F are localized on the apical membrane with the form of these vesicles. (G) HA FERM/FRNK is tightly localized on the apical membrane. (H) Endogenous FAK localization on the apical surface stained with anti-FAK (Novus, NB600-847) and secondary Cy3. (I) Phosphorylated FAK on the residue Tyrosine 397 on the apical surface stained with anti-PY397FAK and secondary Cy3.

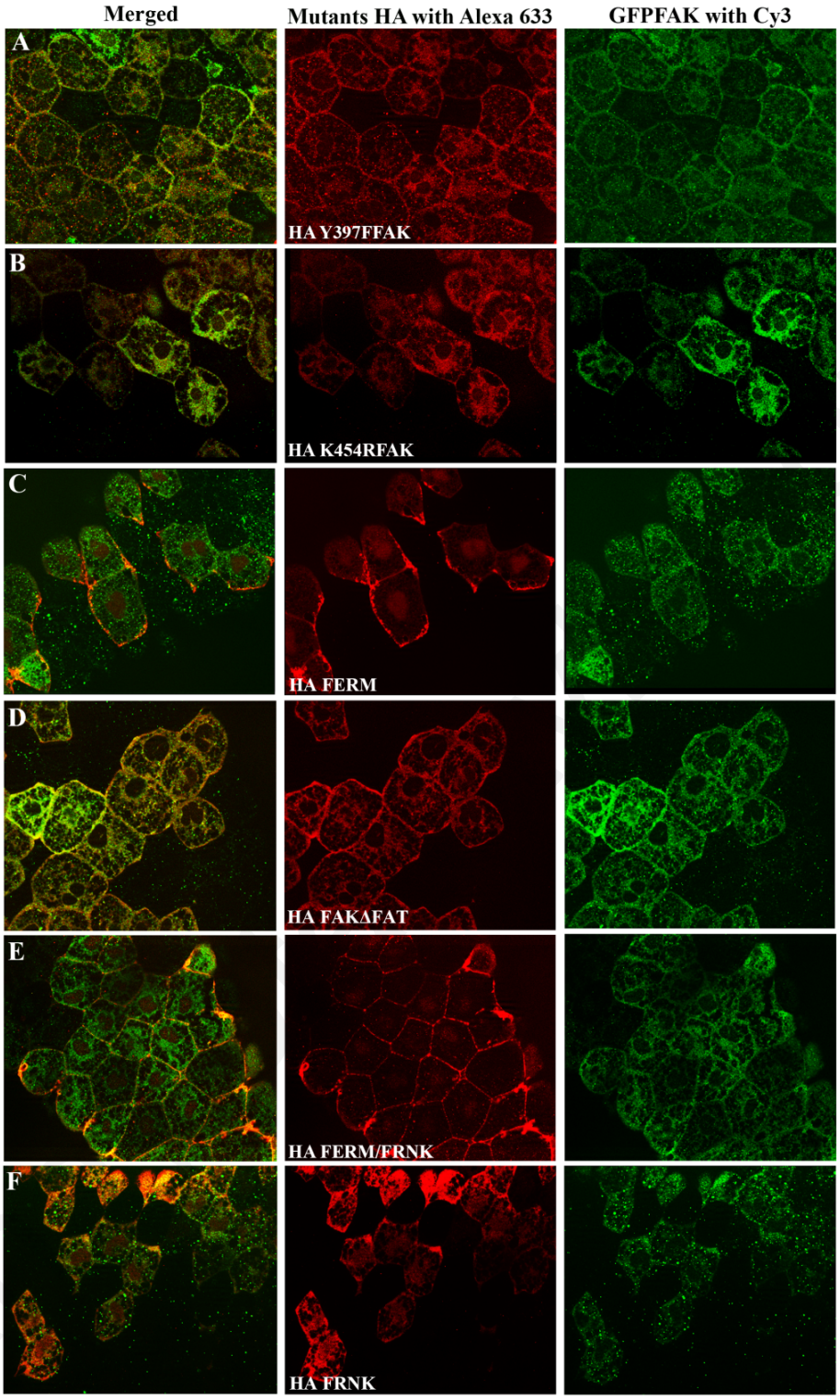

Figure 56. Mutants of FAK and GFPFAK localization at Animal pole cells. (A-F, left column: merged) Optical sections of animal views of stage 12 embryos after clearing with the use of BB/BA. 500pg of each domain was co-injected with 100pg of GFPFAK to one from two cell stage embryo at AP, fixed at stage 12, sectioned, bleached, permeabilized and proceed to immunofluorescence assay. HA monoclonal antibody was used for the mutants of FAK that were generated (red, middle column) and anti-GFP for GFPFAK (green, right column).

Because of the tighter localization of FAT in DMZ cells we decided to examine it further (Figure 54H). As mentioned above FAT domain is necessary and sufficient for the localization of FAK to the focal adhesions (Hildebrand, J. D., Schaller, M. D. et al. 1993). Expression of the FAT via microinjection of AP blastomeres showed that in these cells it is mainly localized in the cytoplasm like FRNK (Figure 53I, J). Visualizing the HA FAT protein in sectioned embryos at the apical side of the plasma membrane of superficial blastomeres, confirmed that like FRNK, the FAT domain is unable to access this region (Figure 55C). This demonstrates that the FAT domain is not responsible for the membrane localization of FAK at least in the apical surface but is probably partially responsible for the cell-cell contact localization of FAK in the cells of the DMZ (Figure 54H).

To further examine the role of the FAT domain in the localization of FAK in the embryo, a deletion of the FAT domain was generated. The HA FAKΔFAT construct fails to localize at the focal adhesions of migrating mesodermal cells plated on fibronectin (Figure 57A). On the other hand a full length HA tagged construct localized on FAs quite strongly confirming that the FAT domain is necessary for targeting FAK to the integrin based focal adhesion complexes (Figure 57B, arrow). In order to examine if the HA FAKΔFAT construct is localized on the plasma membrane, it was compared with the localization of full length FAK at the AP site of the embryo. In embryos coinjected with GFP FAK (100pg) and HA FAKΔFAT at the AP, it appears that the localization of the last construct is strongly correlated with that of full length FAK (Figure 56D). These data are in agreement with the observation that the FAT domain in the AP cells fails to localize on the plasma membrane localization (Figure 53J). The weak membrane localization of both exogenous full length FAK as well as the ΔFAT construct is probably due to the fact that the majority of the protein is in the closed conformation with the FERM domain unable to bind PIP2 or GFRs (growth factor receptors) and take the protein to the membrane.

To verify if this observation is conserved also in the DMZ cells, the injected embryos in the DMZ site were stained with the anti-HA antibody in order to verify the localization of HA FAKΔFAT and HA Y397FΔFAT (Figure 57E, H). Both constructs are localized partially on the membrane and they display diffuse localization in the cytoplasm. Moreover, injected embryos with HA FAKΔFAT were stained with the anti-HA antibody and anti-PY397FAK antibody (Figure 57D-F, G-I). In these cells, there is a slight difference on the membrane localization of this construct (Figure 57D, arrow). In agreement to this, there is elevation in the cytoplasm, which it comes from the construct, and that is the reason why this elevation is not on the membrane. Western Blot analysis

confirmed that this cytoplasmic elevation it comes from the phosphorylated exogenous construct (Figure 57C: lane 1). The above experiment was repeated with the HA Y397FΔFAT construct. Here, it is clear that the HA Y397FΔFAT construct is localized on the cortical cytoskeleton, because the antibody that does not recognize this mutant is now exclusively seen on the plasma membrane (Figure 57G, arrow). This is also in agreement with the localization of the FAT domain in DMZ cells, where it was on the plasma membrane. Therefore, its deletion in these cells may play a role in the localization of FAK on the membrane. However, the FAT domain may not be the only responsible domain for the localization of FAK on the membrane in DMZ cells either, because there is some co-localization with the activated FAK on the plasma membrane.

These results suggests that the C-terminus of FAK (FAT domain) it is not capable of leading full length FAK to the membrane on its own, and that it is possible that other domains of FAK alone, or combined with the FAT domain are necessary for membrane localization.

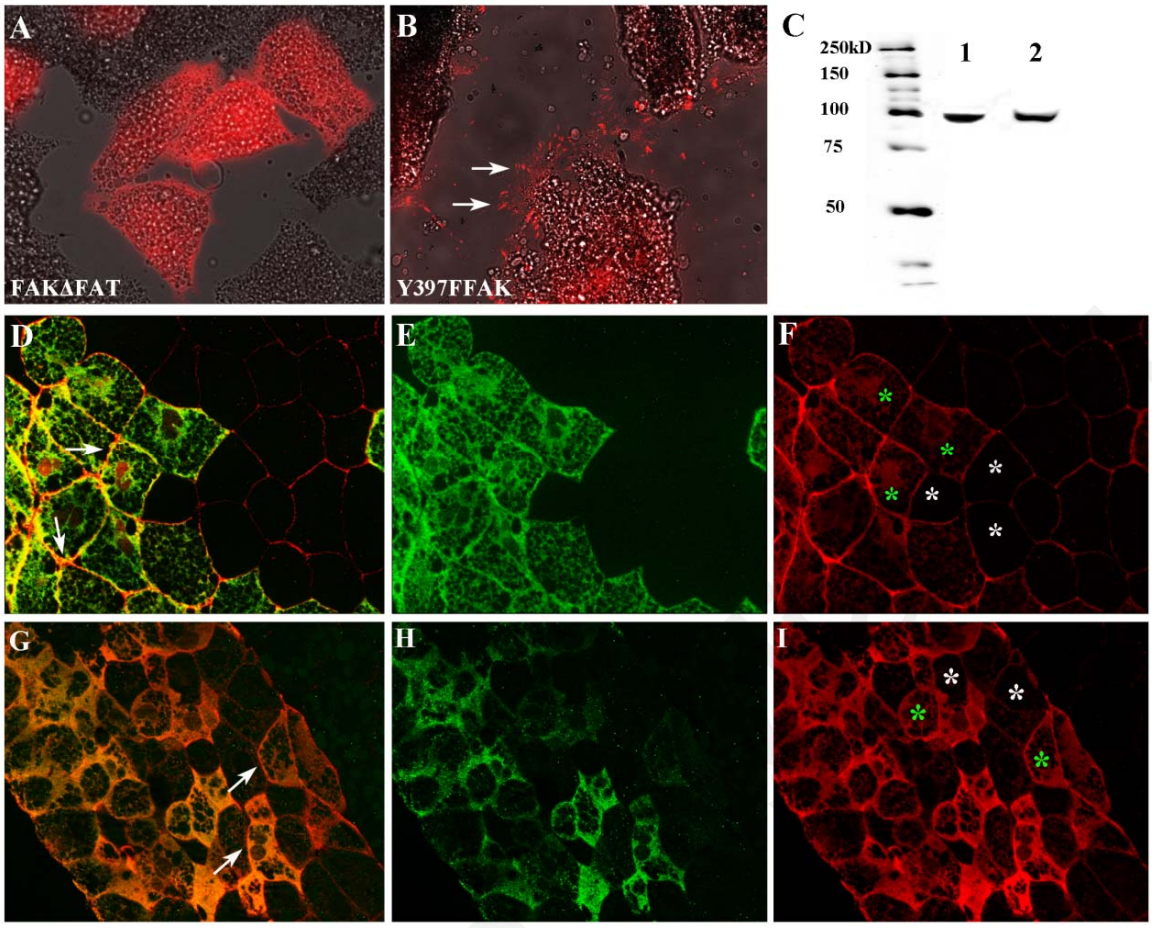

Figure 57. The FAT domain is partially responsible for the plasma membrane localization of FAK. (A-B) Migrating cells on fibronecting coated coverslips after immunofluorescence with HA monoclonal antibody and for secondary Cy3. FAKΔFAT does not have the characteristic linear structures as expect (A) but Y397FFAK does (B, arrows). (C) Western blot analysis of HA FAKΔFAT blotted with P-Y397 (lane 1), and stripped and reprobed with HA (lane 2). (D) Merged image of mid-sagittal optical section of stage 12 embryo with double staining (arrow: place only anti-PY397FAK). 500pg of FAKΔFAT were injected in the DMZ site of the embryo, fixed at stage 12, sagittaly sectioned, permeabilized and proceed to immunofluorescence assay. There is some co-localization with the activated FAK on the membrane in these cells. For FAKΔFAT monoclonal HA antibody was used stained with Alexa 488 (E, green) and for activated FAK polyclonal anti-FAKPY397 used stained with Cy3 (F, red). (G) Merged image of mid sagittal optical section of stage 12 embryo with double staining as above (arrows: place only anti-PY397FAK). For Y397FΔFAT monoclonal HA antibody was used stained with Alexa 488 (H, green) and for activated FAK polyclonal anti-PY397FAK used stained with Cy3 (I, red). Green stars at F and I are cells injected compared to white stars on non injected cells.

3.7 The FERM domain is responsible for the plasma membrane localization of FAK in integrin-free areas and it activates FAK in a Src- dependant manner

3.7.1 The FERM domain of the Focal Adhesion Kinase can autonomously localize at the plasma membrane in *Xenopus* embryos

The data presented so far suggest that the majority of FAK activation during the early stages of *Xenopus* development is achieved through integrin independent mechanisms. This is rather surprising given the fact that most of the emphasis regarding FAK has always been in its role as a focal adhesion protein. However most of the work has been carried out in cell culture where cell ECM interactions are the primary mode of adhesion (Hanks, S. K., Calalb, M. B. et al. 1992; Schaller, M. D., Otey, C. A. et al. 1995; Richardson, A. and Parsons, T. 1996). In the embryo this is not the case and cell-cell interactions govern the three dimensional architecture. Since the FAT domain which is responsible for localization to the focal adhesions is unable to target FAK to the plasma membrane, the next step was to determine which domain was responsible for this localization (Figure 55C). Towards this end the HAFERM construct was used. The FERM domain is known for its inhibitory role of the FAK molecule (Cooper, L. A., Shen, T. L. et al. 2003; Lietha, D., Cai, X. et al. 2007). By interacting with the kinase domain the FERM domain keeps FAK in the inactive closed conformation (Cooper, L. A., Shen, T. L. et al. 2003). FAK phosphorylation on Tyr397 and the more recently described Tyr194 relieves the binding of the FERM on the kinase domain allowing FAK to become active and phosphorylate downstream targets (Lietha, D., Cai, X. et al. 2007; Chen, T. H., Chan, P. C. et al. 2011). The FERM domain has also been shown to be able to bind PIP2 as well as growth factor receptors like HGFR and EGFR making it a good candidate for the membrane localization of FAK (Cai, X., Lietha, D. et al. 2008; Chen, T. H., Chan, P. C. et al. 2011). Therefore, it may be possible that the FERM domain can transport full length FAK to the membrane where its activated.

Overexpression of FERM by injections showed that is localized in the nucleus (as expected (Ossovskaya, V., Lim, S. T. et al. 2008)) and partially on the membrane in DMZ cells (Figure 58A) but tightly on the membrane in AP cells (Figure 58B). In AP cells it displays a characteristic pattern, localizing on plasma membrane associated vesicles (Figure 58B, arrow). Moreover, the FERM domain just like phosphorylated endogenous FAK and unlike FRNK is localized on the apical side of the plasma membrane, which is free of intergins and cadherins (Figure 55B, D, I). The above results suggest that the FERM domain goes to the membrane through binding of PIP2 or growth factor receptors and not

through intergins in this context, suggesting that the FERM domain is crucial in the activation of FAK in the context of the embryo. Since the N-terminus of FAK that contains the FERM domain also contains Tyr397 major site of autophosphorylation of FAK and a site bound by many of FAK partners including PI3K and Src, the mutated HA FERMY397F construct was generated in order to examine if removing the major site of autophosphorylation would affect the constructs localization. The HA FERMY397F point mutant localized in a similar fashion as the HAFERM suggesting that Tyr397 does not play a role in the localization of the FERM domain (Figure 58C, arrow).

As we mentioned before co-injection of 500pg HA FERM with 100pg GFPFAK showed that the membrane localization of FERM alone is tighter than that of the full length FAK (Figure 55C). In order to examine if this membrane localization of FERM is preserved in the DMZ cells, injected embryos with the HA FERM were stained for the PY397FAK antibody. In these cells, FERM partially localizes on the cell-cell boundaries, where it partially co-localizes with phosphorylated FAK (Figure 58G-I).

The fact that the FERM domain is able to go to the plasma membrane more tightly than full length FAK or the C-terminus (FRNK/FAT) in combination with the fact that phosphorylated endogenous FAK is exclusively found on the membrane suggests that the FERM domain is at least partially responsible for the membrane localization of endogenous FAK. The fact that the endogenous phosphorylated FAK is even tighter on the cell-cell boundaries of the DMZ cells than FERM, could indicate either a need for cooperative action between the C-terminus and the N-terminus of FAK for proper localization or that the overexpression of the construct results in saturation of FAK binding sites on the membrane thus causing elevated cytoplasmic localization of the construct.

The FERM domain has been shown to interact *in vitro* with the cytoplasmic tails of β1 integrins therefore it is possible that it can be recruited to the membrane through integrin complexes (Schaller, M. D., Otey, C. A. et al. 1995). However the FERM domain does not co-localize with integrin β1 on the plasma membrane associated vesicles (Figure 59D-F, arrow). It has also been shown that the FERM domain is involved intercellular junctions, so it would be possible that FERM is localized on the membrane through cadherin-based adherens junctions (Stewart, A., Ham, C. et al. 2002). Embryos injected with 500pg of FERM, fixed and stained with the HA (Figure 59B) and the c-cadherin antibody (Figure 59C). No co-localization between FERM and c-cadherin was found on the plasma membrane assosiated vesciles (Figure 59A, arrow). This suggests that FERM is not localized to the membrane through its participation in cell-cell junctions. Therefore, like

activated FAK, the FERM domain is localized on the plasma membrane associated vesicles, and on the apical surface through integrin- and cadherin- independed manners.

There is evidence that the FERM domain can intact directly through its F2 lobe with membrane receptors and phospholipids (Cai, X., Lietha, D. et al. 2008; Chen, T. H., Chan, P. C. et al. 2011). To confirm that the plasma membrane associated vesicles are indeed plasma membrane based structures, embryos were injected with 500pg of HA FERM and 200pg memGFP (membrane GFP: has GAP43 palmitoylation sequence which is indicator of the plasma membrane). FERM and membrane GFP co-localize on these structures confirming that these are plasma membrane derived vesicles (Figure 59G-I, arrow). Moreover, these vesicles are present in non-injected cells, but through an unknown mechanism, are formed more frequently in FERM overexpressing cells. The FERM domain co-localizes with the activated FAK on the apical surface on these vesicles (Figure 58D-F).

Overall, it was shown that the FERM domain of FAK is localized on the plasma membrane where it partially co-localizes with endogenous phosphorylated FAK. The FERM domain alone is also localized at the apical surface of AC cells and on membrane bound vesicles close to the plasma membrane. Neither integrins nor cadherins are found at these membranes. These results suggest that the FERM domain is at least partially responsible for the membrane localization of endogenous activated FAK and not the C-terminal FAT domain which is responsible for integrin based membrane localization of FAK. Finally, the FERM domain is sufficient for membrane localization at the apical surface of the plasma membrane in AC cells while it appears to be only partially sufficient for tight plasma membrane localization in DMZ cells (Figure 58A, B).

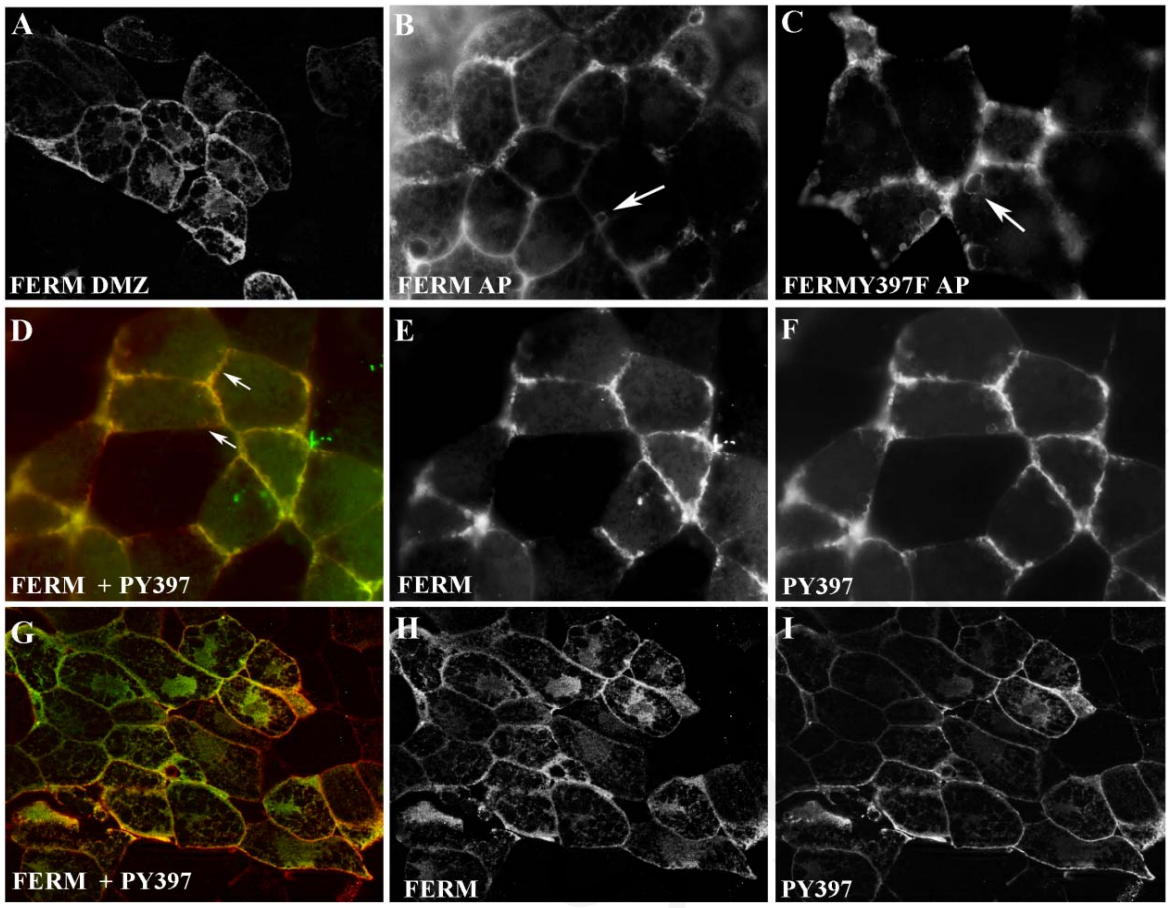

Figure 58. The FERM domain can autonomously localize on the plasma membrane. (A) HAFERM localization at the dorsal marginal zone when the embryo injected with 500pg at four cell stage embryo DMZ. (B) HAFERM localization at the animal pole when the embryo injected with 500pg of FERM mRNA at two cell stage AP (plasma membrane associated vesicles indicated with arrow) (C) HAFERMY397F localization at the animal pole of the embryo when injected with 500pg of FERMY397F mRNA (plasma membrane associated vesicles indicated with arrow). (D) Co-localization of HAFERM (E) (green) overexpressing cells stained with PY397 (F) (red) at the animal pole of the overexpressed cells where activated FAK localizes tightly to the membrane and to the plasma membrane associated vesicles (F). (G) Partially co-localization of HAFERM (H) overexpression stained with PY397 (I) at DMZ cells.

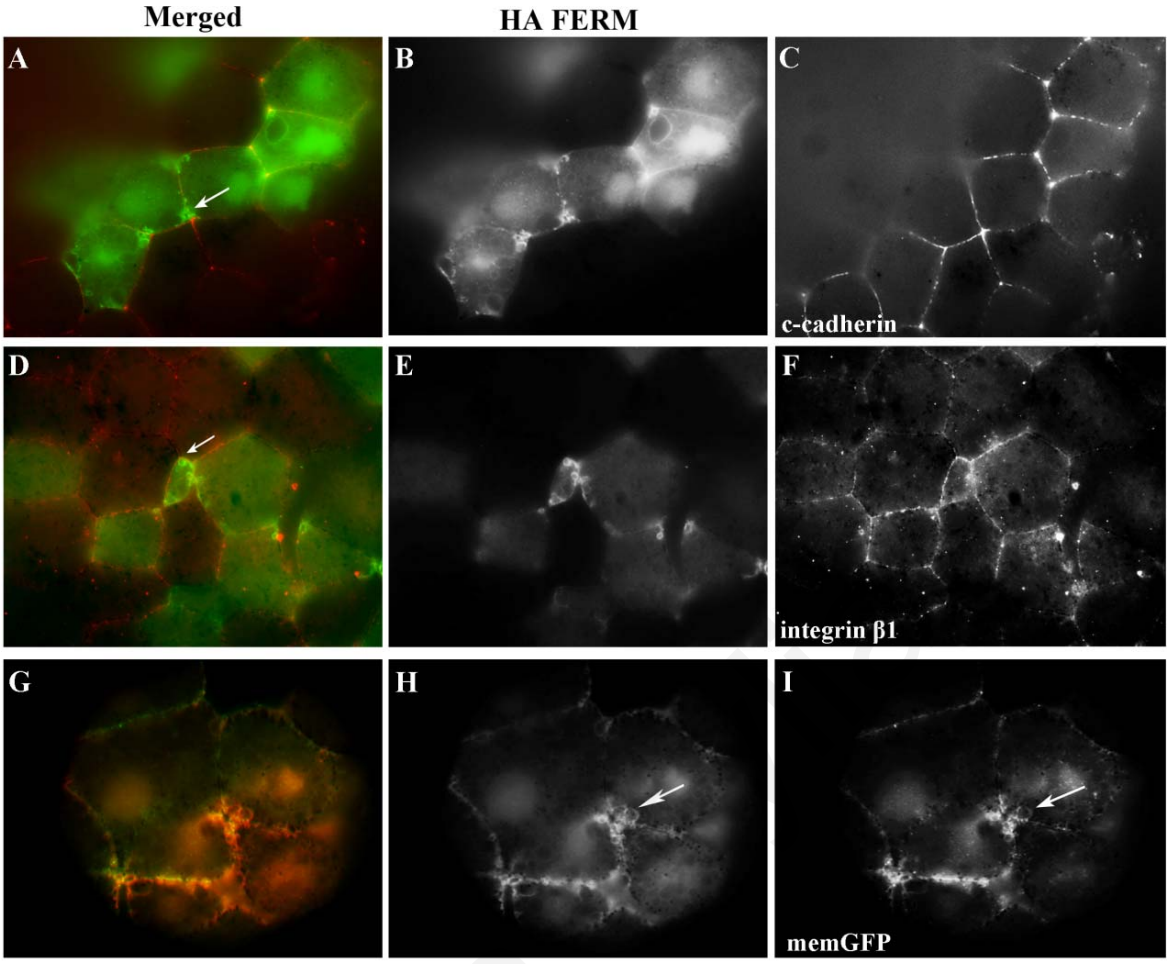

Figure 59. FERM domain of FAK is localized on the plasma membrane through a membrane-based mechanism. (A) AP cells which expressed FERM (green, B) are not co-localized with c-cadherin (red, C) at the vesicles (A, arrow) at the apical surface of the embryo. (D). No co-localization of FERM (green, E) and integrin β1 (red, F) on the plasma associated vesicles (D. Arrow). HA FRNK (500pg) was injected AP at one out two cell stage embryos and stained with HA and cadherin or integrin β1 antibody. (G-I) Co-localization of FERM (green, H) and memGFP (red, I). Arrow indicates plasma membrane derived vesicles at the apical surface of the cells that were expressed both FERM (H) and memGFP (I).

3.7.2 The FERM domain is necessary for the localization of FAK on the membrane

The FERM domain of FAK was found to be localized on the plasma membrane in *Xenopus* embryos as shown above. In order to address the role of the FERM domain in the localization of FAK further an HA Δ375FAK deletion mutant was generated. This deletion removes the first 375 amino acids of FAK including the entire FERM domain. Injection of 500pg of HA Δ375FAK at AP site of two cell embryos followed by immunofluorescence, showed that the localization of this construct was similar to that of endogenous FAK (Figure 60A), albeit with more diffuse membrane localization (Figure 60B). Localization of HA Δ375FAK is also more diffuse than HA FAKΔFAT construct when overexpressed in AP cells (Figure 60C). DMZ-injected embryos with this mutant where stained with the PY397FAK antibody (Figure 60D-F), which can recognize besides the endogenous phosphorylated FAK, this construct as well since it does contain the Tyrosine 397. It is very clear, that without the FERM domain, FAK is not localized tightly on the membrane (Figure 60F). It is interesting to note that there is stronger effect on the membrane localization of FAK when the FERM is deleted in AP cells than when is deleted in DMZ cells. This was actually expected because the localization of the N-terminal domain of FAK is more tight on the membrane in the AP cells than in the DMZ cells (Figure 53G, 54E). These results suggest that the FERM domain is important for the localization of FAK on the membrane at least in AP cells.

Moreover, this construct displayed high catalytic activity (Figure 60E), which is in agreement with the bibliography (Figure 60G, lane 1). It has been previously shown that $FAK^{-/-}$ cells or HEK 293 cells transfected with a truncated FAK (Δ375 or Δ384) showed enhancement of Tyr397 phosphorylation (Cooper, L. A., Shen, T. L. et al. 2003; Jacamo, R. O. and Rozengurt, E. 2005). This is attributed to the role of the FERM domain in FAK autoinhibition as discussed in the introduction.

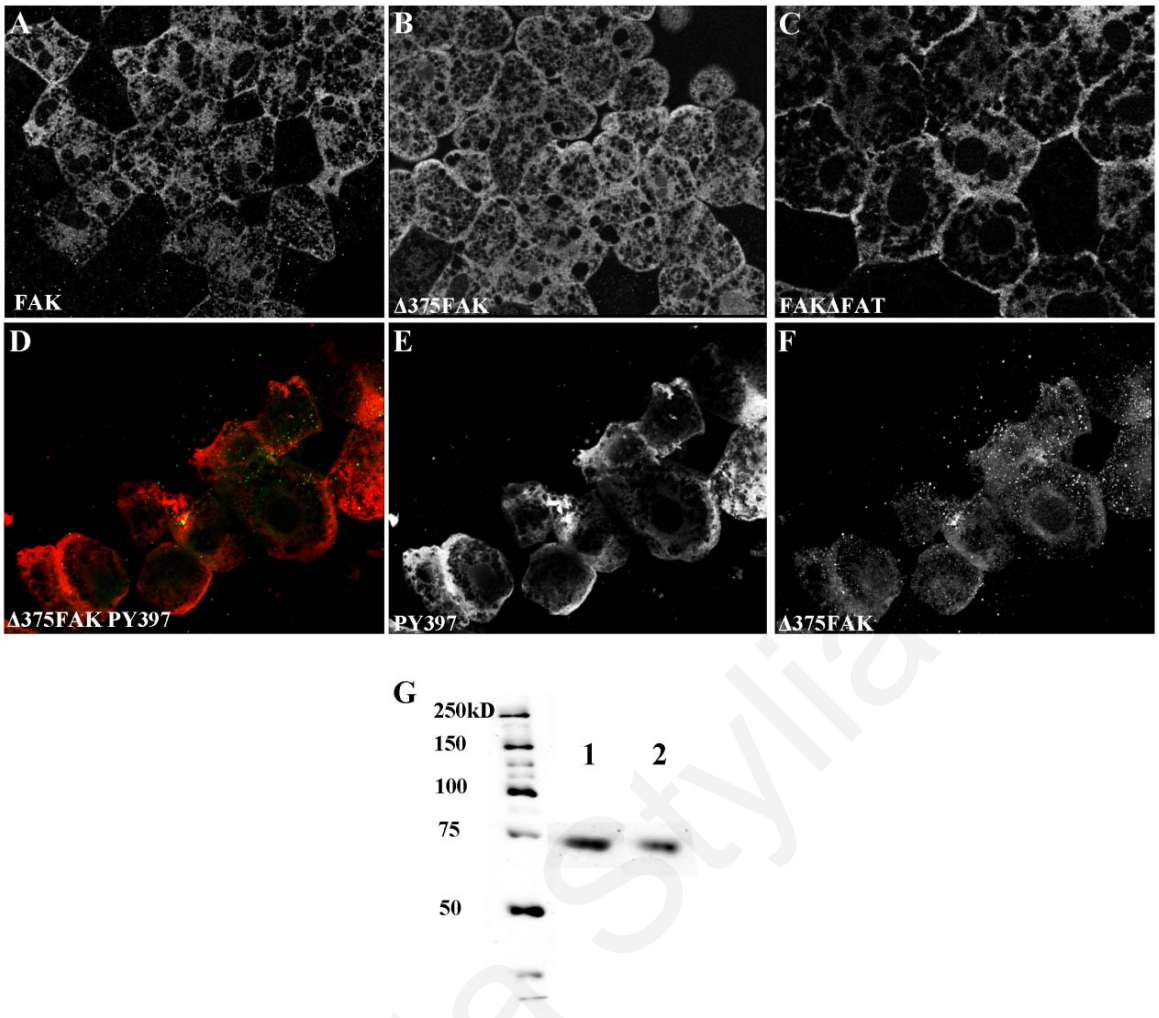

Figure 60. The FERM domain is necessary for the localization of FAK to the membrane. HA FAK (A), HA Δ375FAK (B), HA FAKΔFAT (C) localization at AP cells using HA antibody and Cy3 secondary. 500pg of each RNA injected AP at two cell stage embryo. Localization of HA Δ375FAK (B) is more diffuse than the other two constructs (A and C) when overexpressed in AP cells. (D-F) DMZ-injected embryos with Δ375FAK where stained with Cy3 for the PY397FAK antibody (red, E), which can recognize besides the activated FAK, also this construct. It is very clear, that without the FERM domain, FAK is not localized tightly on the membrane (green, F). (G) Expression of the construct at protein level, lane 1: blot with anti-PY397FAK, lane 2: blot with anti-HA. PY397FAK antibody recognizes the exogenous phosphorylation on Tyrosine 397.

3.7.3 FERM overexpression leads to activation of endogenous FAK

The initial rationale was to create a dominant negative form of FAK to enable down regulation of FAK activity in order to address its function in the developing embryo. Since the FERM domain can localize on the plasma membrane where activated FAK is then it may, unlike FRNK, act as a dominant negative displacing endogenous FAK from the membrane and since it lacks enzymatic activity and would thus block FAKs downstream signalling (Figure 58A, B). In addition FERM overexpression in adherent cells has been shown to down regulate endogenous FAK activity by *in trans* binding its kinase domain (Dunty, J. M., Gabarra-Niecko, V. et al. 2004).

Examination of the phosphorylation state of FAK on Tyr397 was made in FERM overexpressing cells in comparison to controls. FERM overexpressing cells had elevated phospho y397 levels as judged by signal intensity of a phospho specific 397 antibody (PY397FAK) in whole mount immunofluorescence experiments (Figure 61A-C). This elevation could be due to the fact that the FERM construct we were using contains tyrosine 397 which could potentially be phosphorylated *in trans* by endogenous FAK. To test this, a WB was carried out and we confirmed that the exogenous FERM is indeed phosphorylated on Tyr397 (Figure 61M, lane 1). This suggests that active endogenous FAK which is on the plasma membrane phosphorylates the exogenous FERM. This however makes the determination of the phosphorylation status of endogenous FAK on Tyr397 impossible at least via immunofluorescence (Figure 61A-C).

To overcome this, the phosphorylation of endogenous FAK on y576 was examined. The FERM construct does not contain this tyrosine, making it an ideal marker for the effect of the FERM overexpression on endogenous FAK activity. In addition phosphorylation of FAK on residues y576/577 is considered very important since these sites are within the activation loop of the kinase and their phosphorylation confers full enzymatic activity to FAK. Injected embryos with HA FERM were stained with a phospho specific PY576FAK antibody. Py576 was surprisingly elevated in FERM overexpressing cells compared to controls (Figure 61D-F, white and red stars). This elevation was not only observed on the membrane but also in the cytoplasm (Figure 61F, red stars). Closer examination revealed recruitment of endogenous activated FAK on the plasma membrane associated vesicles where FERM is localized (Figure 61G-I, arrow). In order to confirm this elevation, the levels of phospho y861 using another phospho specific antibody were examined. Again this amino acid is not present on the FERM construct so the Ab does not react with the

exogenous protein. Phosphorylated FAK at Tyr861 is moderately co-localized with the FERM wild type domain confirming the lack of cross reactivity between the FERM and the Ab (Figure 61J-L). Despite the fact that there is no strong co-localization, these cells had a noticeable elevation when compared with their neighbouring cells (Figure 61L, red stars). This elevation was once again not only on the membrane but in the cytoplasm as well.

These results suggest that expression of the FERM domain results in elevated phosphorylation of endogenous FAK and presumably its activation through an unknown mechanism. These results are quite surprising given the fact that the FERM domain has been shown to downregulate endogenous FAK phosphorylation *in vitro* and its inhibitory function on the FAK kinase domain is well documented.

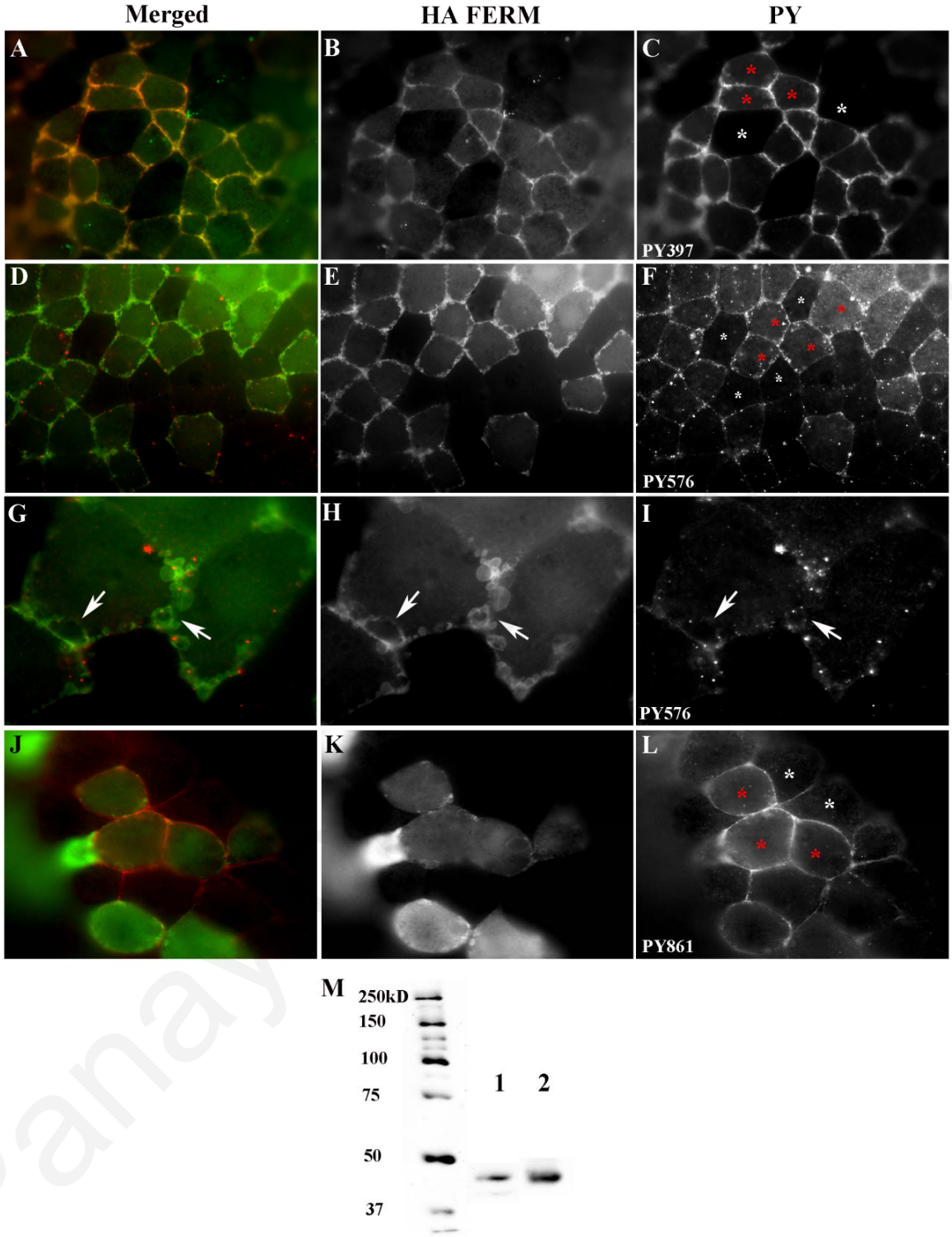

Figure 61. FERM overexpression leads to activation of endogenous FAK. (A-C) Injected embryos with HA FERM (green, 500pg) were stained with Cy3 for the phosphospecific PY397FAK antibody (C, red) and Alexa 488 for anti-HA (B, green). The phosphorylation on Tyrosine 397 level in injected cells is much higher (C, red stars) compared to the controls (C, white stars) as judged by signal intensity of a phospho specific 397 antibody PY397FAK (C) in whole mount immunofluorescence experiments. (D-F) Injected embryos with HA FERM (green, 500pg)

were stained with Cy3 for phospho specific PY576FAK antibody (F, red) and Alexa 488 for anti-HA (E, green). Py576 was surprisingly elevated in FERM overexpressing cells (F, red stars) compared to controls (F, white stars). This elevation was not only observed on the membrane but also in the cytoplasm (F, red stars). (G-I) Closer examination of immunofluorescence with PY576FAK antibody revealed recruitment of endogenous activated FAK on the plasma membrane associated vesicles where FERM is localized (I, arrow). (J-L) Injected embryos with HA FERM (green, 500pg) were stained with Cy3 for the phospho specific PY861FAK antibody (L, red) and with Alexa 488 for anti-HA (K, green). Py861 was surprisingly elevated in FERM overexpressing cells (L, red stars) compared to controls (L, white stars). This elevation was not only observed on the membrane but also in the cytoplasm (L, red stars). (M) Expression of the construct at protein level, lane 1: blot with anti-PY397FAK, lane 2: blot with anti-HA. PY397FAK antibody recognizes the exogenous phosphorylation on Tyr397.

3.7.4 FERM expression results in endogenous FAK activation in a Src dependent manner.

The results above show that somehow expression of the FERM domain leads to elevated phopshorylation of endogenous FAK. This is quite surprising because it suggests that the FERM domain can somehow lead to endogenous FAK activation especially when one considers that phosphorylation on Tyr576 is crucial for full activation of FAKs catalytic activity. Both Tyr576 and Tyr861 are Src phosphorylation sites (Richardson, A., Malik, R. K. et al. 1997; Dunty, J. M., Gabarra-Niecko, V. et al. 2004). Since Tyr397 which is the Src SH2 binding site on FAK is phosphorylated in the exogenously expressed FERM domain we postulated that phosphorylated FERM recruits Src to the membrane where it becomes activated and this leads to increased endogenous FAK phosphorylation (Frame, M. C., Patel, H. et al. 2010).

To test this hypothesis we first examined the status of two known downstream targets of FAK/Src, paxillin and p130Cas. Using indirect immunofluorescence and phospho specific antibodies for these two proteins, the phosphorylation status in FERM overexpressing and control cells was compared. As seen in the Figure 62 both these proteins show elevated phosphorylation in FERM expressing cells and both are recruited at the plasma membrane associated vesicles where FERM is localized. These results strongly suggest that the FERM domain activates FAK in a Src dependent manner and probably by recruiting it to the membrane. The results on p130Cas especially are a strong indicator that this is the case because p130Cas has been shown to be an exclusive Src substrate phsophorylated even in

cells expressing a kinase dead FAK mutant (Ruest, P. J., Shin, N. Y. et al. 2001). This is further supported by the fact that FERM failed to elevate the phosphorylation level of another downstream target of FAK, Akt (Figure 62 G-I). The PI3K/FAK complex activates Akt, when PI3K binds on phosphorylated Tyr397 of FAK (Franke, T. F., Kaplan, D. R. et al. 1997). Previous work in human lung fibroblasts showed that Akt activity was found to be increased after integrin-β1 enforced activation, which led to phosphorylation of FAK on Tyr397 and binding of PI3K. Moreover, Akt phosphorylation was downregulated by using FRNK as a dominant negative of FAK (Xia, H., Nho, R. S. et al. 2004). Based on the above data, the activation of Akt is integrin β1-dependent but the activation caused by the FERM domain in this study, appears to be integrin-independent. This may explains why the FERM domain does not cause elevation of Akt phosphorylation on Ser473.

To confirm that the activation of FAK was indeed through Src the FERMY397F point mutant was used. Substitution of Y397 has been previously shown to abolish Src binding on FAK (Schaller, M. D., Hildebrand, J. D. et al. 1994). Overexpression of this mutant failed to lead to elevation of both endogenous FAK phosphorylation (Tyr576, Tyr861) (Figure 63D-F, G-I) as well as that of downstream signaling molecules, like paxillin (Figure 63A-C). This is a clear indication that the FERM domain acts through Src to lead to FAK activation.

If the above is correct, one would expect Src to co-localize with the FERM domain in the cell because Src can interect with the proline-rich region I with its SH3 domain and with phosphorylated Tyr397 with its SH2 domain (Thomas, J. W., Ellis, B. et al. 1998). We examined if expression of the FERM domain can recruit Src to the plasma membrane associated vesicles where it is localized. Double IF experiments with an HA and Src antibodies showed that in FERM expressing cells of the animal cap Src is found on the FERM positive plasma membrane associated vesicles (Figure 62J-L, arrows). These results in combination with the fact that FERM expression leads to both endogenous FAK phosphorylation as well as paxillin and p130Cas phosphorylation in a Tyr397 dependent manner offer strong evidence that autonomous FERM domain expression leads to activation of FAK in a Src dependent but intergin independent manner. These results demonstrate that in addition to its inhibitory role in integrin based activation of FAK the FERM domain plays an important role in the activation of FAK on the plasma membrane.

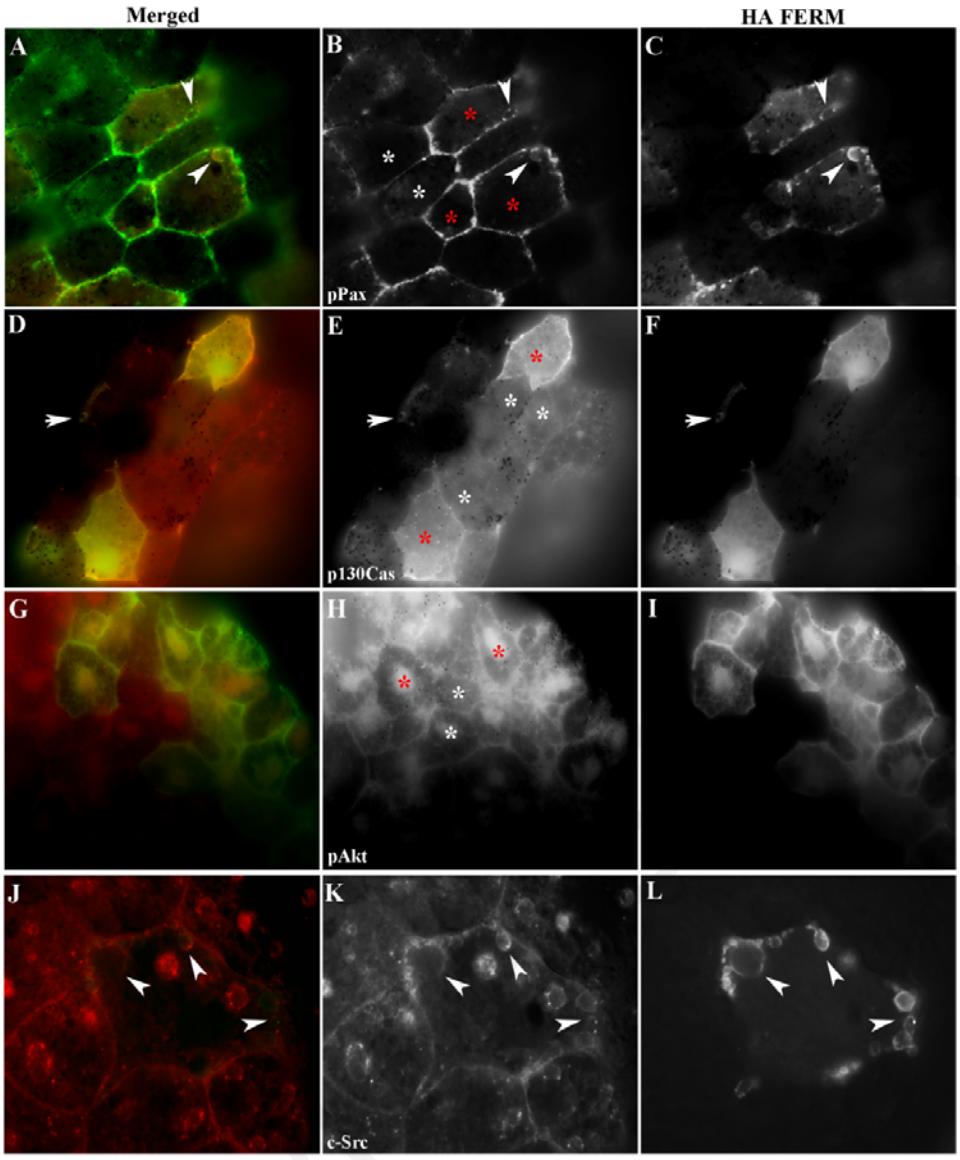

Figure 62. FERM overexpression activates endogenous FAK in a Src-dependent manner. (A-C) Injected embryos with HA FERM (green, 500pg) were stained with Cy3 for the phospho specific of paxillin PY31 antibody (B, red) and Alexa 488 for anti-HA (C, green). The phosphorylation on Tyrosine 31 level in injected cells is elevated (B, red stars) compared to the controls (B, white stars). P-paxillin recruited at the plasma membrane associated vesicles were FERM is localized (A, arrows). (D-F) Injected embryos with HA FERM (green, 500pg) were stained with Cy3 for the phospho specific PY762p130Cas antibody (E, red) and alexa 488 for anti-HA (F, green). PY762 was surprisingly elevated in FERM overexpressing cells (E, red stars) compared to controls (F, white stars). (G-I) Injected embryos with HA FERM (green, 500pg) were stained with Cy3 for the phosphospecific of Akt Ser473 antibody (H, red) and alexa488 for anti-HA (I, green). The phosphorylation on Ser473 level in injected cells (H, red stars) is not higher compared to the controls (E, white stars). (J-L) Injected embryos with HA FERM (green, 500pg) were stained with Cy3 for the c-Src antibody (K, red) and alexa 488 for anti-HA (L, green). Src is

found on the FERM on the plasma membrane derived vesicles in addition to vesicles in the cytosplasm. Co-localization between HA FERM and c-Src. (L, arrows).

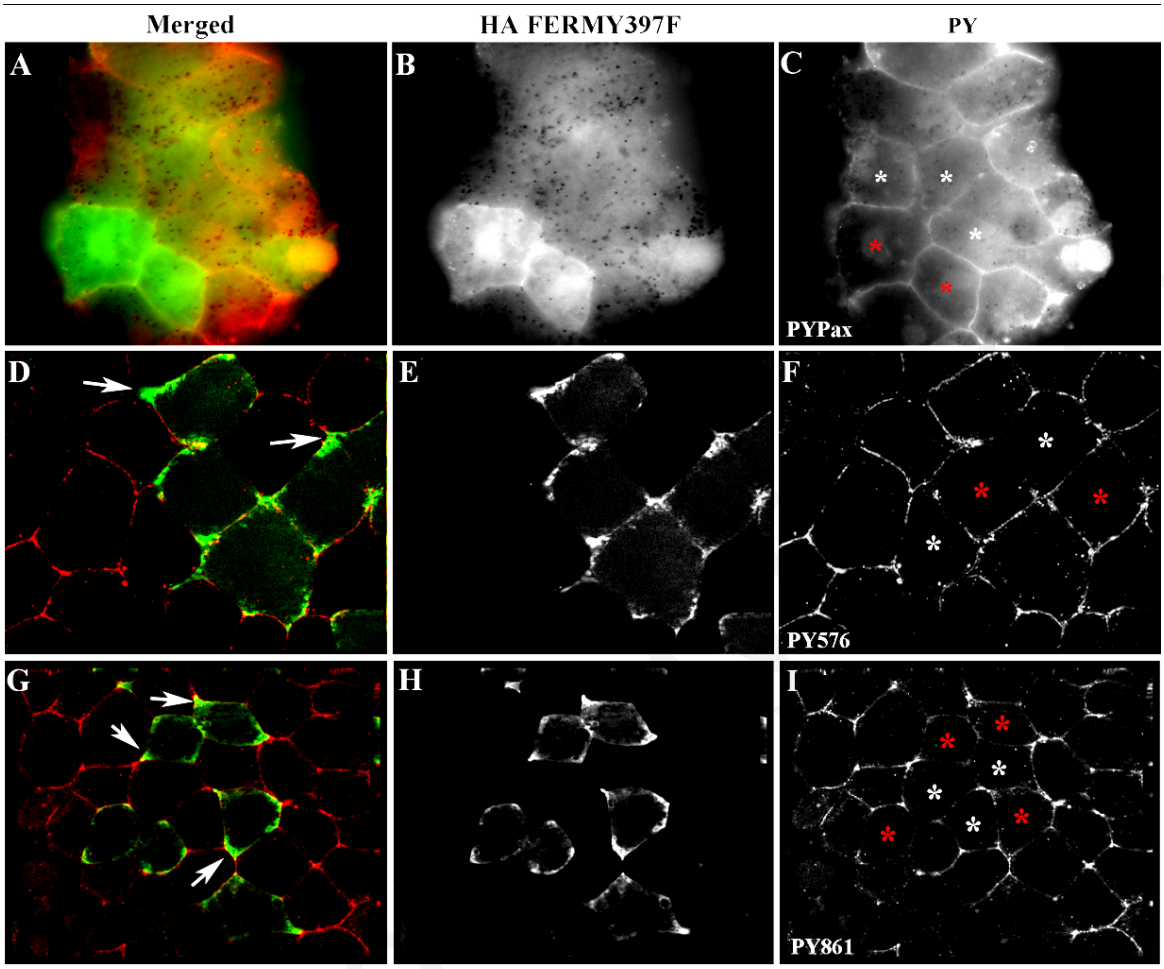

Figure 63. The FERMY397F construct failed to activate endogenous FAK and downstream signaling molecule paxillin. (A-C) Injected embryos with HA FERMY397F (green, 500pg) were stained with Cy3 for the phospho specific of paxillin PY31 antibody (red) and with alexa 488 for anti-HA (green). The phosphorylation on Tyrosine 31 level in injected cells (C, red stars) is not elevated compared to the controls cells (C, white stars) in whole mount immunofluorescence experiments. (D-F) Injected embryos with HA FERMY397F (green, 500pg) were stained with Cy3 for the phospho specific PY576 antibody (red) and with alexa 488 for anti-HA (green). Overexpression of this mutant failed to lead to elevation endogenous FAK phosphorylation to the injected cells (F, red stars) compared to controls (F, white stars). (G-I) Injected embryos with HA FERMY397F (green, 500pg) were stained with Cy3 for the phosphospecific of FAK Tyr861 antibody (red) and anti-HA (green). Overexpression of this mutant failed to lead to elevation of endogenous FAK phosphorylation to injected cells (I, red stars) compared to controls (I, white stars).

3.8 The FERM/FRNK constuct is capable of targeting FAK to the plasma membrane and may be a promissing dominant negative

3.8.1 The FERM and FAT domains cooperate to target FAK on the plasma membrane

Despite the fact that the FERM domain has been previously shown to block FAK activation *in trans* in cultured cells (Cooper, L. A., Shen, T. L. et al. 2003), it actually led to activation of endogenous FAK in the context of the embryo (Cooper, L. A., Shen, T. L. et al. 2003). Context dependence with regard to the activity of the FERM domain has also been seen before *in vitro* by the Beviglia L., group who showed that FERM expression in tumor cell lines (human breast carnicoma cells: BT474 and MCF-7) lead to downregulation of FAK activity whereas in normal cells (epithelial cells: MCF-10A) FERM expression had no effect on FAK activity or phosphorylation (Beviglia, L., Golubovskaya, V. et al. 2003). As shown above, expression of the FERM domain led to elevated phosphorylation of endogenous FAK as well as of the downstream targets paxillin and p130Cas in a Src dependent manner. However, its localization on the cell-cell contact areas in the cells of the involuting mesodermal cells was not as tight as that of endogenous phospho FAK and a large protion of the protein appeared to be in the cytosol and the nucleus (Figures: 54E, 55I). These are the most morphogenetically active cells of the embryo and the cells displaying the highest levels of endogenous FAK phosphorylation during gastrulation (Figures: 41D, 42C-D, 43D). In these cells the FERM domain alone, displays stronger plasma membrane localization compared to full length FAK presumably because it is free to bind PIP2 and GFRs while the majority of the full length FAK is in the closed conformation and unable to use its FERM domain in order to go to the membrane (Figure 54A, E).

On the other hand, active phosphorylated FAK has a free FERM domain which helps it go to the membrane, but the tighter localization of active full length FAK suggests that the C-terminus may cooperate with the N-terminus to confer this tight plasma membrane localization. In agreement with the above is the fact that in these cells the FAT domain localizes to the cell-cell contact areas quite strongly and a comparison between FRNK (which contains the FAT) and FERM reveals similar localization between the two (Figure 54E, G, H). This suggests once again that both are able to target FAK to the plasma membrane in DMZ cells, albeit through different mechanisms.

In order to address this possibility, a C-term and N-term fusion construct was generated that lacks the kinase domain (HA FERM/FRNK) (Figure 51). This construct would presumably have a free FERM domain (no Kinase domain to sequester it) in addition to the FAT domain. Combining the C- and N- termini of FAK in the absence of the kinase domain, resulted in a dramatic change in localization in DMZ cells. The HA FERM/FRNK construct recapitulates the localization of endogenous phospho-FAK closely and the cytoplasmic pool seen with both the FRNK and FERM constructs disappears (Figure 54I). On the other hand, in AP cells, the HA FERM/FRNK mutant exhibits the characteristic pattern of localization of HA FERM (Figure 53G, K). Moreover, HA FERM/FRNK is clearly localized at the integrin-free plasma membrane of the apical surface of the animal cap cells, so as activated FAK (Figure 55G, I). These data suggest that in DMZ cells the FERM and FRNK domains cooperate to target FAK to the membrane while in AP cells the FERM is sufficient and can target the C-terminus of FAK to the plasma membrane and the plasma membrane asosiated vesciles. In addition, co-injections of GFP FAK (100pg) and HAFERM/FRNK (500pg) at the AP of two-cell stage embryos, followed by immunofluorescence using anti-HA and anti-GFP antibodies showed that this mutant is able to compete full length FAK from the membrane (Figure 64). This suggests that combining the C- and the N- termini of FAK creates a construct that can now compete FAK off of its signalling complexes and which may act as a dominant negative (DN). It should be able to competes FAK from both integrin dependent as well as integrin independent complexes and lacks a kinase activity so it will be unable to transduce signals from these complexes.

In order to explore the possibility that the HA FERM/FRNK construct can act as a DN in the context of the embryo, it was injected at the DMZ of four cell stage embryos. When 500pg were injected, the embryos were left to develop and it was observed that expression of the construct led to failure of blastopore closure in nearly 100% of the embryos compared to the controls of the same stage (Figure 65A-C). Most injected embryos died and they rarely developed past the gastrula stage. However, injection of 100pg of FAK mRNA partially rescued this phenotype demonstrating the specificity of the phenotype (Figure 65E-G). A dose response was carried out and it was determined that even 300pg of the HA FERM/FRNK construct resulted in severe embryo abnormalities including a long delay in blastropore closure, blastopore closure failure (Figure 66A, white arrowhead) as well as neural tube closure failure (Figure 66D, red arrowhead). In many embryos it was also clear that there was substantial cell death at and near the site of injection suggesting

that the construct at high doses can cause cell death (Figure 66D, yellow arrow). Embryos which made it past the early neurula stage displayed severe anterior-posterior (AP) axis shortening in addition to diminished head structures (Figure 66G, white arrow). Similar results were obtained using a Y397F point mutant FERM/FRNK that was generated, indicating that the DN activity is independent of the autophosphorylation site of FAK (Figure 66B, E, H, K).

We went on to address the reason behind the apparent toxicity of this construct. We observed that prior to cell death blastomeres near the injection site were enlarged suggesting problems with cell division. We decided to examine dividing cells by co-injecting histone GFP together with HA FERM/FRNK in order to visualize the chromatin in both live and fixed embryos (Figure 67A-E, F-G). As can be seen in Figure 67 expression of HA FERM/FRNK causes the formation of anaphase bridges in dividing cells. As a matter of fact these often fail to resolve leading in divided cells which are connected with thin chromatin filaments several cell diameters in length. The nuclei in these cells take a very characteristic bottle shape due to the unresolved chromatin connection (Figure 67G). This striking effect clearly explains the observed cell death and toxicity of the FERM FRNK construct. This effect was also seen with the HA FERMY397F/FRNK construct (Figure 67H). Moreover, another FAK variant, which is mutated at the site K454R, was tested for the same phenotype. The HA K454RFAK mutant is the most similar to the HA FERM/FRNK because the former is characterized as kinase-inactive and the latter has no kinase domain (Calalb, M. B., Polte, T. R. et al. 1995). This construct did not result in any division problems (Figure 67I). This indicates that this phenotype is not due to the loss of function of the kinase-deficient mutants but to the structure or to the different localization of the HA FERM/FRNK that may cause abnormal interactions with division responsible proteins.

It has been suggested that FAK actually may play a role in mitosis (Ma, A., Richardson, A. et al. 2001). It has also been shown, that cells isolated from FAK knockout mice display proliferation problems (Ilic, D., Kovacic, B. et al. 2003). Serine phosphorylated FAK was shown to be localized on the mitotic spindle of dividing cells and specifically on the centrosomes using a phospho Ser-732 FAK specific antibody (Park, A. Y., Shen, T. L. et al. 2009). Interestingly when FAK antibodies or P-Tyr specific FAK antibodies are used no such localization can be observed because the majority of the protein is found in the cytoplasm and the FAs and only a small subset of Ser-732 phosphorylated FAK is actually on the spindle. This raised the possibility that HA FERM/FRNK acts as a dominant

negative with respect to FAKs role on the centrosomes. Thus, it was examined if the HA FERM/FRNK construct somehow altered the phosphorylation status of FAK on Ser-732. HA FERM/FRNK injected embryos were processed for whole mount immunofluorescence as described before, using a P-Ser732 specific FAK antibody. In control embryos, serine phosphorylated FAK was exclusively nuclear (Figure 67J). Expression of the HA FERM/FRNK construct led to a substantial elevation of the P-Ser732 signal at the injection site (Figure 67K). Interestingly, in several cells expressing HA FERM/FRNK, mis-localization of serine phsophorylated FAK was also observed with almost complete lack of nuclear accumulation and an abundance of cytoplasmic P-Ser732 signal (Figure 67L-N). These results suggest that HA FERM/FRNK may exert its effect on mitosis through elevation of serine phosphorylated FAK levels as well as mis-localization. One possibility is that the HA FERM/FRNK construct becomes itself phosphorylated on Ser-732. Since cytoplasmic dynein has been shown to bind FAK in a Ser-732 phosphorylation dependent manner the phosphorylated FERM/FRNK may be unable to localize on the centrosome and thus sequesters the dynein away from the spindle (Park, A. Y., Shen, T. L. et al. 2009). This could pottentially explain the problems with cell division since knock down of cytoplasmic dynenins results in severe focusing problems of the spindle (Goshima, G., Nedelec, F. et al. 2005).

More experiments are required to understand this effect of FERM/FRNK overespression on mitosis.

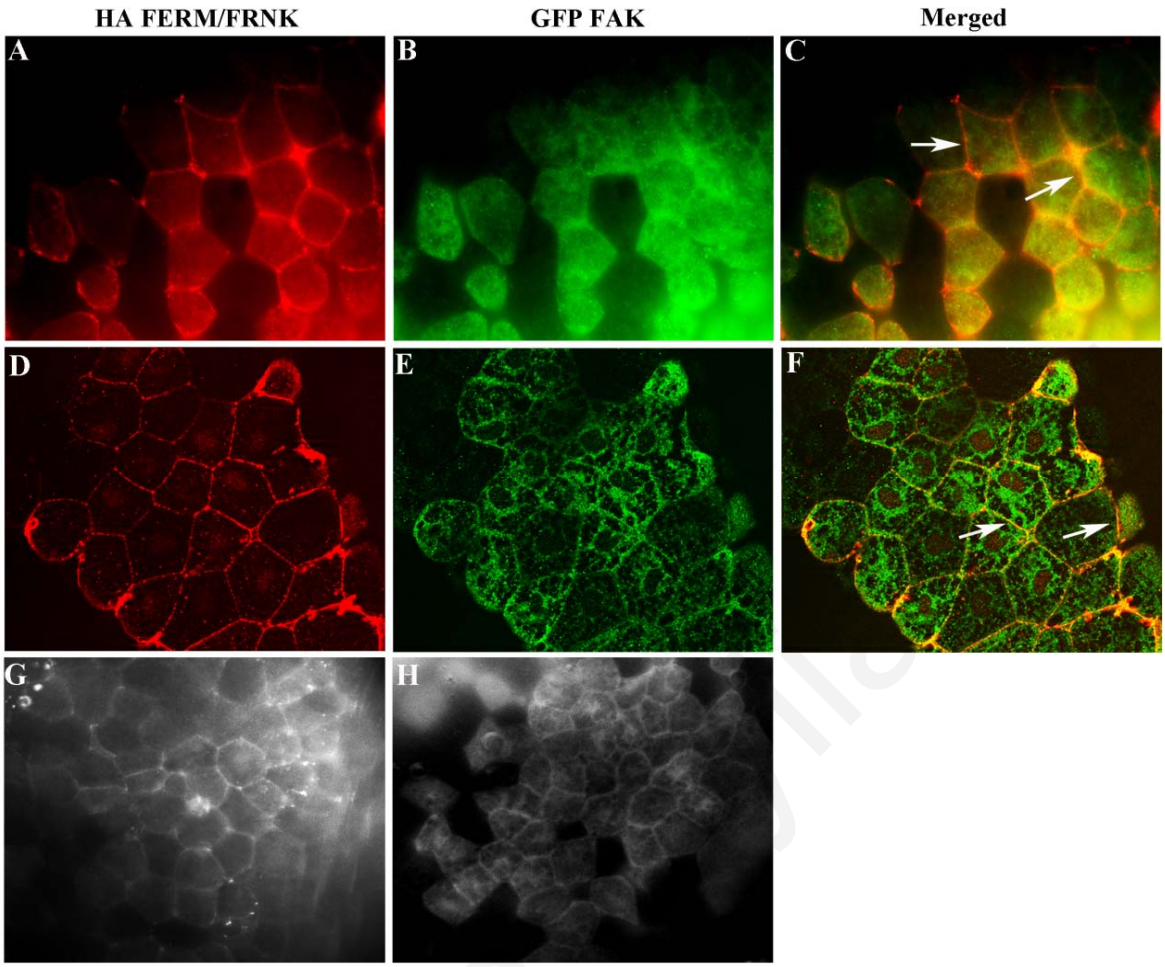

Figure 64. The FERM/FRNK construct competes with FAK for plasma membrane localization. (A-B) HA FERM/FRNK overexpression in AP cells (injected 500pg) stained with Cy3 for anti-HA (A, red) co-injected with GFPFAK (100pg) (B) stained with Alexa 633 for anti-GFP. (C) Merged image of A and B showed that this mutant is able to compete full length FAK from the membrane because of its tight membrane localization (arrows indicate only FERM/FRNK). (D-F) Optical section image of FERM/FRNK and GFPFAK co-expression in AP cells. (G) FERM/FRNK expression in AP cells stained with Cy3 for anti-HA. The localization in tight on the membrane (same as when co-injected with GFPFAK). (H) GFPFAK expression in AP cells stained with Alexa 633 for anti-GFP. The localization is tighter on the membrane (when expressed only full length FAK) and this is an indication that FERM/FRNK competes FAK for the localization to the membrane.

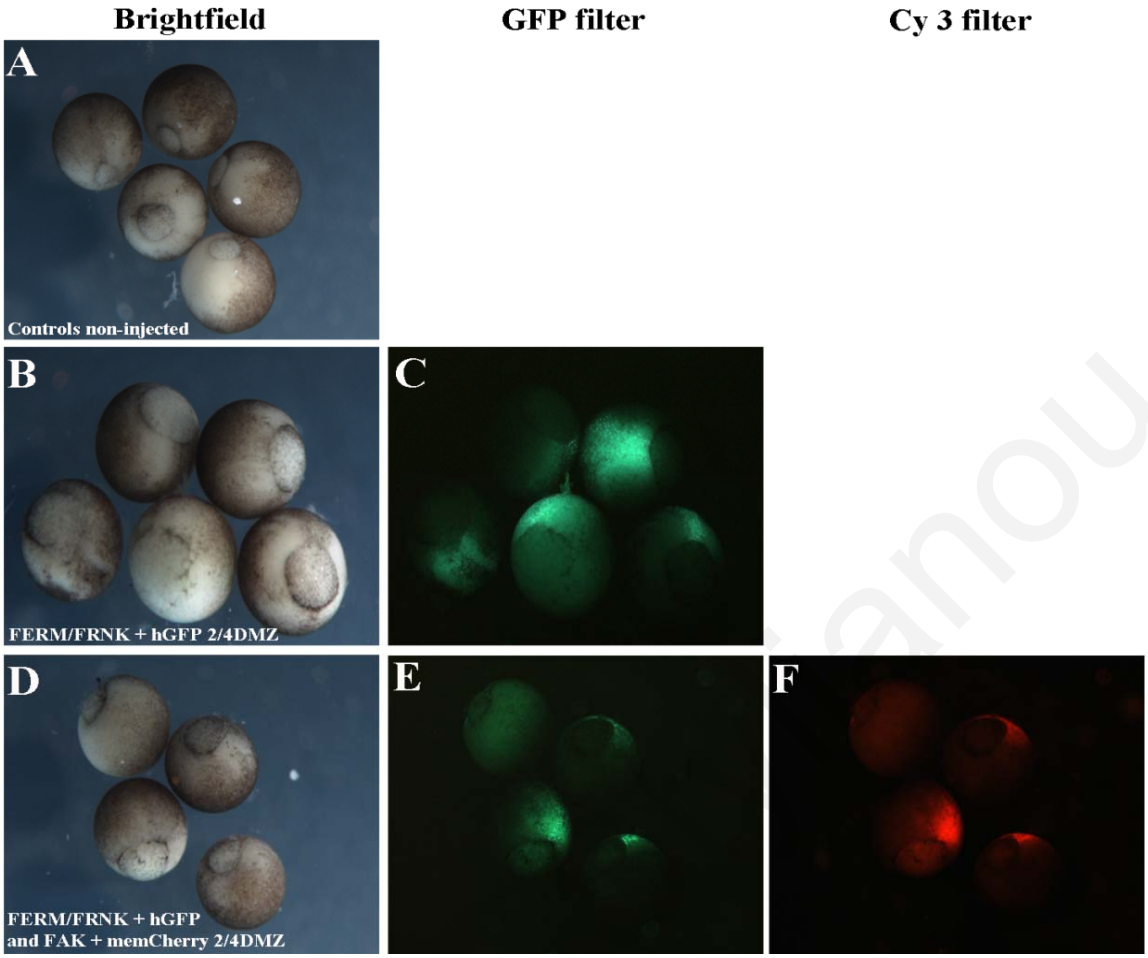

Figure 65. FERM/FRNK phenotype can be rescued when injected with wild type FAK. (A) Control embryos imaged at stage 12. (B-C) Injected embryos with 500pg FERM/FRNK show a delay in blastopore closure (B, C) compared with the controls (A). (D-F) Phenotype of FERM/FRNK can be partially rescued when FERM/FRNK coinjected with full length FAK. Embryos were coinjected with FERM/FRNK (500pg and 100pg histoneGFP for lineage tracer) and FAK (100pg and 100pg membrane Cherry) into both dorsal blastomeres of four cell stage embryo and left to develop. Embryos imaged when the control embryos were stage 12.

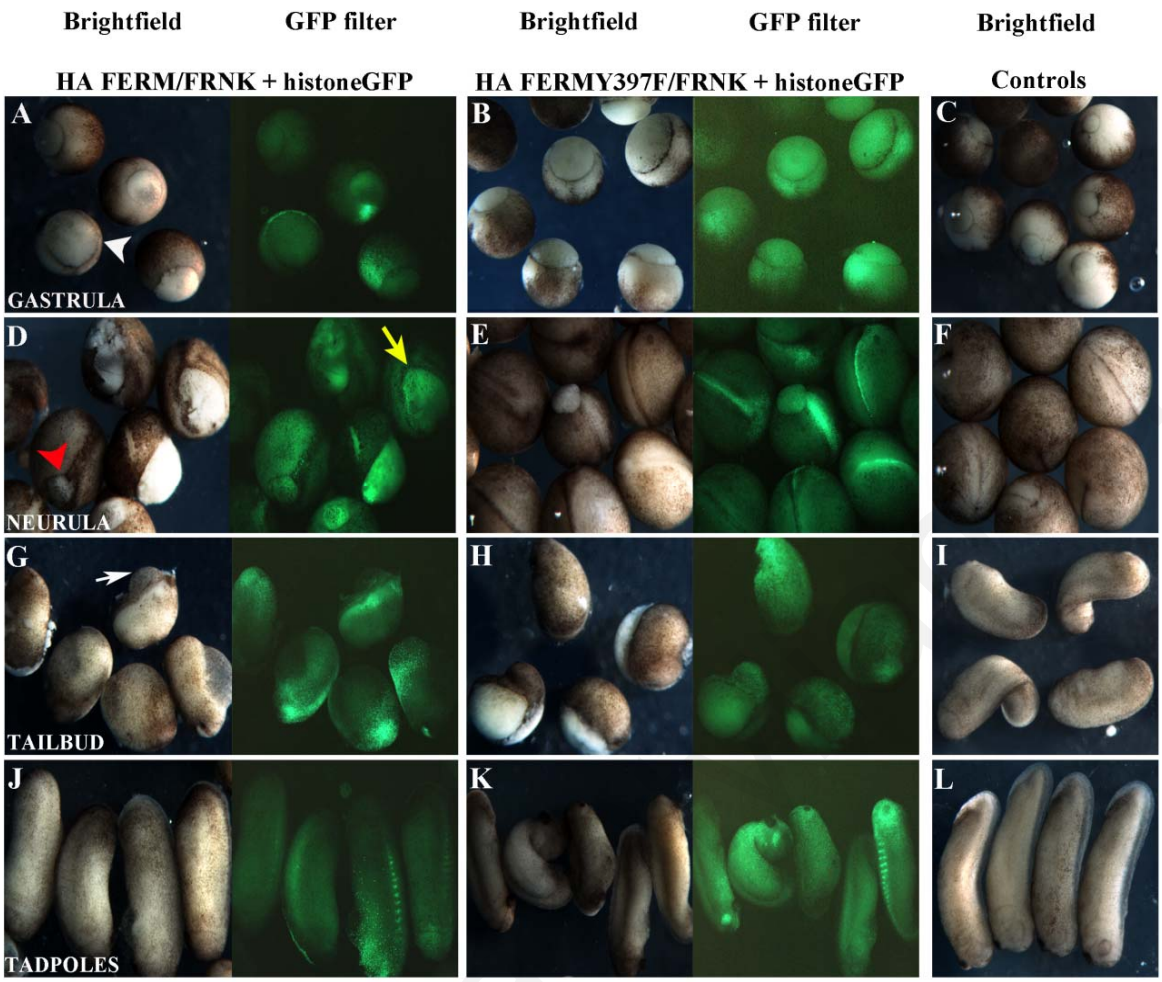

Figure 66. FERM/FRNK and FERMY397F/FRNK phenotypes during *Xenopus* development. (A, D, G, J) First column: Images of injected embryos at the dorsal side into two blastomeres of four cell stage embryo with 300pg of the HA FERM/FRNK (100pg histoneGFP for linage tracer) during *Xenopus* development. Construct resulted in severe embryo abnormalities including a long delay in blastropore closure (A, white arrowhead) as well as neural tube closure failure (B, red arrowhead). In many embryos it was also clear that there was substatial cell death at and near the site of injection suggesting that the construct at this dose can cause cell death (B, yellow arrow). Embryos which made it past the early neurula stage displayed severe anterior-posterior axis shortening (J) in addition to diminished head structures (G, white arrow). (B, E, H, K) Second column: similar results were obtained using a Y397F point mutant FERM/FRNK, indicating that the dominant negative activity is independent of the autophosphorylation site of FAK. (C, F, I, L) Third column: Control embryos at the same stage as the injected one.

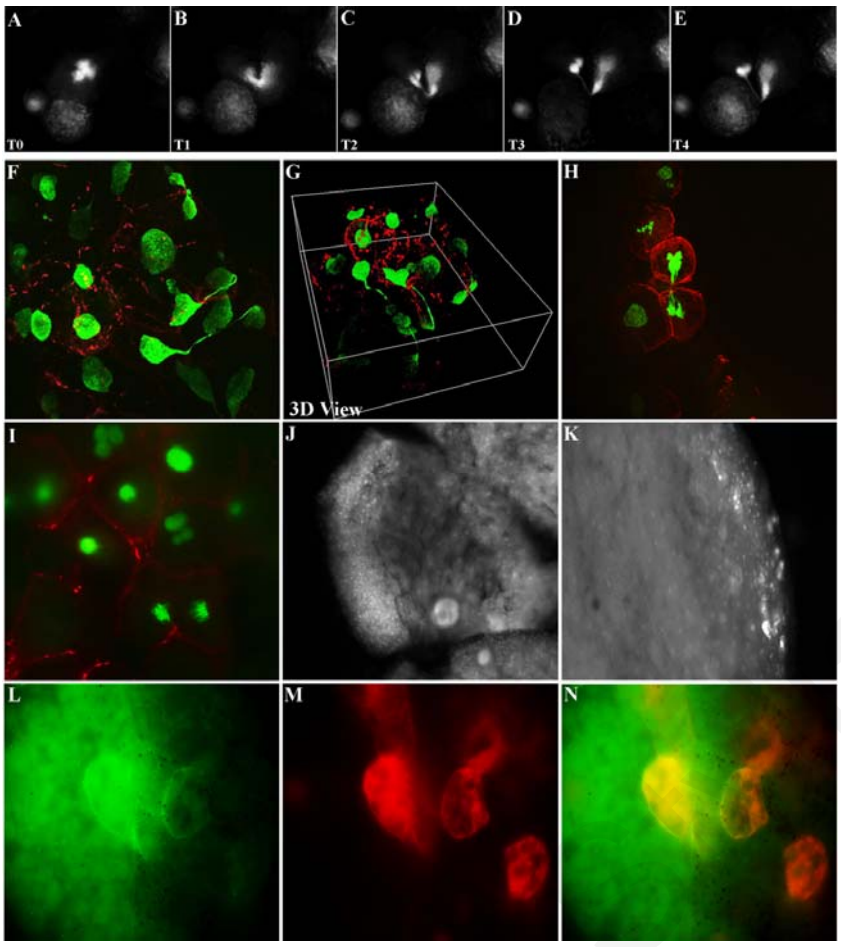

Figure 67. Overexpression of the FERM/FRNK construct leads to the formation of anaphase bridges in dividing cells *in vivo* and *in vitro* and to the mislocalization of P-Ser732. (A-E) Five frames from time lapse movie of dissociated cells on fibronectin coated slides which overexpressing FERM/FRNK (histone GFP). The cells expressing FERM/FRNK (histoneGFP) causes the formation of anaphase bridges in dividing cells *in vivo*. (F-H) This phenotype is conserved and in fixed embryos. Diving cells are connected with thin chromatin filaments several cell diameters in length. The nuclei in these cells take a very characteristic bottle shape due to the unresolved chromatin connection (G, 3D view). This phenotype was conserved also with the FERMY397F/FRNK construct (H). (I) Another FAK variant, K454RFAK, used to test the specificity of the phenotype because is similar to FERM/FRNK construct (dead kinase domain). This construct did not show any division problems. (J-K) Control embryos stained with Cy3 for anti-Ser732 phospho specific FAK antibody. Serine phosphorylated FAK is exclusively nuclear (J). Expression of FERM/FRNK to injected embryos led to a substantial elevation of the P-Ser732 signal in the injected site. (L-N) Higher magnification of the injected site. Cells expressing FERM/FRNK (L), mis-location of serine phosphorylated FAK was observed with almost complete lack of the nuclear accumulation and an abundance of the cytoplasmic P-Ser732 signal (M). The staining of the neighbouring cells is not visible because of the intense of the injected ones. (N) Merged image, FERM/FRNK stained with Alexa 488 for anti-HA (green) and P-Ser732 with Cy3 for anti-Ser732 (red).

3.8.2 FERM/FRNK expression blocks convergent extension by regulating the levels of c-Cadherin

Despite the fact that HA FERM/FRNK expression at relatively high levels can cause cell division problems and eventually lead to cell death at lower levels despite the fact that no cell death can be detected, embryos still displayed severe gastrulation abnormalities and a shortening of the anterior to posterior axis. These results point to a role of FAK in morphogenesis. It has been shown in the past that expression of FRNK can block mesoderm migration without affecting convergent extension movements (Stylianou, P. and Skourides, P. A. 2009). The shortening of the anterior-posterior (AP) axis in HA FERM/FRNK injected embryos suggests an influence of this construct on convergent extension as well (Keller, R. E., Danilchik, M. et al. 1985). First, the effect of FERM/FRNK expression on Mesodermal Migration (MM) was examined. HA FERM/FRNK (500pg) plus histoneGFP (as a linage tracer) were injected in one out of two AP blastomeres at the two cell stage and the embryos were allowed to develop to stage 8. Animal Caps were dissected, dissociated and induced with activin prior to being plated on fibronectin coated coverslips. HA FERM/FRNK blocked mesodermal cell spreading and migration as expected since the C-term FAT domain and the lack of a kinase activity should enable FERM/FRNK to act in a similar fashion as FRNK (Figure 68A, B). Animal cap elongation assays were carried out to determine the effect of HA FERM/FRNK on convergent extension. In these experiments both AP blastomeres of two cell stage embryos were injected with 500pg of HA FERM/FRNK and 100pg of histoneGFP allowed to develop to stage 8, dissected and left to heal in the presence of activin. HA FERM/FRNK injected caps failed to elongate suggesting that it blocks convergent extension. Moreover, for the rescue experiments, the HA FERM/FRNK construct was injected as described above, and in some of those were added 100pg HA FAK and 100pg of memGFP at 2/2 blastomers at the AP site. As can be seen from on Figure 42 the HA FERM/FRNK injected animal caps that had also HA FAK were elongated and rescued (white arrows), whereas those injected only with the HA FERM/FRNK did not elongate (Figure 68C-E).

Inhibition of convergent extension (CE) movements is often associated with effects on the planar cell polarity pathway or on the cadherin based adherens junctions (Winklbauer, R. 2009). Since FAK signaling has been previously implicated in the formation of N-cadherin adherens junctions the effects of HA FERM/FRNK expression on adherens junction formation in the early embryo were examined (Yano, H., Mazaki, Y. et al. 2004). To do this, dissociation re-aggregation assays were carried out in a mixture of HA FERM/FRNK

and control cells. HA FERM/FRNK (500pg) was once again co-injected with hisGFP (100pg) as a linage tracer and a clear re-aggregation of injected cells was observed. HA FERM/FRNK injected cells preferentially aggregate with other injected cells with similar HA FERM/FRNK expression levels (Figure 68F, G). These suggest that the HA FERM/FRNK expression either affected the levels of expression of C-cadherin (the only cadherin expressed in the early embryo) or the formation of adherens junctions (Figure 68) (Heasman, J., Ginsberg, D. et al. 1994). Next, IF was carried out using a c-cadherin specific Ab to examine adherens junctions in HA FERM/FRNK expressing versus control cells. As shown in Figure HA FERM/FRNK expression led to a significant elevation of the C-cadherin signal. Cells with more intense signal of hisGFP (indication of higher levels of HA FERM/FRNK) show more elevated levels of C-cadherin when comparing with their neighbouring cells (Figure 68H-J, arrowheads).

To sum up, mesodermal tissue undergoing CE displays a downregulation of cell-cell based adherens junctions (Winklbauer, R. 2009). Activin induction of AC explants has been shown to reduce the calcium-dependent adhesion between blastomeres and these changes in C-cadherin-mediated adhesion occur without detectable changes in the steady-state levels of C-cadherin or the amount of C-cadherin present on the surface of the cell (Brieher, W. M. and Gumbiner, B. M. 1994). Diminished cell-cell adhesion is presumably required to allow the sliding between cells required for CE to occur (Winklbauer, R. 2009). This taken together with our data suggests that FERM/FRNK block CE by strengthening cell-cell C-cadherin based adhesion.

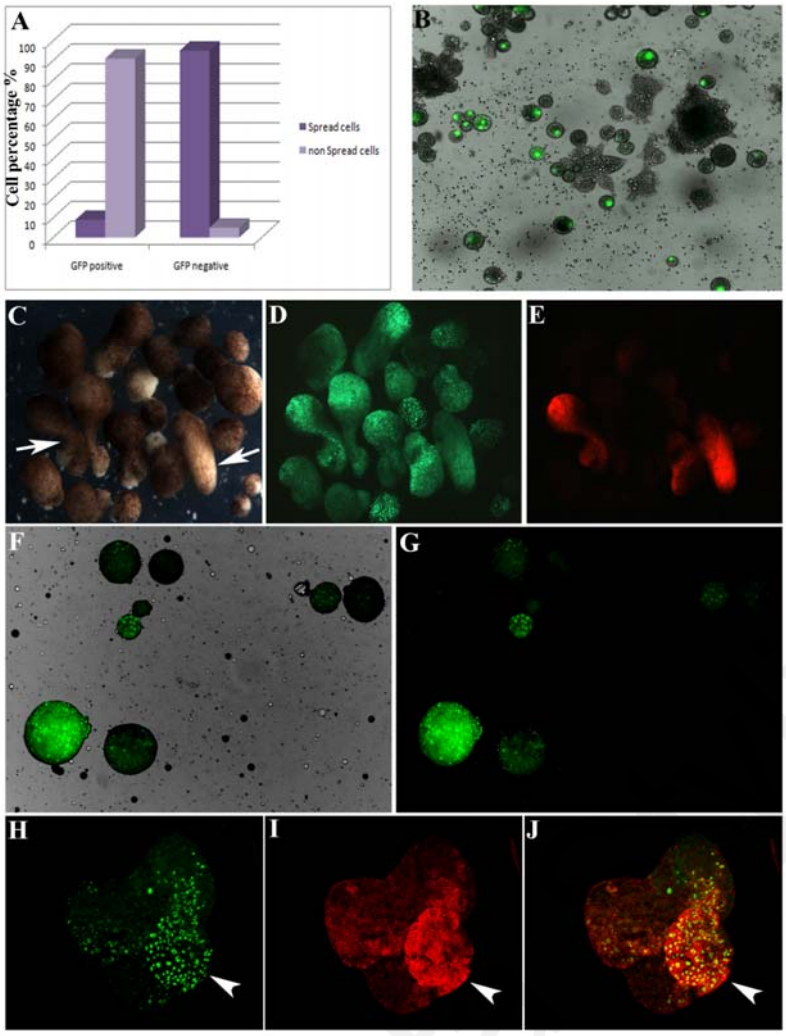

Figure 68. FERM/FRNK blocks convergent extension by regulating the levels of c-Cadherin. (A) Percentage of GFP positive (500pg FERM/FRNK overexpressing cells) and GFP negative (control cells) during mesoderm migration. 91% of positive GFP cells are rounded up compared to the controls (GFP negative). (C-E) Elogation assay where injected FERM/FRNK (500pg) caps failed to elongated suggesting that it blocks convergent extension (D, histoneGFP positive caps). In some of those were added 100pg FAK (E, membrane Cherry caps). As seen in C the FERM/FRNK injected animal caps that had also FAK were elongated and rescued (arrows) where those injected only with FERM/FRNK did not elongated. (F-G) Dissociation re-aggregation assays were carried out in a mixture of HA FERM/FRNK and control cells. HA FERM/FRNK (500pg) co-injected with hisGFP (100pg) as a linage tracer and a clear re-aggregation of injected cells was observed. HA FERM/FRNK injected cells preferentially aggregate with other injected cells with similar HA FERM/FRNK expression levels. (H-J) Immmunofluorescence was carried out using a c-cadherin specific Ab (I) to examine adherents junctions in HA FERM/FRNK expressing versus control cells (H). FERM/FRNK expression led to a significant elevation of the C-cadherin signal (J, arrowhead). Cells with more intense signal of hisGFP (indication of higher levels of HA FERM/FRNK, H: arrowhead) show more elevated levels of C-cadherin when comparing with their neighboring cells (I, arrowhead).

4. DISCUSSION

This project had two main goals. The first goal of this project was the use of Near Infra Red (NIR) Quantum Dots (QD's) for imaging of deep tissue morphogenetic movements in *Xenopus laevis* embryos *in vivo*. Specifically, we were able to visualize mesoderm migration by targeting QD's to specific tissues via microinjection.

Quantum Dots provide distinct advantages over traditional fluorescent markers. In addition to extremely high fluorescence intensity, QD's offer wide excitation spectra, narrow and tunable emission spectra, large stokes shift and resistance to photobleaching (Medintz, I. L., Uyeda, H. T. et al. 2005; Michalet, X., Pinaud, F. F. et al. 2005). The NIR region of the spectrum (700–950 nm) is ideal for imaging through tissues because light scattering diminishes with increasing wavelength, and hemoglobin electronic and water vibrational overtone absorptions approach their minimum over this spectral domain (Franceschini, M. A., Moesta, K. T. et al. 1997; Hawrysz, D. J. and Sevick-Muraca, E. M. 2000; Intes, X., Ripoll, J. et al. 2003; Weissleder, R. and Ntziachristos, V. 2003 ; Kalchenko, V., Shivtiel, S. et al. 2006 ; Rao, J., Dragulescu-Andrasi, A. et al. 2007). Furthermore, autofluorescence of living tissues reaches a minimum at this range and the fluorescent signal can, even in the case of organic fluorophores, be detected *in vivo* at sub-nanomolar quantities and at depths sufficient for experimental or clinical imaging (Weissleder, R., Tung, C. H. et al. 1999; Tung, C. H., Mahmood, U. et al. 2000).

NIR deep tissue imaging is an emerging technology which has never before been utilized for imaging purposes in *Xenopus* or any other developmental model. In addition, although NIR QD's have recently been used for locating and visualizing static tissues like tumors it is the first time deep tissue imaging had been employed to create time lapse movies of morphogenetic processes (Voura, E. B., Jaiswal, J. K. et al. 2004; Gao, X., Cui, Y. et al. 2004). Previous experiments with the use of green QD's have demonstrated that QD's can be used to observe labeled tissues for extended periods of time without significant loss of the fluorescent signal. QD´s in conjunction with time lapse video-microscopy allowed the authors to follow injected cells from the four cell stage all the way to the tadpole stage with single cell resolution (Dubertret, B., Skourides, P. et al. 2002). The experiments using green QD could not provide deep tissue imaging and visualization was restricted to the superficial layers. Due to these limitations of visible spectrum fluorophores deep tissue movements in *Xenopus* have been mapped using images from fixed and sectioned *Xenopus* embryos by Mike Danilchick. This raised the possibility of using QD´s emitting in the NIR region for *in vivo* imaging of morphogenesis in *Xenopus*.

4.1 Developing Near Infra Red (NIR) Quantum Dots (QD's) based imaging tools for imaging of deep tissue morphogenetic movements in *Xenopus in vivo*

By taking advantage of Near Infra Red Quantum Dots we were able to image mesoderm migration with single cell resolution via microinjection into individual blastomeres. Using this approach, we achieved a detailed single resolution view of mesoderm migration *in vivo* in *Xenopus* (movies 1 and 2). Labeled embryos were monitored on a customized NIR QD capable epifluorescence microscope with the use of time lapse microscopy to collect high resolution 4D data. The data produced from this analysis provided us quantitative *in vivo* measurements regarding migration rates and directionality.

NIR QD's microinjected at the dorsal marginal zone of eight cell stage embryos failed to provide clear delineation of individual cells due to the uniform nature of the labeling. NIR QD's were evenly inherited by the progeny of the injected cells thus leading to diffuse signal and making cell boundaries hard to distinguish. Despite this, we were able to obtain movies showing the progress of the leading edge (injection in dorsal side) and mesodermal mantle closure (injection doth in dorsal and ventral side). In addition, for the first time, we were able to calculate the average displacement rate of the leading edge *in vivo*, which was 1.9 ± 0.28μm/min (stable temperature at 20°C). These rates did not vary as much as previously recorded *in vitro* rates (1-3μm/min) (Winklbauer, R. 1990; Winklbauer, R. and Nagel, M. 1991; Winklbauer, R. and Keller, R. 1996). Our rates were slower than previously published *in vivo* rates (~4μm/min) (Davidson, L. A., Hoffstrom, B. G. et al. 2002) but faster than the rates calculated from the analysis of *in vivo* MRI based time lapse movies (~1,3μm/min) (Papan, C., Boulat, B. et al. 2007; Papan, C., Boulat , B. et al. 2007). The differences between the rates measured by us and others are most likely due to differences in the temperature at which the embryos or explants were filmed.

In order to improve the visualization we proceeded by injecting NIR QDs in 32 cell stage embryos at blastomeres C1 or B1. Using this approach, individual cells were tracked and migration rates were easily determined. Individual cell migration rates were calculated and they ranged between 1.9μm/min and 2.9μm/min. These measurements show that individual cells can attain sustained migration rates, which are significantly higher than the migration rate of the mesoderm leading edge. In *Xenopus*, prechordal mesoderm moves as a multilayered coherent cell mass held together by cadherin based cell-cell adhesions (Winklbauer R., Nagel M. et al. 1996). However, it is clear from the QD based visualization of the anterior mesoderm that there is free movement of individual cells within the cell mass and that a surprising amount of mixing takes place during this

movement. Individual cells break free from their neighbours and become interspersed within non labelled regions (movie). In addition, cells can be seen undergoing division and the daughter cells follow different paths. These data are in agreement with previously published work suggesting that contacts between individual dorsal marginal zone cells are significantly less stable than those between ventral marginal zone cells (Reintsch, W. E. and Hausen, P. 2001).

Another approach that resulted in single cell visualization was the use of Qtracker 800 Cell labelling QD's. These QDs were injected in the blastocoels of late blastula to early gastrula embryos. Mid-gastrula injections enabled single cell visualization and tracking albeit with lower resolution than single blastomere injections. In addition, the Qtracker® 800 Cell Labeling QD's tended to aggregate inside the cells and the signal from labelled cells did not persist as long as that of non-targeted QD's.

In order to further improve our imaging capabilities we tried to create functionalized NIR QD's which were targeted the nucleus. Individual nuclei are well spaced within the embryo in all dimensions and thus create better contrast. Several commercial streptavidin QD's, including NIR QD's (800nm), were used and incubated with NLS. With this approach, only NLS QD's 500nm localized to the nucleus. It appears that the diameter of the longer wavelength QD's were too large to enter the nucleus. This was confirmed by using carboxyl QD's and NLS creating covalent NLS-QD's conjugates, in an effort to minimise the diameter, also failed to accumulate nucleus. We also tested InAr/ZnS core shell QD's synthesized by the Bawendi group (Zimmer, J. P., Kim, S. W. et al. 2006). These QD's have similar emission spectra with the QDot 800 QD's from invitrogen but have a significantly smaller hydrodynamic radius and readily accumulate in the nucleus. The quantum yield of these lab synthesized particles is relatively low (6-9%), compared to the commercially available CdSe/ZnS core shell QD´s making them unsuitable for deep tissue imaging at this time. Their relatively low quantum yield requires the use of higher amounts before the signal intensity reaches sufficient levels for *in vivo* detection in deep tissues and such amounts are toxic to the embryo.

In summary, we established a new imaging technology by using NIR QD's and have begun re-mapping deep tissue morphogenetic movements in *Xenopus laevis in vivo*. The visualization of mesoderm migration was performed successfully providing quantitative data, by targeting QD's to specific tissues via microinjection.

The second and major goal of this project was to explore the role of Focal Adhesion Kinase (FAK) *in vitro* and *in vivo* during *Xenopus laevis* early development.

FAK has been widely studied in many contexts due to its important role in signaling pathways that control cell morphology, migration, spreading, motility, and survival. In addition, FAK is overexpressed in many metastatic human tumors and has been shown to be necessary for embryonic development since FAK null mice ($FAK^{-/-}$) die by embryonic day 8.5 (Ilic, D., Furuta, Y. et al. 1995). FAK mutant knock-in mouse models were also generated by researchers to explore the role of FAK signaling pathways in development and its function *in vivo*. Mutant FAK^{Δ} is expressed at normal levels and as an active kinase but $FAK^{\Delta/\Delta}$ embryos display various defects and overall developmental retardation at E13.5-14.5 and eventually die (Corsi, J. M., Houbron, C. et al. 2009). $FAK^{K454R/K454R}$ mutant embryos also exhibited embryonic lethality (lethal at E9.5) and extensive defects in blood vessel formation and disorganized EC (endothelial cells) pattering (Lim, S. T., Chen, X. L. et al. 2010). In *Xenopus*, *Drosophila* and the chick FAKs expression suggests a role in gastrulation but there are no data to further support this (Hens, M. D. and DeSimone, D. W. 1995; Zhang, X., Wright, C. V. et al. 1995; Fox, G. L., Rebay, I. et al. 1999; Fujimoto, J., Sawamoto, K. et al. 1999).

Despite the wealth of evidence for FAK involvement in diverse cellular processes and the embryonic lethality of its absence during development, little is known regarding the specific role of this protein in morphogenesis and *in vivo* studies are generally lacking. Overall, studies regarding FAK have focused heavily on its role in integrin signaling and for the most part were carried out in *in vitro* cell culture systems. It has been shown that FAK localizes prominently at integrin rich focal adhesions, which suggested a role in controlling cell behaviour resulting from interactions with the extracellular matrix (Hanks, S. K., Ryzhova, L. et al. 2003; Schlaepfer, D. D. and Mitra, S. K. 2004). This has led to the generation of a large amount of data and has contributed to a good understanding of certain aspects of FAKs function. However, this has also produced conflicting reports which highlight the importance of the context in which the molecule is studied. One example is the finding that FAK acts as a negative regulator of cell migration on collagen while in the more widespread fibronectin based studies, it has been shown by several groups to act as a positive regulator (Owen, J. D., Ruest, P. J. et al. 1999; Sieg, D. J., Hauck, C. R. et al. 1999; Schaller, M. D. 2004). This, and other examples, in combination with the fact that cell culture based experiments are unable to recapitulate physiological conditions support the need for more studies examining FAK *in vivo*.

4.2 Focal Adhesion Kinase is present at focal adhesion complexes and is necessary for active mesoderm migration in *Xenopus* embryos *in vitro* and *in vivo*

We have shown that QD's can be used to track migrating mesodermal cells during gastrulation *in vivo* and this gave us the opportunity to use this tool to analyze gastrulation movements in live embryos. We decided to analyze the role of focal adhesions and specifically, FAK, in mesodermal cell migration using QD's.

The presence of focal adhesions in migrating cells on fibronectin coated slides *in vitro* was confirmed with the use of antibodies against well characteristic focal adhesion proteins. Focal adhesion complexes were mainly concentrated at the cell periphery especially in cells with a motile phenotype and were weaker and smaller than the ones seen on mammalian cells grown on fibronectin (Stylianou, P. and Skourides, P. A. 2009). But double labelling of these proteins with actin revealed that the focal adhesion complexes formed at the ends of actin filaments in a similar fashion as described in mammalian adherent cells (Maher, P. A., Pasquale, E. B. et al. 1985; Yap, A. S., Stevenson, B. R. et al. 1995).

Detection of these complexes *in vivo* was not very successful; however, all focal adhesion proteins examined were enriched in the interface between the BCR and the adherent mesodermal cells including phosphorylated FAK (Stylianou, P. and Skourides, P. A. 2009). Work by other groups using substrates of varying flexibility have shown that cells plated in relatively flexible substrates display a less organized cytoskeleton and absence of linear focal adhesions. Instead, they form focal adhesion like structures that appear punctuate and are much smaller (Robert, J. P. and and Wang, Y.-L. 1997). Since the BCR is less rigid than glass it is likely that focal contacts in the embryo are very small compared to the ones formed *in vitro* making them harder to image but the concentration of focal adhesion proteins in the interface between mesendoderm and the BCR suggests that such complexes do indeed form in the embryo.

The observation that FAK is expressed in *Xenopus* migrating mesodermal cells and that it is localized to the focal adhesions formed by these cells make it a good candidate to explore its potential role in mesoderm migration. In order to examine this possibility we used FRNK, a known dominant negative splice variant of FAK, via microinjection and carried out various *in vivo* and *in vitro* assays (Schaller, M. D., Borgman, C. A. et al. 1993; Richardson, A. and Parsons, T. 1996; Richardson, A., Malik, R. K. et al. 1997). FRNK was able to downregulate FAK in *Xenopus leavis* embryos *in vitro* in adherent, migrating mesodermal cells plated on fibronectin, by competing endogenous FAK off of integrin

based complexes but had no effect on the intercalative behaviour of explants undergoing convergent extension. In rescue experiments co-expression of FAK, resulted in cells exhibiting a migratory morphology; however, their average migration rate was slower than the control cells. These results suggest that FRNK can specifically and cell autonomously inhibit mesoderm migration on FN *in vitro* and suggests that FAK is necessary for this morphogenetic movement but is not important for convergent extension.

Since FRNK can inhibit mesoderm migration *in vitro*, we wanted to determine the effects of FRNK expression *in vivo.* For such experiments, microinjections were targeted the dorsal mesoderm since it is the tissue most actively engaged in this type of morphogenetic movement (Wacker, S., Brodbeck, A. et al. 1998).

FRNK over-expression led to blastopore closure delay and in the most severe cases led to neural tube closure problems. FRNK injected embryos which gastrulated normally were morphologically normal but blastopore closure was delayed. These results are in agreement with previous data showing that use of adhesion blocking antibodies and peptides (Ab´s against fibronectin and RGD containing peptides) leads to a delay or failure of blastopore closure (Ramos, J. W. and DeSimone, D. W. 1996; Winklbauer, R. and Keller, R. 1996). Since the dorsal most mesoderm is more migratory, we postulated that FRNK expression in less active tissues would be less detrimental to the gastrulation process. This prediction was tested by marginal zone injections (progressively more lateral) of FRNK into four cell stage embryos. As the injections were targeted to more lateral blastomeres (away from the DMZ), the percentage of embryos failing to close their blastopore decreases, further supporting the prediction that blocking mesoderm migration in less active tissues should result in milder phenotypes. Evidence for the specificity of the FRNK phenotype was established by co-injection of FAK which can rescue the FRNK phenotype and significantly reduce the number of embryos failing to reach the tadpole stage. The partial rescue of the FRNK phenotype by co-expression of FAK is consistent with the partial rescue observed in dissociated cells. *Whole mount in situ hybridization* for Xbra indicates that mesoderm specification is not affected in FRNK expressing embryos (two blastomeres of four cell stage embryos were injected at the dorsal marginal region with FRNK 500pg per blastomere). However, the position of chordamesoderm in FRNK injected embryos is mildly affected (slightly shortened trunk) compared to the controls.

Having established a technique for imaging mesoderm migration *in vivo* and determined that FAK is necessary for this movement, we went on to image FRNK expressing mesoderm *in vivo* with the use of NIR QD´s. Using the same approach as used in the

control embryos, FRNK expressing embryos were visualized. Control cells reached the top of the BCR but the FRNK injected cells lacked directionality and only a small number of these cells reached the top of the BCR. FRNK positive cells that were in direct contact with controls cells initially migrated directionally towards the top of the BCR, possibly pulled by neighbouring FRNK negative cells, however, they were soon left behind and began migrating randomly.

This, is to our knowledge, is the first time that inhibition of this morphogenetic movement (mesoderm migration) has been imaged *in vivo* and offers strong evidence regarding the *in vivo* inhibition of mesoderm migration by FRNK. The behavior of the FRNK expressing cells correlates well with the *in vitro* data, further strengthening our conclusion that FAK is necessary for this movement.

4.3 The role of Tyrosine 397 auto-phosphorylation site of Focal Adhesion Kinase during Xenopus development

Y397FFAK overexpression led to developmental defects, such as blastopore closure delay, blastopore closure failure and neural tube closure failure. These phenotypes were observed in all tested expression levels but with varying severity. Higher amounts of Y397FFAK led to embryo lethality, whereas lower amounts lead to blastopore closure failure. The blastopore closure failure however, was rescued by overexpression of HA FAK, indicating the specificity of this phenotype. These results indicate that phosphorylation of the major autophosphorylation site of FAK may be critical during gastrulation in *Xenopus* embryos. These results are in agreement with our previous published data showing that FRNK injected embryos failed to reach blastopore closure which led to neural tube closure problems compared to the non injected embryos (Stylianou, P. and Skourides, P. A. 2009). In addition, similar *in vivo* experiments were performed in mice to explore the role of FAK signalling pathways in development. FAK^{Δ} mutant (deleted exon 15 which contains major phosphorylation site Y397) was expressed at normal levels and as an active kinase, however, $FAK^{\Delta/\Delta}$ mouse embryos displayed various defects (haemorrhages, edema, multiple organ abnormalities) and overall developmental retardation at E13.5-14.5 followed by death (Corsi, J. M., Houbron, C. et al. 2009).

From our results, it appears that autophosphorylation of FAK is required for blastopore closure during gastrulation of the embryo. Therefore, we wanted to test its importance in the process of mesoderm migration. Y397FFAK was able to block cell spreading (almost totally up to 95%) *in vitro*. Surprisingly, when we used deletions of FAT domain the point mutant Y397FΔFAK also blocked spreading. This suggest that the point mutant Y397FΔFAK is acting via competition of FAK in complexes independent of focal adhesions or that it exerts an effect which is more global and upstream of FAs formation. Rescue experiments performed by overexpression of HA FAK, indicated the specificity of this phenotype. Overall, these results suggest that the Y397F point mutant does not exert its effect at the focal adhesions but rather acts on signaling complexes of FAK unrelated to focal adhesion complexes.

It is known that embryonic fibroblasts of $FAK^{-/-}$ mice have defects in migration and reduction in the rate of cell spreading (Ilic, D., Furuta, Y. et al. 1995; Corsi, J. M., Houbron, C. et al. 2009). Similar problems appear in $FAK^{\Delta/\Delta}$ cells (deleted exon 15 which contains major phosphorylation site Y397) which exhibit multiple thinner membrane

protrusions and show delayed spreading compared to $FAK^{+/+}$ mouse embryonic fibroblasts (MEFs) cultured *in vitro* (Corsi, J. M., Houbron, C. et al. 2009). These results are in agreement with our findings showing a spreading defect in adherent mesodermal cells expressing the Y397FFAK mutant.

The failure of the blastopore to close in Y397FFAK embryos is an indication that convergent extension movements are possibly blocked. This was confirmed by the fact that Y397FFAK expression blocked convergent extension movements in animal cap elogation assays. This phenotype could not be rescued by co-injecting HA FAK. The inability of wild type FAK to rescue the convergent extension movements suggests that expression of Y397FFAK leads to irreversible changes in the tissue and it is possible that the expression of this mutant leads to changes in cell fate specification or patterning of the mesoderm.

Whole mount in situ hybridization for Xbra and Chordin indicated that mesoderm specification was not somewhat affected in Y397FFAK expressing embryos with lower levels of Xbra compared to controls. In addition, the position of mesoderm in Y397FFAK injected embryos was mildly affected compared to the controls. Furthermore, the expression levels of the two neural markers, Sox2 and Sox3 (neural plate), were comparable to uninjected control embryos. RT PCR analysis was performed in order to obtain more quantitative data and in this case it was evident that Y397FFAK, expression led to a reduction of Xbra levels. These results were quite difficult to explain since Y397FFAK expression appears to reduce the expression levels of Xbra but this appears to be a non cell autonomous effect. It is possible that expression of this construct alters mesodermal patterning without blocking mesoderm induction. This would explain the inability to rescue convergent extension since the amount of FAK used for the rescue would in theory affect the type of mesoderm being induced. Failure to specifically induce chordal mesoderm would in effect abolish convergent extension movements even if prechordal or lateral mesoderm were in fact present. More work is required in order to point the precise effects of Y397FFAK expression on mesodermal patterning and polarity.

In summary, our results confirm the essential role of the FAK autophosphorylation site Tyr397 on cell spreading and migration and in addition suggest a possible role for FAK in mesodermal patterning and polarity. The behavior of the Y397FFAK expressing embryos correlates well with the *in vitro* data, further strengthening our conclusion that phosphorylated FAK is necessary for mesoderm migration during gastrulation.

4.4 Focal Adhesion Kinase is activated by integrin-independent mechanisms in the context of the embryo

One of the major finding of this proposal is that throughout embryogenesis (including the blastula stages), FAK is heavily phosphorylated on the major autophosphorylation site Y397, on the activation loop of the kinase domain (Y576/577), as well as at the C-terminus Src phosphorylation site (Y861). Moreover, FAK is phosphorylated on the Grb2 binding site (Y925) predominantly at the mesodermal belt in blastula stage, at the blastopore lip (dorsal and ventral) during gastrula stages and at the apical side of the archenteron at later stages. This is in contrast with what Hens and DeSimone suggested, where FAK is phosphorylated for the first time at the onset of gastrulation and levels increases through stage 17 and beyond (Hens, M. D. and DeSimone, D. W. 1995). Our results suggest that FAK must be activated primarily by integrin independent mechanisms in the embryo due to the fact that prior to gastrulation there is no fibronectin secretion and no laminin expression and thus, no associated cell-ECM signaling (Fey, J. and Hausen, P. 1990; Danker, K., Hacke, H. et al. 1993).

Further support for this is the observation that activated FAK is localized tightly on the membrane of the cells in the entire embryo (on residues Tyrosine 397 and 576), even in integrin-free areas such as in the apical surface of the superficial cells of the animal cap. Moreover, the fact that FAK is heavily phosphorylated in pre gastrula stage embryos shows that the kinase has an early role independent of cell movements and integrin activation. Despite the fact that FAK is found primarily in the cytoplasm of all cells in the embryo, the phosphorylated forms are only located at the plasma membrane including the apical membrane, suggesting that FAK activation takes place on the membrane. It is important to note that diffusion of the activated FAK from the baseolateral sites of the cell, to the apical surface is not possible because of the presence of tight junctions. It was shown that the biogenesis of the tight junctions in the early *Xenopus* embryo is a cell autonomous mechanism and that during this process the apical-basolateral membrane boundary is preserved (Fesenko, I., Kurth, T. et al. 2000).

As a result, activated FAK seen on the apical surface, becomes activated there, and activated FAK from the cell-cell contact areas cannot diffuse to the apical side. This difference, between cell-cell contacts and apical membrane localization of FAK gives *Xenopus laevis* embryos a very useful advantage when compared to cell culture studies. In the context of the embryo, the integrin –dependent and –independent mechanisms can be

separated, whereas in cell cultures, they cannot be distinguished because the cell-ECM interactions are the primary mode of adhesion.

The notion that FAK activation in the embryo is largely integrin-independent is also supported by the fact that the autonomously expressed C-terminal domain of FAK (FRNK), which is known for its function as a dominant negative in the integrin dependent activation of FAK by competing endogenous FAK from focal adhesions in several systems, fails to downregulate FAK activity in the context of the embryo (Richardson, A., Malik, R. K. et al. 1997; Heidkamp, M. C., Bayer, A. L. et al. 2002). This was quite surprising because its been shown *in vitro* that the C-terminus of FAK (FAT) is necessary and sufficient to target FAK at focal adhesions complexes (Hildebrand, J. D., Schaller, M. D. et al. 1993). Moreover, we showed that FRNK is able to downregulate FAK in *Xenopus laevis* embryos *in vitro* in adherent, migrating mesodermal cells plated on fibronectin, by competing endogenous FAK off of integrin based complexes (Stylianou, P. and Skourides, P. A. 2009). Also, this was shown *in vivo* at the stage of somitogenesis (Kragtorp, K. A. and Miller, J. R. 2006) where it blocks phosphorylation of endogenous FAK.

So far, FRNK has not been found to be expressed in *Xenopus laevis* embryos (Hens, M. D. and DeSimone, D. W. 1995). However, we failed to detect any dowregulation of the phosphotyrosine levels (P-Y397, P-Y576) of endogenous FAK by overexpression of FRNK in the embryo. We cannot exclude the possibility that some reduction was in fact present; however examination of the phospho Tyr levels using whole mount indirect immunofluorescence is a semi-quantitative method which cannot detect small changes in epitope abundance. It is on the other hand, a better option in this system than total protein western blotting experiments, which would underestimate such phospho Tyr level changes between injected and control embryos stemming from the fact that only a small subset of cells in the embryo is actually expressing the dominant negative construct.

More evidence in support for a limited role of integrin signalling with regards to FAK activation in the embryo comes from the observation that FRNK fails to localize tightly on the plasma membrane and at the apical surface of the blastomeres, suggesting that the C-terminus is not sufficient for membrane localization of FAK in the embryo. In addition, autonomously expressed FAT domain also fails to localize on the plasma membrane in the above areas, where there are no integrin-based complexes.

It has been reported that FAK is localized in the apicolateral junctions *in vivo* and therefore, it might become activated by cell-cell interactions (Ridyard, M. S. and Sanders, E. J. 1999). However, we also show that activated FAK does not colocalize with C-

cadherin at the apical surface of the embryos. This leads to the conclusion that FAK becomes activated in certain areas of the embryo via integrin- and cadherin-independent mechanisms.

4.5 The FERM domain is responsible for the plasma membrane localization of FAK in integrin-free areas and it activates FAK in a Src- dependent manner

The above results suggest that the localization and activation of FAK in gastrula embryos is probably regulated by another domain of FAK that is known to be involved in integrin-independent complexes. In order to identify this domain, the localization pattern of each domain of FAK was examined separately. The N-terminal domain of FAK was found to be localized at the apical surface of the cells, tightly on the plasma membrane in AP cells and partially on the plasma membrane in DMZ cells. Focusing on its localization in the AP cells, the FERM domain was found to be sufficient for targeting the C-terminus of FAK on the plasma membrane. The HAFERM/FRNK construct, localized in an identical fashion of the HAFERM suggesting that the FAT domain has no role in the localization of FAK on the apical side of the cells of the outermost epithelium. Moreover, the FERM domain was found to be necessary for the localization of FAK on the plasma membrane at least in AP cells and on the apical surface of superficial cells. Deletion of the FERM domain (HA Δ375FAK) eliminated membrane localization in AP cells and reduce the localization in DMZ cells.

This observation immediately made the FERM domain a good candidate of downregulating FAK *in vivo* because endogenous FAK and exogenous FERM may compete for membrane localization. In agreement with this possibility, is that it has been shown that the FERM domain can inhibit FAK by its ability to bind the kinase domain intramolecularly and intermolecularly (Cooper, L. A., Shen, T. L. et al. 2003; Lietha, D., Cai, X. et al. 2007).

Surprisingly, overexpression of the N-terminal domain of FAK led to the activation of endogenous FAK in a Src dependent manner. This activation was demonstrated not only by elevated phosphotyrosine levels of endogenous FAK (P-Y576, P-Y861), but also of downstream targets of FAK, such as Y31 of paxillin and Y762 of p130Cas. All the above tyrosines (those of FAK and those of the downstream targets) are phosphorylated by Src. In addition, overexpression of the FERM domain failed to elevate the levels of phosphorylated Ser473 Akt. PI3K binds the P-Y397 of FAK through its p85 subdomain and this leads to the activation of Akt (Franke, T. F., Kaplan, D. R. et al. 1997). Previous work in human lung fibroblasts showed that Akt activity was found to be increased after integrin-β1 enforced activation, which led to phosphorylation of FAK on Tyr397 and binding of PI3K. Moreover, Akt phosphorylation was downregulated by FRNK (Xia, H.,

Nho, R. S. et al. 2004). Based on the above data, the activation of Akt is integrin β1-dependent, but the activation caused by the FERM domain in this study is integrin-independent. This may explain why the FERM domain does not cause elevation of phospho Ser473. Moreover, in FERM expressing cells Src is localized on the FERM positive plasma membrane associated vesicles. In agreement to this, overexpression of the FERMY397F (point mutant on autophosphorylation site of FERM) construct that cannot bind Src, did not had the ability to elevate the phosphorylation levels of endogenous FAK or paxillin. Therefore, the FERM domain can activate FAK in a Src dependent but integrin independent manner.

The FERM domain is known to interact with many membrane receptors, and having in mind the fact that these vesicles are membrane-based structures (co-localization with mem GFP) it is possible that in the context of the embryo FAK becomes activated by growth factor receptors. In support of this, it has been shown that the F2 lobe of FERM domain can interact with PtdIns(4,5)P_2. This interaction causes conformational changes in the structure of FAK and leads to its activation (Cai, X., Lietha, D. et al. 2008). Moreover, the F2 lobe of the FERM domain was also found to interact with the HGF receptor that leads to the phosphorylation of the FERM domain at Tyr194, which in turn leads to the phosphorylation and activation of FAK (Chen, T. H., Chan, P. C. et al. 2011). In addition, FAK mutated on the basic patch of the F2 lobe (KAKTLR) of the FERM domain showed lower levels of FAK phosphorylation. This is most likely because it abolishes the binding of the FERM domain on PIP2 or on HGFR (Dunty, J. M., Gabarra-Niecko, V. et al. 2004). Combining these, with the results of this study, overexpression of the FERM domain could activate FAK through an interaction with Src.

Therefore, a possible model that can explain the activation of FAK caused by FERM overexpression on plasma membrane-associated vesicles is the following: the FERM domain is localized to integrin-free areas because it has the ability to bind PIP2s or GFRs. The FERM domain is probably localized in the same complexes where activated FAK is, because endogenous FAK is found on the plasma membrane associated vesicles formed by the FERM domain. Active FAK can phosphorylate the FERM domain on the Tyr397 *in trans*; creating a potential SH-2 binding site for Src (Figure 69A). Phosphorylated FERM on Tyr397, together with the upstream proline-rich region included in the HA FERM construct, create a high affinity binding site for Src through its SH-2 and SH-3 domains respectively. As a result, overexpression of the FERM domain leads to the recruitment of more Src molecules and probably to its activation (Figure 69B). Src is activated by the

binding of an SH-2 and an SH-3 site, and by phosphorylation on the residue Tyr416 (Boggon, T. J. and Eck, M. J. 2004). Combining the possibility that endogenous FAK and exogenous FERM are localized at the same complexes with the fact that Src is recruited by FERM to these complexes, leads to elevated phosphorylation of Src downstream substrates. Active Src can phosphorylate endogenous FAK on Tyrosine 576/577, 861 and its other downstream targets such as paxillin and p130Cas (Figure 69C). Combining the fact that Tyrosine 397 is an exclusive substrate of FAK autophosphorylation (because in kinase dead expressing cells, this site is not phosphorylated) (Hildebrand, J. D., Schaller, M. D. et al. 1993) with the fact that activated FAK localizes exclusively on the plasma membrane indicates that the FERM domain can not become activated in the cytoplasm and then translocated to the plasma membrane associated vesicles.

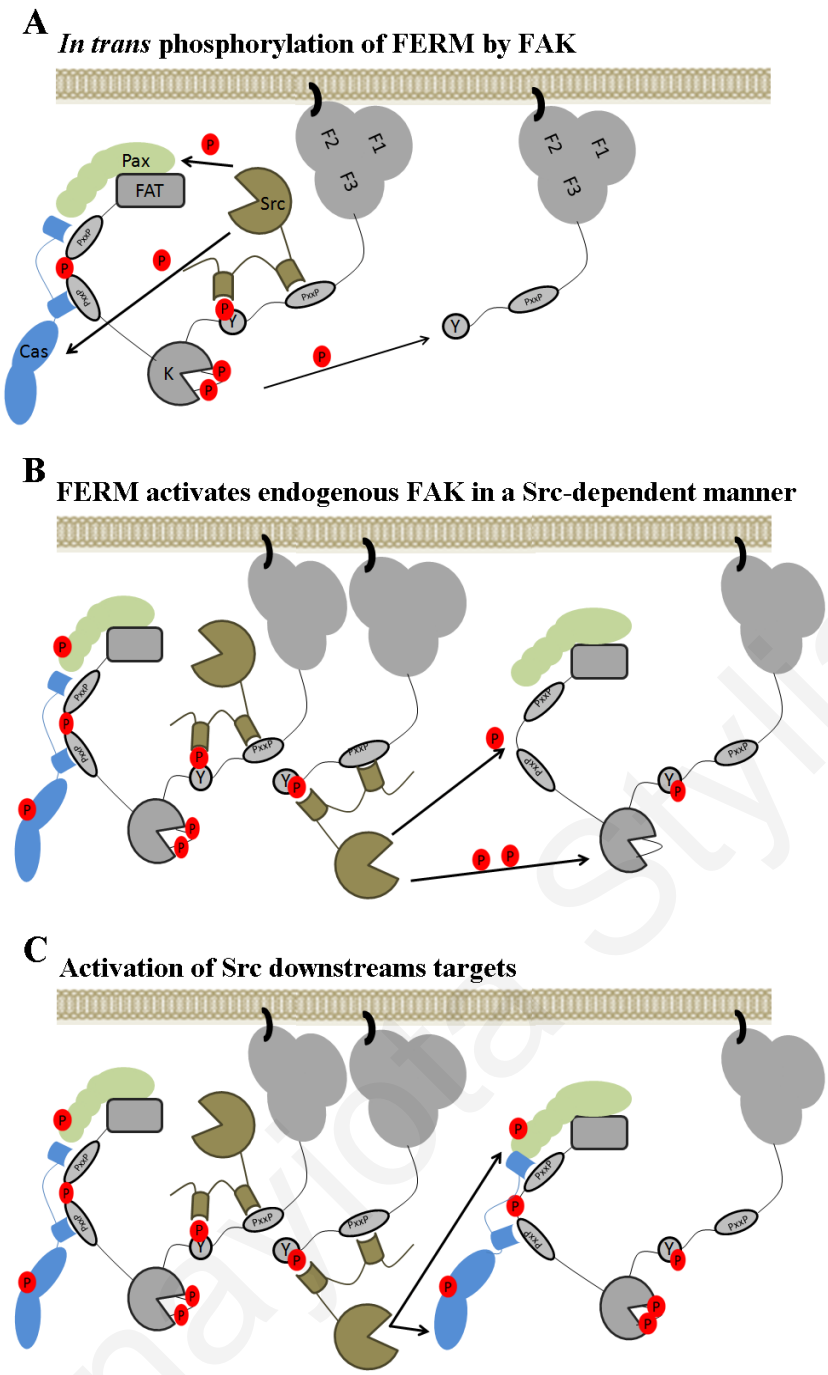

Figure 69. Model for integrin-independent activation of FAK caused by the FERM domain. (A) Endogenous phosphorylated FAK on Tyrosine 397, 576/577 and 861 is bound on plasma membrane-associated vesicles, which are integrin-free areas through an interaction between its F2 lobe and PIP2 or GFRs. In these areas there are bound FERM molecules through their F2 lobe that become phosphorylated by FAK *in trans* on Tyr397. Activated FAK is bound through the FAT domain on phosphorylated paxillin on Tyr31 and through the Pro-2 and Pro-3 domains on phosphorylated p130Cas on Tyr762. All these tyrosines are phosphorylated by Src (B) This phosphorylation of the FERM construct on Tyr397 creates a high affinity binding site for Src. Src recruitment on the FERM domain leads to the phosphorylation of neighboring FAK molecules on Tyr576/577 and Tyr861. As a result FAK becomes activated in integrin-free areas. (C) Src further phosphorylates its downstream targets on Tyr31 of paxillin and on Tyr762 of p130Cas.

4.6 FERM/FRNK is a promissing dominant negative of FAK

The failure of the FERM and FRNK domains to act as dominant negatives in the context of the embryo and the different localization of the N-terminus and C-terminus in the various regions of the embryo led to the conclusion that different domains of FAK are responsible for its localization and activation in integrin-free and integrin based regions of the embryo. More specifically, the FERM domain seems to be responsible for the localization of FAK in the AP cells and partially in the DMZ cells. The FAT domain seems to be partially responsible for the localization of FAK in the DMZ cells but has no role in the localization of the protein in AP cells. This is supported by the fact that FAKΔFAT mutant localization in AP cells is identical to full length FAK localization. This raised the possibilitity that a construct containing the two domains that are responsible for the two different modes of FAK localization could act as a dominant negative.

The FERM/FRNK construct recapitulated the tight localization of endogenous phosphorylated FAK in the AP and DMZ cells and on the apical surface of the cells of the outermost epithelium. Therefore, in the context of the embryo, the FERM and FAT domains appear to cooperate to target activated FAK on the plasma membrane.

Moreover, FERM/FRNK appears to act as a dominat negative. Firstly FERM/FRNK was able to compete full length FAK from the membrane; something that neither FERM or FRNK can accomplish. Further support for this notion comes from the severe phenotype caused by the construct's expression. These are significantly more pronounced effects, and occur at much lower expression levels compared those observed by expression of the well characterized *in vitro* studies using the FRNK construct. FRNK overexpression *in vivo* did not cause any severe phenotypes or embryonic leathality (Kragtorp, K. A. and Miller, J. R. 2006; Stylianou, P. and Skourides, P. A. 2009), whereas FAK deficient mice die very early, at the embryonic day 8.5 (Ilic, D., Furuta, Y. et al. 1995). Therefore, a dominant negative of FAK should cause the same phenotype as that observed in FAK-/- mice, however, FRNK does not seem to do this. FERM/FRNK overexpression led to developmental defects, such as cell death, blastopore closure delay, blastopore closure failure, neural tube closure failure, shortening of the antero-posterior axis and diminished head structures. These severity of these phenotypes showed a clear dose dependence with cell death and division problems appearing at high expression levels and progressively milder phenotypes at low expression levels. For example, higher amounts of FERM/FRNK led to cell lethality, whereas, lower amounts lead to bp closure failure. However, the blastopore closure failure was rescued by overexpression of HA FAK, indicating the

specificity of this phenotype. In addition, the cells near and around the injection site exhibited accute toxicity and death. Injected cells were enlarged an indication of problems with cell divsion. Upon closer examination it was revealed that these cells formed anaphase bridges which were probably reasponsible for the toxicity caused by this construct. The cell division problems seem to stem from the fact that overexpression of this construct leads to elevated and mislocalized of phosphorylated Ser732 FAK from the nucleus to the cytoplasm. It is likely that the observed misslocalization of phosphorylated Ser732 is due to the fact that the exogenous construct is phosphorylated on Ser732. Misslocalized Ser732 phosphorylated FAK may sequester dynein away from the spindle leading to the observed defects in mitosis. In support of this, loss of dynein has been shown to lead to severe spindle abnormalities and defective mitosis (Goshima, G., Nedelec, F. et al. 2005).

Additionally, FERM/FRNK overexpression led to severe defects in gastrulation movements. FERM/FRNK is able to block spreading and mesodermal migration *in vitro*. Also the observed shortening of the anterior-posterior axis in FERM/FRNK expressing embryos is an indication that convergent extension movements are blocked (Winklbauer, R. 2009). Confirming the above, FERM/FRNK overexpression in animal cap elongation assays blocked convergent extension movement. Once again, this phenotype proved to be specific because it could be rescued by co-injecting HA FAK. A possible explanation of the elongation failure in FERM/FRNK overexpressing animal caps, may be the observed elevation of C-cadherin expression in FERM/FRNK expressing cells. Dissociation and re-aggregation assays showed that FERM/FRNK expressing cells aggregate separately from control cells and that their levels of C-cadherin show a dose dependent increase according to the levels of expression of the FERM/FRNK construct. These demonstrate that FERM/FRNK overexpression leads to the strengthening of the cell-cell contacts and as a result, in failure of covergent extension.

It is interesting to note that FERMY397F/FRNK also led to the above phenotypes with the same severity indicating that y397 is not important in the elicited phenotype.

5. CONCLUSIONS AND FUTURE PLANS

In conclusion, we have established a new imaging technology by using NIR QD's and have begun re-mapping deep tissue morphogenetic movements in *Xenopus laevis in vivo*. The visualization of mesoderm migration was performed successfully generating the first *in vivo* quantitative measurements concerning this movement. We are planning to simultaneously target superficial tissues with visible spectrum emitting QD's and deep tissues with Near Infra Red QD's. This way, individual movements will be imaged with different colours and their relationships will be easier to analyze. The data produced from this *in vivo* analysis will also be useful for determining the role of individual pathways in morphogenesis and lead to a better understanding of the mechanisms though which they act. The ability to image morphogenetic movements *in vivo* creates the opportunity to address questions regarding individual movements during gastrulation *in vivo.*

In addition, the generation of time lapse movies of deep tissues of embryos in which mesoderm migration is blocked using FRNK (dominant negative Focal Adhesion Kinase) was accomplished. Inhibition of FAK blocks mesoderm spreading and migration both *in vitro* and *in vivo*. Also quantitative measurements regarding the effect of FRNK in mesoderm migration *in vivo* and *in vitro* were accomplished. These results provide new insights about the role of FAK and of focal adhesions during gastrulation and provide a new tool for the study of morphogenesis *in vivo*. We will further analyse the role of other proteins in *Xenopus laevis* morphogenesis using dominant negative RNAs that will be targeted to a tissue together with NIR QD's and the tissues will be monitored and imaged *in vivo*. The creation of improved QD imaging tools will improve both the depth penetration as well as the quality of *in vivo* imaging data. The ability to image morphogenetic movements *in vivo* creates the opportunity to address questions regarding the *in vivo* role of individual movements during the process of gastrulation as a whole. These experiments will provide quantitative measurements regarding the effects of selected genes on morphogenetic movements *in vivo* and *q*uantitative data regarding the relationship between convergent extension and mesoderm migration.

Studying the pattern of FAK localization and activation in the *Xenopus laevis* embryo has revealed that FAK activation takes place on the plasma membrane and is primarily integrin-independent. Mapping the region of FAK responsible for its membrane localization in the context of the embryo, we have shown that the FERM domain is both necessary and sufficient for this, in integrin-independent regions. The activation of FAK in the embryo seems to be regulated by the FERM domain in AP cells and on their apical

surfaces, and by the FERM and FAT domain together in DMZ cells. In addition, both the N- and C- terminus of FAK cooperate for its plasma membrane localization in integrin-containing regions of the embryo. Extensive experiments addressing the function of the FERM domain also showed that in *Xenopus laevis* embryos, the FERM domain can upregulate endogenous FAK in a Src-dependent manner.

Finally, a potential dominant negative was generated comprising the N- and C- termini of FAK. There are several indications that this construct is a promising dominant negative and more experiments on its effects on the phosphorylation status of FAK will demonstrate this and potentially lead to its establisment as a dominant negative that can downregulate FAK *in vivo.*

REFERENCES

Alfandari, D., Ramos, J., et al. (1996). "The RGD-dependent and the Hep II binding domains of fibronectin govern the adhesive behaviors of amphibian embryonic cells." Mechanisms of Development **56**: 83-92.

Ariizumi, T., Sawamura, K., et al. (1991). "Dose and time-dependent mesoderm induction and outgrowth formation by activin A in Xenopus laevis." Int J Dev Biol **35**(4): 407-414.

Arya, H., Kaul, Z., et al. (2005). "Quantum dots in bio-imaging: Revolution by the small." Biochem Biophys Res Commun **329**(4): 1173-1177.

Asashima, M., Nakano, H., et al. (1990). "Mesodermal induction in early amphibian embryos by activin A (erythroid differentiation factor)." Dev. Biol **198**: 330-335.

Beviglia, L., Golubovskaya, V., et al. (2003). "Focal adhesion kinase N-terminus in breast carcinoma cells induces rounding, detachment and apoptosis." Biochem J **373**(Pt 1): 201-210.

Boggon, T. J. and Eck, M. J. (2004). "Structure and regulation of Src family kinases." Oncogene **23**(48): 7918-7927.

Boppart, S. A., Tearney, G. J., et al. (1997). "Noninvasive assessment of the developing Xenopus cardiovascular system using optical coherence tomography." Proc Natl Acad Sci U S A **9**: 4256-4261.

Brieher, W. M. and Gumbiner, B. M. (1994). "Regulation of C-cadherin function during activin induced morphogenesis of Xenopus animal caps." J Cell Biol **126**(2): 519-527.

Bruchez, M., Jr., Moronne, M., et al. (1998). "Semiconductor nanocrystals as fluorescent biological labels." Science **281**(5385): 2013-2016.

Burridge, K. and Chrzanowska-Wodnicka, M. (1996). "Focal adhesions, contractility, and signaling." Annu Rev Cell Dev Biol. **12**: 463-518.

Burridge, K., Fath, K., et al. (1988). "Focal adhesions: transmembrane junctions between the extracellular matrix and the cytoskeleton." Annu Rev Cell Biol. **4**: 487-525.

Cai, X., Lietha, D., et al. (2008). "Spatial and temporal regulation of focal adhesion kinase activity in living cells." Mol Cell Biol **28**(1): 201-214.

Calalb, M. B., Polte, T. R., et al. (1995). "Tyrosine phosphorylation of focal adhesion kinase at sites in the catalytic domain regulates kinase activity: a role for Src family kinases." Mol Cell Biol **15**(2): 954-963.

Calalb, M. B., Zhang, X., et al. (1996). "Focal adhesion kinase tyrosine-861 is a major site of phosphorylation by Src." Biochem Biophys Res Commun **228**(3): 662-668.

Cary, L. A., Chang, J. F., et al. (1996). "Stimulation of cell migration by overexpression of focal adhesion kinase and its association with Src and Fyn." J Cell Sci **109 (Pt 7)**: 1787-1794.

Cary, L. A. and Guan, J. L. (1999). "Focal adhesion kinase in integrin-mediated signaling." Front Biosci **4**: D102-113.

Chan, W. C., Maxwell, D. J., et al. (2002). "Luminescent quantum dots for multiplexed biological detection and imaging." Curr Opin Biotechnol **13**(1): 40-46.

Chen, H. C., Appeddu, P. A., et al. (1996). "Phosphorylation of tyrosine 397 in focal adhesion kinase is required for binding phosphatidylinositol 3-kinase." J Biol Chem **271**(42): 26329-26334.

Chen, T. H., Chan, P. C., et al. (2011). "Phosphorylation of focal adhesion kinase on tyrosine 194 by Met leads to its activation through relief of autoinhibition." Oncogene **30**(2): 153-166.

Choi, Y. S., Sehgal, R., et al. (1990). "A cadherin-like protein in eggs and cleaving embryos of Xenopus laevis is expressed in oocytes in response to progesterone." J Cell Biol **110**(5): 1575-1582.

Cohen, L. A. and Guan, J. L. (2005). "Residues within the first subdomain of the FERM-like domain in focal adhesion kinase are important in its regulation." J Biol Chem **280**(9): 8197-8207.

Cooper, L. A., Shen, T. L., et al. (2003). "Regulation of focal adhesion kinase by its amino-terminal domain through an autoinhibitory interaction." Mol Cell Biol **23**(22): 8030-8041.

Corsi, J. M., Houbron, C., et al. (2009). "Autophosphorylation-independent and -dependent functions of focal adhesion kinase during development." J Biol Chem **284**(50): 34769-34776.

Crawford, B. D., Henry, C. A., et al. (2003). "Activity and distribution of paxillin, focal adhesion kinase, and cadherin indicate cooperative roles during zebrafish morphogenesis." Mol Biol Cell. **14**: 3065-3081.

Dale, L. and Slack, J. M. (1987). "Fate map for the 32-cell stage of Xenopus laevis." Development **99**(4): 527-551.

Danker, K., Hacke, H., et al. (1993). "V(+)-fibronectin expression and localization prior to gastrulation in Xenopus laevis embryos." Mech Dev **44**(2-3): 155-165.

Davidson, L. A., Hoffstrom, B. G., et al. (2002). "Mesendoderm extension and mantle closure in Xenopus laevis gastrulation: combined roles for integrin alpha(5)beta(1), fibronectin, and tissue geometry." Dev Biol **242**: 109-129.

Demetriou, M. C., Stylianou, P., et al. (2008). "Spatially and temporally regulated alpha6 integrin cleavage during Xenopus laevis development." Biochem Biophys Res Commun **366**(3): 779-785.

Deramaudt, T. B., Dujardin, D., et al. (2011). "FAK phosphorylation at Tyr-925 regulates cross-talk between focal adhesion turnover and cell protrusion." Mol Biol Cell **22**(7): 964-975.

Doherty, J. T., Conlon, F. L., et al. (2010). "Focal adhesion kinase is essential for cardiac looping and multichamber heart formation." Genesis **48**(8): 492-504.

Du, Q. S., Ren, X. R., et al. (2001). "Inhibition of PYK2-induced actin cytoskeleton reorganization, PYK2 autophosphorylation and focal adhesion targeting by FAK." J Cell Sci. **114**: 2977-2987.

Dubertret, B., Skourides, P., et al. (2002). "In vivo imaging of quantum dots encapsulated in phospholipid micelles." Science. **298**: 1759-1762.

Dunty, J. M., Gabarra-Niecko, V., et al. (2004). "FERM domain interaction promotes FAK signaling." Mol Cell Biol **24**(12): 5353-5368.

Eide, B. L., Turck, C. W., et al. (1995). "Identification of Tyr-397 as the primary site of tyrosine phosphorylation and pp60src association in the focal adhesion kinase, pp125FAK." Mol Cell Biol **15**(5): 2819-2827.

Fesenko, I., Kurth, T., et al. (2000). "Tight junction biogenesis in the early Xenopus embryo." Mech Dev **96**(1): 51-65.

Fey, J. and Hausen, P. (1990). "Appearance and distribution of laminin during development of Xenopus laevis." Differentiation **42**(3): 144-152.

Fox, G. L., Rebay, I., et al. (1999). "Expression of DFak56, a Drosophila homolog of vertebrate focal adhesion kinase, supports a role in cell migration in vivo." Proc Natl Acad Sci U S A **96**(26): 14978-14983.

Frame, M. C., Patel, H., et al. (2010). "The FERM domain: organizing the structure and function of FAK." Nat Rev Mol Cell Biol **11**(11): 802-814.

Franceschini, M. A., Moesta, K. T., et al. (1997). "Frequency-domain techniques enhance optical mammography: Initial clinical results." Proc. Natl. Acad. Sci. USA **94**: 6468-6473.

Franke, T. F., Kaplan, D. R., et al. (1997). "PI3K: downstream AKTion blocks apoptosis." Cell **88**(4): 435-437.

Franke, T. F., Kaplan, D. R., et al. (1997). "Direct regulation of the Akt proto-oncogene product by phosphatidylinositol-3,4-bisphosphate." Science **275**(5300): 665-668.

Fujimoto, J., Sawamoto, K., et al. (1999). "Cloning and characterization of Dfak56, a homolog of focal adhesion kinase, in Drosophila melanogaster." J Biol Chem **274**(41): 29196-29201.

Furuta, Y., Ilic, D., et al. (1995). "Mesodermal defect in late phase of gastrulation by a targeted mutation of focal adhesion kinase, FAK." Oncogene **11**(10): 1989-1995.

Gabarra-Niecko, V., Keely, P. J., et al. (2002). "Characterization of an activated mutant of focal adhesion kinase: 'SuperFAK'." Biochem J **365**(Pt 3): 591-603.

Gao, X., Cui, Y., et al. (2004). "In vivo cancer targeting and imaging with semiconductor quantum dots." Nat Biotechnol. **22**: 969-976.

Gervais, F. G., Thornberry, N. A., et al. (1998). "Caspases cleave focal adhesion kinase during apoptosis to generate a FRNK-like polypeptide." J Biol Chem **273**(27): 17102-17108.

Gilbert, S. (2006). Developmental Biology. Sunderland, Massachusetts USA Sinauer Associates, Inc., Puplishers.

Gilmore, A. P. and Romer, L. H. (1996). "Inhibition of focal adhesion kinase (FAK) signaling in focal adhesions decreases cell motility and proliferation." Mol Biol Cell **7**(8): 1209-1224.

Gilmore, A. P. and Romer, L. H. (1996). "Inhibition of focal adhesion kinase (FAK) signaling in focal adhesions decreases cell motility and proliferation." Mol Biol Cell. **7**: 1209-1224.

Ginsberg, D., DeSimone, D., et al. (1991). "Expression of a novel cadherin (EP-cadherin) in unfertilized eggs and early Xenopus embryos." Development **111**(2): 315-325.

Godfrey, E. W. and Sanders, G. E. (2004). "Effect of water hardness on oocyte quality and embryo development in the African clawed frog (Xenopus laevis)." Comp Med **54**(2): 170-175.

Goshima, G., Nedelec, F., et al. (2005). "Mechanisms for focusing mitotic spindle poles by minus end-directed motor proteins." J Cell Biol **171**(2): 229-240.

Grigera, P. R., Jeffery, E. D., et al. (2005). "FAK phosphorylation sites mapped by mass spectrometry." J Cell Sci **118**(Pt 21): 4931-4935.

Hanks, S. K., Calalb, M. B., et al. (1992). "Focal adhesion protein-tyrosine kinase phosphorylated in response to cell attachment to fibronectin." Proc Natl Acad Sci U S A **89**(18): 8487-8491.

Hanks, S. K., Ryzhova, L., et al. (2003). "Focal adhesion kinase signaling activities and their implications in the control of cell survival and motility." Front Biosci. **8**: d982-996.

Hardin, J. and Keller, R. (1988). "The behaviour and function of bottle cells during gastrulation of Xenopus laevis." Development **103**(1): 211-230.

Harte, M. T., Hildebrand, J. D., et al. (1996). "p130Cas, a substrate associated with v-Src and v-Crk, localizes to focal adhesions and binds to focal adhesion kinase." J Biol Chem **271**(23): 13649-13655.

Haskell, R. C., Williams, M. E., et al. (2004). "Visualizing early frog development with motion-sensitive 3-D optical coherence microscopy." Conf Proc IEEE Eng Med Biol Soc. **7**: 5296-5299.

Hawrysz, D. J. and Sevick-Muraca, E. M. (2000). "Developments toward diagnostic breast cancer imaging using near-infrared optical measurements and fluorescent contrast agents." Neoplasia **2**: 388-417.

Hayashi, I., Vuori, K., et al. (2002). "The focal adhesion targeting (FAT) region of focal adhesion kinase is a four-helix bundle that binds paxillin." Nat Struct Biol **9**(2): 101-106.

Heasman, J., Ginsberg, D., et al. (1994). "A functional test for maternally inherited cadherin in Xenopus shows its importance in cell adhesion at the blastula stage." Development **120**(1): 49-57.

Heasman, J., Kofron, M., et al. (2000). "Beta-catenin signaling activity dissected in the early Xenopus embryo: a novel antisense approach." Dev Biol **222**(1): 124-134.

Heidkamp, M. C., Bayer, A. L., et al. (2002). "GFP-FRNK disrupts focal adhesions and induces anoikis in neonatal rat ventricular myocytes." Circ Res **90**: 1282-1289.

Heidkamp, M. C., Bayer, A. L., et al. (2002). "GFP-FRNK disrupts focal adhesions and induces anoikis in neonatal rat ventricular myocytes." Circ Res **90**(12): 1282-1289.

Henry, C. A., Crawford, B. D., et al. (2001). "Roles for zebrafish focal adhesion kinase in notochord and somite morphogenesis." Dev Biol **240**(2): 474-487.

Hens, M. D. and DeSimone, D. W. (1995). "Molecular analysis and developmental expression of the focal adhesion kinase pp125FAK in Xenopus laevis." Dev Biol **170**(2): 274-288.

Hens, M. D. and DeSimone, D. W. (1995). "Molecular analysis and developmental expression of the focal adhesion kinase pp125FAK in Xenopus laevis." Dev Biol. **170**: 274-288.

Hildebrand, J. D., Schaller, M. D., et al. (1993). "Identification of sequences required for the efficient localization of the focal adhesion kinase, pp125FAK, to cellular focal adhesions." J Cell Biol **123**(4): 993-1005.

Hildebrand, J. D., Schaller, M. D., et al. (1995). "Paxillin, a tyrosine phosphorylated focal adhesion-associated protein binds to the carboxyl terminal domain of focal adhesion kinase." Mol Biol Cell **6**(6): 637-647.

Hilken, G., Dimigen, J., et al. (1995). "Growth of Xenopus laevis under different laboratory rearing conditions." Lab Anim **29**(2): 152-162.

Hynes, R. O. (1992). "Integrins: versatility, modulation, and signaling in cell adhesion." Cell **69**(1): 11-25.

Hynes, R. O., George, E. L., et al. (1992). "Toward a genetic analysis of cell-matrix adhesion." Cold Spring Harb Symp Quant Biol **57**: 249-258.

Iioka, H., Iemura, S., et al. (2007). "Wnt signalling regulates paxillin ubiquitination essential for mesodermal cell motility." Nat Cell Biol. **9**: 813-821.

Ilic, D., Furuta, Y., et al. (1995). "Reduced cell motility and enhanced focal adhesion contact formation in cells from FAK-deficient mice." Nature **377**(6549): 539-544.

Ilic, D., Kovacic, B., et al. (2003). "Focal adhesion kinase is required for blood vessel morphogenesis." Circ Res **92**(3): 300-307.

Intes, X., Ripoll, J., et al. (2003). "In vivo continuous-wave optical breast imaging enhanced with Indocyanine Green." Med Phys. **30**: 1039-1047.

Jacamo, R. O. and Rozengurt, E. (2005). "A truncated FAK lacking the FERM domain displays high catalytic activity but retains responsiveness to adhesion-mediated signals." Biochem Biophys Res Commun **334**(4): 1299-1304.

Joos, T. O., Whittaker, C. A., et al. (1995). "Integrin alpha 5 during early development of Xenopus laevis." Mech Dev **50**(2-3): 187-199.

Kalchenko, V., Shivtiel, S., et al. (2006). "Use of lipophilic near-infrared dye in whole-body optical imaging of hematopoietic cell homing." J Biomed Opt.(11): 050507.

Katz, B. Z., Romer, L., et al. (2003). "Targeting membrane-localized focal adhesion kinase to focal adhesions: roles of tyrosine phosphorylation and SRC family kinases." J Biol Chem **278**(31): 29115-29120.

Kawasaki, E. S. and Player, A. (2005). "Nanotechnology, nanomedicine, and the development of new, effective therapies for cancer." Nanomedicine **1**(2): 101-109.

Keller, R. E. (1980). "The cellular basis of epiboly: an SEM study of deep-cell rearrangement during gastrulation in Xenopus laevis." J Embryol Exp Morphol **60**: 201-234.

Keller, R. E. (1981). "An experimental analysis of the role of bottle cells and the deep marginal zone in gastrulation of Xenopus laevis." J Exp Zool **216**(1): 81-101.

Keller, R. E., Danilchik, M., et al. (1985). "The function and mechanism of convergent extension during gastrulation of Xenopus laevis." J Embryol Exp Morphol **89 Suppl**: 185-209.

Kim, S., Lim, Y. T., et al. (2003). "Near-infrared fluorescent type II quantum dots for sentinel lymph node mapping." Nature Biotechnology **22**: 93-97.

Kragtorp, K. A. and Miller, J. R. (2006). "Regulation of somitogenesis by Ena/VASP proteins and FAK during Xenopus development." Development **133**(4): 685-695.

Kragtorp, K. A. and Miller, J. R. (2006). "Regulation of somitogenesis by Ena/VASP proteins and FAK during Xenopus development." Development. **133**: 685-695.

Kurth, T. and Hausen, P. (2000). "Bottle cell formation in relation to mesodermal patterning in the Xenopus embryo." Mech Dev **97**(1-2): 117-131.

Kwan, K. M. and Kirschner, M. W. (2003). "Xbra functions as a switch between cell migration and convergent extension in the Xenopus gastrula." Development **130**(9): 1961-1972.

Leu, T. H. and Maa, M. C. (2002). "Tyr-863 phosphorylation enhances focal adhesion kinase autophosphorylation at Tyr-397." Oncogene **21**: 6992-7000.

Leu, T. H. and Maa, M. C. (2002). "Tyr-863 phosphorylation enhances focal adhesion kinase autophosphorylation at Tyr-397." Oncogene **21**(46): 6992-7000.

Lietha, D., Cai, X., et al. (2007). "Structural basis for the autoinhibition of focal adhesion kinase." Cell **129**(6): 1177-1187.

Lim, S. T., Chen, X. L., et al. (2010). "Knock-in mutation reveals an essential role for focal adhesion kinase activity in blood vessel morphogenesis and cell motility-polarity but not cell proliferation." J Biol Chem **285**(28): 21526-21536.

Lim, S. T., Mikolon, D., et al. (2008). "FERM control of FAK function: implications for cancer therapy." Cell Cycle **7**(15): 2306-2314.

Longo, D., Peirce, S. M., et al. (2004). "Multicellular computer simulation of morphogenesis: blastocoel roof thinning and matrix assembly in Xenopus laevis." Dev Biol **271**(1): 210-222.

Ma, A., Richardson, A., et al. (2001). "Serine phosphorylation of focal adhesion kinase in interphase and mitosis: a possible role in modulating binding to p130(Cas)." Mol Biol Cell **12**(1): 1-12.

Maher, P. A., Pasquale, E. B., et al. (1985). "Phosphotyrosine-containing proteins are concentrated in focal adhesions and intercellular junctions in normal cells." Proc Natl Acad Sci U S A. **82**: 6576-6580.

Marsden, M. and DeSimone, D. W. (2001). "Regulation of cell polarity, radial intercalation and epiboly in Xenopus: novel roles for integrin and fibronectin." Development **128**(18): 3635-3647.

Marsden, M. and DeSimone, D. W. (2001). "Regulation of cell polarity, radial intercalation and epiboly in Xenopus: novel roles for integrin and fibronectin." Development **128**: 3635-3647.

Medintz, I. L., Uyeda, H. T., et al. (2005). "Quantum dot bioconjugates for imaging, labelling and sensing." Nat Mater **4**: 435-446.

Michalet, X., Pinaud, F. F., et al. (2005). "Quantum dots for live cells, in vivo imaging, and diagnostics." Science **307**(5709): 538-544.

Michalet, X., Pinaud, F. F., et al. (2005). "Quantum dots for live cells, in vivo imaging, and diagnostics." Science. **307**: 538-544.

Nakatsuji, N. (1986). "Presumptive mesoderm cells from Xenopus laevis gastrulae attach to and migrate on substrata coated with fibronectin or laminin." Journal of Cell Science **86**: 109-118.

Nakatsuji, N. and Johnson, K. E. (1983b). "Conditioning of a culture substratum by the ectodermal layer promotes attachment and oriented locomotion by amphibian gastrula mesodermal cells. ." Journal of Cell Science **59**: 43-60.

Nandadasa, S., Tao, Q., et al. (2009). "N- and E-cadherins in Xenopus are specifically required in the neural and non-neural ectoderm, respectively, for F-actin assembly and morphogenetic movements." Development **136**(8): 1327-1338.

Needles, A., Yang, V. X. D., et al. (2003). "Structural and Doppler imaging of Xenopus Laevis embryos in vivo: a comparison of ultrasound biomicroscopy and optical coherence tomography." Ultrasonics, IEEE Symposium **1**: 758-761.

Nolan, K., Lacoste, J., et al. (1999). "Regulated expression of focal adhesion kinase-related nonkinase, the autonomously expressed C-terminal domain of focal adhesion kinase." Mol Cell Biol **19**(9): 6120-6129.

Nutt, S. L., Bronchain, O. J., et al. (2001). "Comparison of morpholino based translational inhibition during the development of Xenopus laevis and Xenopus tropicalis." Genesis **30**(3): 110-113.

Ossovskaya, V., Lim, S. T., et al. (2008). "FAK nuclear export signal sequences." FEBS Lett **582**(16): 2402-2406.

Otey, C. A. (1996). "pp125FAK in the focal adhesion." Int Rev Cytol **167**: 161-183.

Owen, J. D., Ruest, P. J., et al. (1999). "Induced focal adhesion kinase (FAK) expression in FAK-null cells enhances cell spreading and migration requiring both auto- and activation loop phosphorylation sites and inhibits adhesion-dependent tyrosine phosphorylation of Pyk2." Mol Cell Biol **19**(7): 4806-4818.

Papan, C., Boulat , B., et al. (2007). "Formation of the dorsal marginal zone in Xenopus laevis analyzed by time-lapse microscopic magnetic resonance imaging." Dev Biol. **305**: 161-171.

Papan, C., Boulat, B., et al. (2007). "Two-dimensional and three-dimensional time-lapse microscopic magnetic resonance imaging of Xenopus gastrulation movements using intrinsic tissue-specific contrast." Dev Dyn. **236**: 494-501.

Park, A. Y., Shen, T. L., et al. (2009). "Role of focal adhesion kinase Ser-732 phosphorylation in centrosome function during mitosis." J Biol Chem **284**(14): 9418-9425.

Parsons, J. T. and Parsons, S. J. (1997). "Src family protein tyrosine kinases: cooperating with growth factor and adhesion signaling pathways." Curr Opin Cell Biol **9**(2): 187-192.

Ramos, J. W. and DeSimone, D. W. (1996). "Xenopus embryonic cell adhesion to fibronectin: position-specific activation of RGD/synergy site-dependent migratory behavior at gastrulation." J Cell Biol **134**(1): 227-240.

Rao, J., Dragulescu-Andrasi, A., et al. (2007). "Fluorescence imaging in vivo: recent advances." Curr Opin Biotechnol **18**(1): 17-25.

Reintsch, W. E. and Hausen, P. (2001). "Dorsoventral differences in cell-cell interactions modulate the motile behaviour of cells from the Xenopus gastrula." Dev Biol(240): 387-403.

Reiske, H. R., Kao, S. C., et al. (1999). "Requirement of phosphatidylinositol 3-kinase in focal adhesion kinase-promoted cell migration." J Biol Chem **274**(18): 12361-12366.

Richardson, A., Malik, R. K., et al. (1997). "Inhibition of cell spreading by expression of the C-terminal domain of focal adhesion kinase (FAK) is rescued by coexpression of Src or catalytically inactive FAK: a role for paxillin tyrosine phosphorylation." Mol Cell Biol **17**(12): 6906-6914.

Richardson, A., Malik, R. K., et al. (1997). "Inhibition of cell spreading by expression of the C-terminal domain of focal adhesion kinase (FAK) is rescued by coexpression

of Src or catalytically inactive FAK: a role for paxillin tyrosine phosphorylation." Mol Cell Biol **17**: 6906-6914.

Richardson, A. and Parsons, T. (1996). "A mechanism for regulation of the adhesion-associated proteintyrosine kinase pp125FAK." Nature **380**: 538-540.

Ridyard, M. S. and Sanders, E. J. (1999). "Potential roles for focal adhesion kinase in development." Anat Embryol (Berl) **199**(1): 1-7.

Robert, J. P. and and Wang, Y.-L. (1997). "Cell locomotion and focal adhesions are regulated by substrate flexibility." Proc. Natl. Acad. Sci. **94**: 13661-13665.

Ruest, P. J., Shin, N. Y., et al. (2001). "Mechanisms of CAS substrate domain tyrosine phosphorylation by FAK and Src." Mol Cell Biol **21**(22): 7641-7652.

Sato, S. M. and Sargent, T. D. (1989). "Development of neural inducing capacity in dissociated Xenopus embryos." Dev Biol. **134**: 263-266.

Schaller, M. D. (2004). "FAK and paxillin: regulators of N-cadherin adhesion and inhibitors of cell migration?" J Cell Biol **166**(2): 157-159.

Schaller, M. D., Borgman, C. A., et al. (1992). "pp125FAK a structurally distinctive protein-tyrosine kinase associated with focal adhesions." Proc Natl Acad Sci U S A **89**(11): 5192-5196.

Schaller, M. D., Borgman, C. A., et al. (1993). "Autonomous expression of a noncatalytic domain of the focal adhesion-associated protein tyrosine kinase pp125FAK." Mol Cell Biol **13**: 785-791.

Schaller, M. D., Borgman, C. A., et al. (1993). "Autonomous expression of a noncatalytic domain of the focal adhesion-associated protein tyrosine kinase pp125FAK." Mol Cell Biol **13**(2): 785-791.

Schaller, M. D., Hildebrand, J. D., et al. (1994). "Autophosphorylation of the focal adhesion kinase, pp125FAK, directs SH2-dependent binding of pp60src." Mol Cell Biol **14**(3): 1680-1688.

Schaller, M. D., Otey, C. A., et al. (1995). "Focal adhesion kinase and paxillin bind to peptides mimicking beta integrin cytoplasmic domains." J Cell Biol **130**(5): 1181-1187.

Schlaepfer, D. D., Hanks, S. K., et al. (1994). "Integrin-mediated signal transduction linked to Ras pathway by GRB2 binding to focal adhesion kinase." Nature **372**(6508): 786-791.

Schlaepfer, D. D., Hauck, C. R., et al. (1999). "Signaling through focal adhesion kinase." Prog Biophys Mol Biol **71**(3-4): 435-478.

Schlaepfer, D. D. and Hunter, T. (1996). "Evidence for in vivo phosphorylation of the Grb2 SH2-domain binding site on focal adhesion kinase by Src-family protein-tyrosine kinases." Mol Cell Biol **16**(10): 5623-5633.

Schlaepfer, D. D. and Mitra, S. K. (2004). "Multiple connections link FAK to cell motility and invasion " Curr OpinGenet Dev **14**: 92-101.

Schlaepfer, D. D., Mitra, S. K., et al. (2004). "Control of motile and invasive cell phenotypes by focal adhesion kinase." Biochim Biophys Act. **1692**: 77-102.

Schlaepfer, D. D., Mitra, S. K., et al. (2004). "Control of motile and invasive cell phenotypes by focal adhesion kinase." Biochim Biophys Acta **1692**(2-3): 77-102.

Shen, Y. and Schaller, M. D. (1999). "Focal adhesion targeting: the critical determinant of FAK regulation and substrate phosphorylation." Mol Biol Cell **10**(8): 2507-2518.

Sieg, D. J., Hauck, C. R., et al. (2000). "FAK integrates growth-factor and integrin signals to promote cell migration." Nat Cell Biol **2**: 249-256.

Sieg, D. J., Hauck, C. R., et al. (1999). "Required role of focal adhesion kinase (FAK) for integrin- stimulated cell migration." J Cell Sci **112** 2677-2691.

Sieg, D. J., Hauck, C. R., et al. (1999). "Required role of focal adhesion kinase (FAK) for integrin-stimulated cell migration." J Cell Sci **112 (Pt 16)**: 2677-2691.

Sive, H. L., Grainger, R. M., et al. (2000). Early Development of *Xenopus laevis*. A Laboratory Manual. Cold Spring Harbor, New York., Cold Spring Harbor Laboratory Press, New York.

Skourides, P. A., Perera, S. A., et al. (1999). "Polarized distribution of Bcr-Abl in migrating myeloid cells and co-localization of Bcr-Abl and its target proteins." Oncogene **18**(5): 1165-1176.

Smith, A. M., Duan, H., et al. (2008). "Bioconjugated quantum dots for in vivo molecular and cellular imaging." Adv Drug Deliv Rev **60**(11): 1226-1240.

Smith, J. C., Conlon, F. L., et al. (2000). "Xwnt11 and the regulation of gastrulation in Xenopus." Philos Trans R Soc Lond B Biol Sci **355**(1399): 923-930.

Smith, W. C. and Harland, R. M. (1991). "Injected Xwnt-8 RNA acts early in Xenopus embryos to promote formation of a vegetal dorsalizing center." Cell **67**(4): 753-765.

Stepniak, E., Radice, G. L., et al. (2009). "Adhesive and signaling functions of cadherins and catenins in vertebrate development." Cold Spring Harb Perspect Biol **1**(5): a002949.

Stewart, A., Ham, C., et al. (2002). "The focal adhesion kinase amino-terminal domain localises to nuclei and intercellular junctions in HEK 293 and MDCK cells

independently of tyrosine 397 and the carboxy-terminal domain." Biochem Biophys Res Commun **299**(1): 62-73.

Stroh, M., Zimmer, J. P., et al. (2005). "Quantum dots spectrally distinguish multiple species within the tumor milieu in vivo." Nat Med. **11**: 678-682.

Stylianou, P. and Skourides, P. A. (2009). "Imaging morphogenesis, in Xenopus with Quantum Dot nanocrystals." Mech Dev **126**(10): 828-841.

Tada, M. and Smith, J. C. (2000). "Xwnt11 is a target of Xenopus Brachyury: regulation of gastrulation movements via Dishevelled, but not through the canonical Wnt pathway." Development **127**(10): 2227-2238.

Takashi Ariizumi, Naomi Moriya, et al. (1991). "Concentration-dependent inducing activity of activin A " Development Genes and Evolution **200**: 230-233.

Taylor, J. M., Mack, C. P., et al. (2001). "Selective expression of an endogenous inhibitor of FAK regulates proliferation and migration of vascular smooth muscle cells." Mol Cellular Biol **21**: 1565-1572.

Taylor, J. M., Mack, C. P., et al. (2001). "Selective expression of an endogenous inhibitor of FAK regulates proliferation and migration of vascular smooth muscle cells." Mol Cell Biol **21**(5): 1565-1572.

Thomas, J. W., Ellis, B., et al. (1998). "SH2- and SH3-mediated interactions between focal adhesion kinase and Src." J Biol Chem **273**(1): 577-583.

Toutant, M., Costa, A., et al. (2002). "Alternative splicing controls the mechanisms of FAK autophosphorylation." Mol Cell Biol **22**(22): 7731-7743.

Tung, C. H., Mahmood, U., et al. (2000). "In vivo Imaging of Proteolytic Enzyme Activity Using a Novel Molecular Reporter." Cancer Research **60**: 4953-4958.

Ubbels, G. A., Hara, K., et al. (1983). "Evidence for a functional role of the cytoskeleton in determination of the dorsoventral axis in Xenopus laevis eggs." J Embryol Exp Morphol **77**: 15-37.

van Seventer, G. A., Salmen, H. J., et al. (2001). "Focal adhesion kinase regulates beta1 integrin-dependent T cell migration through an HEF1 effector pathway." Eur J Immunol **31**: 1417-1427.

Voura, E. B., Jaiswal, J. K., et al. (2004). "Tracking metastatic tumor cell extravasation with quantum dot nanocrystals and fluorescence emission-scanning microscopy." Nat Med. **10**: 993-998.

Wacker, S., Brodbeck, A., et al. (1998). "Patterns and control of cell motility in the Xenopus gastrula." Development **125**: 1931-1942.

Walling, M. A., Novak, J. A., et al. (2009). "Quantum dots for live cell and in vivo imaging." Int J Mol Sci **10**(2): 441-491.

Wallingford, J. B., Rowning, B. A., et al. (2000). "Dishevelled controls cell polarity during Xenopus gastrulation." Nature **405**(6782): 81-85.

Weissleder, R. and Ntziachristos, V. (2003). "Shedding light onto live molecular targets." Nat Med. **9**: 123-128.

Weissleder, R., Tung, C. H., et al. (1999). "In vivo imaging of tumors with protease-activated near-infrared fluorescent probes." **17**: 375-378.

Winklbauer, R. (1990). "Mesodermal cell migration during Xenopus gastrulation." Dev Biol. **142**: 155-168.

Winklbauer, R. (1990). "Mesodermal cell migration during Xenopus gastrulation. ." Dev Biol. **142**: 155-168.

Winklbauer, R. (2009). "Cell adhesion in amphibian gastrulation." Int Rev Cell Mol Biol **278**: 215-275.

Winklbauer, R. and Keller, R. (1996). "Fibronectin, mesoderm migration, and gastrulation in Xenopus." Dev Biol. **177**: 413-426.

Winklbauer, R. and Nagel, M. (1991). "Directional mesodermal cell migration in the Xenopus gastrula." Dev Biol. **148**: 573-589.

Winklbauer, R. and Schürfeld, M. (1999). "Vegetal rotation, a new gastrulation movement involved in the internalization of the mesoderm and endoderm in Xenopus." Development **16**: 3703-3713.

Winklbauer R., Nagel M., et al. (1996). "Mesoderm migration in the Xenopus gastrula." Int J Dev Biol. **40**: 305-311.

Xia, H., Nho, R. S., et al. (2004). "Focal adhesion kinase is upstream of phosphatidylinositol 3-kinase/Akt in regulating fibroblast survival in response to contraction of type I collagen matrices via a beta 1 integrin viability signaling pathway." J Biol Chem **279**(31): 33024-33034.

Xing, Y. and Rao, J. (2008). "Quantum dot bioconjugates for in vitro diagnostics & in vivo imaging." Cancer Biomark **4**(6): 307-319.

Yano, H., Mazaki, Y., et al. (2004). "Roles played by a subset of integrin signaling molecules in cadherin-based cell-cell adhesion." J Cell Biol **166**(2): 283-295.

Yap, A. S., Stevenson, B. R., et al. (1995). "Vinculin localization and actin stress fibers differ in thyroid cells organized as monolayers or follicles." Cell Motil Cytoskeleton. **32**: 318-331.

Zachary, I. (1997). "Focal adhesion kinase." Int J Biochem Cell Biol **29**(7): 929-934.

Zhang, X., Wright, C. V., et al. (1995). "Cloning of a Xenopus laevis cDNA encoding focal adhesion kinase (FAK) and expression during early development." Gene **160**(2): 219-222.

Zhang, X., Wright, C. V., et al. (1995). "Cloning of a Xenopus laevis cDNA encoding focal adhesion kinase (FAK) and expression during early development." Gene **160**: 219-222.

Zimmer, J. P., Kim, S. W., et al. (2006). "Size series of small indium arsenide-zinc selenide core-shell nanocrystals and their application to in vivo imaging." J Am Chem Soc **128**: 2526-2527.

ANNEXES

I. Abbreviations

aa: amino acids

AC: Animal Cap

AJs: Adheren Junctions

AP: Animal Pole

BB:BA: Two parts Benzyl Benzoate and one part Benzyl Alcohol, Murray's Clearing Medium

Bleaching Solution: 1% H_2O_2, 5% Formamide, 0.5X SSC (standard saline citrate)

BC: Blastocoel

BCL: Blastopore Floor

BCR: Blastocoel Roof

BP: Blastopore

BSA: Bovine Serum Albumin

CE: Convergent Extension

CHO : Chinese hamster ovary

CMFM: Ca^{++} /Mg^{++} ions free buffer

DMZ: Dorsal Marginal Zone

DN: Dominant Negative

ECM: Extracellular Matrix

EGFR: Epidermal Growth Factor Receptor

HGFR: Hepatocyte Growth Factor Receptor

EDC: ethyl-N'-dimethylaminopropyl-carbodiimide

IMZ: Involuting Marginal Zone

IF: Immunofluoresence

FAs: Focal Adhesions

FAK: Focal Adhesion Kinase

FAK MO: FAK-specific antisense morpholino

FAT: Focal Adhesion Targeting

FERM: Four-point-one, Ezrin, Radaxin, Moesin

FL: Full Length

FN: Fibronectin

FRNK: FAK-Related Non Kinase

GFR: Growth Factor Receptors

Graf: GTPase Regulator Associated with FAK

Grb2: Growth factor Receptor-Bound protein 2

Grb7: Growth factor Receptor-Bound protein 7

hisGFP: histone Green Fluorescent Protein

MIP: Maximum intensity projection

memCherry: membrane Cherry

MMR: Marc's Modified Ringers

MM: Mesoderm Migration

MK's modified lysis buffer: 50 mM Tris HCl pH8, 150 mM NaCl, 1 mM EGTA, 0.5% NP-40, 0.5% Triton-X100, 5mM NaF

MZ: Marginal Zone

NES: Nuclear Export Signal

NIR QD's: Near Infra Red Quantum Dots

NLS: Nuclear Localization Signal

PBDT: 0.5% Triton, 5% BSA, 1% DMSO and 1% Normal Goat or Normal Donkey serum

PBS: Phosphate Buffer Saline

PBS++: PBS contains 0.5mM $MgCl_2$ and 0.5mM $CaCl_2$

PBT: 1X PBS + 0.1% Triton X-100

PC-γ: Phospholipase C-γ

PDGFR: Platelet-Derived Growth Factor Receptor

PFA: Paraformaldehyde 4%

PI3K: Phosphoinositide 3-Kinase

PIP2: Phosphatidylinositol-4,5-bisphosphate

Pro: Proline-Rich

PTw: 1X PBS + 0.1% Tween -20

QD's: Quantum dots

RIPA lysis buffer: 50 mM TrisHCl pH7.4, 150 mM NaCl, 2 mM EDTA, 1% NP-40, 0.1% SDS, 1% deoxycholate 24mM

RT: Room Temperature

SH: Src Homology

Ser: Serine

TBSTw: 1XTBS buffer + 0.1%Tween

Tyr: Tyrosine

VMZ: Ventral Marginal Zone

VP : vegetal pole

WISH: whole mount in situ hybridization

WT: wild type

II. Puplications

1. **Stylianou P**, Skourides PA. Imaging morphogenesis, in *Xenopus* with Quantum Dot nanocrystals. Mech Dev. 2009 Oct; 126 (10):828-41.*
2. Demetriou MC, **Stylianou P**, Andreou M, Yiannikouri O, Tsaprailis G. Cress A.E, Skourides P. Spatially and temporally regulated alpha6 integrin cleavage during *Xenopus laevis* development. Biochem Biophys Res Commun. 2008 Feb 15; 366 (3):779-85.*

*** Copy of the papers attached**

III. Conference announcements

Poster

1. "Nanotheranostics- Fabrication and Safety Concerns" International Conference, 27th- 30th April 2010, Agia Napa, Cyprus
2. 2010: Santa Cruz Developmental Biology Meeting, June 30th - July 3rd 2010

Title of the poster:

Imaging morphogenesis, in *Xenopus* with Quantum Dot nanocrystals

P. Stylianou and P.A. Skourides*

Department of Biological Sciences, Laboratory of Developmental Biology and BioImaging Technology

University of Cyprus, P.O. Box 20537,

CY 1678, Nicosia, Cyprus

* Corresponding author's e-mail address: skourip@ucy.ac.cy